

PHOTOGRAPH THIS SHEET

AD-A155 025

DTIC ACCESSION NUMBER

II

LEVEL

1

INVENTORY

FPRC-83-M-1

DOCUMENT IDENTIFICATION

Feb. 1984

This document has been approved
for public release and sale; its
distribution is unlimited.

DISTRIBUTION STATEMENT

ACCESSION FOR

NTIS GRA&I ☒

DTIC TAB ☐

UNANNOUNCED ☐

JUSTIFICATION

BY

DISTRIBUTION /

AVAILABILITY CODES

DIST

AVAIL AND/OR SPECIAL

A-1

DISTRIBUTION STAMP



DTIC
ELECTE
S JUN 13 1985 D
E

DATE ACCESSIONED

DATE RETURNED

85 06 13 138

DATE RECEIVED IN DTIC

REGISTERED OR CERTIFIED NO.

PHOTOGRAPH THIS SHEET AND RETURN TO DTIC-DDAC

AD-A155 025

EVALUATION OF CYLINDER, SOLENOID VALVE
AND SERVOVALVE CONTAMINANT SENSITIVITY

FINAL REPORT

30 September 1981 to 30 September 1982

PREPARED FOR

U. S. ARMY MOBILITY EQUIPMENT RESEARCH
AND DEVELOPMENT COMMAND
FORT BELVOIR, VIRGINIA 22060

PREPARED BY

PERSONNEL OF THE
FLUID POWER RESEARCH CENTER
OKLAHOMA STATE UNIVERSITY
STILLWATER, OKLAHOMA

Contract No. DAAK 70-81-C-0066

85 06 13 138

EVALUATION OF CYLINDER, SOLENOID VALVE
AND SERVOVALVE CONTAMINANT SENSITIVITY

FINAL REPORT

30 September 1981 to 30 September 1982

PREPARED FOR

U. S. ARMY MOBILITY EQUIPMENT RESEARCH
AND DEVELOPMENT COMMAND
FORT BELVOIR, VIRGINIA 22060

PREPARED BY

PERSONNEL OF THE
FLUID POWER RESEARCH CENTER
OKLAHOMA STATE UNIVERSITY
STILLWATER, OKLAHOMA

Contract No. DAAK 70-81-C-0066

Unclassified

SECURITY CLASSIFICATION OF THIS PAGE (When Data Entered)

REPORT DOCUMENTATION PAGE		READ INSTRUCTIONS BEFORE COMPLETING FORM
1. REPORT NUMBER FPRC-83-M-1	2. GOVT ACCESSION NO.	3. RECIPIENT'S CATALOG NUMBER
4. TITLE (and Subtitle) Evaluation of Cylinder, Solenoid, Valve, and Servovalve Contaminant Sensitivity		5. TYPE OF REPORT & PERIOD COVERED Final Report 30 Sept. 1981-30 Sept. 1982
		6. PERFORMING ORG. REPORT-NUMBER FPRC-83-M-1
7. AUTHOR(s) Hong, I. T., Izawa, K., Ito, T.		8. CONTRACT OR GRANT NUMBER(s) DAAK70-81-C-0066
9. PERFORMING ORGANIZATION NAME AND ADDRESS Fluid Power Research Center Oklahoma State University Stillwater, OK 74078		10. PROGRAM ELEMENT, PROJECT, TASK AREA & WORK UNIT NUMBERS
11. CONTROLLING OFFICE NAME AND ADDRESS U.S. Army Mobility Equipment Research & Development Command Procurement and Production Office / Ft. Belvoir, VA 22060		12. REPORT DATE February 1984
		13. NUMBER OF PAGES 218
14. MONITORING AGENCY NAME & ADDRESS (if different from Controlling Office) ONRRP, Rm. 582, Federal Bldg., 300 E. 8th Street Austin, TX 78701		15. SECURITY CLASS. (of this report) Unclassified
		15a. DECLASSIFICATION/DOWNGRADING SCHEDULE
16. DISTRIBUTION STATEMENT (of this Report) Approved for Public Release: Distribution Unlimited		
17. DISTRIBUTION STATEMENT (of the abstract entered in Block 20, if different from Report)		
18. SUPPLEMENTARY NOTES		
19. KEY WORDS (Continue on reverse side if necessary and identify by block number) hydraulic cylinder, servovalve, solenoid valve, Omega Rating, Beta Ten model, contamination, contaminant sensitivity, contaminant lock, silting force, seal, wear, leakage		
20. ABSTRACT (Continue on reverse side if necessary and identify by block number) This report presents the results of a series of investigations of hydraulic cylinders, solenoid valves, and servovalves contaminant sensitivity evaluations. Contamination theories used to evaluate these components were developed and verified experimentally. Test procedures for each component were also presented.		

DD FORM 1473
1 JAN 73

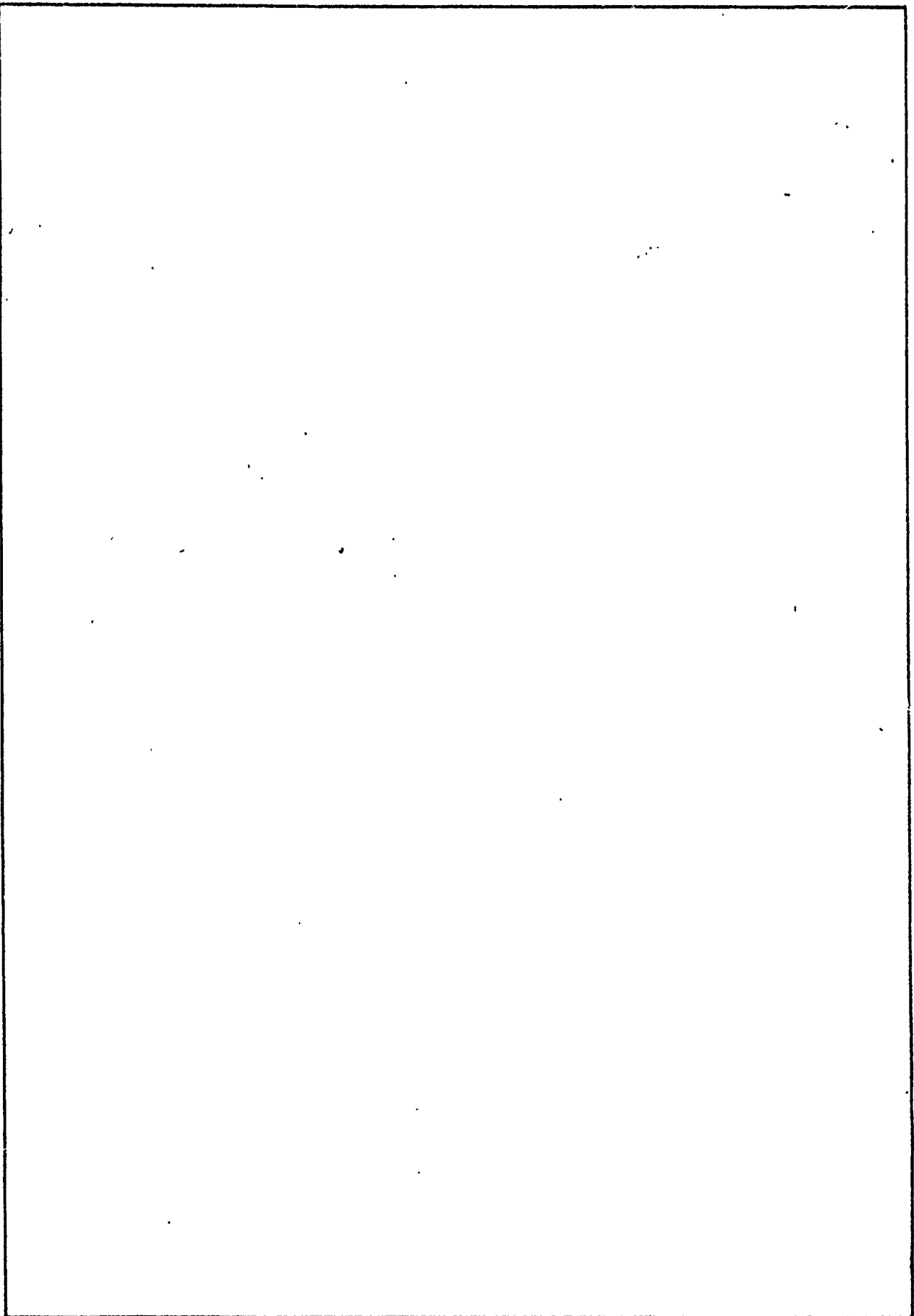
EDITION OF 1 NOV 65 IS OBSOLETE
S/N 0102-1F-014-6601

Unclassified

SECURITY CLASSIFICATION OF THIS PAGE (When Data Entered)

Unclassified

SECURITY CLASSIFICATION OF THIS PAGE (When Data Entered)



S/N 0102- LF- 014- 6601

Unclassified

SECURITY CLASSIFICATION OF THIS PAGE(When Data Entered)

SUMMARY

In previous MERADCOM-sponsored research activities, the Fluid Power Research Center has developed contaminant sensitivity test procedures for fixed displacement pumps and motors, pressure compensated pumps, directional control valves, and relief valves. All of these procedures either have been accepted as national or international standards or are currently in the study range for such acceptance. In each case, the test procedures led to a single number figure of merit which identifies the contaminant sensitivity of these components -- that is, how their service lives are affected by controlled exposure to particulate contaminant.

Contaminant sensitivity ratings have not been developed for three other major components normally found in modern hydraulic systems -- servovalves, solenoid valves and cylinders. With this in mind, the effort of this research is to investigate the contaminant sensitivity of these components. Accordingly, the purpose of this research is to:

1. Develop test procedures to determine the contaminant sensitivity of hydraulic servovalves, solenoids, and cylinders.
2. Develop interpretation techniques for the test results to determine the contamination protection requirements.

The objectives of this project have been met successfully.

This report presents the results of work carried out to achieve the listed project objectives. In order to provide the potential

readers a clearer view of each component under study, research results are presented in three major parts -- Part I, II, and III for hydraulic servovalves, solenoid valves and cylinders individually. Each part is composed of several specific chapters in the order of Introduction, Investigation (Theoretical Background and Analysis, Test Results, etc.), Discussion, and Conclusion.

PREFACE

This report was prepared by the staff of the Fluid Power Research Center (FPRC), Oklahoma State University, under the general direction of Dr. E. C. Fitch. The work reported here was authorized by U. S. Army MERADCOM Contract No. DAAK70-81-C-0066. The report documents the work completed under the subject contract covering the period 30 September 1981 to 30 September 1982.

The principal investigators for this effort were Dr. R. Inoue (Servovalves, Solenoid Valves) and Mr. D. Ahlberg, former research engineers at the FPRC. Project personnel were:

K. Izawa

T. Ito

Dr. I. T. Hong has served as Program Coordinator and has organized this report.

The Contract Officer Technical Representative for this contract was Mr. Delmar Craft.

TABLE OF CONTENTS

Part		Page
I	SERVOVALVES	1-1
	Introduction	1-2
	Review of Previous Studies	1-5
	Theoretical Background	1-18
	Servovalve Contaminant Sensitivity Theory	1-40
	Test Stand	1-57
	Test Procedure	1-65
	Test Results	1-82
	Conclusions and Recommendations	1-105
	References	1-108
II	SOLENOID VALVES	2-1
	Introduction	2-2
	Review of Previous Studies	2-4
	Development of the Solenoid Valve Omega Theory	2-14
	Test Procedure	2-36
	Test Stand	2-50
	Results of Valve Tests	2-57
	Conclusions & Recommendations	2-62
III	HYDRAULIC CYLINDERS	3-1
	Introduction	3-2
	Cylinder Contaminant Sensitivity Rating Method	3-5
	Cylinder Test Facility	3-15
	Fluid Power Cylinder Contaminant Test Procedure	3-21
	Experimental Verification	3-25
	Discussion and Conclusion	3-31

LIST OF FIGURES
PART I-SERVOVALVES

Figure		Page
2.1	Flow Chart of Failure Diagnosis	1-8
2.2	Lockheed's Electrohydraulic Valve Test Procedure	1-10
2.3	Lockheed's Servovalve Contaminant Sensitivity Test Results	1-11
2.4	Moog's Servovalves Contaminant Sensitivity Test Result	1-14
3.1	The Schematical Structure of Servovalves	1-20
3.2	Types of First Stage Hydraulic Amplifiers	1-21
3.3	Effect of Dither on Pressure Distributions with Inverse Taper Spool	1-28
3.4	Valve Contaminant Lock Sensitivity vs. Contaminant Size for Directional Control Valves	1-29
3.5	Moving Force of the Spool vs. Contaminant Concentration	1-31
3.6	Erosion Characteristic Curves of SAE 1020 Steel at Various Impact Velocities	1-35
3.7	Erosion Rate vs. Impact Angles at Various Particle Size Ranges	1-36
3.8	Typical Erosion Angle of Attack Characteristic	1-37

Figure		Page
3.9	Particle Impinging Process at the Spool Orifice	1-38
4.1	Illustration of Particles Destruction Characteristics	1-49
4.2	Linearized Particle Destruction Time Constant Relationship for OSU Test Pump No. 102	1-50
5.1	Test Circuit	1-58
5.2	Qualification Test Results	1-61
6.1	The Beta Ten Filter Model	1-66
6.2	Test Circuit	1-72
6.3	Hysteresis Increase Characteristic Curve	1-79
6.4	Pressure Gain Degradation Curve	1-80
7.1	Test Result of Servovalve A -- Hysteresis Increase	1-89
7.2	Test Result of Servovalve B -- Hysteresis Increase	1-90
7.3	Test Result of Servovavle C -- Hysteresis Increase	1-91
7.4	Hysteresis Increase of Beta Model for Servovalve A	1-93
7.5	Hysteresis Increase of Beta Model for Servovalve B	1-94
7.6	Hysteresis Increase of Beta Model for Servovalve C	1-95
7.7	Measured Pressure Degradation for Servovalves A, B, and C	1-99
7.8	Total Pressure Gain Profile for Valve B	1-100
7.9	Contaminant Tolerance Profiles	1-103

PART II-SOLENOID VALVES

Figure		Page
2.1	Test Circuit	2-7
2.2	Silting Force vs. Contaminant Size at Stationary Time of 16 Min. ACFTD	2-8
2.3	Silting Force vs. Average Contaminant Size at Stationary Time of 16 Min. Carbonyl Iron	2-9
2.4	The Nature of Silting Force Contaminant Lock	2-11
2.5	Effect of Increase in X and Y Parameters	2-12
3.1	Beta Ten Profile	2-15
3.2	Valve Contaminant Lock Sensitivity vs. Contaminant Size	2-17
3.3	Force vs. Reference Gravimetric Level	2-19
3.4	Algorithm to Find Solenoid Valve Omega	2-23
3.5	Solenoid Omega Computer Algorithm	2-27
3.6	Program Listing of Solenoid Omega	2-28
3.7	Omega Conversion Chart	2-35
4.1	Test Circuit	2-42
4.2	Solenoid Valve Actuation Mechanism	2-45
4.3	Force-Voltage Characteristic Curve	2-46
5.1	Schematic of Test Circuit	2-51
6.1	Test Stand Qualification Test Result	2-54
6.2	Variation of Solenoid Force due to the AC Induced Vibration	2-60

PART III-HYDRAULIC CYLINDERS

Figure		Page
2.1	Particle Ingression Process	3-12
2.2	Cylinder Contaminant Sensitivity Rating Concept	3-14
3.1	Test Circuit	3-16
3.2	Schematic of Pressure Path -- Upward Process	3-17
3.3	Schematic of Pressure Path -- Downward Process	3-19
4.1	Test Circuit	3-22
5.1	Cylinder Contaminant Sensitivity Test Results	3-29

LIST OF TABLES PART I-SERVOVALVES

Table		Page
2.1	Test Schedule of Threshold Sensitivity Test	1-13
2.2	Test Result Due to Flow Variation	1-16
4.1	Particle Distribution of the Lower Cut Dust	1-44
5.1	ACFTD Chemical Property	1-64
6.1	Accuracy Limits	1-70
6.2	Contaminant Lock Sensitivity Data Sheet	1-76
6.3	Contaminant Wear Sensitivity Data Sheet	1-77
7.1	Contaminant Lock Sensitivity Test Result-A	1-86
7.2	Contaminant Lock Sensitivity Test Result-B	1-87
7.3	Contaminant Lock Sensitivity Test Result-C	1-88
7.4	Summary of Calculation on Coefficient X and Y	1-92
7.5	Summary of Contaminant Lock Omega Rating	1-97
7.6	Summary of Contaminant Wear Omega Rating	1-102

PART II-SOLENOID VALVES

3.1	Particle Size Distribution of Converted Beta Ten Profile	2-20
3.2	Particle Distribution of Lower Cut Dust	2-22
3.3	Silting Force vs. Pressure Difference	2-24

Table		Page
3.4	Solenoid Valve Omega Rating Test Data Recording Form	2-32
3.5	Solenoid Valve Omega Rating Test Work Sheet	2-33
3.6	Solenoid Valve Omega Rating Test Report Form	2-34
4.1	Accuracy Limits	2-40
6.1	Summary of Omega Ratings of Tested Valves	2-59

PART III-HYDRAULIC CYLINDERS

2.1	Cylinder Test Results -- Internal Leakage	3-9
4.1	Cylinder Contaminant Sensitivity Test Report	3-24
5.1	Test Program	3-26
5.2	Test Results -- Ingression Approach	3-28

• PART I

SERVOVALVES

CHAPTER I - INTRODUCTION

Electrohydraulic servovalves were originally developed for the aerospace industry because their compactness and high response capabilities offered distinct advantages. As the technology of electrohydraulic servomechanisms evolved, the use of servovalves has broadened to include machine tools, mobile equipment, and many other applications where a load must be positioned accurately.

As the application of servovalves spread, one serious problem became evident -- contaminant sensitivity. Since servomechanisms are manufactured with very precise and close tolerances to satisfy high performance requirements, they are more sensitive to contaminant than most other hydraulic components. Servovalves installed in missiles and aircraft are usually protected by intensive filtration; however, servovalves used in mobile equipment are generally exposed to severe contaminant environments. The contaminant level found in a mobile hydraulic system is usually much higher than that in missile and aircraft systems. Also, servovalves used in mobile hydraulic systems are expected to have longer operating lives. Protection from contaminant is essential if the desired operating life is to be achieved.

To determine the protection required for a servovalve, the contaminant sensitivity of the valve must be evaluated; however, test procedures which evaluate the contaminant sensitivity are not yet available.

The objectives of the project which are the subject of this report include:

1. Develop test procedures to evaluate the contaminant sensitivity of servovalves.
2. Conduct the contaminant sensitivity tests on servovalves.
3. Develop interpretation techniques for the test results to determine the contamination protection requirements.

The plan of attack used to accomplish the objectives of this study was:

1. Construction of the test system.
2. Development of test procedures necessary to evaluate the contaminant sensitivity of servovalves.
3. Evaluation of the contaminant effects on servovalve hysteresis and threshold. (Different sizes of classified AC Fine Test Dust were used to establish the relationship between contaminant size and sensitivity. Clogging of the filter will be avoided during testing.)
4. Increase of hysteresis was measured as a function of contaminant level and size, while time of exposure to contaminant was kept constant.
5. Evaluation of the change of pressure gain due to contaminant wear.
6. Interpretation of test results. (Interpretation techniques for the test results were developed to select the servovalve best

suited for the particular application and to determine the filter protection requirements.)

CHAPTER II - REVIEW OF PREVIOUS STUDIES

Contamination effect on electrohydraulic servovalves has been discussed recurrently by virtue of the potential of the servovalves for automation and their capability to interface with microelectronics. The results acquired from many investigations on contaminant sensitivity of the servovalves have given users the negative impression that they are very sensitive to contaminants. This position has been engrained by such statements as that by Williams [1] that "The operating environment of servovalves must approach surgical cleanliness standards." Williams, however, claimed that present day servovalves are reliable based on field experiences and the studies done on new servovalve design. A survey conducted by Nair [2] among leading manufacturers and users of the electrohydraulic servovalves, on the contrary, shows that the contaminant related problems of servovalves still need to be studied scientifically and that the effective use of servovalves must be promoted.

As shown in Williams' paper and Nair's survey, there seem to be some misunderstandings among users and manufacturers. Neither have any evaluation technique to accurately evaluate servovalve performance in contaminated systems.

This study is intended to fill or at least alleviate this gap between the users and the manufacturers by developing an evaluation technique for servovalve contaminant sensitivity as well as providing

a filter selection technique for particular servovalves. A summary of some previous servovalve studies is presented below.

WADC STUDY [3]

A technical report published by WADC (Wright Air Development Center) discusses an attempt to ascertain the susceptibility of the servovalves to a high degree of contamination in hydraulic fluids. The report includes a survey of servovalve vendors and users. The survey from the vendors shows that design improvements have decreased contaminant related problems. Main emphasis from the vendors was aimed at built-in filter design, torque motor design, and more powerful first stage amplifier.

From the user standpoint, servovalves operating under relatively low temperature, below 160 F, had the least contamination problems. Servovalves operated in high temperature were felt to be likely to meet contamination problems. A missile manufacturer stated that all oil was passed through a set of filters which consisted of a 10 μ m filter in series with a 2 μ m filter to eliminate contaminants. The servovalve users which had little difficulty from oil contamination paid a great deal of attention to their systems by maintaining the assembly and test area clean, providing high-quality filters, and by emphasis on good maintenance practices.

One of the objectives of the WADC study, was to formulate experimental procedures. The experiment evaluated position feedback of the actuator to the servo amplifier. When contaminant of a particular size

range was added to the system, a temporary command signal was applied to the servovalve, and the position response was recorded. The contaminant addition and the valve operation were continued until the valve ceased to operate satisfactorily. The total contaminant added and total operating time before failure were recorded as well as spool end pressure and actuator end pressure for the failure analysis.

The deleterious effects of the servosystem were observed by the position output of the actuator. The failure symptoms which they defined were sluggishness, hard-over, and oscillation. The causes of failure were perceived based on the progressive dismantling and cleaning procedure. The procedure is shown in the flow chart in Fig. 2.1. The report in the procedure section mentioned that the filters, orifices, or nozzles were removed and cleaned one at a time when a "hard-over" condition happened.

From the test results tabulated in the report, 20 failures were due to filter clogging, ten due to orifice, three due to nozzle, three due to second stage failure. It was stated that the servovalves were less susceptible when the first stage quiescent flows were less. In conjunction with this statement, it is concluded that the tests were more of a filter test than a valve design test, because the valve malfunction in most cases resulted from filter clogging.

LOCKHEED STUDY [4]

A contamination study performed by Vought Electronics under contract from Lockheed Aircraft Corporation concluded that the major

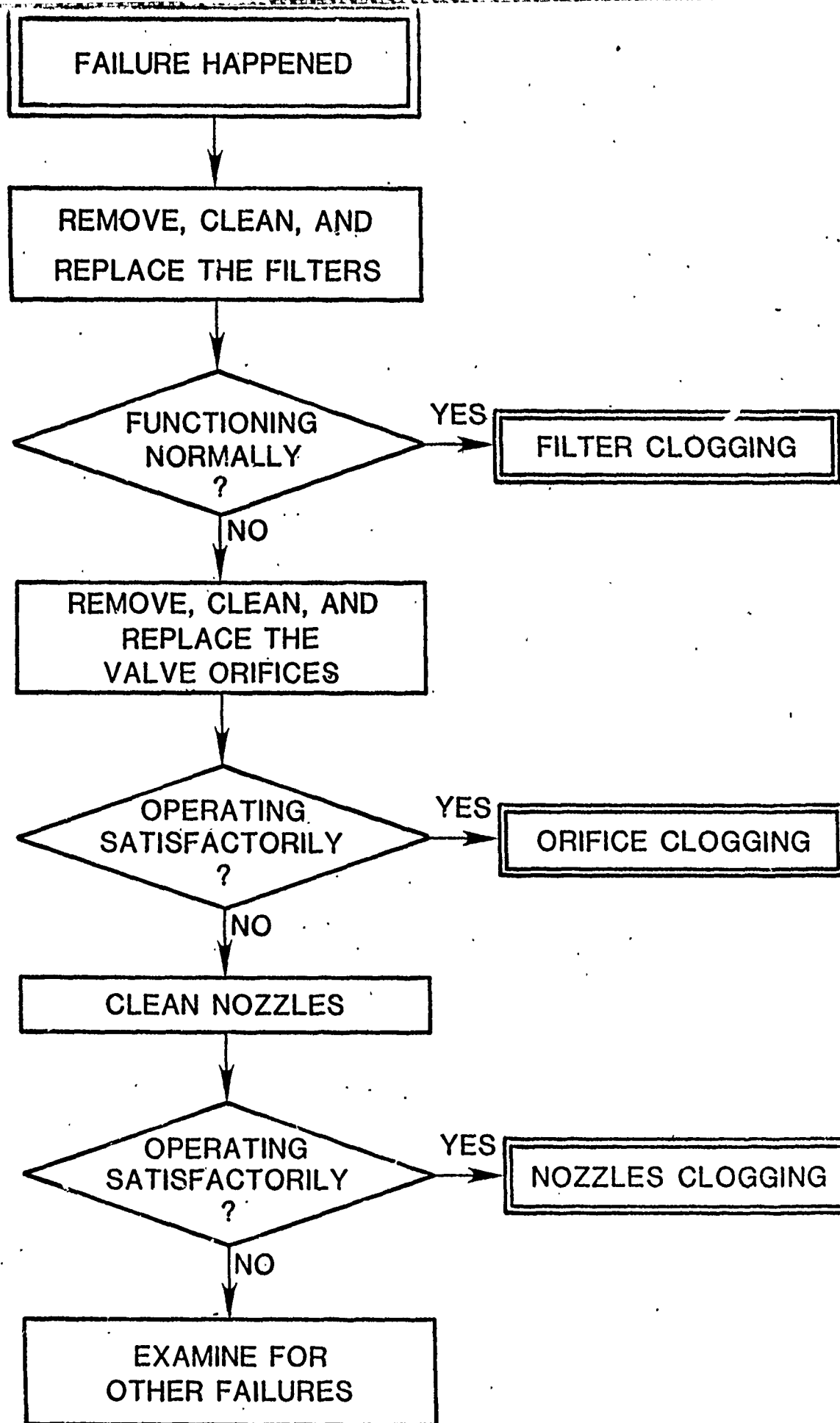


Fig. 2.1 Flow Chart of Failure Diagnosis

cause of the failure of the electrohydraulic servovalves tested was erosion of targets, nozzles, flappers, spool valves, etc. The report stated that there were no failures related to clogging of orifices or filters except one valve which failed because of a collapsed built-in filter. The failure in terms of erosion was designated when the valve went hard-over or failed to respond to the maximum input current.

The test procedure they developed is summarized in flow chart form in Fig. 2.2. The contaminant used in their study was a mixture of 90 percent standard AC Fine Test Dust (ACFTD) and 10 percent carbonyl iron powder.

Failure analysis was performed by disassembly. Since some of the servovalves tested used a wet torque motor, iron filings were found in the air gap around the motor poles. The servovalves consisting of dry torque motor were found to have no deposit around the torque motors. The fixed orifices, nozzles, flappers, etc., were carefully examined for erosion or damage. The nozzle-flappers of some servovalves were eroded so that pilot pressure gain was decreased. This caused less driving capability of the second stage spool valve. The report showed one failure due to the collapse of built-in filters over the supply orifices. Scoring on the spool valve surfaces occurred in all valves.

From the test results, one of the servovalves tested failed to operate with only a 6 mg/L total contaminant concentration while another one survived 528 mg/L. Using the data obtained from the report, threshold performance degradation was redrawn as a function of contaminant concentration in Fig. 2.3

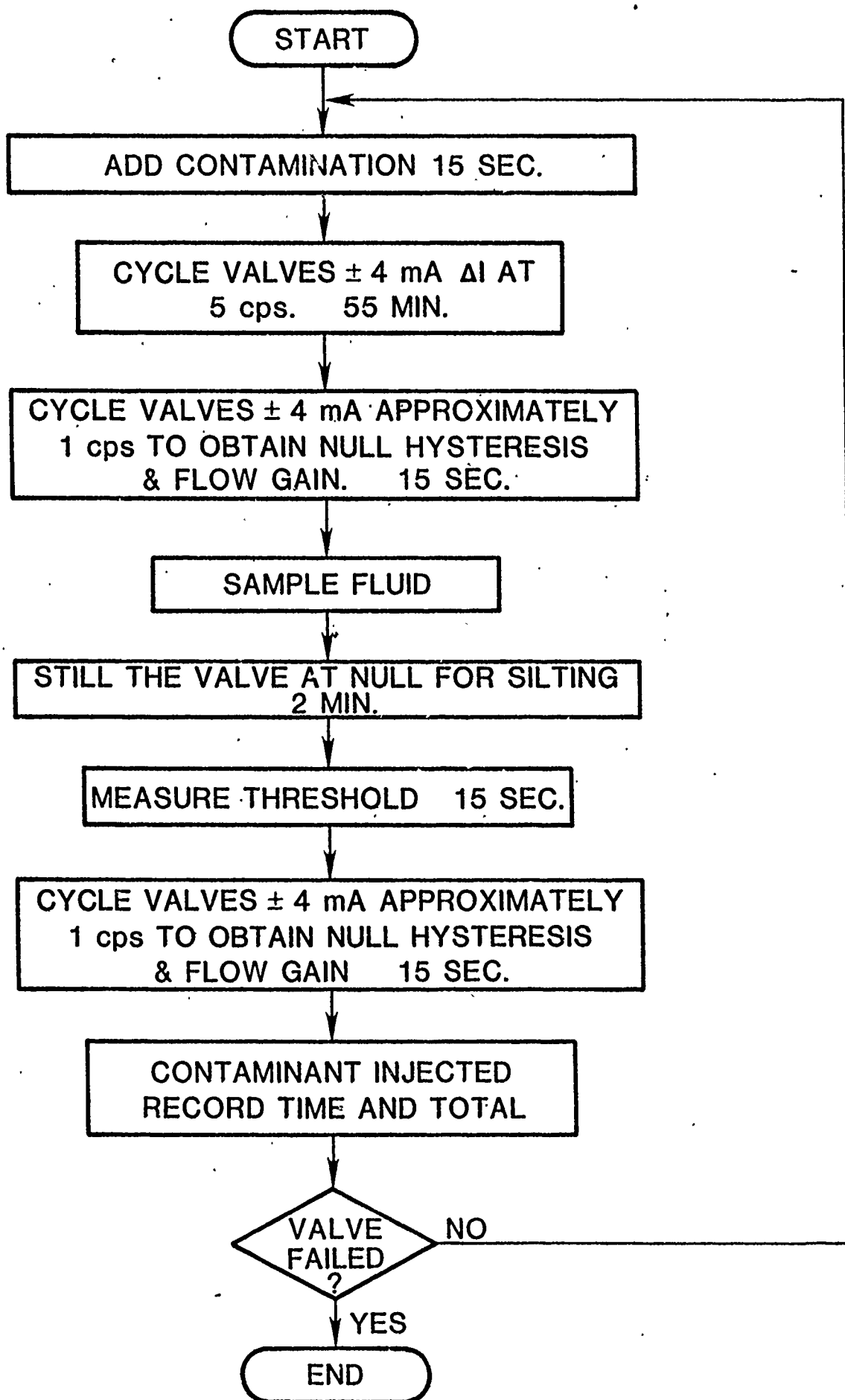


Fig. 2.2 Lockheed's Electrohydraulic Valve Test Procedure

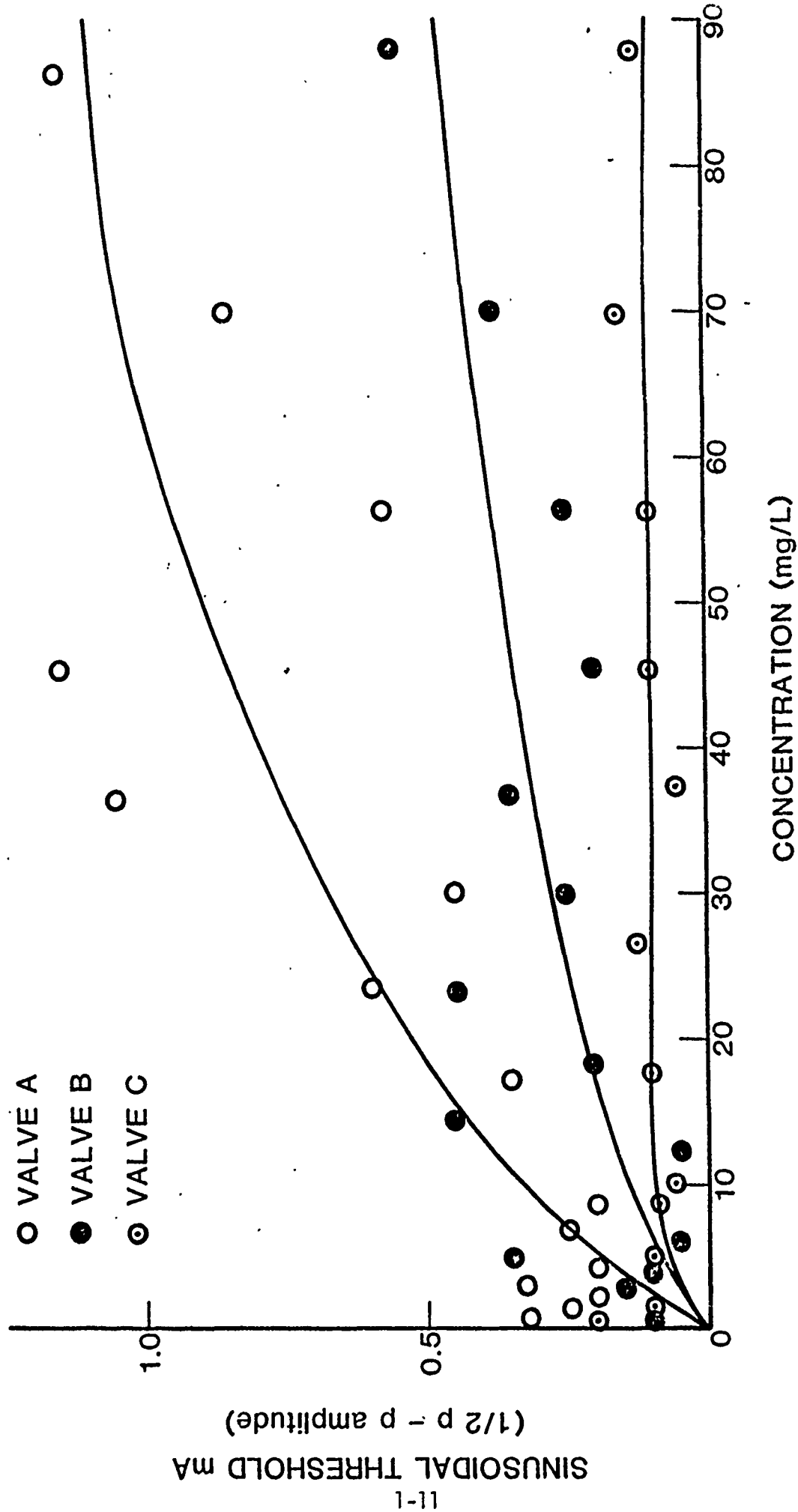


Fig. 2.3 Lockheed's Servovalve Contaminant Sensitivity Test Results

MOOG STUDY [5]

Moog attacked the problem more scientifically. The contaminant sensitivity was classified into two categories: temporary performance degradation and permanent performance degradation. The temporary performance degradation was detected by measuring threshold increase during contaminant injection. The permanent performance degradation was measured from leakage flow.

The effect of the particle size on performance was studied. It was found that the servovalve threshold would increase as a function of fine particles, 1-5 μm . Because larger particles cause clogging of orifices or built-in filters, the use of 0-10 μm classified ACFTD was recommended to evaluate the threshold sensitivity of the servovalves. This procedure simplified the test procedure. The other point to be noted from this report is the failure criteria of testing. It was suggested that threshold sensitivity degradation beyond 10 percent of rated signal was of no value, since such a large threshold would not be acceptable to most users. Using 0-10 μm test dust, the threshold was measured according to the schedule summarized in Table 2.1. The threshold increase was redrawn from the Moog results, as shown in Fig. 2.4. The threshold was measured at concentrations of 2, 4, 8, and 16 mg/L.

The permanent performance degradation measured from leakage flow was evaluated as the degree of wear on sharp orifices on the second stage spool. As in the previous test, 0-10 μm ACFTD was used. It was concluded that the measurement of the sensitivity for different particle

Table 2.1. Test Schedule of Threshold Sensitivity Test.

Time (min)	0	2	5	7	10	12	15	17	20
0-10 m Concentration (mg/L)		2		4		8		16	
Addition of Contaminants (mg/L)	2		2		4		8		
Hysteresis Measurements		↔		↔		↔		↔	
Test Condition: 0.5 Hz sinewave ±10% of rated current System Pressure 300psi	↔								

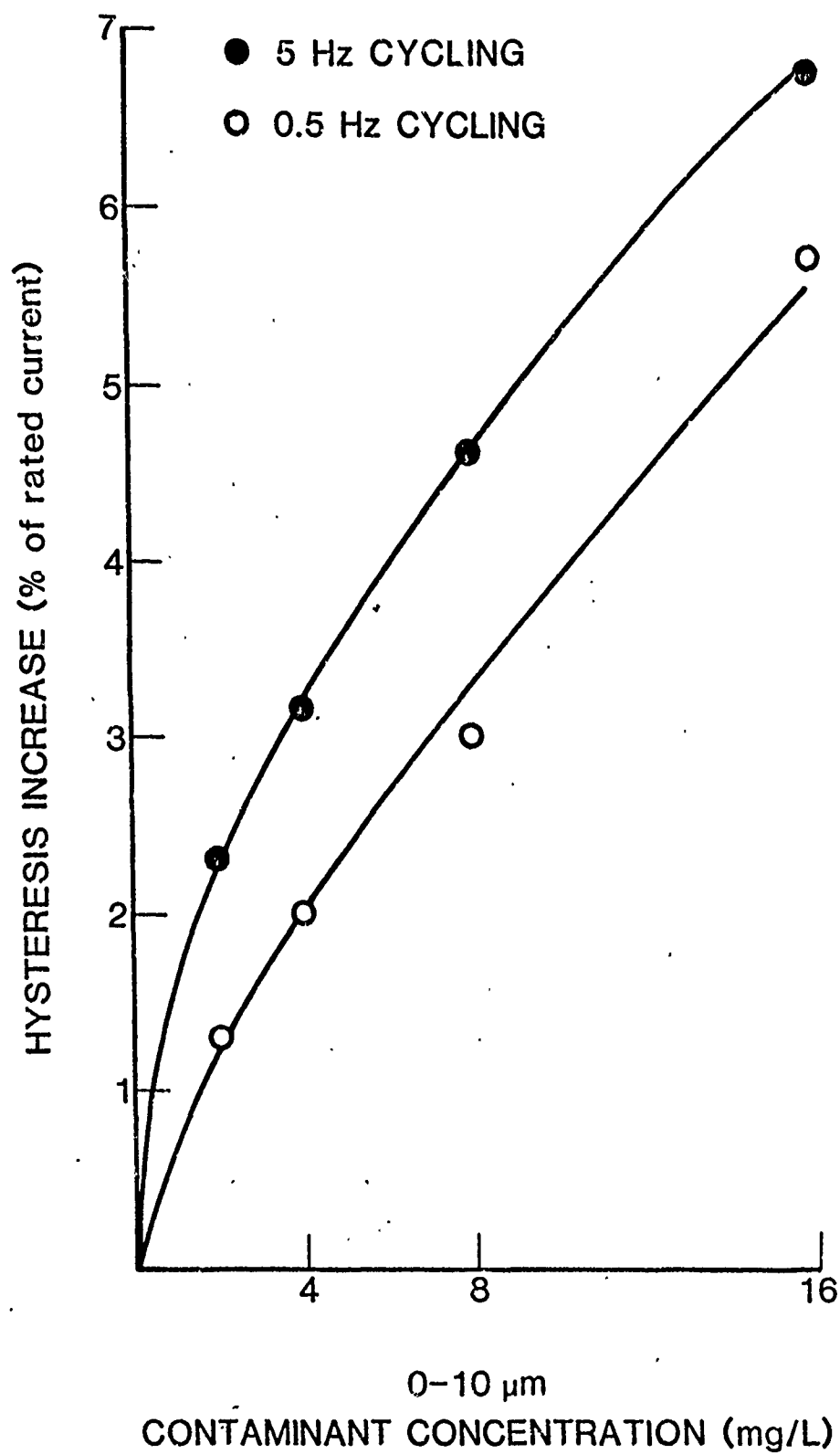


Fig. 2.4 Moog's Servovalves Contaminant Sensitivity Test Result

size distributions (i.e., 0-5 μm , 0-10 μm , etc.) on the same specimen was not feasible because the performance degradation starts high and progressively decreases as wear increases the clearance and rounds the corners of the spool orifices. The wear due to 0-10 μm contaminant was caused by cycling the servovalves for 40 minutes with 20 mg/L of contaminant concentration. The leakage flow was measured after two successive 40-minute periods of operation. The internal leakage flow increased from 2 percent of rated flow to 23 percent.

The effect of flow rate through the spool orifice edges was also investigated by removing the first stage assembly and installing special spool stops in the second stage assembly to fix the spool at various valve openings. For small openings, internal leakage did not increase appreciably because of the silting effect. For larger openings, there was no appreciable effect of flow rate on the leakage rate, as shown in Table 2.2.

Using the same equipment prepared for the above test, the effect of particle impact on the spool orifice edges was tested by adding different particle size ranges: 0-5 μm , 0-10 μm , and 0-80 μm . The concentration for this test was 300 mg/L. The result showed that larger particles caused more erosion than the smaller particles.

The report listed the overall permanent degradation on servovalve performance after the sensitivity tests. These included:

1. Slight increase in gain at null.
2. Hysteresis and threshold increase by 1 percent.

Table 2.2. Test Result Due to Flow Variation.

0-80 m		50 mg/L	Contaminants
Flow	Linear Valve Opening	Leakage Increase	Comment
10%	22 μm	none	silted up completely
20%	44 μm	2%	partially silted
40%	88 μm	7.7%	
130%	286 μm	7.7%	

3. Seventeen percent decrease of original pressure gain value.
4. Decrease in first stage gain.
5. Increase in first stage leakage flow.

DISCUSSION

Each of these studies reached a milestone for the evaluation technique of servovalve contaminant sensitivity. Their accomplishments have been invaluable in this project.

These studies pointed out some of the myths concerning servovalves while bringing out some interesting anomalies. For instance, the valve which survived a concentration level of 528 mg/L would probably be operating long after most hydraulic pumps would have been destroyed by contaminant. Other test valves would not survive in ultra-clean systems..

CHAPTER III - THEORETICAL BACKGROUND

TYPES OF SERVOVALVES

Electrohydraulic servovalves can be classified by their internal configurations, the number of stages in power amplification, and the control mode. From the flow and response requirements, the servovalves can be categorized as single-stage, two-stage, and three-stage. Single-stage servovalves consist of a torque motor and a four-way valve. Because of their simplicity, single-stage servovalves are less expensive, and their response is high compared with multiple-stage servovalves. Their disadvantages are the flow capacity due to steady-state flow forces and stability which depends on the load dynamics.

Two-stage servovalves, which are the most common, are composed of a second-stage valve driven by a single-stage servovalve, while three-stage servovalves consist of a third-stage valve driven by a two-stage servovalve. By compounding the servovalve in the above fashion, the disadvantages of the single-stage servovalves are overcome, but such valves become more complex and expensive.

Multiple-stage servovalves have some sort of feedback between the first stage and second stage. There are three basic methods of feeding back the signal from second stage to first stage:

- * Centering springs on the spool end of the second stage to create a force balance between the stages.
- * A feedback spring deflected by the second-stage spool displacement to create a force feedback to the torque motor.

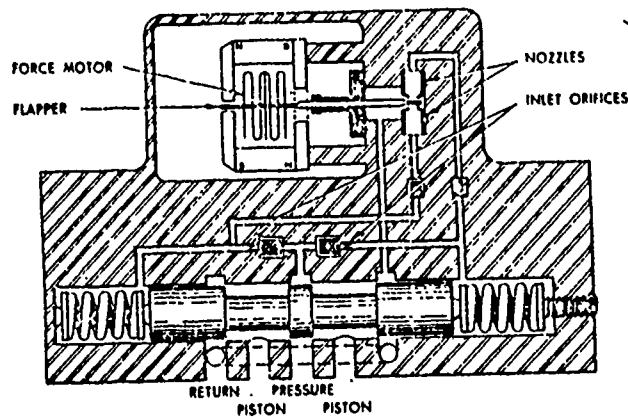
- * Position feedback accomplished by direct position feedback similar to hydraulic followers (Fig. 3.1).

The classification can also be made from the configuration of the first-stage hydraulic amplifiers. The most common designs are nozzle flapper, jet pipe, jet deflector, and spool types. Schematics of each design are shown in Fig. 3.2.

With respect to the control modes of the servovalves, there are six types available:

- * flow control
- * pressure control
- * pressure-flow control
- * dynamic pressure feedback
- * static load error washout
- * acceleration switching

The flow control servovalves are basic and the most common. They control load flow proportional to the electrical input current at constant load. This type of servovalve has high resolution and stiffness but low damping. Pressure control servovalves provide a differential pressure output in response to an electrical input current while pressure-flow control servovalves regulate flow in response to both the electrical input current and the differential load pressure. This function provides effective damping in high-resonant loaded servosystems at the expense of lowering system stiffness. The servovalves combining the functions of the flow control servovalves, which provide stiffness on the steady state, and the pressure flow control servovalves, which



TWO-STAGE SERVOVALVE WITH OPEN CENTER FIRST STAGE

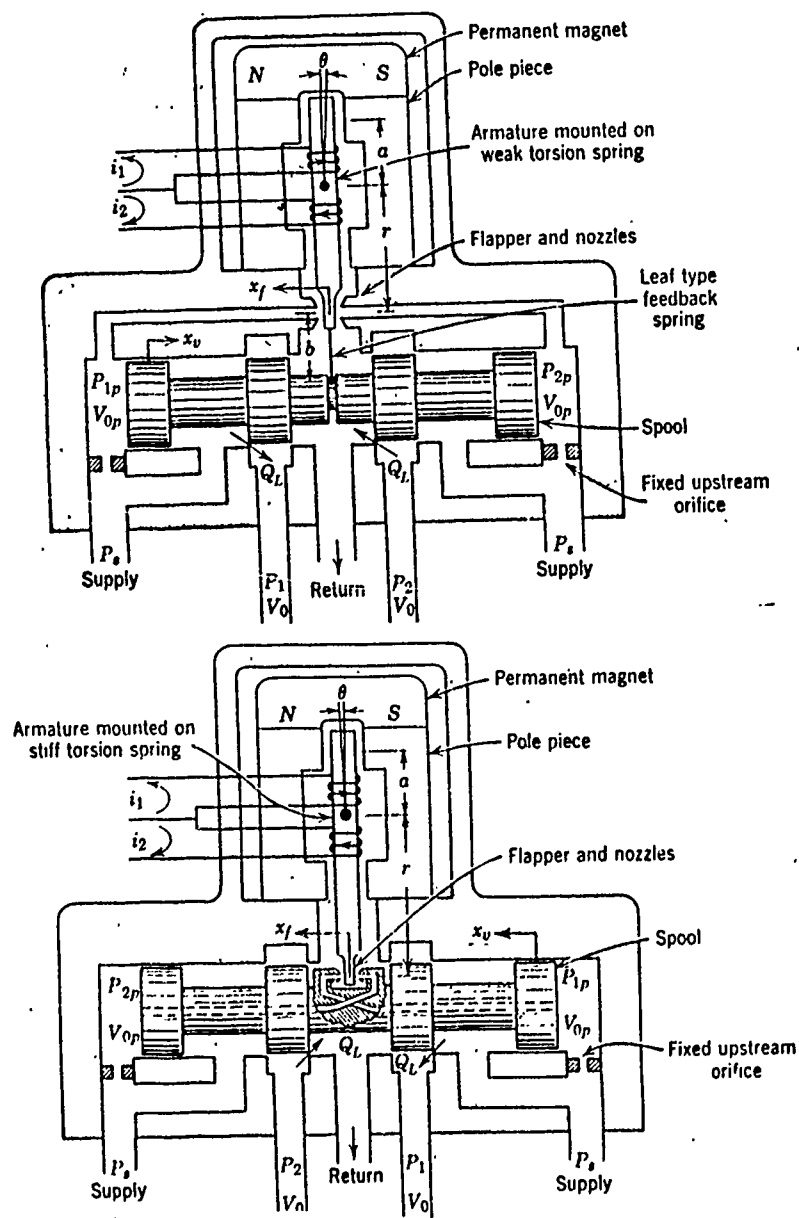
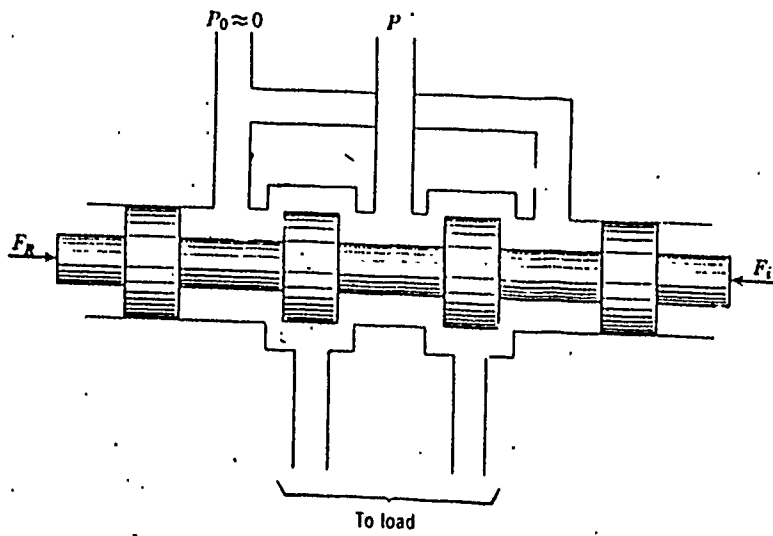
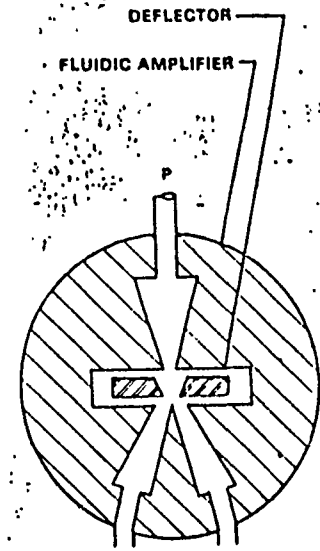


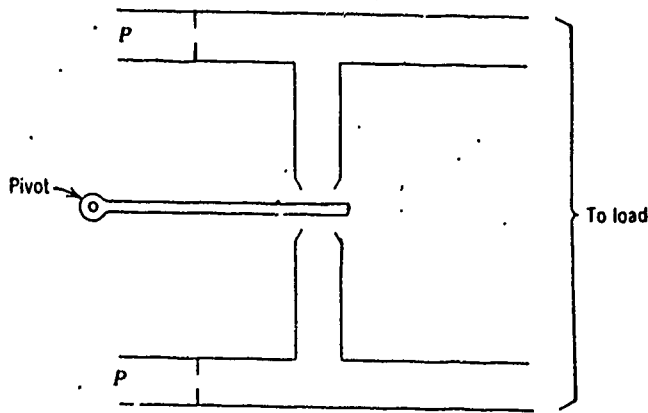
Fig. 3.1 The Schematical Structure of Servovalves



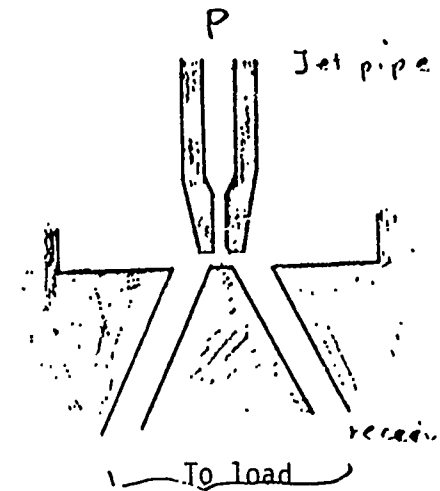
(a) Spool Valve



(c) Deflective Jet Valve



(b) Double Nozzle Flapper Valve



(d) Jet Pipe Valve

Fig. 3.2 Types of First Stage Hydraulic Amplifiers

provide effective damping under dynamic conditions, are called the dynamic pressure feedback servovalves. The static load error washout servovalves have a further feature besides the dynamic pressure feedback technique. This type includes an additional static pressure feedback to compensate load position errors caused by the load structural compliance. The acceleration switching servovalves are quite distinct from the others, although the construction of these valves is similar to the flow control servovalve aforementioned. The input signal to the torque motor is a high frequency pulse length modulated wave instead of conventional DC input current.

Regardless of the way in which the servovalve is described, one thing remains common -- small clearances. Spool displacements as low as 0.25 to 0.5 mm are common, while radial clearances of 0.7 to 1.5 μm are found in some aerospace applications. Unless careful design practices are utilized, these clearances will invariably pose serious contamination sensitivity problems.

SERVOVALVE PERFORMANCE PARAMETERS

To obtain better performance, the electrohydraulic servovalves are fabricated with very close tolerances. Typical high performance servovalves for industrial applications have spool laps of 20 μm for all null edges. This spool lap condition governs the system performance and stability.

To determine the performance of the servovalves, several parameters should be examined. Some of these parameters are dependent upon the spool lap conditions. The important parameters are:

flow gain

flow-pressure coefficient

pressure sensitivity

hysteresis

threshold

internal leakage flow

The first three parameters are called valve coefficients. These coefficients influence the stability of the servosystems. The flow gain affects open-loop gain. The flow-pressure coefficient provides systems damping and is related to the leakage characteristics of the valve. The pressure sensitivity is expressed by the ratio of flow gain to the flow-pressure coefficient and represents the ability of a valve-motor or valve-piston combination to accelerate an inertial load under large loads with little error. The larger the pressure sensitivity, the lower the system compliance.

Hysteresis is a nonlinearity caused by the magnetic effect of the torque motor and the friction on the spool. Threshold is also induced by friction on the spool. These nonlinearities should be kept as small as possible to avoid trouble in stability. In general, a system having strong nonlinearities might exhibit limit cycle oscillations or jump resonance.

Internal leakage flow is mainly related to energy consumption. In missile applications, for example, very low internal leakage rates are normally selected in order to supply fluid to the system for a certain period of time. Internal leakage flow is subjected not only to

first-stage hydraulic amplifier configuration but also second-stage spool valve lap conditions. Underlapped spool valves cause large amounts of internal leakage flow and also can be the cause of higher wear rates on metering orifices.

EFFECT OF CONTAMINANTS ON SERVOVALVE PERFORMANCE PARAMETERS

Servo valve reliability and performance are a function of several factors. The valve design, discussed in previous sections, is one of them. Another factor might be the performance and efficiency of the filters selected for the servosystems. Also, the material of the contaminants affects servo valve performance severely.

The effect of contaminants on the servo valves appears in the form of contaminant lock force on the spool, wear on the critical surface and orifices, and clogging of small fixed or variable orifices. The contaminant lock force is created by the silting of small particles in the tight clearance between the spool and the sleeve. The result of silting then emerges as sluggish response due to increased friction on the spool or perhaps unstable servosystem response. If the second-stage spool driving force is not large enough to overcome the frictional force due to silting, hard-over or total loss of flow capability results. This kind of sudden failure, so-called catastrophic failure, can be disastrous on some equipment.

In contrast to the contaminant lock mode, which causes temporary performance degradation, contaminant wear brings about permanent performance deteriorations, so-called perceptible failure. Even though

the working fluid is moderately clean, contaminant wear remains a concern. Scoring and abrading between the spool and sleeve surfaces may occur, as may wear in orifices. The most critical of the orifices are the control orifices on the spool that regulate the flow to load according to a signal. Rounding off the sharp edges of the orifices causes a change in the discharge coefficient of the orifices and change in valve performance parameters. A different rate of wear in the orifices causes a null-shift in servovalves. Excessive null shift causes asymmetric flow. Rounding off the fixed orifices of the servovalves also changes their discharge coefficients but has less effect on the servovalve performance.

Clogging small fixed and variable orifices and built-in filters leads to other disastrous results in servosystems. This problem had been considered the general cause of valve failure in the past, but some documents indicate that no failure due to plugged or clogged orifices occurred [4].

It is unquestionably valuable to correlate the effect of particulate contaminants with servovalve performance parameters to evaluate their susceptibility to contaminants. A critical parameter, which represents not only the degradation of the servovalve performance but also variation on the static and dynamic characteristics, must be selected from the performance parameters.

As mentioned, contaminant-related problems are categorized as contaminant lock and contaminant wear.

CONTAMINANT LOCK ON SPOOL-TYPE VALVES

Spool-type valves are highly sensitive to contaminant-induced friction. Even without contaminants, spool-type valves have a tendency to lock in the spool sleeve at higher pressure. This phenomenon is termed hydraulic lock. The combination of higher pressure and dirty operating fluid makes the situation worse for these valves.

Some factors affecting the friction force on the spool valves are:

- * Valve material, geometrical irregularities, size of annular clearance, and spool diameter
- * Particle materials and sizes
- * Contaminant size distribution
- * Contaminant concentration
- * Oscillation or movement of the spool
- * Pressure acting on the spool
- * Boundary layer characteristics of the fluid used

Valve material and geometrical irregularities have a strong influence on contaminant susceptibility of the spool valves, while the remaining factors are external influences on the valve performance. Selection of valve materials and quality of the valve surface finish can significantly change the contaminant effects on valve performance.

As mentioned previously, the hydraulic lock phenomenon can occur, even though the fluid is relatively clean. This is because surface irregularities and some geometrical configurations create pressure distribution asymmetries along the valve clearance. This increases

the possibility of a large lateral force, which can cause an increase in friction. Apparent surface irregularities could be the result of contaminants in the clearance. If these contaminants are softer than the valve and the sleeve surface and are easily fractured, there may not be a large frictional force. If the contaminants are very hard, they might score the surfaces of the sleeve and spool, possibly resulting in a jammed spool. Figure 3.3, the results of Kusama and others [6], shows the effect of contaminants on the pressure distribution along an inversely tapered spool, which is effective in avoiding hydraulic lock and large lateral force.

Summarizing the above discussion, the lateral force on the spool could be minimized if the spool has good symmetry, fine surface finish, good roundness, straightness of the axes, and an inverse taper. These consequently can minimize friction force on the spool.

Another influential factor inducing a large contaminant lock force is the contaminant particle size. Figure 3.4 shows the results of the study on the contaminant lock sensitivity of directional control valves conducted at the FPRC [7]. The curves depict the relationship between contaminant lock sensitivity and contaminant size. Each valve indicated especially high sensitivity to one particular particle size. For instance, OSU Valve 104-2 is especially sensitive to 10 micrometre particles; whereas, OSU Valve 101 showed sensitivity to 25 micrometre particles.

The effect of the concentration of contaminants on the locking

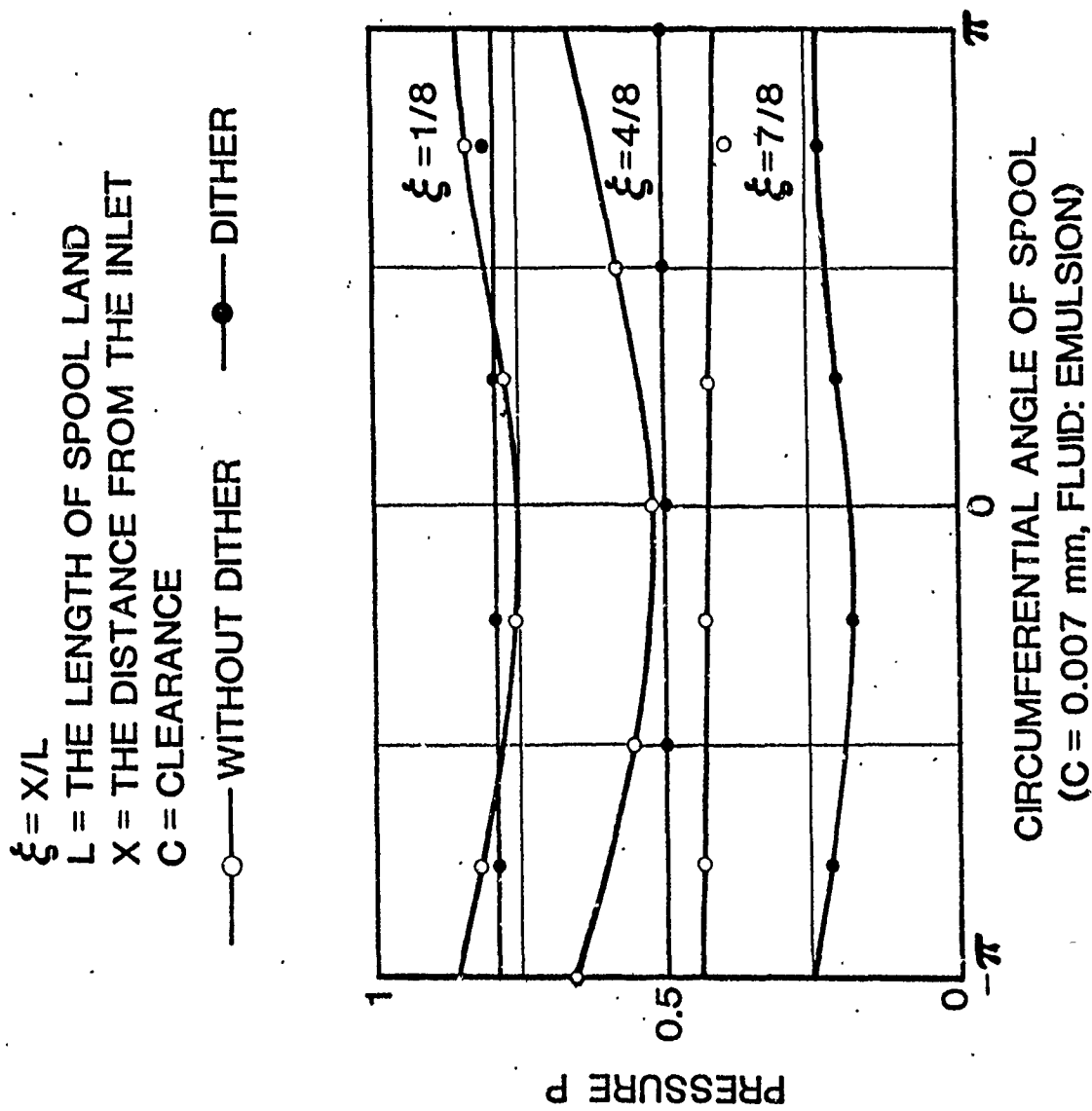


Fig. 3.3 Effect of Dither on Pressure Distributions with Inverse Taper Spool

FC-0074-5.60. -14-JN-VALVE CONTAM. LOCK SENSITIVITY VS CONTAM. SIZE

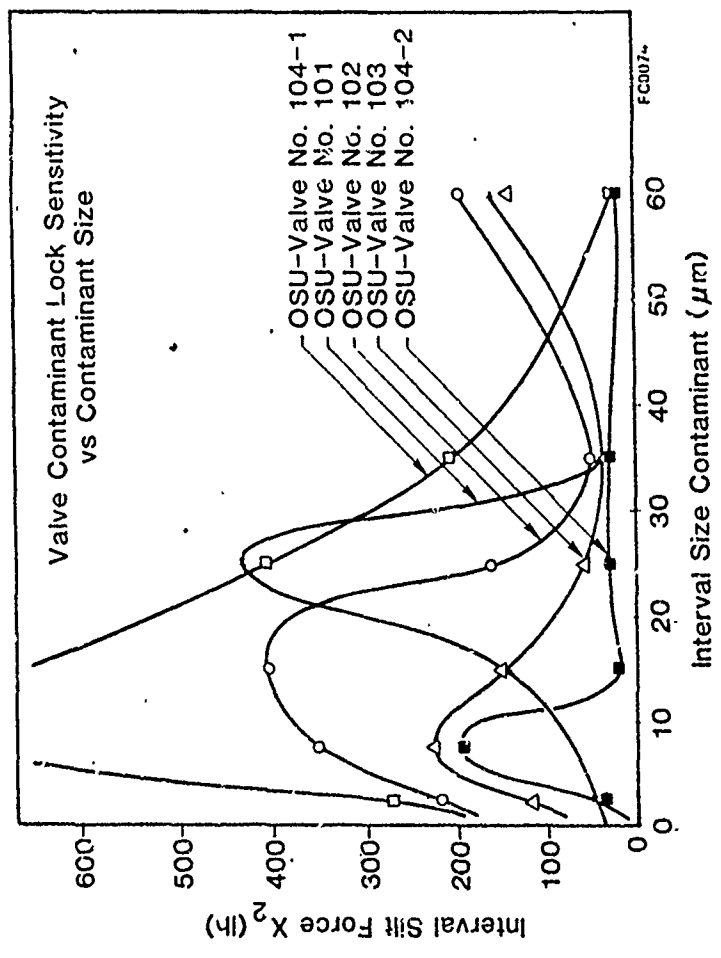


Fig. 3.4 Valve Contaminant Lock Sensitivity vs. Contaminant Size for Directional Control Valves

force is represented in Fig. 3.5 [8]. It is clearly revealed that friction force increases as contaminant concentration increases. The friction force does not diverge but approaches an asymptotic level. The study also stated that the increase of the concentration considerably accelerates the friction locking process. The higher the concentration, the shorter the time before the valve clearance clogs completely, and the frictional force reaches its maximum value.

CONTAMINANT WEAR ON SHARP ORIFICE EDGES OF THE SPOOL

A major area of concern in servovalve contaminant sensitivity has been small orifice clogging and spool sticking. The significance of contaminant wear, however, has not been fully appreciated among design engineers. This fact can be seen in the literature available concerning servovalve performance degradation due to contaminant wear. The study presented by Black [5] is one of a few references which discuss wear on spool orifices.

In view of the fact that the orifice lap condition is vital to the overall servosystem performance, the susceptibility of servovalves to fluid contamination should be obvious. It is not realistic to pursue surgically or super clean systems for servovalves. Rather, it is desirable to use servovalves in "normal" clean systems; that is, in systems where no special care is provided for servovalves, which could cause accelerated wear on the critical orifices and loss of desirable performance. This is mainly due to particles impinging on the sharp corners of orifices and removing material, resulting in a rounding off

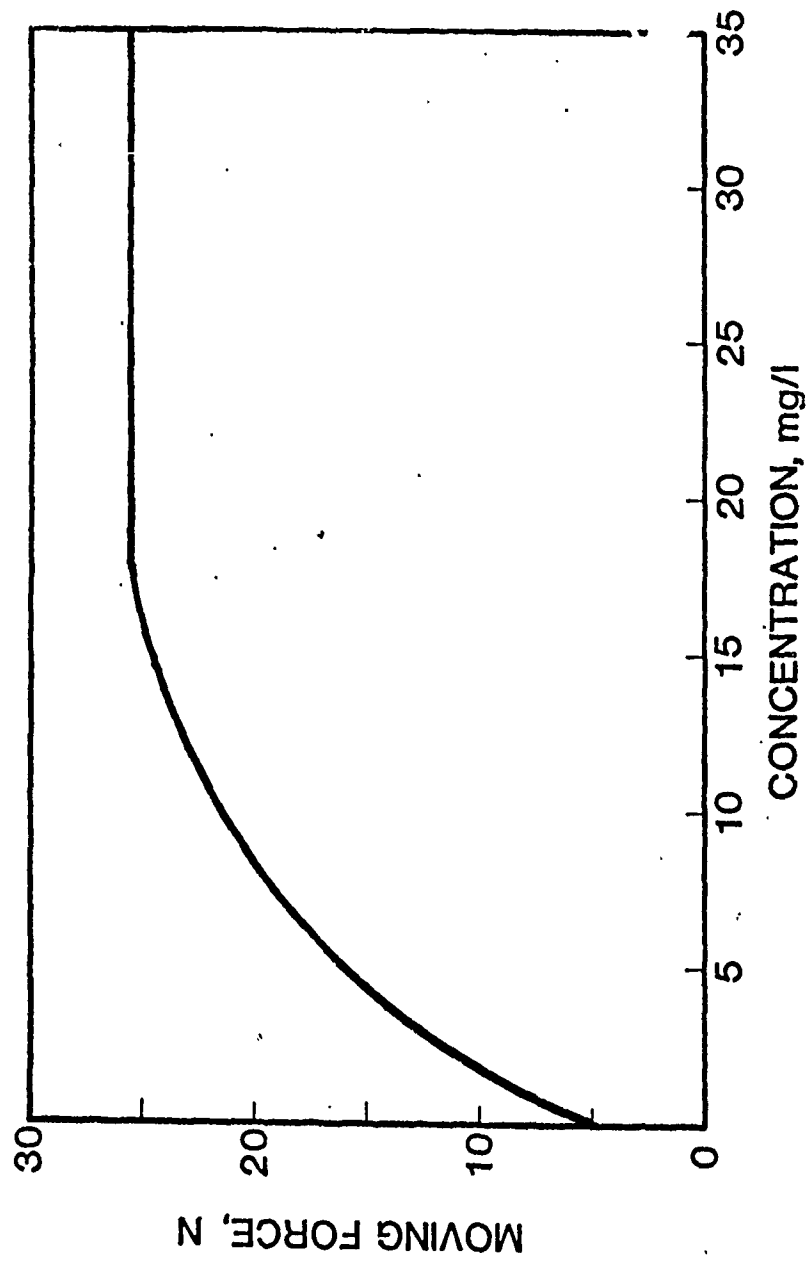


Fig. 3.5 Moving Force of the Spool vs. Contaminant Concentration

of the edges. It is intuitive that, the larger the number of particles impinging on orifices, the quicker the wear occurs. It is also instinctively perceived that larger particles cause more destructive damage to the orifices by virtue of their higher kinetic energy.

Particle impingement erosion has long been observed in many fields. Coal slurry transmission converts coal to a fluid flow for transporting. The pumps and hydraulic lines in such systems are subjected to particle impingement erosion. Gas turbine engines, gasifiers, and catalytic cracking systems have also suffered damage due to high speed particle impact on the component surfaces.

Many theoretical and experimental investigations have been carried out in these fields of applications. In fluid power systems, particle impingement erosion can be observed on poppets in relief valves and balls in check valves as well as servovalve spool orifices. In Ref. [9], it was stated that performance degradation due to particle impingement erosion poses the most serious threat to the reliable operation of relief valves. A study by Pai [10] demonstrated the effect of particle impact angle on erosion. A brief review of Pai's study is presented below in order to have insight into the erosion phenomenon on the servovalve spool orifices.

A number of experiments were conducted to obtain the relationship between contaminant concentration, particle size, and particle impact angle. A theory developed by Bitter and later modified by Neilson and

Gilchrist was used to predict particle impingement erosion on fluid power components. The theory is further revised to be more coincident with Bitter's theoretical curves. The wear formulae are, as a result, represented in Eqs. (3-1) and (3-2):

$$Q = \frac{\frac{1}{2} M V^2 \cos^2 \alpha}{\phi} + \frac{\frac{1}{2} M (V \sin \alpha - K)^2}{\epsilon} \quad (\alpha > \alpha_0) \quad (3-1)$$

$$Q = \frac{\frac{1}{2} M V^2 \cos^2 \alpha \sin n(\alpha - \alpha_{el})}{\phi} + \frac{\frac{1}{2} M (V \sin \alpha - K)^2}{\epsilon} \quad (\alpha \leq \alpha_0) \quad (3-2)$$

where M = Total mass of impinging particles

V = Particle velocity

K = Threshold velocity at which the elastic limit is just reached

ϕ = Cutting wear factor

a = Deformation wear factor

α = Angle of impact

α_0 = Angle of impact at which parallel component of velocity just becomes zero when collision ends

α_{el} = Threshold angle at which the normal component of velocity just reaches the threshold velocity, K

n = A constant on the erosion curve

The ratio of the cutting wear factor, ϕ , to the deformation wear factor, ϵ , represents the characteristics of the impinging particles and the material being impinged. The erosion characteristics are said to be brittle when ϕ/ϵ is less than one; ductile when ϕ/ϵ is greater than one. A ductile system was chosen for Pai's study where ϕ/ϵ was reported to be 0.625.

Experimental data and theoretical curves show correlation, and the theory predicted the particle impingement erosion well, as depicted in Fig. 3.6. The experiment reveals insignificant effect of particle size on the erosion, as plotted in Fig. 3.7. The result can be explained from Eq. (3.1); the erosion is not a function of particle size. This fact, however, conflicts with the experiment on servovalve spool orifice wear conducted by Moog [5]. The effect of concentration level could not be predicted, although the wear equations anticipate a proportional increase of wear as the concentration level increases. In addition, an impact angle of 50 deg caused the maximum wear.

In general, the erosion characteristics of servovalve spools and contaminant material pertain to brittle systems in which ϕ/ϵ is greater than one. This condition in terms of particles and servovalve spool materials is similar to Pai's study. In the study, the maximum erosion occurred at 40 to 50 degrees of impact angle in ductile systems. Thus, 40 to 50 degrees of impact angle could also cause severe erosion on servovalve spool control orifices. Figure 3.8 depicts erosion versus angle of impact characteristics with different ϕ/ϵ ratios plotted by Neilson and Gilchrist [11]. In the figure, erosion characteristics of servovalves could be full in the region between Figure 3.8(b) and (c). These figures show that larger impact angles cause more severe erosion.

It is well known that the jet from a small spool orifice forms along the axis whose angle from the spool axis is 69 deg. As depicted in Fig. 3.9, impinging angle of particles on both surfaces or corners of the

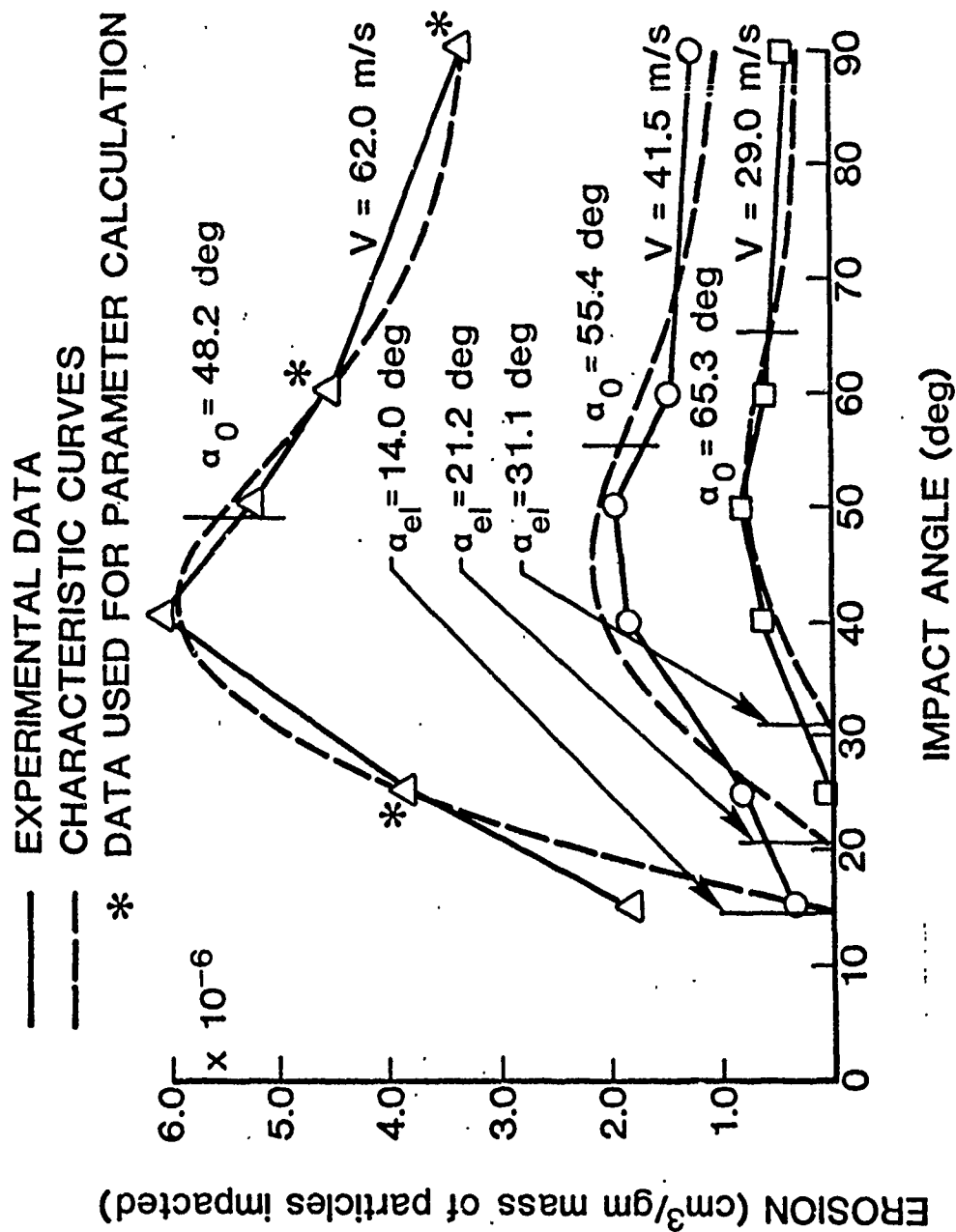


Fig. 3.6 Erosion Characteristic Curves of SAE1020 Steel at Various Impact Velocities. Particle Size Range = 40 μ m- μ p, Concentration Level = 150 mg/L

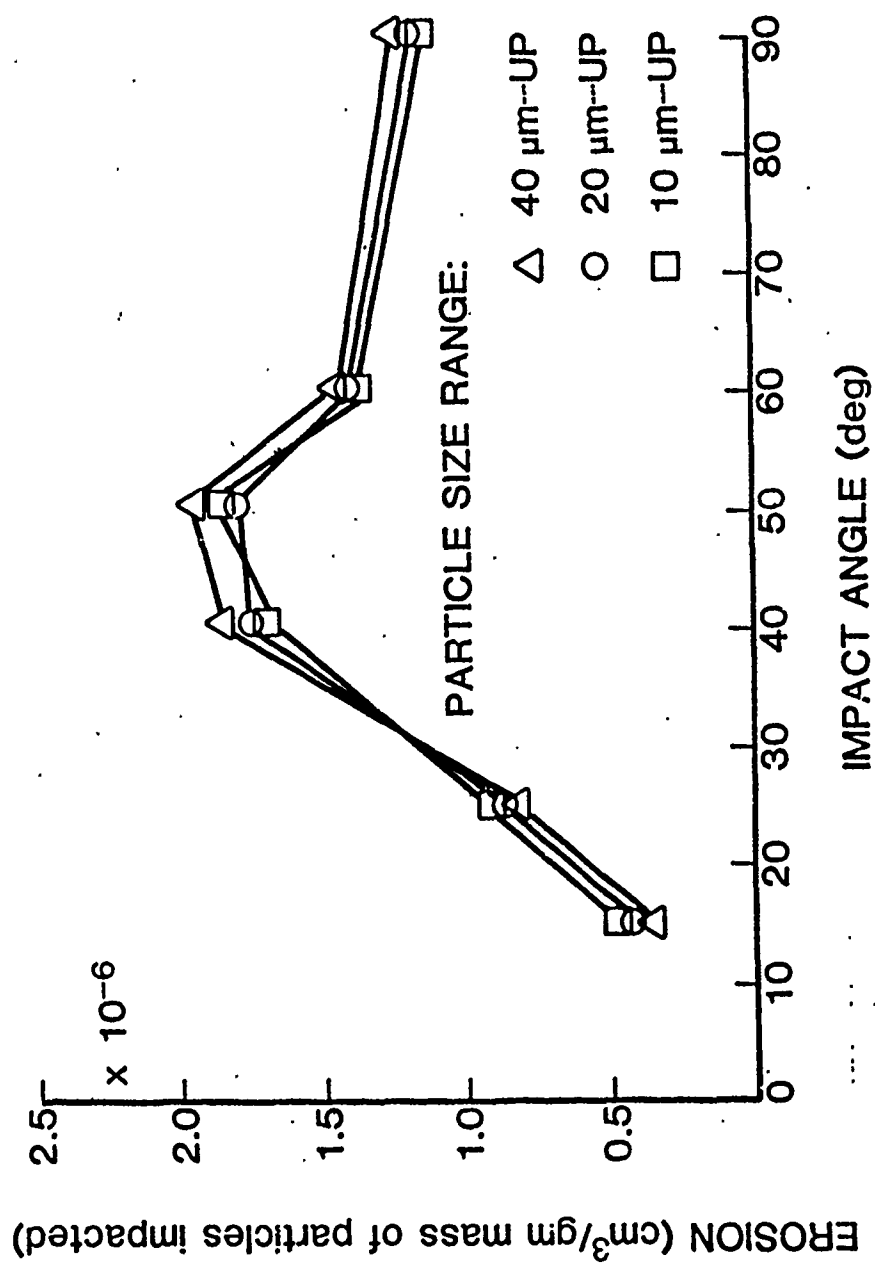


Fig. 3.7 Erosion Rate vs. Impact Angles at Various Particle Size Ranges. Concentration Level = 150 mg/L. Impact Velocity = 41.5 m/s

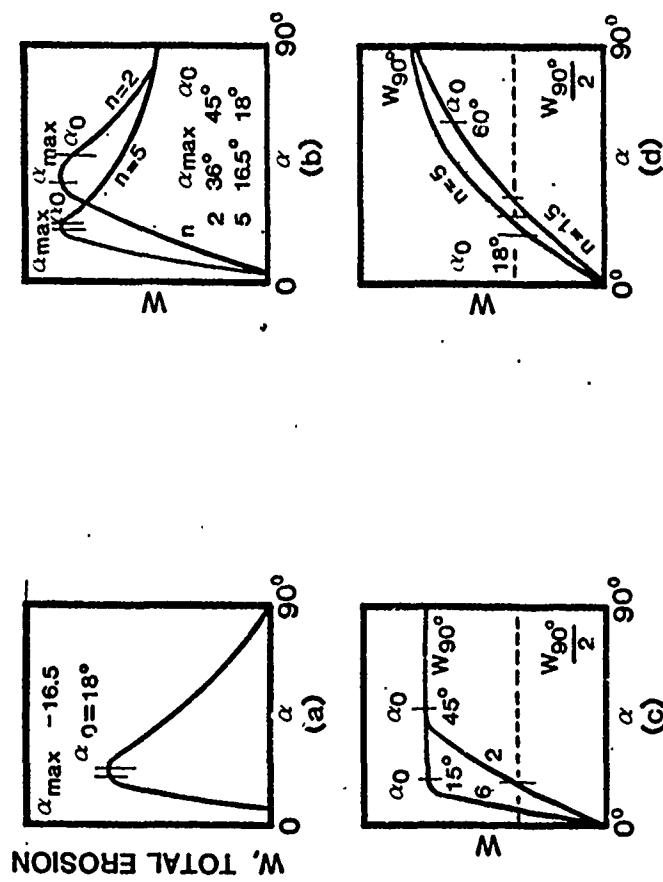


Fig. 3.8 Typical Erosion-Angle of Attack Characteristic

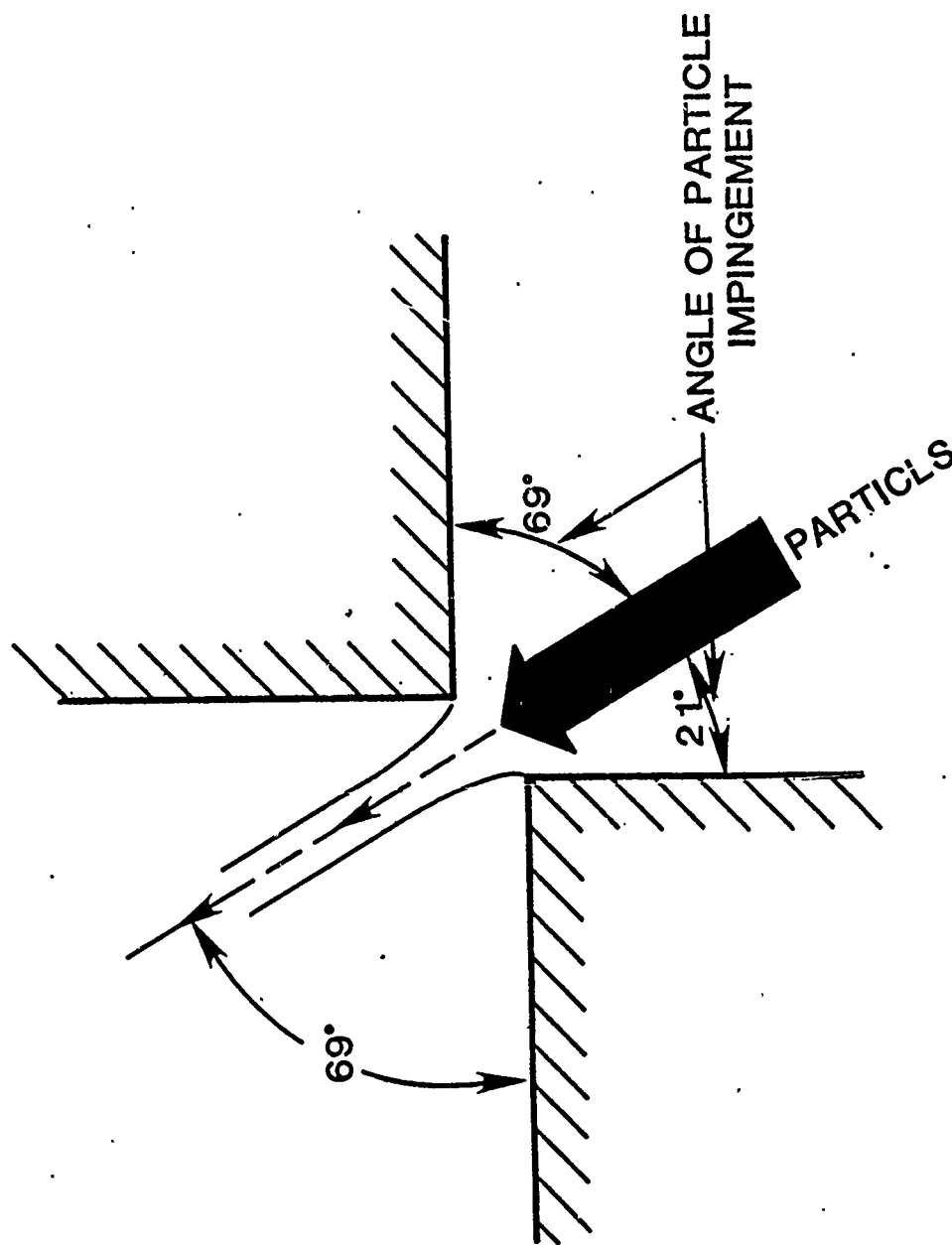


Fig. 3.9 Particle Impinging Process at the Spool Orifice

spool and the sleeve would, then, be 69 deg and 21 deg, respectively. Particles impinging to the surface at 69 deg would cause heavier erosion and round off the sharp corners more than those impinging at 21 deg.

CHAPTER IV - SERVOVALVE CONTAMINANT SENSITIVITY THEORY

The servovalve contaminant sensitivity theory must encompass both contaminant wear and contaminant lock. Contaminant lock sensitivity is evaluated from the increase of hysteresis due to contaminant-induced friction as a function of contaminant concentration and particle size intervals. It is an indication of how the servovalves tolerate the maximum contamination level within the specified performance.

Contaminant wear sensitivity, on the other hand, is evaluated from the variation in pressure gain, which shows direct performance deviation from the initial specifications as a function of particle size. It is an indication of servovalve life demonstrating how many hours the servovalves can operate acceptably within the specified performance.

CONTAMINANT LOCK SENSITIVITY

The evaluation of contaminant lock sensitivity is established based on the semi-empirical theory for spool type directional control valves developed by the FPRC [7].

The contaminant lock theory for spool valves is supported by the constant pressure filtration, as is the contaminant lock mechanism of spool valves. The primary assumptions made to support this theory are as follows:

- * The capture mechanism of direct interception of particles from the fluid stream lines is adjacent to the pore walls.
- * The particle retention on the walls of the pores is achieved in such a way that the volume passage decreases in direct proportion

to the volume of filtrate which passes through the flow path.

- * Leakage flow follows Poiseuille's Law.

- * The silting force which resists spool movement is proportional to the volume of contaminant retained in the clearance between the valve spool and the housing.

The result of the above assumptions led to the final form of the equation showing the relationships among the silting force, F , stationary time, t , valve geometry, fluid viscosity, μ , pressure differential, ΔP , across the leakage path, and contaminant concentration, V_p , as shown in Eq. (4-1).

$$F = k_1 \left(1 - \frac{1}{\sqrt{k_2 \frac{V_p \Delta P}{\mu} t + 1}} \right) \quad (4-1)$$

Values k_1 and k_2 are geometric parameters of the valve spool and are attained empirically from test data. These values are distinctive from valve to valve and between various particle size ranges. The semi-empirical model has been verified by the development of a contaminant monitor [2] as well as a directional control valves study [7].

Application of the theory to servovalves is made with little modification. Measuring silting force on the servovalve spools is impractical. Besides, the silting force does not indicate direct contaminant susceptibility of servovalves because of the capability of the first-stage hydraulic amplifiers to drive second-stage spools.

If the servovalves have sufficient driving capability to overcome larger silting forces, the valve might demonstrate no degradation on output performance parameters. A better parameter is the hysteresis increase due to friction, which is in turn due to silting force. Thus, Eq. (4-1) can be used to determine the change of silting force with an increase of hysteresis. For the servovalve contaminant sensitivity, contaminant concentration is selected as an independent variable. This makes the test process shorter and minimizes the destruction of larger particles.

Equation (4-1) is rewritten for the form of the servovalve contaminant lock sensitivity as:

$$b_i = x_i \left(1 - \frac{1}{\sqrt{y_i V_p + 1}} \right) \quad (4-2)$$

Parameters x_i and y_i depend only on the contaminant size (5-10 μm , 10-20 μm , 20-30 μm) when all other conditions remain constant. These parameters, called contaminant lock coefficients, are determined by finding the best fit curve to a set of data (V_p, b_i) obtained from testing. Unfortunately, it is not practical to use double-cut AC Fine Test Dust (5-10, 10-20, etc.). Therefore, lower cut ACFTD (0-5 μm , 0-10 μm , 0-20 μm , 0-30 μm) is substituted, and the result is converted to the equations for interval contaminant size. The conversion is performed from the particle size distribution relations in each dust fraction. The size distribution of the lower cut dust is tabulated

in Table 4.1. This table is used in Eq. (4-3) to calculate the effect of each particle size interval. It is assumed that there are no particles larger than 5 μm in 0-5 μm lower cut dust; no particle larger than 10 μm in 0-10 μm ; etc. The contribution of each particle size interval to the lock coefficient for lower cut dust is calculated from Eq. (4-3). Weighting factors in Eq. (4-3) are obtained from particle distribution of the lower cut dust, as shown in Table 4.1.

$$\begin{aligned} X_{0-10} &= 0.942 X_{0-5} + 0.258 X_{5-10} \\ Y_{0-10} &= 0.942 Y_{0-5} + 0.258 Y_{5-10} \\ X_{0-20} &= 0.687 X_{0-5} + 0.239 X_{5-10} + 0.074 X_{10-20} \\ Y_{0-20} &= 0.687 Y_{0-5} + 0.239 Y_{5-10} + 0.074 Y_{10-20} \end{aligned} \quad (4-3)$$

To determine the Omega rating value, contaminant lock coefficients X_β for the Beta 10 filter model are calculated. The relationship between the lock coefficients for Beta 10 model and particle size interval calculated above is derived based on the curve of Beta 10 = 2. Contribution of each particle size interval to the lock coefficients is evaluated from this curve, assuming that the total number of particles is counted from particles greater than 1 μm . As a result, the contaminant lock coefficients for the Beta 10 model are calculated from Eq. (4-4).

$$\begin{aligned} X_\beta &= 0.964 X_{0-5} + 0.035 X_{5-10} + 0.001 X_{10-20} \\ Y_\beta &= 0.964 Y_{0-5} + 0.035 Y_{5-10} + 0.001 X_{10-20} \end{aligned} \quad (4-4)$$

THE LOWER CUT DUST

INTERVAL μm	0-10	0-20	0-30	0-40	0-50	0-60	0-70
0/5	74.2%	68.7%	67.9%	67.8%	67.7%	67.7%	67.7%
5/10	25.8	23.9	23.6	23.6	23.5	23.5	23.5
10/20		7.4	7.4	7.4	7.4	7.4	7.4
20/30			1.1	1.0	1.0	1.0	1.0
30/40				0.2	0.3	0.26	0.26
40/50					0.1	0.11	0.10
50/60						0.03	0.03
60/70							0.01

FPRC-OSU-80-86

Table 4.1 Particle Distribution of the Lower Cut Dust

Substituting the values of X_β and Y_β from Eq. (4-4) in place of X_i and Y_i into Eq. (4-2), the relationship between hysteresis increase and gravimetric level is obtained for the Beta 10 filter model. From this relationship, the Omega rating value is defined as the Beta 10 filter needed to ensure a performance degradation of no more than 2 percent of hysteresis increase after one minute of stationary time in the standard system. The standard system is defined as a hydraulic system having a flow rate of 20 gpm and an ingression rate of 10^8 particles per minute greater than $10 \mu\text{m}$.

The Omega rating value is based on this standard system and a Beta 10 = 2 filter.

CONTAMINANT WEAR

Wear on the spool orifices changes the performance of a servovalve. Worn orifices cause higher loop gain, which brings about an oscillatory system response and reduced stiffness, which increases the error due to external disturbances.

Servovalve wear is dependent on the valve material and design. Assuming that the contaminant in the hydraulic system has the same characteristics as AC Fine Test Dust and that its properties do not change, the major factors which affect performance degradation are contaminant concentration level and contaminant particle size. The term "contaminant concentration level" includes a time factor. For example, consider an electrohydraulic servovalve regulating flow to an actuator in a hydraulic system whose contaminant level is 10 mg/L.

After 100 hours of operation, the servovalve is removed to check the performance degradation and the pressure gain is found to have decreased to 80 percent of the original. Another identical servovalve in operation in another system with the same conditions, except with contaminant concentration level of 20 mg/L, may experience a decrease in pressure gain to 80 percent of the original in only 50 hours.

The performance degradation is then expressed as a function of contaminant particle size and contaminant concentration, which is a function of time. Defining the contaminant sensitivity, S_i , of the component at each contaminant size interval, i , the relationship between the performance degradation and the contaminant is shown by Eq. (4-5). This parametric representation simplifies the concept of contaminant sensitivity.

$$P_1 - P_2 = - S_i \bar{N}_i \quad (4-5)$$

where $P_1 - P_2$ is performance degradation

\bar{N}_i is total amount of contaminant to which the component is exposed.

The total amount of contaminant, \bar{N}_i , is expressed in terms of flow rate $Q(t)$, and contaminant concentration, $N_i(t)$, as:

$$\bar{N}_i = Q(t) n_i(t) (t_1 - t_2) \quad (4-6)$$

Substituting Eq. (4-6) into Eq. (4-5) gives:

$$P_1 - P_2 = - S_i Q(t) n_i(t) (t_1 - t_2) \quad (4-7)$$

Representing this discrete equation in continuous form, Eq. (4-7) becomes:

$$\frac{dP}{dt} = - S_i Q(t) n_i(t) \quad (4-8)$$

In the laboratory, the particles destroyed in the test system are not replenished; whereas, in the field, contaminant ingress and filtration create a more or less steady contaminant level. Expressing it in the term, n_i , in the above equations, n_i is constant in the field. In the laboratory, particle numbers could vary, depending on the components in the test system, especially a pump and its operating time. The number of larger particles decreases due to destruction, mainly in a pump, and smaller increase in number until destruction of all of the larger particles takes place.

This process continues until all of the contaminants become small enough to be unharmed to a test component. The destruction process could be expressed in mathematical model as in Eq. (4-9a):

$$n_i(t) = n_0 e^{-t/\tau} \quad (4-9a)$$

Where n_0 is the initial number of particles per liter and t the time constant in the particle destruction process.

The particle destruction process changes due to the pump used in the test system. Component contaminant sensitivity would alter as a result. An analysis on the particle destruction process is introduced below from the work at the FPRC [9].

Figure 4.1 is a result obtained from the particle destruction analysis under the test condition that contaminant size 0-80 μm of classified AC Fine Test Dust was injected into the test system to set the contaminant concentration level to 100 mg/L. Population changes on each particle interval show replenishing of smaller particles due to destruction of larger particles.

Figure 4.2 illustrates the time constant, t , in different particle size intervals. The dotted line in the graph is obtained from a least squares fit exponential to describe the particle population change as a function of particle size intervals. Smaller particle size ranges replenished by the destruction process of larger particles exhibit longer time constants; whereas, larger particle size ranges show shorter time constants because these particles are destroyed but not replenished. The time constant obtained for larger particles could be used directly for data interpretation because no replenishment of particles clearly represents laboratory test conditions. Extrapolating the time constant values of greater than 30 μm to smaller size to 10 μm was performed, as shown in Fig. 4.2.

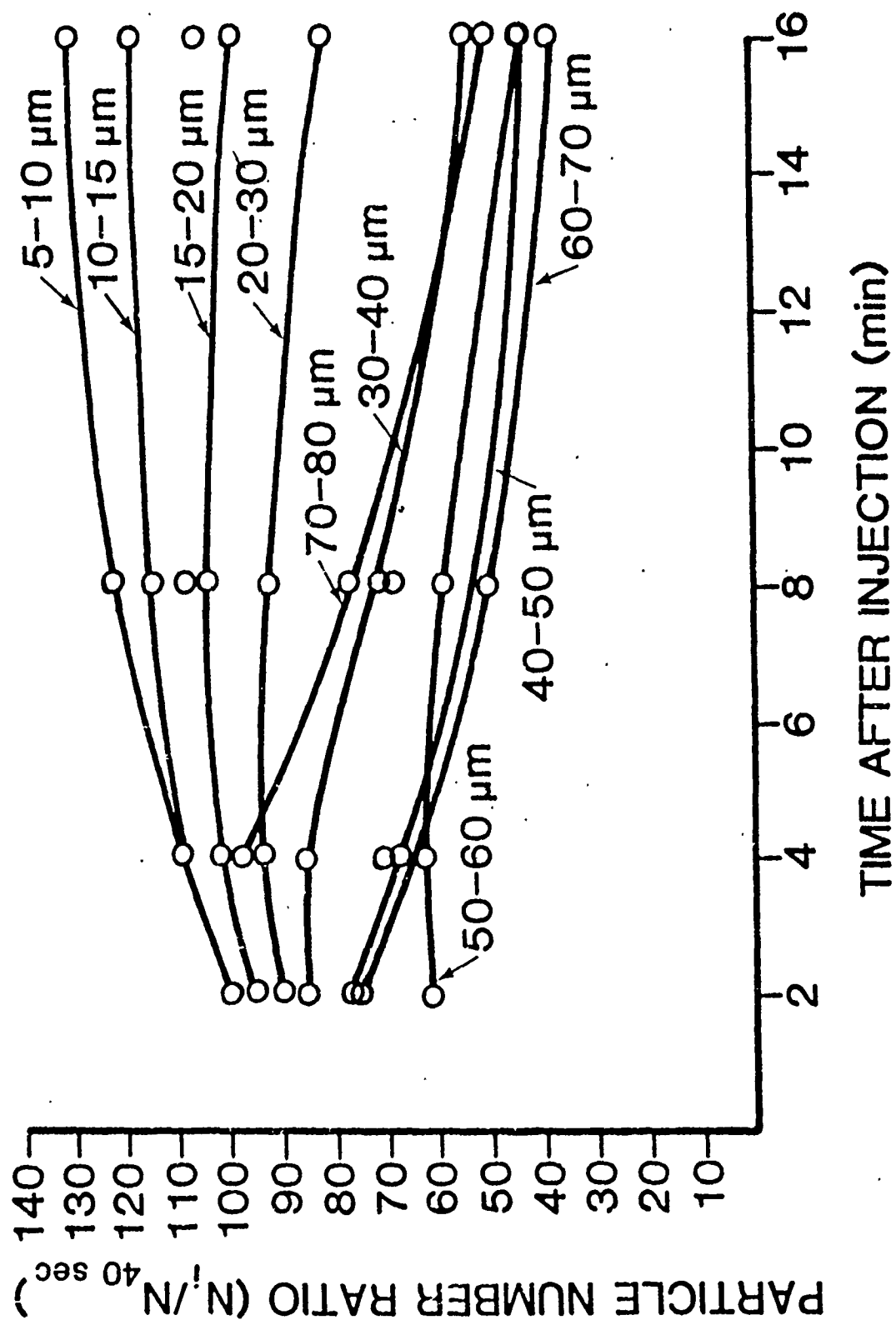


Fig. 4.1 Illustration of Particles Destruction Characteristic

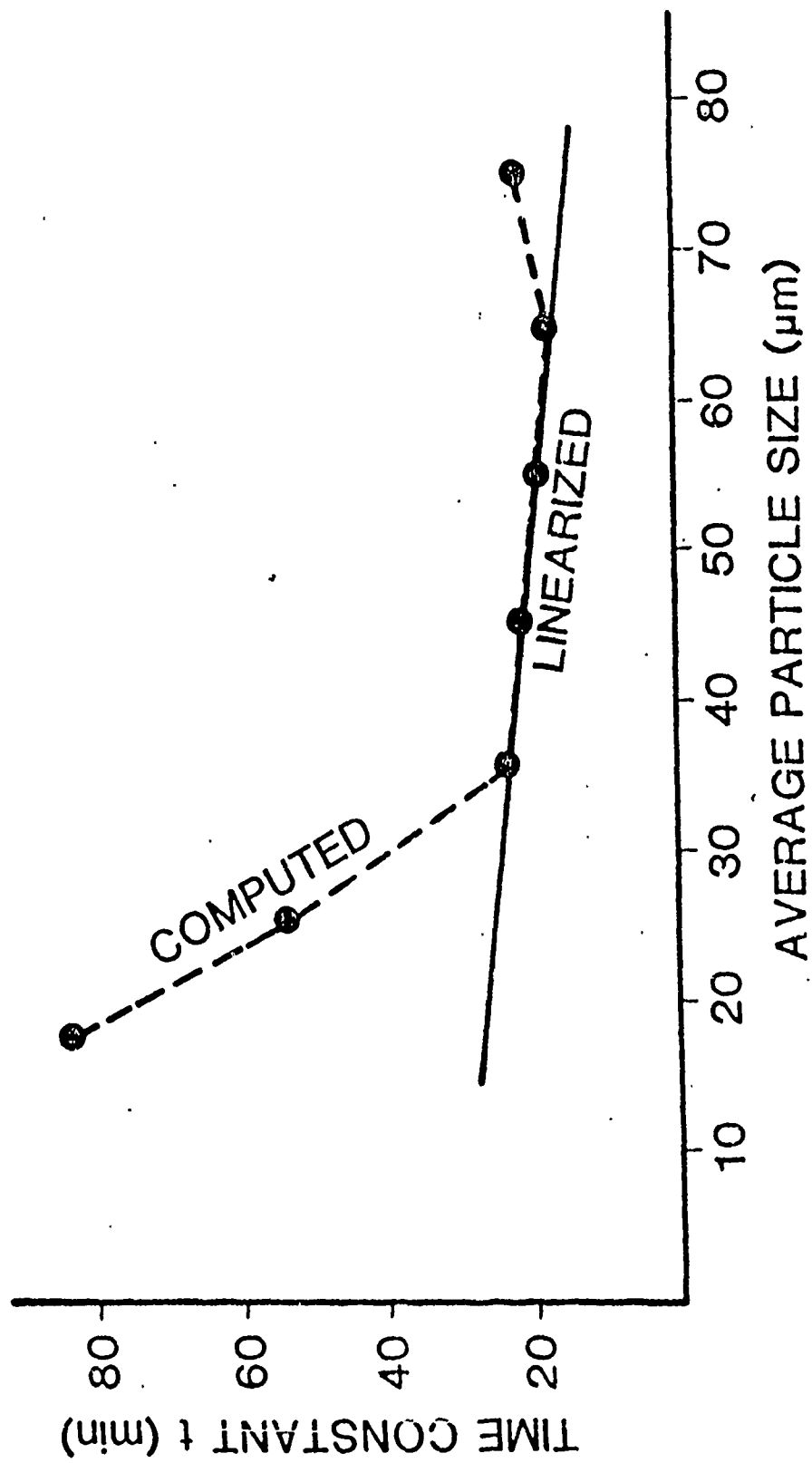


Fig. 4.2 Linearized Particle Destruction Time Constant Relationship for OSU Test Pump No. 102

The destruction process for smaller particles, especially 0-10 μm particles, has proved to have a negligible effect on particle number. This fact leads to the assumption that the particle population of these smaller sizes is constant and expressed as in Eq. (4-9b):

$$n_i(t) = n_{0i} \quad (4-9b)$$

It has been verified that the contaminant sensitivity of a component is a proportional function of the concentration. This relation is expressed in Eq. (4-10) defining the contaminant wear coefficient, α .

$$S_i(n) = \alpha_i n_i(t) \quad (4-10)$$

The performance degradation equation now becomes:

$$\frac{dP}{dt} = -\alpha_i n_{0i}^2 Q(t) e^{-2t/\tau} \quad (4-11)$$

For servovalves, performance degradation is analogous to pressure gain variation; therefore, Eq. (4-11) is transformed into Eq. (4-12):

$$\frac{dK_p}{dt} = -\alpha_i n_{0i}^2 Q_L e^{-2t/\tau} \quad (4-12)$$

In this equation, controlled load flow, Q_L , is kept constant. Integration yields an expression for pressure gain at any time t after the concentration n_0 has been initially established.

$$k_p = k_{p0} - \frac{1}{2} \tau \alpha n_0^2 Q_L (1 - e^{-2t/\tau}) \quad (4-13a)$$

Where k_{p0} is the initial pressure gain prior to contaminant injection. In the assumption made in the previous paragraphs, Eq. (4-13a) can be expressed as in Eq. (4-13b).

$$k_p = k_{p0} - \alpha_i n_{oi}^2 Q_L t \quad (4-13b)$$

This equation is only valid for particle sizes up to 10 μm . From Eq. (4-13a & b) the contaminant wear coefficient can be expressed as:

$$(\tau \alpha)_i = \frac{(k_{p0} - k_{pf})_i}{\frac{1}{2} n_{oi}^2 Q_L (1 - e^{-2t/\tau})} \quad (4-14a)$$

$$(\alpha)_i = \frac{(k_{p0} - k_{pf})}{n_{oi}^2 Q_L t} \quad (\text{for } D \leq 10 \mu m) \quad (4-14b)$$

Where the subscript i identifies the particle size interval injected.

Using Eqs. (4-14a) or (b), the relationship between gravimetric level and pressure gain can be obtained reforming Eq. (4-14a) in terms of gravimetric levels for X and Y .

From the above equations and the fact that Q_2 , t , and a do not change their values due to different gravimetric levels:

$$\frac{G_x^2}{G_1^2} = \frac{(k_{p1} - k_{pf})_x}{(k_{p0} - k_{pf})_y} \quad (4-15)$$

Equation (4-15) shows direct relationship between gravimetric level and pressure gain degradation.

Since lower cut test dust is used for testing, pressure gain degradation must be converted, as in the contaminant lock sensitivity theory. For the size range of 0-10 μm test dust, the total pressure degradation due to the lower cut dust 0-10 μm could be contributed to each size interval, as shown in the equation below.

$$\Delta k_{p0-10} = \Delta k_{p \frac{0-5}{0-10}} + \Delta k_{p \frac{5-10}{0-10}} \quad (4-16)$$

where $\Delta k_{p \frac{0-5}{0-10}}$ is the degradation due to the percentage of 0-5 μm test dust in the range of 0-10 μm .

$\Delta k_{p \frac{5-10}{0-10}}$ is the degradation due to the amount of 5-10 μm test dust in the range of 0-10 μm .

PART I

SERVOVALVES

CHAPTER I - INTRODUCTION

Electrohydraulic servovalves were originally developed for the aerospace industry because their compactness and high response capabilities offered distinct advantages. As the technology of electrohydraulic servomechanisms evolved, the use of servovalves has broadened to include machine tools, mobile equipment, and many other applications where a load must be positioned accurately.

As the application of servovalves spread, one serious problem became evident -- contaminant sensitivity. Since servomechanisms are manufactured with very precise and close tolerances to satisfy high performance requirements, they are more sensitive to contaminant than most other hydraulic components. Servovalves installed in missiles and aircraft are usually protected by intensive filtration; however, servovalves used in mobile equipment are generally exposed to severe contaminant environments. The contaminant level found in a mobile hydraulic system is usually much higher than that in missile and aircraft systems. Also, servovalves used in mobile hydraulic systems are expected to have longer operating lives. Protection from contaminant is essential if the desired operating life is to be achieved.

To determine the protection required for a servovalve, the contaminant sensitivity of the valve must be evaluated; however, test procedures which evaluate the contaminant sensitivity are not yet available.

The objectives of the project which are the subject of this report include:

1. Develop test procedures to evaluate the contaminant sensitivity of servovalves.
2. Conduct the contaminant sensitivity tests on servovalves.
3. Develop interpretation techniques for the test results to determine the contamination protection requirements.

The plan of attack used to accomplish the objectives of this study was:

1. Construction of the test system.
2. Development of test procedures necessary to evaluate the contaminant sensitivity of servovalves.
3. Evaluation of the contaminant effects on servovalve hysteresis and threshold. (Different sizes of classified AC Fine Test Dust were used to establish the relationship between contaminant size and sensitivity. Clogging of the filter will be avoided during testing.)
4. Increase of hysteresis was measured as a function of contaminant level and size, while time of exposure to contaminant was kept constant.
5. Evaluation of the change of pressure gain due to contaminant wear.
6. Interpretation of test results. (Interpretation techniques for the test results were developed to select the servovalve best

suited for the particular application and to determine the filter protection requirements.)

CHAPTER II - REVIEW OF PREVIOUS STUDIES

Contamination effect on electrohydraulic servovalves has been discussed recurrently by virtue of the potential of the servovalves for automation and their capability to interface with microelectronics. The results acquired from many investigations on contaminant sensitivity of the servovalves have given users the negative impression that they are very sensitive to contaminants. This position has been engrained by such statements as that by Williams [1] that "The operating environment of servovalves must approach surgical cleanliness standards." Williams, however, claimed that present day servovalves are reliable based on field experiences and the studies done on new servovalve design. A survey conducted by Nair [2] among leading manufacturers and users of the electrohydraulic servovalves, on the contrary, shows that the contaminant related problems of servovalves still need to be studied scientifically and that the effective use of servovalves must be promoted.

As shown in Williams' paper and Nair's survey, there seem to be some misunderstandings among users and manufacturers. Neither have any evaluation technique to accurately evaluate servovalve performance in contaminated systems.

This study is intended to fill or at least alleviate this gap between the users and the manufacturers by developing an evaluation technique for servovalve contaminant sensitivity as well as providing

a filter selection technique for particular servovalves. A summary of some previous servovalve studies is presented below.

WADC STUDY [3]

A technical report published by WADC (Wright Air Development Center) discusses an attempt to ascertain the susceptibility of the servovalves to a high degree of contamination in hydraulic fluids. The report includes a survey of servovalve vendors and users. The survey from the vendors shows that design improvements have decreased contaminant related problems. Main emphasis from the vendors was aimed at built-in filter design, torque motor design, and more powerful first stage amplifier.

From the user standpoint, servovalves operating under relatively low temperature, below 160 F, had the least contamination problems. Servovalves operated in high temperature were felt to be likely to meet contamination problems. A missile manufacturer stated that all oil was passed through a set of filters which consisted of a 10 μ m filter in series with a 2 μ m filter to eliminate contaminants. The servovalve users which had little difficulty from oil contamination paid a great deal of attention to their systems by maintaining the assembly and test area clean, providing high-quality filters, and by emphasis on good maintenance practices.

One of the objectives of the WADC study was to formulate experimental procedures. The experiment evaluated position feedback of the actuator to the servo amplifier. When contaminant of a particular size

range was added to the system, a temporary command signal was applied to the servovalve, and the position response was recorded. The contaminant addition and the valve operation were continued until the valve ceased to operate satisfactorily. The total contaminant added and total operating time before failure were recorded as well as spool end pressure and actuator end pressure for the failure analysis.

The deleterious effects of the servosystem were observed by the position output of the actuator. The failure symptoms which they defined were sluggishness, hard-over, and oscillation. The causes of failure were perceived based on the progressive dismantling and cleaning procedure. The procedure is shown in the flow chart in Fig. 2.1. The report in the procedure section mentioned that the filters, orifices, or nozzles were removed and cleaned one at a time when a "hard-over" condition happened.

From the test results tabulated in the report, 20 failures were due to filter clogging, ten due to orifice, three due to nozzle, three due to second stage failure. It was stated that the servovalves were less susceptible when the first stage quiescent flows were less. In conjunction with this statement, it is concluded that the tests were more of a filter test than a valve design test, because the valve malfunction in most cases resulted from filter clogging.

LOCKHEED STUDY [4]

A contamination study performed by Vought Electronics under contract from Lockheed Aircraft Corporation concluded that the major

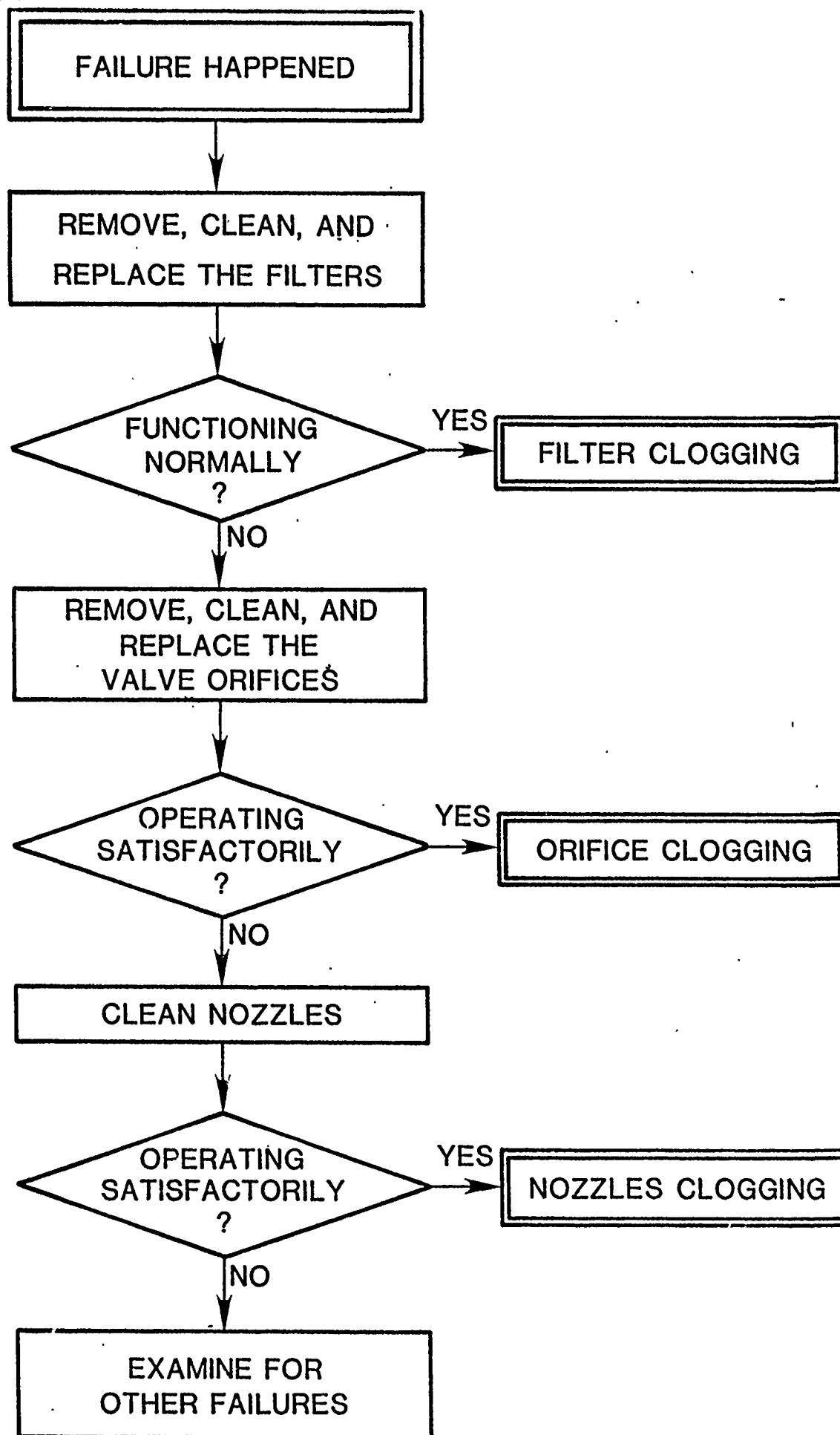


Fig. 2.1 Flow Chart of Failure Diagnosis

cause of the failure of the electrohydraulic servovalves tested was erosion of targets, nozzles, flappers, spool valves, etc. The report stated that there were no failures related to clogging of orifices or filters except one valve which failed because of a collapsed built-in filter. The failure in terms of erosion was designated when the valve went hard-over or failed to respond to the maximum input current.

The test procedure they developed is summarized in flow chart form in Fig. 2.2. The contaminant used in their study was a mixture of 90 percent standard AC Fine Test Dust (ACFTD) and 10 percent carbonyl iron powder.

Failure analysis was performed by disassembly. Since some of the servovalves tested used a wet torque motor, iron filings were found in the air gap around the motor poles. The servovalves consisting of dry torque motor were found to have no deposit around the torque motors. The fixed orifices, nozzles, flappers, etc., were carefully examined for erosion or damage. The nozzle-flappers of some servovalves were eroded so that pilot pressure gain was decreased. This caused less driving capability of the second stage spool valve. The report showed one failure due to the collapse of built-in filters over the supply orifices. Scoring on the spool valve surfaces occurred in all valves.

From the test results, one of the servovalves tested failed to operate with only a 6 mg/L total contaminant concentration while another one survived 528 mg/L. Using the data obtained from the report, threshold performance degradation was redrawn as a function of contaminant concentration in Fig. 2.3

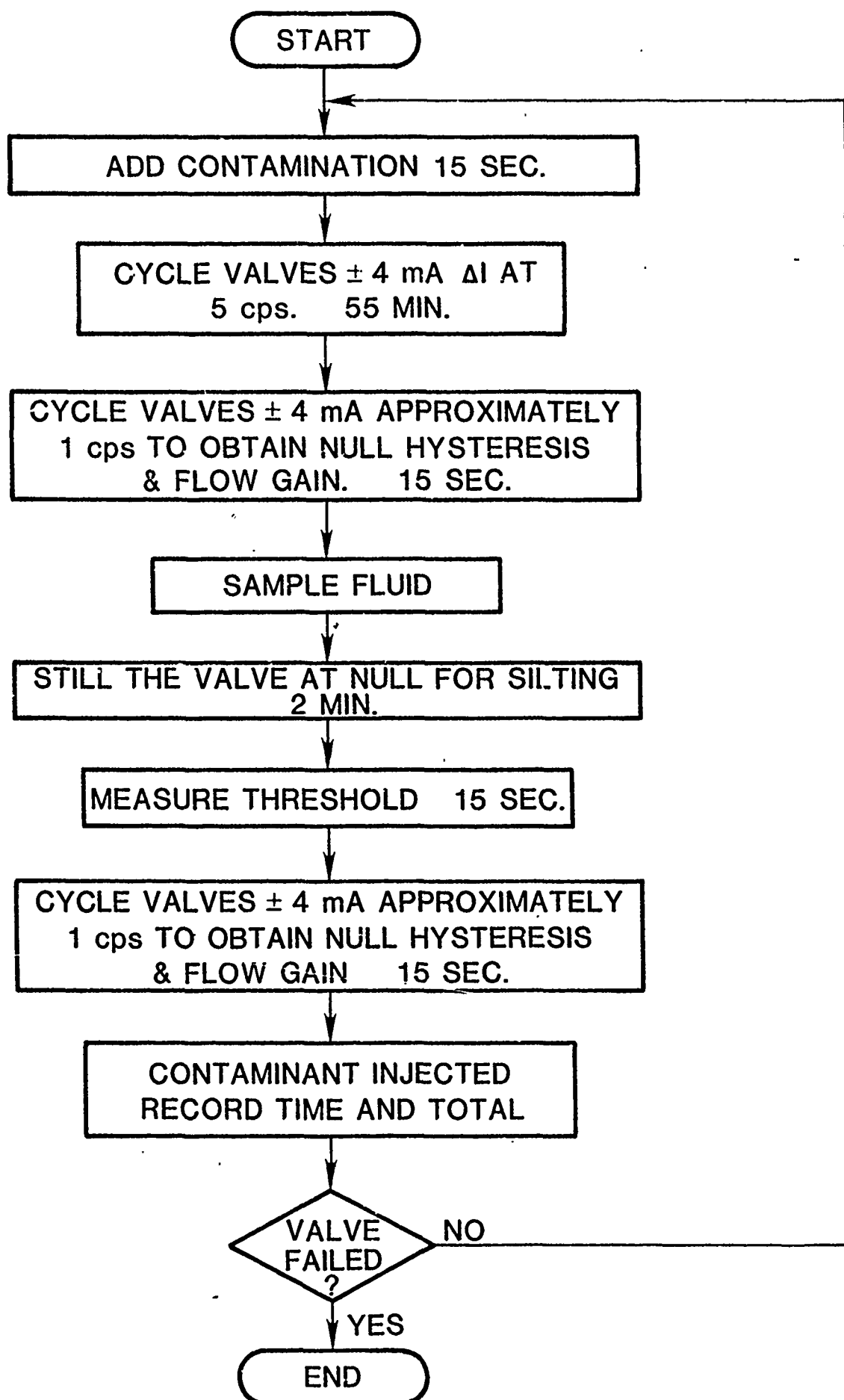


Fig. 2.2 Lockheed's Electromechanical Valve Test Procedure

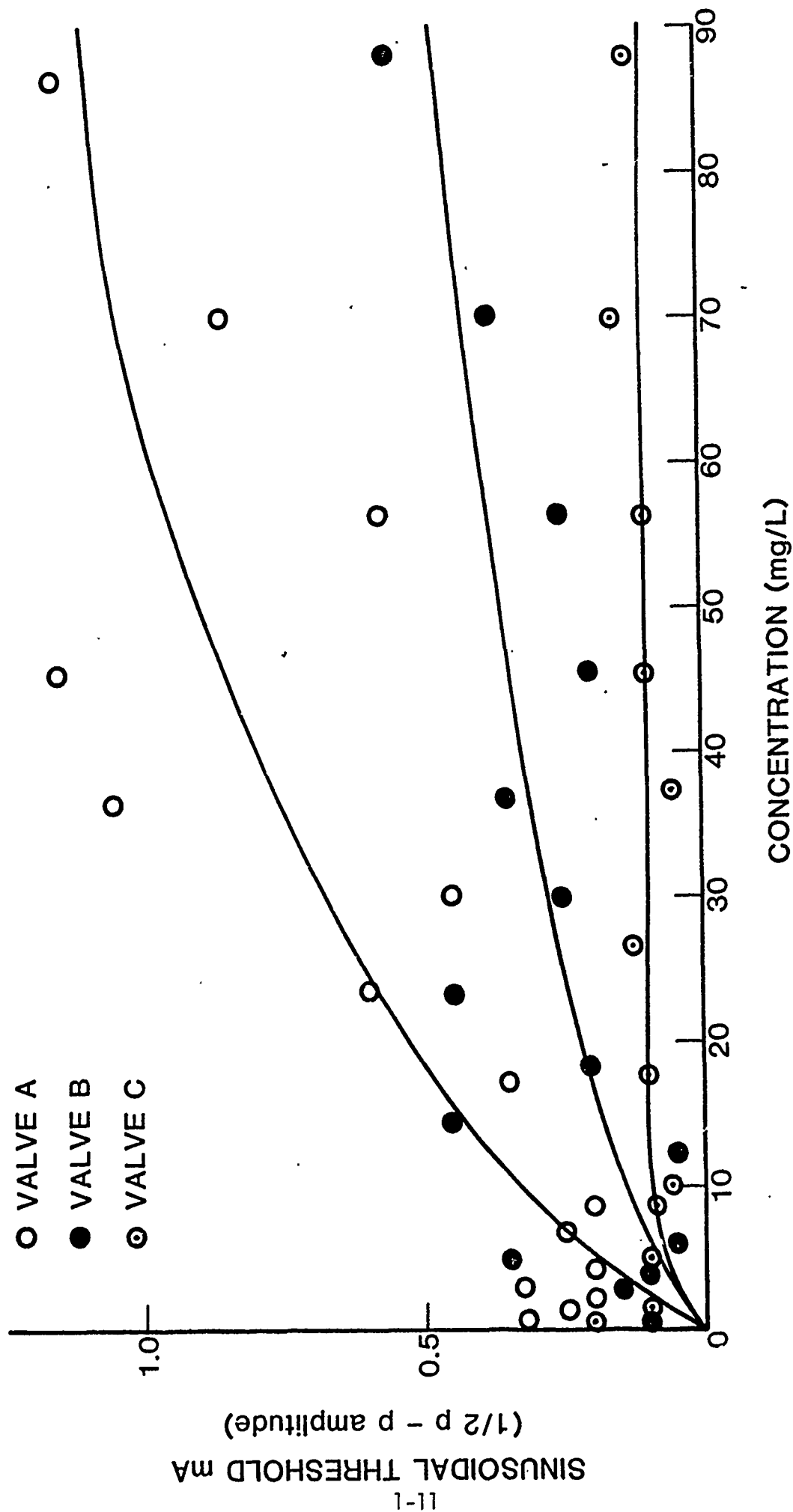


Fig. 2.3 Lockheed's Servovalve Contaminant Sensitivity Test Results






MOOG STUDY [5]

Moog attacked the problem more scientifically. The contaminant sensitivity was classified into two categories: temporary performance degradation and permanent performance degradation. The temporary performance degradation was detected by measuring threshold increase during contaminant injection. The permanent performance degradation was measured from leakage flow.

The effect of the particle size on performance was studied. It was found that the servovalve threshold would increase as a function of fine particles, 1-5 μm . Because larger particles cause clogging of orifices or built-in filters, the use of 0-10 μm classified ACFTD was recommended to evaluate the threshold sensitivity of the servovalves. This procedure simplified the test procedure. The other point to be noted from this report is the failure criteria of testing. It was suggested that threshold sensitivity degradation beyond 10 percent of rated signal was of no value, since such a large threshold would not be acceptable to most users. Using 0-10 μm test dust, the threshold was measured according to the schedule summarized in Table 2.1. The threshold increase was redrawn from the Moog results, as shown in Fig. 2.4. The threshold was measured at concentrations of 2, 4, 8, and 16 mg/L.

The permanent performance degradation measured from leakage flow was evaluated as the degree of wear on sharp orifices on the second stage spool. As in the previous test, 0-10 μm ACFTD was used. It was concluded that the measurement of the sensitivity for different particle

Table 2.1. Test Schedule of Threshold Sensitivity Test.

Time (min)	0	2	5	7	10	12	15	17	20	
0-10 m Concentration (mg/L)		2		4		8		16		Cleaning up the system.
Addition of Contaminants (mg/L)	2		2		4		8			
Hysteresis Measurements										
Test Condition: 0.5 Hz sinewave ±10% of rated current System Pressure 300psi										

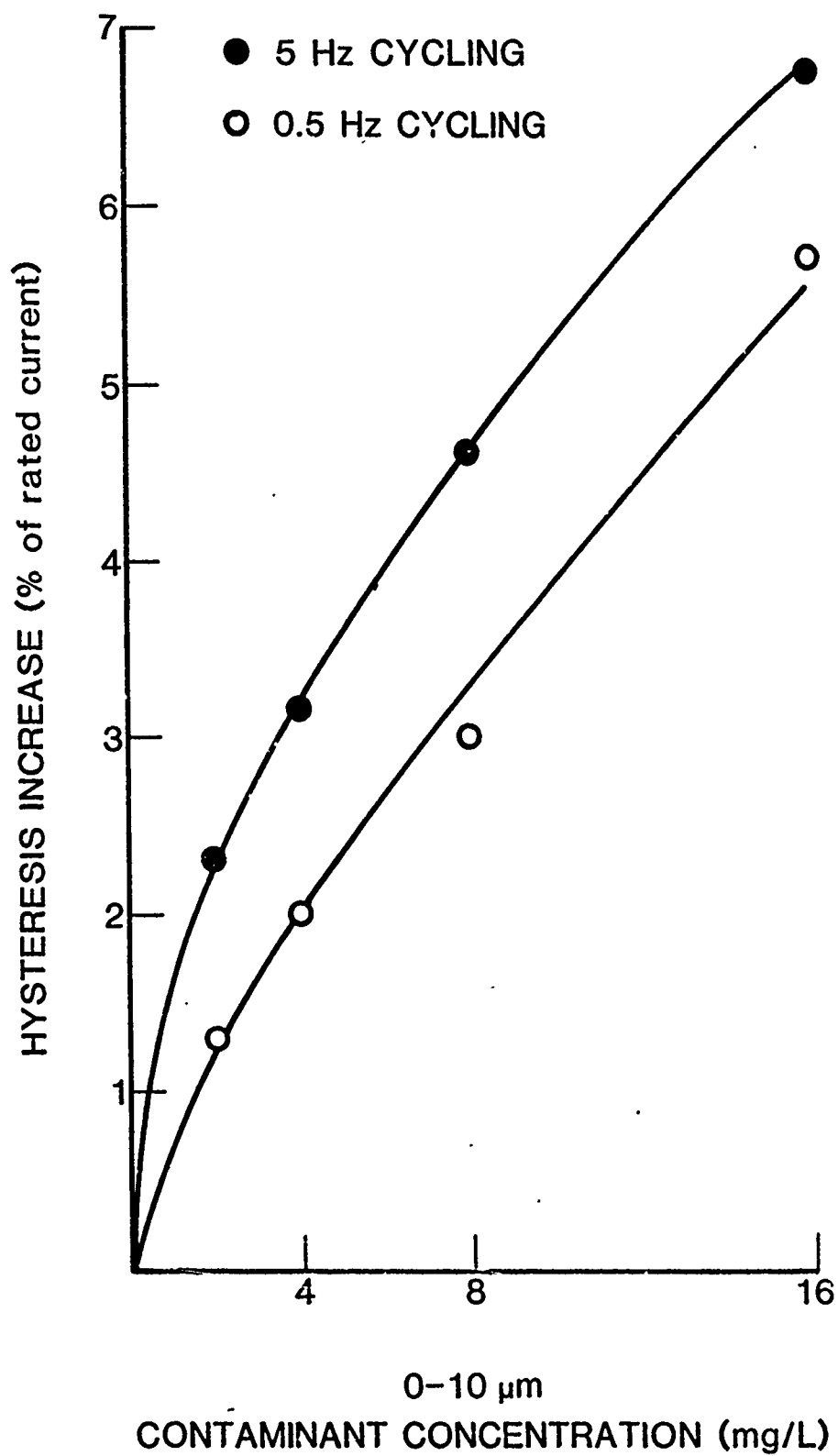


Fig. 2.4 Moog's Servovalves Contaminant Sensitivity Test Result

size distributions (i.e., 0-5 μm , 0-10 μm , etc.) on the same specimen was not feasible because the performance degradation starts high and progressively decreases as wear increases the clearance and rounds the corners of the spool orifices. The wear due to 0-10 μm contaminant was caused by cycling the servovalves for 40 minutes with 20 mg/L of contaminant concentration. The leakage flow was measured after two successive 40-minute periods of operation. The internal leakage flow increased from 2 percent of rated flow to 7 percent.

The effect of flow rate through the spool orifice edges was also investigated by removing the first stage assembly and installing special spool stops in the second stage assembly to fix the spool at various valve openings. For small openings, internal leakage did not increase appreciably because of the silting effect. For larger openings, there was no appreciable effect of flow rate on the leakage rate, as shown in Table 2.2.

Using the same equipment prepared for the above test, the effect of particle impact on the spool orifice edges was tested by adding different particle size ranges: 0-5 μm , 0-10 μm , and 0-80 μm . The concentration for this test was 300 mg/L. The result showed that larger particles caused more erosion than the smaller particles.

The report listed the overall permanent degradation on servovalve performance after the sensitivity tests. These included:

1. Slight increase in gain at null.
2. Hysteresis and threshold increase by 1 percent.

Table 2.2. Test Result Due to Flow Variation.

	0-80 m	50 mg/L	Contaminants
Flow	Linear Valve Opening	Leakage Increase	Comment
10%	22 μm	none	silted up completely
20%	44 μm	2%	partially silted
40%	88 μm	7.7%	
130%	286 μm	7.7%	

3. Seventeen percent decrease of original pressure gain value.
4. Decrease in first stage gain.
5. Increase in first stage leakage flow.

DISCUSSION

Each of these studies reached a milestone for the evaluation technique of servovalve contaminant sensitivity. Their accomplishments have been invaluable in this project.

These studies pointed out some of the myths concerning servovalves while bringing out some interesting anomalies. For instance, the valve which survived a concentration level of 528 mg/L would probably be operating long after most hydraulic pumps would have been destroyed by contaminant. Other test valves would not survive in ultra-clean systems.

CHAPTER III - THEORETICAL BACKGROUND

TYPES OF SERVOVALVES

Electrohydraulic servovalves can be classified by their internal configurations, the number of stages in power amplification, and the control mode. From the flow and response requirements, the servovalves can be categorized as single-stage, two-stage, and three-stage. Single-stage servovalves consist of a torque motor and a four-way valve. Because of their simplicity, single-stage servovalves are less expensive, and their response is high compared with multiple-stage servovalves. Their disadvantages are the flow capacity due to steady-state flow forces and stability which depends on the load dynamics.

Two-stage servovalves, which are the most common, are composed of a second-stage valve driven by a single-stage servovalve, while three-stage servovalves consist of a third-stage valve driven by a two-stage servovalve. By compounding the servovalve in the above fashion, the disadvantages of the single-stage servovalves are overcome, but such valves become more complex and expensive.

Multiple-stage servovalves have some sort of feedback between the first stage and second stage. There are three basic methods of feeding back the signal from second stage to first stage:

- * Centering springs on the spool end of the second stage to create a force balance between the stages.
- * A feedback spring deflected by the second-stage spool displacement to create a force feedback to the torque motor.

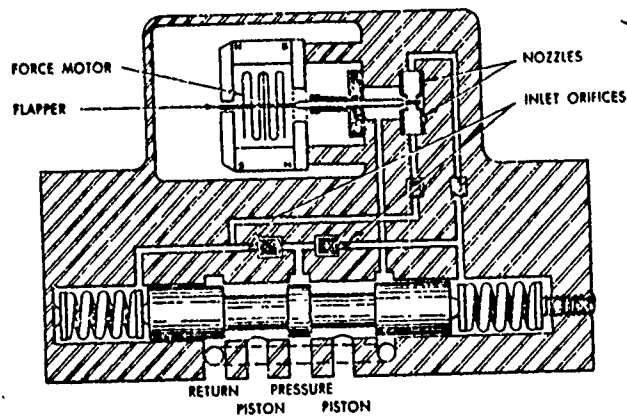
- * Position feedback accomplished by direct position feedback similar to hydraulic followers (Fig. 3.1).

The classification can also be made from the configuration of the first-stage hydraulic amplifiers. The most common designs are nozzle flapper, jet pipe, jet deflector, and spool types. Schematics of each design are shown in Fig. 3.2.

With respect to the control modes of the servovalves, there are six types available:

- * flow control
- * pressure control
- * pressure-flow control
- * dynamic pressure feedback
- * static load error washout
- * acceleration switching

The flow control servovalves are basic and the most common. They control load flow proportional to the electrical input current at constant load. This type of servovalve has high resolution and stiffness but low damping. Pressure control servovalves provide a differential pressure output in response to an electrical input current while pressure-flow control servovalves regulate flow in response to both the electrical input current and the differential load pressure. This function provides effective damping in high-resonant loaded servosystems at the expense of lowering system stiffness. The servovalves combining the functions of the flow control servovalves, which provide stiffness on the steady state, and the pressure flow control servovalves, which



TWO STAGE SERVOVALVE WITH OPEN CENTER FIRST STAGE

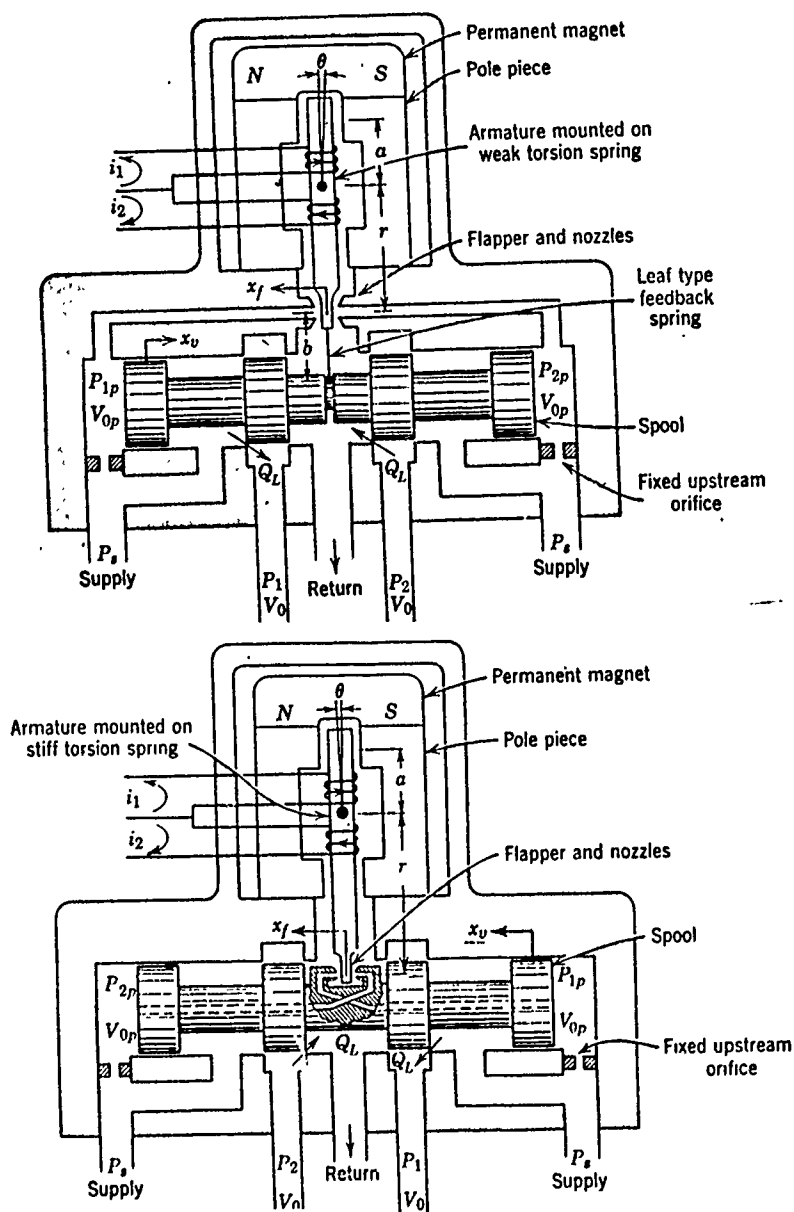
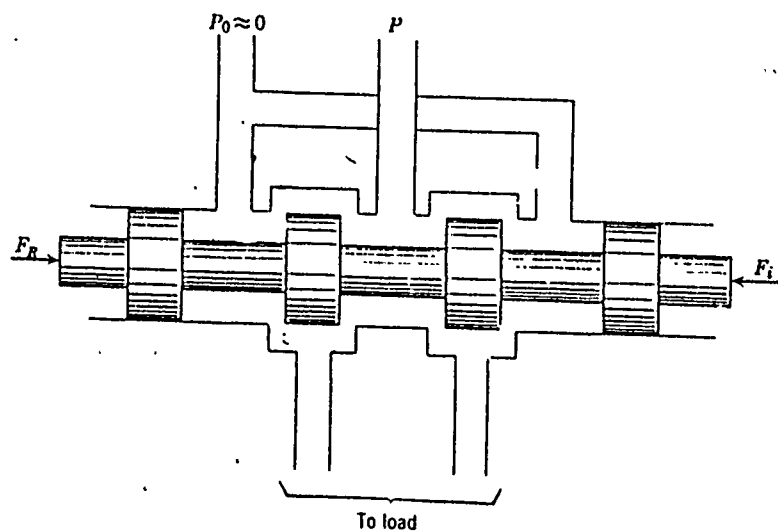
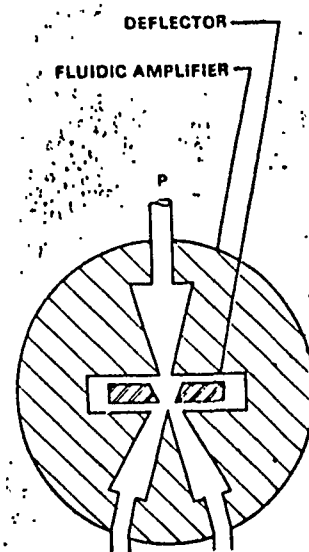


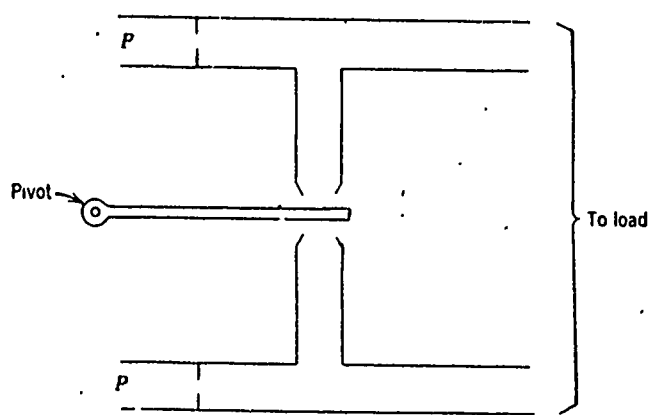
Fig. 3.1 The Schematical Structure of Servovalves



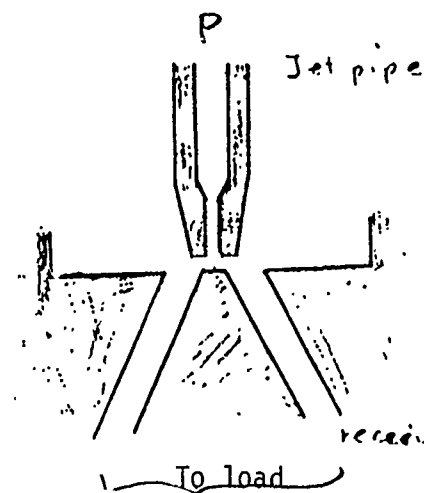
(a) Spool Valve



(c) Deflective Jet Valve.



(b) Double Nozzle Flapper Valve



(d) Jet Pipe Valve

Fig. 3.2 Types of First Stage Hydraulic Amplifiers

provide effective damping under dynamic conditions, are called the dynamic pressure feedback servovalves. The static load error washout servovalves have a further feature besides the dynamic pressure feedback technique. This type includes an additional static pressure feedback to compensate load position errors caused by the load structural compliance. The acceleration switching servovalves are quite distinct from the others, although the construction of these valves is similar to the flow control servovalve aforementioned. The input signal to the torque motor is a high frequency pulse length modulated wave instead of conventional DC input current.

Regardless of the way in which the servovalve is described, one thing remains common -- small clearances. Spool displacements as low as 0.25 to 0.5 mm are common, while radial clearances of 0.7 to 1.5 μm are found in some aerospace applications. Unless careful design practices are utilized, these clearances will invariably pose serious contamination sensitivity problems.

SERVOVALVE PERFORMANCE PARAMETERS

To obtain better performance, the electrohydraulic servovalves are fabricated with very close tolerances. Typical high performance servovalves for industrial applications have spool laps of 20 μm for all null edges. This spool lap condition governs the system performance and stability.

To determine the performance of the servovalves, several parameters should be examined. Some of these parameters are dependent upon the spool lap conditions. The important parameters are:

- flow gain
- flow-pressure coefficient
- pressure sensitivity
- hysteresis
- threshold
- internal leakage flow

The first three parameters are called valve coefficients. These coefficients influence the stability of the servosystems. The flow gain affects open-loop gain. The flow-pressure coefficient provides systems damping and is related to the leakage characteristics of the valve. The pressure sensitivity is expressed by the ratio of flow gain to the flow-pressure coefficient and represents the ability of a valve-motor or valve-piston combination to accelerate an inertial load under large loads with little error. The larger the pressure sensitivity, the lower the system compliance.

Hysteresis is a nonlinearity caused by the magnetic effect of the torque motor and the friction on the spool. Threshold is also induced by friction on the spool. These nonlinearities should be kept as small as possible to avoid trouble in stability. In general, a system having strong nonlinearities might exhibit limit cycle oscillations or jump resonance.

Internal leakage flow is mainly related to energy consumption. In missile applications, for example, very low internal leakage rates are normally selected in order to supply fluid to the system for a certain period of time. Internal leakage flow is subjected not only to

first-stage hydraulic amplifier configuration but also second-stage spool valve lap conditions. Underlapped spool valves cause large amounts of internal leakage flow and also can be the cause of higher wear rates on metering orifices.

EFFECT OF CONTAMINANTS ON SERVOVALVE PERFORMANCE PARAMETERS

Servo valve reliability and performance are a function of several factors. The valve design, discussed in previous sections, is one of them. Another factor might be the performance and efficiency of the filters selected for the servosystems. Also, the material of the contaminants affects servo valve performance severely.

The effect of contaminants on the servo valves appears in the form of contaminant lock force on the spool, wear on the critical surface and orifices, and clogging of small fixed or variable orifices. The contaminant lock force is created by the silting of small particles in the tight clearance between the spool and the sleeve. The result of silting then emerges as sluggish response due to increased friction on the spool or perhaps unstable servosystem response. If the second-stage spool driving force is not large enough to overcome the frictional force due to silting, hard-over or total loss of flow capability results. This kind of sudden failure, so-called catastrophic failure, can be disastrous on some equipment.

In contrast to the contaminant lock mode, which causes temporary performance degradation, contaminant wear brings about permanent performance deteriorations, so-called perceptible failure. Even though

the working fluid is moderately clean, contaminant wear remains a concern. Scoring and abrading between the spool and sleeve surfaces may occur, as may wear in orifices. The most critical of the orifices are the control orifices on the spool that regulate the flow to load according to a signal. Rounding off the sharp edges of the orifices causes a change in the discharge coefficient of the orifices and change in valve performance parameters. A different rate of wear in the orifices causes a null-shift in servovalves. Excessive null shift causes asymmetric flow. Rounding off the fixed orifices of the servovalves also changes their discharge coefficients but has less effect on the servovalve performance.

Clogging small fixed and variable orifices and built-in filters leads to other disastrous results in servosystems. This problem had been considered the general cause of valve failure in the past, but some documents indicate that no failure due to plugged or clogged orifices occurred [4].

It is unquestionably valuable to correlate the effect of particulate contaminants with servovalve performance parameters to evaluate their susceptibility to contaminants. A critical parameter, which represents not only the degradation of the servovalve performance but also variation on the static and dynamic characteristics, must be selected from the performance parameters.

As mentioned, contaminant-related problems are categorized as contaminant lock and contaminant wear.

CONTAMINANT LOCK ON SPOOL-TYPE VALVES

Spool-type valves are highly sensitive to contaminant-induced friction. Even without contaminants, spool-type valves have a tendency to lock in the spool sleeve at higher pressure. This phenomenon is termed hydraulic lock. The combination of higher pressure and dirty operating fluid makes the situation worse for these valves.

Some factors affecting the friction force on the spool valves are:

- * Valve material, geometrical irregularities, size of annular clearance, and spool diameter
- * Particle materials and sizes
- * Contaminant size distribution
- * Contaminant concentration
- * Oscillation or movement of the spool
- * Pressure acting on the spool
- * Boundary layer characteristics of the fluid used

Valve material and geometrical irregularities have a strong influence on contaminant susceptibility of the spool valves, while the remaining factors are external influences on the valve performance. Selection of valve materials and quality of the valve surface finish can significantly change the contaminant effects on valve performance.

As mentioned previously, the hydraulic lock phenomenon can occur, even though the fluid is relatively clean. This is because surface irregularities and some geometrical configurations create pressure distribution asymmetries along the valve clearance. This increases

the possibility of a large lateral force, which can cause an increase in friction. Apparent surface irregularities could be the result of contaminants in the clearance. If these contaminants are softer than the valve and the sleeve surface and are easily fractured, there may not be a large frictional force. If the contaminants are very hard, they might score the surfaces of the sleeve and spool, possibly resulting in a jammed spool. Figure 3.3, the results of Kusama and others [6], shows the effect of contaminants on the pressure distribution along an inversely tapered spool, which is effective in avoiding hydraulic lock and large lateral force.

Summarizing the above discussion, the lateral force on the spool could be minimized if the spool has good symmetry, fine surface finish, good roundness, straightness of the axes, and an inverse taper. These consequently can minimize friction force on the spool.

Another influential factor inducing a large contaminant lock force is the contaminant particle size. Figure 3.4 shows the results of the study on the contaminant lock sensitivity of directional control valves conducted at the FPRC [7]. The curves depict the relationship between contaminant lock sensitivity and contaminant size. Each valve indicated especially high sensitivity to one particular particle size. For instance, OSU Valve 104-2 is especially sensitive to 10 micrometre particles; whereas, OSU Valve 101 showed sensitivity to 25 micrometre particles.

The effect of the concentration of contaminants on the locking

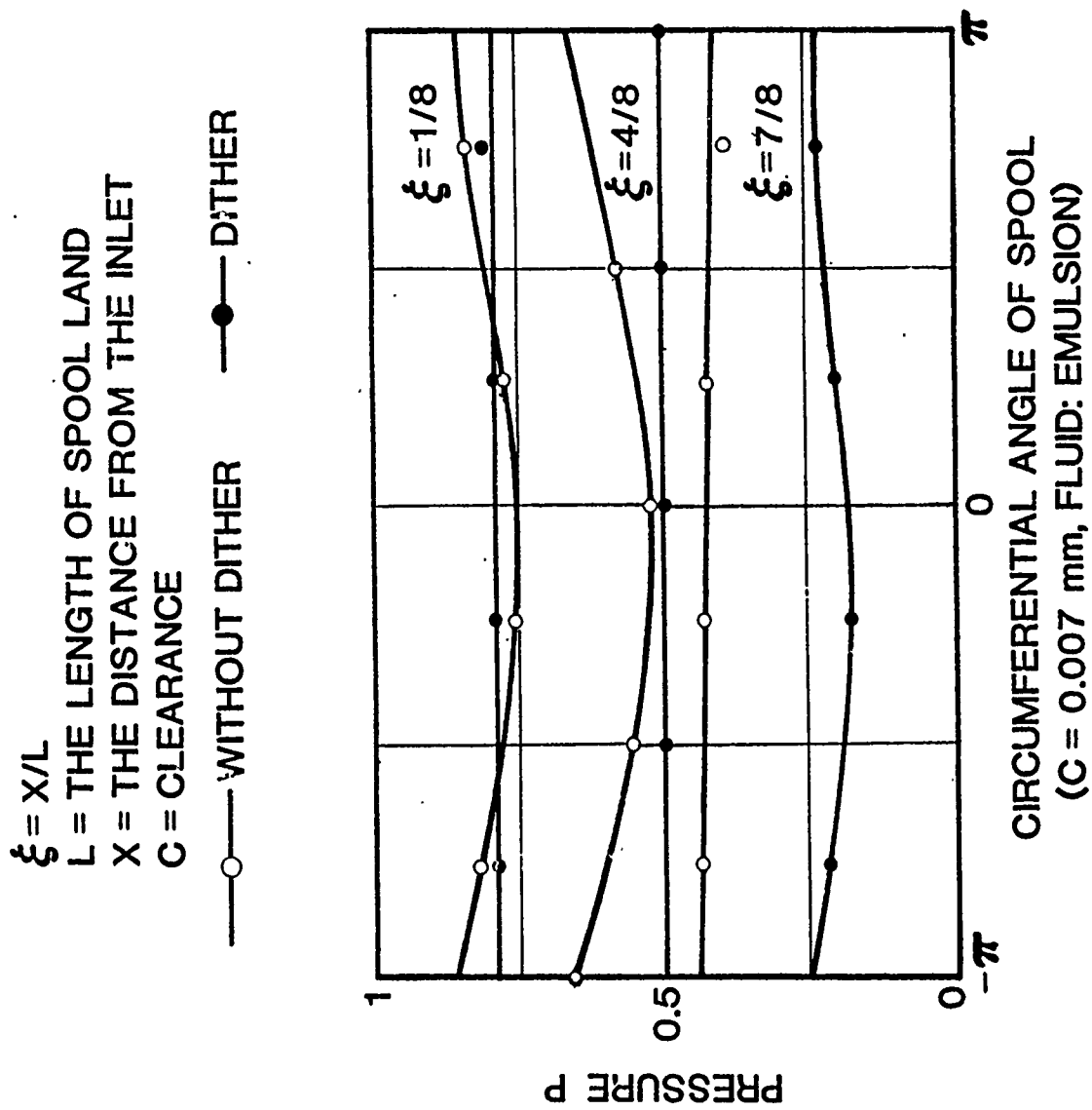


Fig. 3.3 Effect of Dither on Pressure Distributions with Inverse Taper Spool

FC-0074-5.60. -14-JN-VALVE CONTAM. LOCK SENSITIVITY VS CONTAM. SIZE

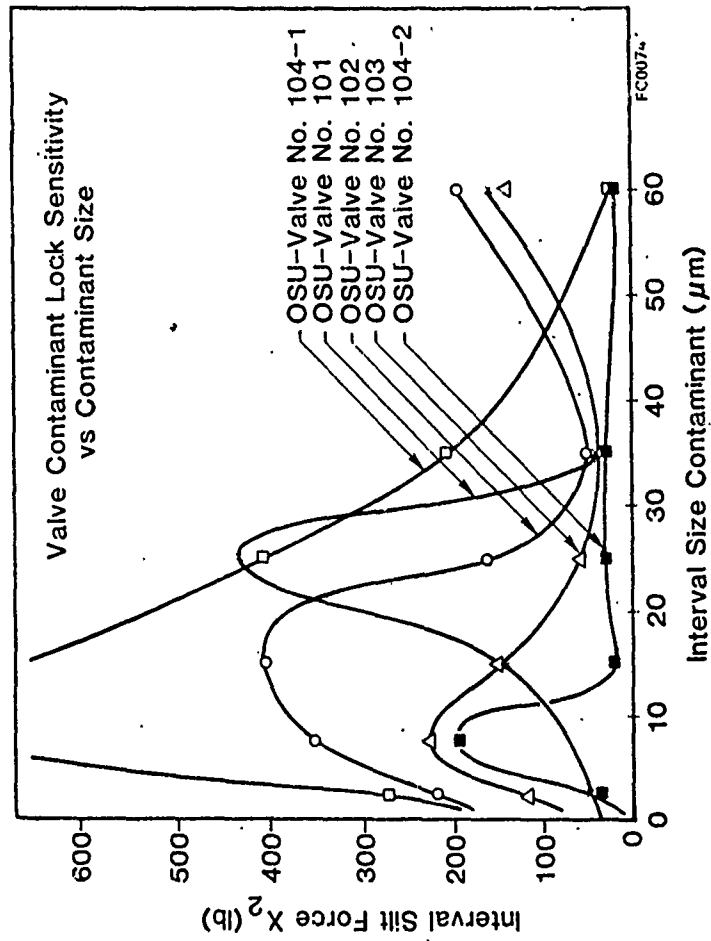


Fig. 3.4 Valve Contaminant Lock Sensitivity vs. Contaminant Size for Directional Control Valves

force is represented in Fig. 3.5 [8]. It is clearly revealed that friction force increases as contaminant concentration increases. The friction force does not diverge but approaches an asymptotic level.. The study also stated that the increase of the concentration considerably accelerates the friction locking process. The higher the concentration, the shorter the time before the valve clearance clogs completely, and the frictional force reaches its maximum value.

CONTAMINANT WEAR ON SHARP ORIFICE EDGES OF THE SPOOL

A major area of concern in servovalve contaminant sensitivity has been small orifice clogging and spool sticking. The significance of contaminant wear, however, has not been fully appreciated among design engineers. This fact can be seen in the literature available concerning servovalve performance degradation due to contaminant wear. The study presented by Black [5] is one of a few references which discuss wear on spool orifices.

In view of the fact that the orifice lap condition is vital to the overall servosystem performance, the susceptibility of servovalves to fluid contamination should be obvious. It is not realistic to pursue surgically or super clean systems for servovalves. Rather, it is desirable to use servovalves in "normal" clean systems; that is, in systems where no special care is provided for servovalves, which could cause accelerated wear on the critical orifices and loss of desirable performance. This is mainly due to particles impinging on the sharp corners of orifices and removing material, resulting in a rounding off

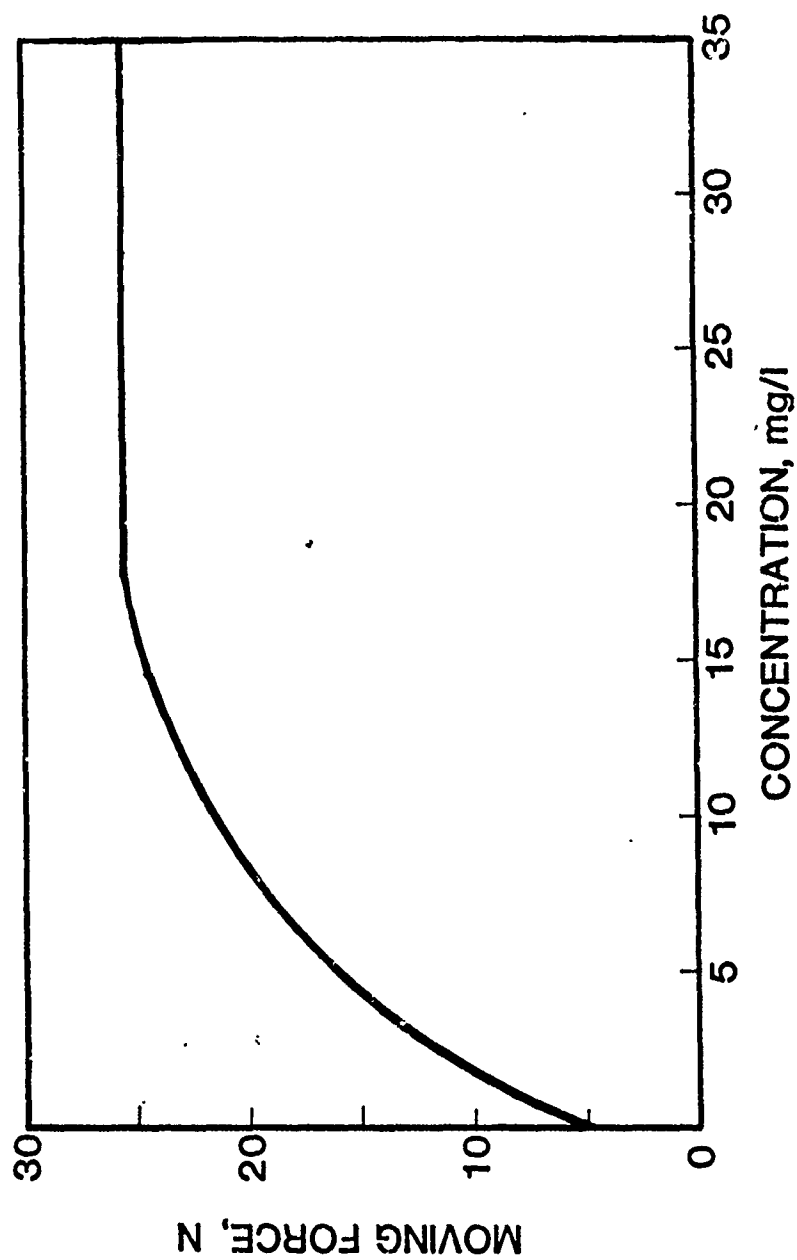


Fig. 3.5 Moving Force of the Spool vs. Contaminant Concentration

of the edges. It is intuitive that, the larger the number of particles impinging on orifices, the quicker the wear occurs. It is also instinctively perceived that larger particles cause more destructive damage to the orifices by virtue of their higher kinetic energy.

Particle impingement erosion has long been observed in many fields. Coal slurry transmission converts coal to a fluid flow for transporting. The pumps and hydraulic lines in such systems are subjected to particle impingement erosion. Gas turbine engines, gasifiers, and catalytic cracking systems have also suffered damage due to high speed particle impact on the component surfaces.

Many theoretical and experimental investigations have been carried out in these fields of applications. In fluid power systems, particle impingement erosion can be observed on poppets in relief valves and balls in check valves as well as servovalve spool orifices. In Ref. [9], it was stated that performance degradation due to particle impingement erosion poses the most serious threat to the reliable operation of relief valves. A study by Pai [10] demonstrated the effect of particle impact angle on erosion. A brief review of Pai's study is presented below in order to have insight into the erosion phenomenon on the servovalve spool orifices.

A number of experiments were conducted to obtain the relationship between contaminant concentration, particle size, and particle impact angle. A theory developed by Bitter and later modified by Neilson and

Gilchrist was used to predict particle impingement erosion on fluid power components. The theory is further revised to be more coincident with Bitter's theoretical curves. The wear formulae are, as a result, represented in Eqs. (3-1) and (3-2):

$$Q = \frac{\frac{1}{2} M V^2 \cos^2 \alpha}{\phi} + \frac{\frac{1}{2} M (V \sin \alpha - K)^2}{\epsilon} \quad (\alpha > \alpha_0) \quad (3-1)$$

$$Q = \frac{\frac{1}{2} M V^2 \cos^2 \alpha \sin n(\alpha - \alpha_{el})}{\phi} + \frac{\frac{1}{2} M (V \sin \alpha - K)^2}{\epsilon} \quad (\alpha \leq \alpha_0)^{n-2}$$

where M = Total mass of impinging particles

V = Particle velocity

K = Threshold velocity at which the elastic limit is just reached

ϕ = Cutting wear factor

ϵ = Deformation wear factor

α = Angle of impact

α_0 = Angle of impact at which parallel component of velocity just becomes zero when collision ends

α_{el} = Threshold angle at which the normal component of velocity just reaches the threshold velocity, K

n = A constant on the erosion curve

The ratio of the cutting wear factor, ϕ' , to the deformation wear factor, ϵ , represents the characteristics of the impinging particles and the material being impinged. The erosion characteristics are said to be brittle when ϕ/ϵ is less than one; ductile when ϕ/ϵ is greater than one. A ductile system was chosen for Pai's study where ϕ/ϵ was reported to be 0.625.

Experimental data and theoretical curves show correlation, and the theory predicted the particle impingement erosion well, as depicted in Fig. 3.6. The experiment reveals insignificant effect of particle size on the erosion, as plotted in Fig. 3.7. The result can be explained from Eq. (3.1); the erosion is not a function of particle size. This fact, however, conflicts with the experiment on servovalve spool orifice wear conducted by Moog [5]. The effect of concentration level could not be predicted, although the wear equations anticipate a proportional increase of wear as the concentration level increases. In addition, an impact angle of 50 deg caused the maximum wear.

In general, the erosion characteristics of servovalve spools and contaminant material pertain to brittle systems in which ϕ/ϵ is greater than one. This condition in terms of particles and servovalve spool materials is similar to Pai's study. In the study, the maximum erosion occurred at 40 to 50 degrees of impact angle in ductile systems. Thus, 40 to 50 degrees of impact angle could also cause severe erosion on servovalve spool control orifices. Figure 3.8 depicts erosion versus angle of impact characteristics with different ϕ/ϵ ratios plotted by Neilson and Gilchrist [11]. In the figure, erosion characteristics of servovalves could be full in the region between Figure 3.8(b) and (c). These figures show that larger impact angles cause more severe erosion.

It is well known that the jet from a small spool orifice forms along the axis whose angle from the spool axis is 69 deg. As depicted in Fig. 3.9, impinging angle of particles on both surfaces or corners of the

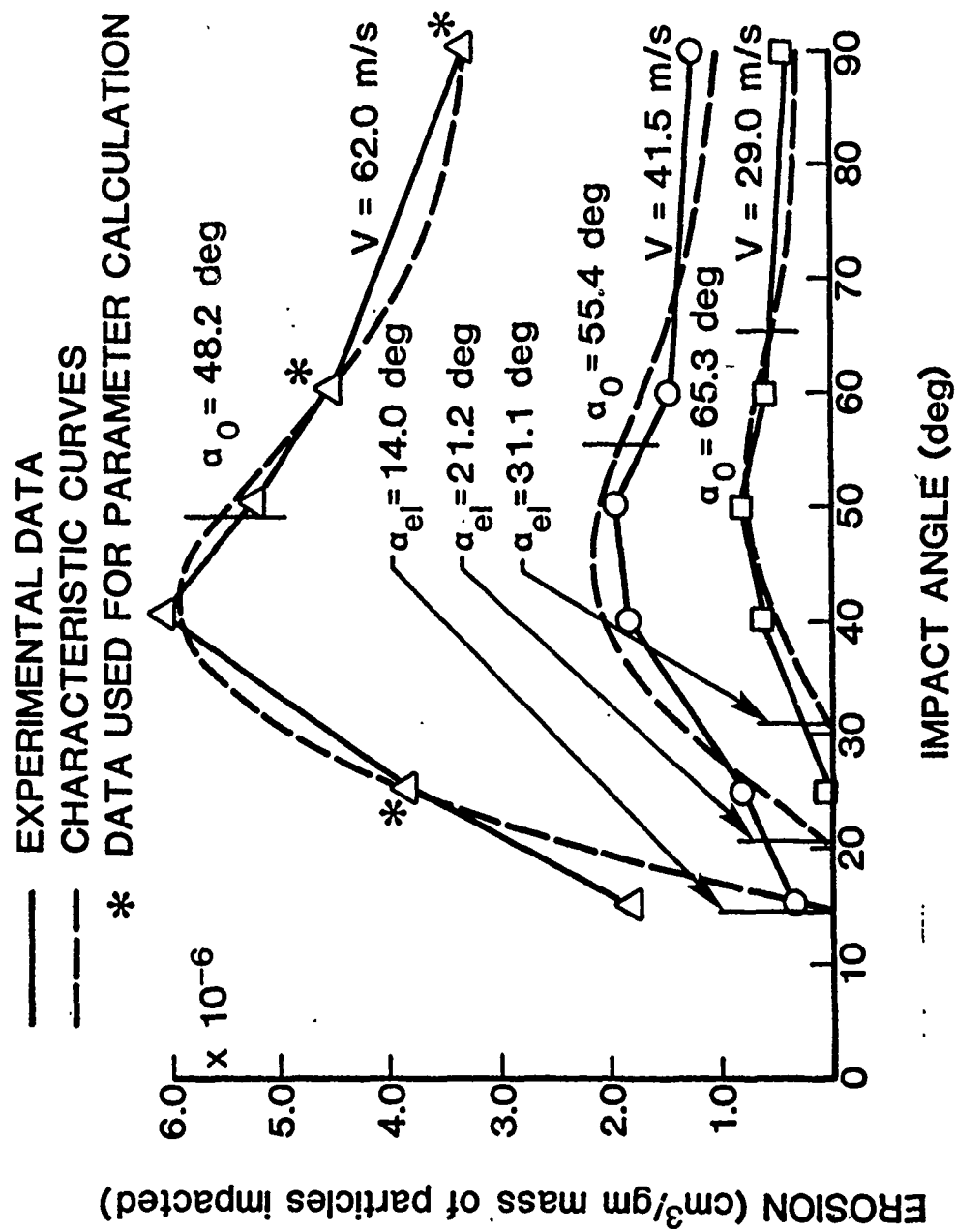


Fig. 3.6 Erosion Characteristic Curves of SAE1020 Steel at Various Impact Velocities. Particle Size Range = 40 μm -up, Concentration Level = 150 mg/L

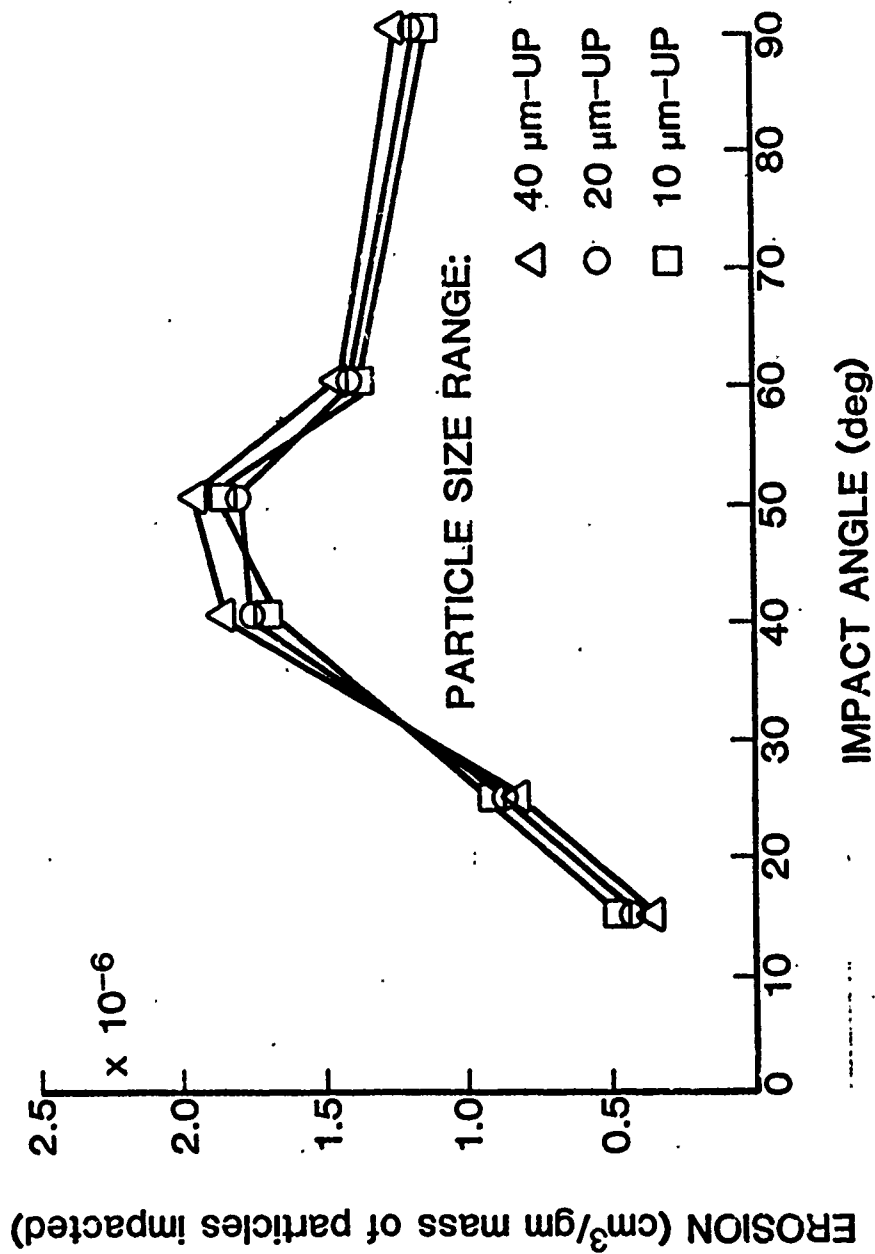


Fig. 3.7 Erosion Rate vs. Impact Angles at Various Particle Size Ranges. Concentration Level = 150 mg/L. Impact Velocity = 41.5 m/s

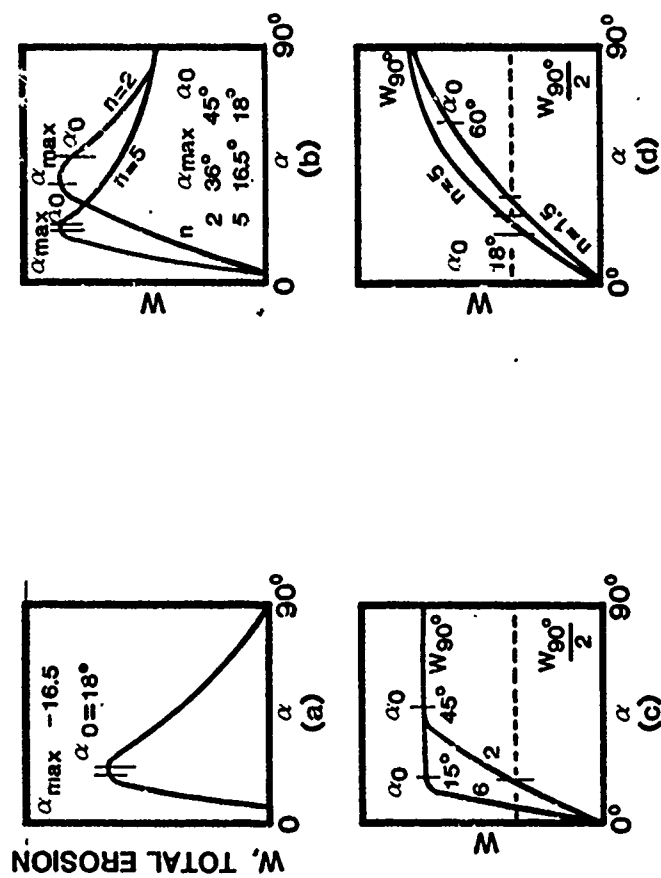


Fig. 3.8 Typical Erosion-Angle of Attack Characteristic

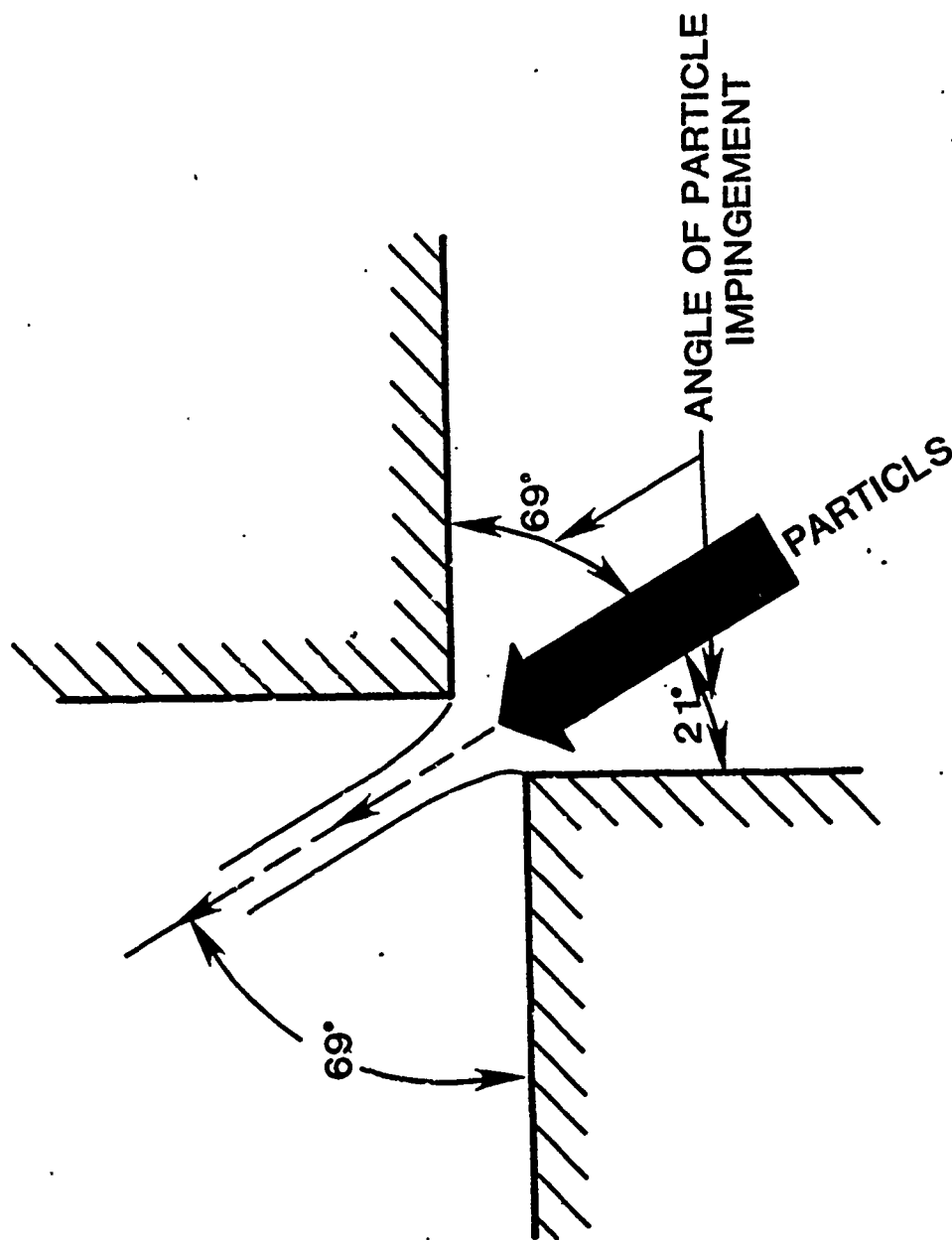


Fig. 3.9 Particle Impinging Process at the Spool Orifice

spool and the sleeve would, then, be 69 deg and 21 deg, respectively. Particles impinging to the surface at 69 deg would cause heavier erosion and round off the sharp corners more than those impinging at 21 deg.

CHAPTER IV - SERVOVALVE CONTAMINANT SENSITIVITY THEORY

The servovalve contaminant sensitivity theory must encompass both contaminant wear and contaminant lock. Contaminant lock sensitivity is evaluated from the increase of hysteresis due to contaminant-induced friction as a function of contaminant concentration and particle size intervals. It is an indication of how the servovalves tolerate the maximum contamination level within the specified performance.

Contaminant wear sensitivity, on the other hand, is evaluated from the variation in pressure gain, which shows direct performance deviation from the initial specifications as a function of particle size. It is an indication of servovalve life demonstrating how many hours the servovalves can operate acceptably within the specified performance.

CONTAMINANT LOCK SENSITIVITY

The evaluation of contaminant lock sensitivity is established based on the semi-empirical theory for spool type directional control valves developed by the FPRC [7].

The contaminant lock theory for spool valves is supported by the constant pressure filtration, as is the contaminant lock mechanism of spool valves. The primary assumptions made to support this theory are as follows:

- * The capture mechanism of direct interception of particles from the fluid stream lines is adjacent to the pore walls.
- * The particle retention on the walls of the pores is achieved in such a way that the volume passage decreases in direct proportion

to the volume of filtrate which passes through the flow path.

* Leakage flow follows Poiseuille's Law.

* The silting force which resists spool movement is proportional to the volume of contaminant retained in the clearance between the valve spool and the housing.

The result of the above assumptions led to the final form of the equation showing the relationships among the silting force, F , stationary time, t , valve geometry, fluid viscosity, μ , pressure differential, ΔP , across the leakage path, and contaminant concentration, V_p , as shown in Eq. (4-1).

$$F = k_1 \left(1 - \frac{1}{\sqrt{k_2 \frac{V_p \Delta P}{\mu} t + 1}} \right) \quad (4-1)$$

Values k_1 and k_2 are geometric parameters of the valve spool and are attained empirically from test data. These values are distinctive from valve to valve and between various particle size ranges. The semi-empirical model has been verified by the development of a contaminant monitor [2] as well as a directional control valves study [7].

Application of the theory to servovalves is made with little modification. Measuring silting force on the servovalve spools is impractical. Besides, the silting force does not indicate direct contaminant susceptibility of servovalves because of the capability of the first-stage hydraulic amplifiers to drive second-stage spools.

If the servovalves have sufficient driving capability to overcome larger silting forces, the valve might demonstrate no degradation on output performance parameters. A better parameter is the hysteresis increase due to friction, which is in turn due to silting force. Thus, Eq. (4-1) can be used to determine the change of silting force with an increase of hysteresis. For the servovalve contaminant sensitivity, contaminant concentration is selected as an independent variable. This makes the test process shorter and minimizes the destruction of larger particles.

Equation (4-1) is rewritten for the form of the servovalve contaminant lock sensitivity as:

$$b_i = X_i \left(1 - \frac{1}{\sqrt{Y_i V_p + 1}} \right) \quad (4-2)$$

Parameters X_i and Y_i depend only on the contaminant size (5-10 μm , 10-20 μm , 20-30 μm) when all other conditions remain constant. These parameters, called contaminant lock coefficients, are determined by finding the best fit curve to a set of data (V_p , b_i) obtained from testing. Unfortunately, it is not practical to use double-cut AC Fine Test Dust (5-10, 10-20, etc.). Therefore, lower cut ACFTD (0-5 μm , 0-10 μm , 0-20 μm , 0-30 μm) is substituted, and the result is converted to the equations for interval contaminant size. The conversion is performed from the particle size distribution relations in each dust fraction. The size distribution of the lower cut dust is tabulated

in Table 4.1. This table is used in Eq. (4-3) to calculate the effect of each particle size interval. It is assumed that there are no particles larger than 5 μm in 0-5 μm lower cut dust; no particle larger than 10 μm in 0-10 μm ; etc. The contribution of each particle size interval to the lock coefficient for lower cut dust is calculated from Eq. (4-3). Weighting factors in Eq. (4-3) are obtained from particle distribution of the lower cut dust, as shown in Table 4.1.

$$\begin{aligned} X_{0-10} &= 0.742 X_{0-5} + 0.258 X_{5-10} \\ Y_{0-10} &= 0.742 Y_{0-5} + 0.258 Y_{5-10} \\ X_{0-20} &= 0.687 X_{0-5} + 0.239 X_{5-10} + 0.074 X_{10-20} \\ Y_{0-20} &= 0.687 Y_{0-5} + 0.239 Y_{5-10} + 0.074 Y_{10-20} \end{aligned} \quad (4-3)$$

To determine the Omega rating value, contaminant lock coefficients X_β for the Beta 10 filter model are calculated. The relationship between the lock coefficients for Beta 10 model and particle size interval calculated above is derived based on the curve of Beta 10 = 2. Contribution of each particle size interval to the lock coefficients is evaluated from this curve, assuming that the total number of particles is counted from particles greater than 1 μm . As a result, the contaminant lock coefficients for the Beta 10 model are calculated from Eq. (4-4).

$$\begin{aligned} X_\beta &= 0.964 X_{0-5} + 0.035 X_{5-10} + 0.001 X_{10-20} \\ Y_\beta &= 0.964 Y_{0-5} + 0.035 Y_{5-10} + 0.001 X_{10-20} \end{aligned} \quad (4-4)$$

THE LOWER CUT DUST

INTERVAL μm	μm 0-10	0-20	0-30	0-40	0-50	0-60	0-70
0/5	74.2%	68.7%	67.9%	67.8%	67.7%	67.7%	67.7%
5/10	25.8	23.9	23.6	23.6	23.5	23.5	23.5
10/20		7.4	7.4	7.4	7.4	7.4	7.4
20/30			1.1	1.0	1.0	1.0	1.0
30/40				0.2	0.3	0.26	0.26
40/50					0.1	0.11	0.10
50/60						0.03	0.03
60/70							0.01

FFRC-OSU-80-86

Table 4.1 Particle Distribution of the Lower Cut Dust

Substituting the values of X_B and Y_B from Eq. (4-4) in place of X_i and Y_i into Eq. (4-2), the relationship between hysteresis increase and gravimetric level is obtained for the Beta 10 filter model. From this relationship, the Omega rating value is defined as the Beta 10 filter needed to ensure a performance degradation of no more than 2 percent of hysteresis increase after one minute of stationary time in the standard system. The standard system is defined as a hydraulic system having a flow rate of 20 gpm and an ingression rate of 10^8 particles per minute greater than $10 \mu\text{m}$.

The Omega rating value is based on this standard system and a Beta 10 = 2 filter.

CONTAMINANT WEAR

Wear on the spool orifices changes the performance of a servovalve. Worn orifices cause higher loop gain, which brings about an oscillatory system response and reduced stiffness, which increases the error due to external disturbances.

Servovalve wear is dependent on the valve material and design. Assuming that the contaminant in the hydraulic system has the same characteristics as AC Fine Test Dust and that its properties do not change, the major factors which affect performance degradation are contaminant concentration level and contaminant particle size. The term "contaminant concentration level" includes a time factor. For example, consider an electrohydraulic servovalve regulating flow to an actuator in a hydraulic system whose contaminant level is 10 mg/L.

After 100 hours of operation, the servovalve is removed to check the performance degradation and the pressure gain is found to have decreased to 80 percent of the original. Another identical servovalve in operation in another system with the same conditions, except with contaminant concentration level of 20 mg/L, may experience a decrease in pressure gain to 80 percent of the original in only 50 hours.

The performance degradation is then expressed as a function of contaminant particle size and contaminant concentration, which is a function of time. Defining the contaminant sensitivity, S_i , of the component at each contaminant size interval, i , the relationship between the performance degradation and the contaminant is shown by Eq. (4-5). This parametric representation simplifies the concept of contaminant sensitivity.

$$P_1 - P_2 = - S_i \bar{N}_i \quad (4-5)$$

where $P_1 - P_2$ is performance degradation

\bar{N}_i is total amount of contaminant to which the component is exposed.

The total amount of contaminant, \bar{N}_i , is expressed in terms of flow rate $Q(t)$, and contaminant concentration, $N_i(t)$, as:

$$\bar{N}_i = Q(t) n_i(t) (t_1 - t_2) \quad (4-6)$$

Substituting Eq. (4-6) into Eq. (4-5) gives:

$$P_1 - P_2 = -S_i Q(t) n_i(t) (t_1 - t_2) \quad (4-7)$$

Representing this discrete equation in continuous form, Eq. (4-7) becomes:

$$\frac{dP}{dt} = -S_i Q(t) n_i(t) \quad (4-8)$$

In the laboratory, the particles destroyed in the test system are not replenished; whereas, in the field, contaminant ingress and filtration create a more or less steady contaminant level. Expressing it in the term, n_i , in the above equations, n_i is constant in the field. In the laboratory, particle numbers could vary, depending on the components in the test system, especially a pump and its operating time. The number of larger particles decreases due to destruction, mainly in a pump, and smaller increase in number until destruction of all of the larger particles takes place.

This process continues until all of the contaminants become small enough to be unharmed to a test component. The destruction process could be expressed in mathematical model as in Eq. (4-9a):

$$n_i(t) = n_o e^{-t/\tau} \quad (4-9a)$$

Where n_0 is the initial number of particles per liter and t the time constant in the particle destruction process.

The particle destruction process changes due to the pump used in the test system. Component contaminant sensitivity would alter as a result. An analysis on the particle destruction process is introduced below from the work at the FPRC [9].

Figure 4.1 is a result obtained from the particle destruction analysis under the test condition that contaminant size 0-80 μm of classified AC Fine Test Dust was injected into the test system to set the contaminant concentration level to 100 mg/L. Population changes on each particle interval show replenishing of smaller particles due to destruction of larger particles.

Figure 4.2 illustrates the time constant, t , in different particle size intervals. The dotted line in the graph is obtained from a least squares fit exponential to describe the particle population change as a function of particle size intervals. Smaller particle size ranges replenished by the destruction process of larger particles exhibit longer time constants; whereas, larger particle size ranges show shorter time constants because these particles are destroyed but not replenished. The time constant obtained for larger particles could be used directly for data interpretation because no replenishment of particles clearly represents laboratory test conditions. Extrapolating the time constant values of greater than 30 μm to smaller size to 10 μm was performed, as shown in Fig. 4.2.

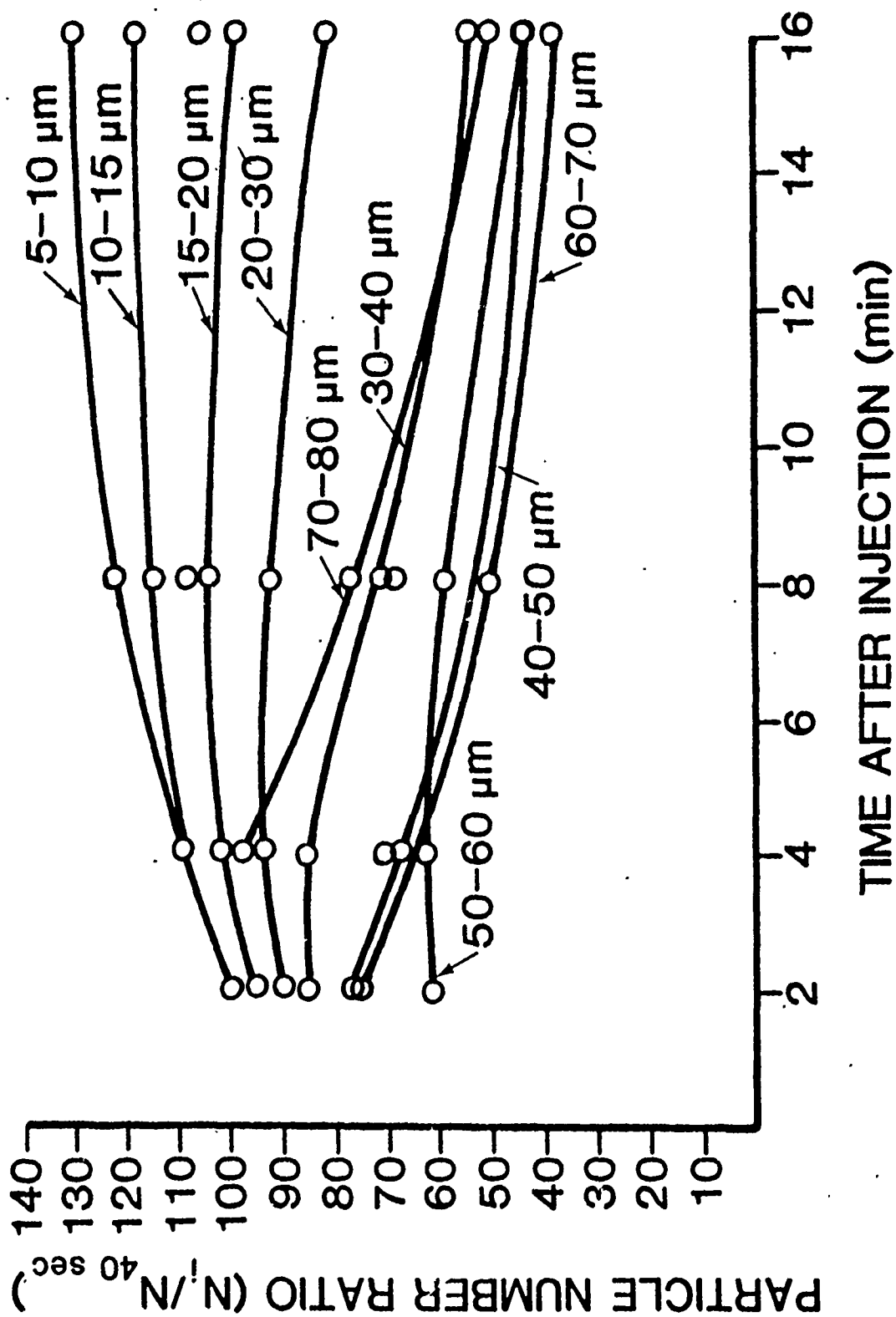


Fig. 4.1 Illustration of Particles Destruction Characteristic

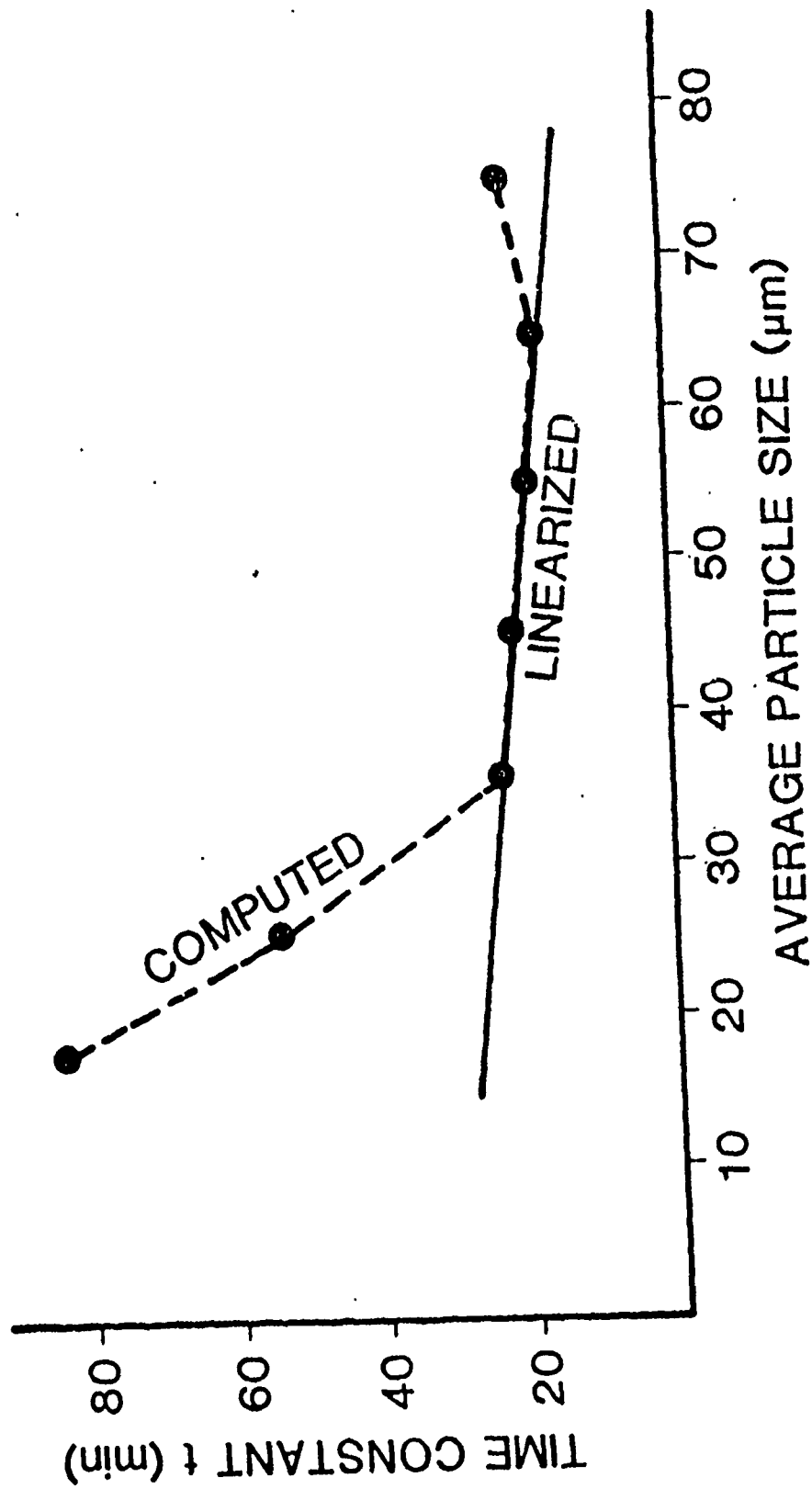


Fig. 4.2 Linearized Particle Destruction Time Constant Relationship for OSU Test Pump No. 102

The destruction process for smaller particles, especially 0-10 μm particles, has proved to have a negligible effect on particle number. This fact leads to the assumption that the particle population of these smaller sizes is constant and expressed as in Eq. (4-9b):

$$n_i(t) = n_{0i} \quad (4-9b)$$

It has been verified that the contaminant sensitivity of a component is a proportional function of the concentration. This relation is expressed in Eq. (4-10) defining the contaminant wear coefficient, α .

$$S_i(n) = \alpha_i n_{0i}(t) \quad (4-10)$$

The performance degradation equation now becomes:

$$\frac{dP}{dt} = -\alpha_i n_{0i}^2 Q(t) e^{-2t/\tau} \quad (4-11)$$

For servovalves, performance degradation is analogous to pressure gain variation; therefore, Eq. (4-11) is transformed into Eq. (4-12):

$$\frac{dK_p}{dt} = -\alpha_i n_{0i}^2 Q_L e^{-2t/\tau} \quad (4-12)$$

In this equation, controlled load flow, Q_L , is kept constant. Integration yields an expression for pressure gain at any time t after the concentration n_0 has been initially established.

$$k_p = k_{p0} - \frac{1}{2} \tau \alpha n_0^2 Q_L (1 - e^{-2t/\tau}) \quad (4-13a)$$

Where k_{p0} is the initial pressure gain prior to contaminant injection. In the assumption made in the previous paragraphs, Eq. (4-13a) can be expressed as in Eq. (4-13b).

$$k_p = k_{p0} - \alpha_i n_{0i}^2 Q_L t \quad (4-13b)$$

This equation is only valid for particle sizes up to $10 \mu m$. From Eq. (4-13a & b) the contaminant wear coefficient can be expressed as:

$$(\tau \alpha)_i = \frac{(k_{p0} - k_{pf})_i}{\frac{1}{2} n_{0i}^2 Q_L (1 - e^{-2t/\tau})} \quad (4-14a)$$

$$(\alpha)_i = \frac{(k_{p0} - k_{pf})}{n_{0i}^2 Q_L t} \quad (\text{for } D \leq 10 \mu m) \quad (4-14b)$$

Where the subscript i identifies the particle size interval injected.

Using Eqs. (4-14a) or (b), the relationship between gravimetric level and pressure gain can be obtained reforming Eq. (4-14a) in terms of gravimetric levels for X and Y .

From the above equations and the fact that Q_2 , t , and a do not change their values due to different gravimetric levels:

$$\frac{G_x^2}{G_y^2} = \frac{(k_{p0} - k_{pf})_x}{(k_{p0} - k_{pf})_y} \quad (4-15)$$

Equation (4-15) shows direct relationship between gravimetric level and pressure gain degradation.

Since lower cut test dust is used for testing, pressure gain degradation must be converted, as in the contaminant lock sensitivity theory. For the size range of 0-10 μm test dust, the total pressure degradation due to the lower cut dust 0-10 μm could be contributed to each size interval, as shown in the equation below.

$$\Delta k_{p0-10} = \Delta k_{p \frac{0-5}{0-10}} + \Delta k_{p \frac{5-10}{0-10}} \quad (4-16)$$

where $\Delta k_{p \frac{0-5}{0-10}}$ is the degradation due to the percentage of 0-5 μm test dust in the range of 0-10 μm .

$\Delta k_{p \frac{5-10}{0-10}}$ is the degradation due to the amount of 5-10 μm test dust in the range of 0-10 μm .

Further manipulation yields Eq. (4-17) from Eq. (4-14).

$$k_{pf} = -\alpha_{0-5} n_{0 \frac{0-5}{0-10}}^2 Q_L t - \alpha_{5-10} n_{0 \frac{5-10}{0-10}}^2 Q_L t + k_{p0} \quad (4-17)$$

Where $n_{0 \frac{0-5}{0-10}}$, $\frac{5-10}{0-10}$ represent the particle number per unit volume of 0-5 μm and 5-10 μm contaminant included in 0-10 μm contaminant injection, respectively.

Rearranging Eq. (4-17) yields Eq. (4-18):

$$\alpha_{5-10} = \frac{1}{n_{0 \frac{5-10}{0-10}}^2} \left[\frac{k_{p0} - k_{pf0-10}}{Q_L t} - \alpha_{0-5} n_{0 \frac{0-5}{0-10}}^2 \right] \quad (4-18)$$

Similarly, the equations for 10-20, 20-30, 30-40 μm , and 40-50 μm particle size intervals are obtained. The contaminant wear coefficient of all interval size contaminants is summarized in the following using the fact that the particle destruction occurs as discussed in previous paragraphs. The time constants for the interval particles are denoted as t_{10-20} , t_{20-30} , and so forth. Major contaminant destruction can be assumed to take place in the pumps of the servovalve test hydraulic systems.

$$\alpha_{0-5} = \frac{1}{n_{0-5}^2} \frac{(k_{p0} - k_{pf})_{0-5}}{Q_L t}$$

$$\alpha_{5-10} = \frac{1}{n_{0-10}^2} \left\{ \frac{(k_{p0} - k_{pf})_{0-10}}{Q_L t} - \alpha_{0-5} n_{0-5}^2 \right\}$$

$$\alpha_{10-20} = \frac{1}{\frac{1}{2} n_{0-20}^2 Q_L \tau_{10-20} (1 - e^{-2t/\tau_{10-20}})}$$

$$\left\{ (k_{p0} - k_{pf})_{0-20} - Q_L t (\alpha_{0-5} n_{0-5}^2 + \alpha_{5-10} n_{0-10}^2) \right\} \quad (4.19)$$

$$\alpha_i = \frac{1}{\frac{1}{2} n_{0-i}^2 Q_L \tau_i (1 - e^{-2t/\tau_i})}$$

$$\left\{ (k_{p0} - k_{pf})_i - Q_L t (\alpha_{0-5} n_{0-5}^2 + \alpha_{5-10} n_{0-10}^2) \right.$$

$$\left. - \frac{1}{2} Q_L \sum_{j=3}^{i-1} \alpha_j n_{0-j}^2 \tau_j (1 - e^{-2t/\tau_j}) \right\}$$

$$i = 4, 5, 6 \quad ; \quad j = r$$

where: Subscript 3 corresponding to 0-20 or 10-20

Subscript 4 corresponding to 0-30 or 20-30

Subscript 5 corresponding to 0-40 or 30-40

Subscript 6 corresponding to 0-50 or 40-50

These contaminant wear coefficients were derived from laboratory test data and represent the characteristic susceptibility to contaminant wear for a particular servovalve. In other words, these coefficients are an inherent property of a particular servovalve.

As mentioned, contaminant particles remain at some constant condition in the field. Thus, field contaminant concentration N_{fi}

becomes as Eq. (4-20)

$$n_i(t) = n_{Fi} \quad (4-20)$$

Pressure gain as a function of time for a reference field condition can be derived by a similar process as before. The resulting equation becomes :

$$K_P = K_{P0} - Q_L \left\{ \sum n_{Fi}^2 \alpha_i \right\} t \quad (4-21)$$

From Eq. (4-21), a reference contaminant life equation is obtained :

$$T = \frac{K_{P0} - K_{PT}}{Q_L \sum_{i=1}^6 n_{Fi}^2 \alpha_i} \quad (4-22)$$

where K_{PT} is pressure gain corresponding to time T .

Calculating Eq. (4-22) gives the contaminant service life according to the specified contaminant environment. A contaminant tolerance profile can be drawn from Eq. (4-22). The profile is the locus of tangency points and is obtained from the contaminant particle distribution curves for the same contaminant service life.

The Omega rating value for servovalves is defined as the Beta 10 filter value required to assure a 1000 hour life in the standard system.

From the Omega rating value, the necessary filter requirement for servovalves can be specified to ensure a service life with the required performance limitations.

CHAPTER V - TEST STAND

In order to conduct the tests described in the previous chapter, a contaminant sensitivity test facility was constructed. It was determined that the test stand must meet the following criteria:

1. It must accept a variety of valves up to four-way, three position.
2. It must have facilities for a controlled rate of injection of contaminants into the fluid stream.
3. The components in the test system must not be contaminant sensitive, and they must neither generate nor trap the test contaminant so that the gravimetric level of the contaminants will remain constant.
4. It must be compatible with mineral base fluids as well as the entire range of fire resistant fluids.
5. It must have a cleanup system to remove the contaminants after each test.

To meet these criteria, a stand was fabricated using the schematic diagram shown in Fig. 5.1. The stand was provided with a manifold suitable for mounting a variety of valves on their individual adapters.

To meet these criteria, a stand was fabricated using the schematic diagram shown in Fig. 5.1. The stand was provided with a manifold suitable for mounting a variety of valves on their individual adapters.

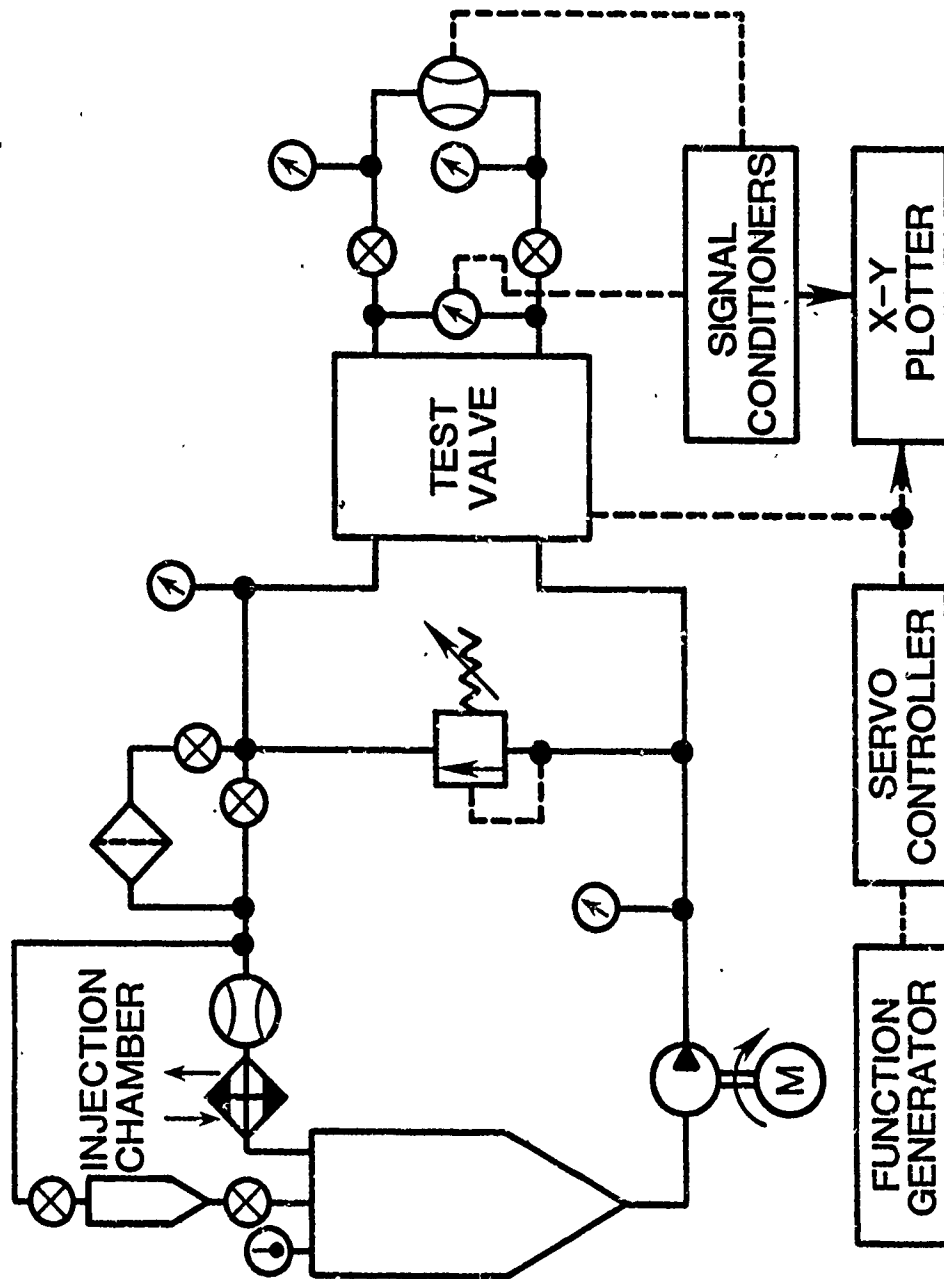


Fig. 5.1 Test Circuits

The injection chamber provides the means for injecting the ACFTD contaminants at a controlled rate. The chamber is constructed of glass so that the injection process can be observed and to ensure that the contaminant does not adhere to the side walls. The base of the chamber is conical.

Contaminant is put into the chamber as a slurry. The injection valve is then opened to allow the slurry to flow into the test reservoir, where it is thoroughly mixed with the test fluid by the agitating action of the diffuser through which all return fluid flows. Residual contaminants are removed from the injection chamber by allowing a portion of the return fluid to flow through the chamber.

The components used in the stand were chosen based either on previously-conducted contaminant sensitivity tests or on known contaminant insensitive designs. For instance, the main system pump has a demonstrated high contaminant tolerance, while the charge pump uses a centrifugal design, which is not only insensitive to contaminants but also does little damage to the ACFTD particles.

The flow meter on the high pressure portion of the system was target-type. A rotameter was used on the low pressure side of the system. The shut-off valves and three-way valves were of stainless steel construction to resist abrasion, while the pressure relief valve had been tested at the FPRC and was known to be very contaminant tolerant.

To ensure that a constant contaminant gravimetric level could be maintained by the test system, qualification tests were conducted in accordance with Clause 11 of the Test Procedure of Chapter IV with the exception that a gravimetric level of 250 mg/L was used rather than the 100 mg/L specified in the procedure. This was done because it was originally proposed to test the valves at this higher contaminant concentration. Unfortunately, the higher level caused some long-term damage to the test stand components, so it was decided to reduce the concentration.

The qualification test results are shown in Fig. 5-2. The ability of the stand to maintain the injected level for at least one hour is clearly shown.

To ensure compatibility with fire resistant hydraulic fluids, most system components were fabricated of stainless steel. Where elastomeric seals were required, Viton seals were specified.

The filter elements used in the cleanup circuit have a Beta 10 rating of greater than 75.

MAJOR TEST STAND COMPONENTS

The following is a listing of the major components used in the fabrication of the valve test stand.

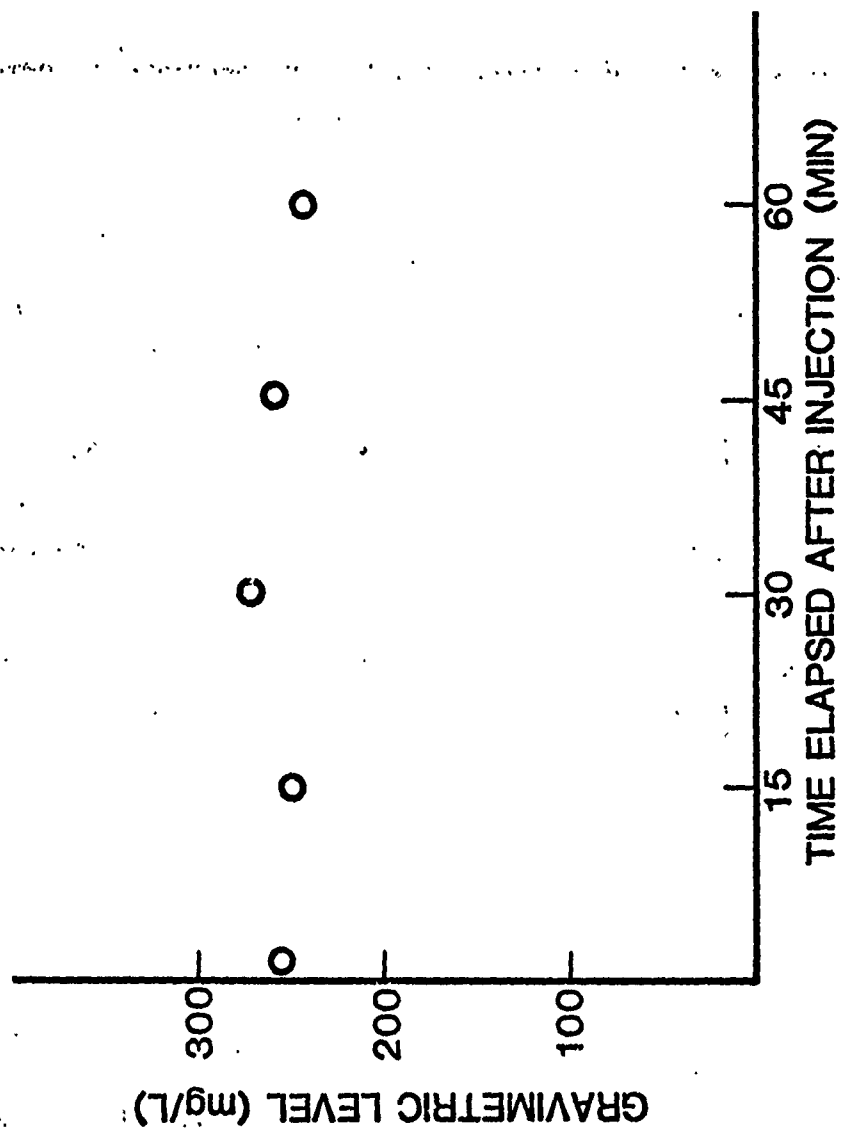


Fig. 5.2 Qualification Test Results

Hydraulic System

- Hydraulic pump

Dynex/Rivett fixed displacement piston pump model PF4015-1584

- Hydraulic Pressure Relief Valve

Vickers Balanced Piston type relief valve model CG-03-H-20

- Heat Exchangers

Basco two pass all 304 stainless steel model 04024

- Injection Chamber

Made of glass tube

- Reservoir

Conical shape with diffuser at the end of hydraulic tubing

- Charge Pump

Dayton centrifugal pump and electrical motor model GK580

- Filter Elements

Hilco Model PL-718-26

Instrumentation

- Flowmeter

Ramapo target type model Mark V- $\frac{1}{2}$ -SSB

- Rotameter

Fischer and Porter model 10A 1755S

- Differential Pressure Gauge

Sensotec Model A-5

- Strain Gauge Amplifier

Daytronic Strain Gage Conditioner/Indicator Model 3278

- . Strain Gauge Amplifier
Ramapo digital flow indicator Model SGA-350 RMD
- . Servovalve Amplifier
Thompson Controls Model T6-R
- . Low Frequency Oscillator
Hewlett Packard Model 202 CR
- . X-Y Recorder
Hewlett Packard Model 7046A

TEST CONTAMINANTS

Air Cleaner Fine Test Dust (ACFTD) was selected as the test contaminant. This contaminant has been approved both nationally and internationally as a standard for contamination control tests. The result of chemical analysis of AC Fine Test Dust is tabulated in Table 5-1 for different size ranges with the raw dust reported by the manufacturer. Mechanical properties of the test contaminants are listed below:

Density = $2.66 \times 10^{-3} \text{ kg/cm}^3$

Poisson's Ratio = 0.2

Young's Modulus of Elasticity = $2.74 \times 10^3 \text{ MPa}$

Contaminant sensitivity tests on servovalves are conducted using lower cut classified AC Fine Test Dust (zero to some size "D") because of the resemblance of the size distribution of these cuts to the result of downstream particle size distribution of the system filter associated with the standard multipass test.

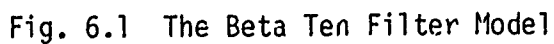
Table 5.1 ACFTD Chemical Property

CHEMICAL ANALYSIS OF AC FINE TEST DUST						
SAMPLE	LOI	SiO ₂	Fe ₂ O ₃	Al ₂ O ₃	CaO	MgO
AC FINE	2.72	69.2	4.35	13.6	0.05	1.64
0-5 μm	5.60	61.3	5.03	17.8	0.04	2.43
50 μm AND UP	0.60	76.5	4.12	11.4	0.14	1.68
RAW DUST	2.68	68.5	4.58	16.0	2.91	0.77

CHAPTER VI - TEST PROCEDURE

A detailed review of the accomplishments, reported in Refs. [3], [4], and [5], has led to the establishment of the following procedure for the assessment of servovalve contaminant sensitivity. Maximum contaminant size injected is limited to 20 to 30 μm to avoid contaminant clogging of the built-in filters which was experienced by Ref. [3]. Furthermore, the population of larger particle sizes in filtered hydraulic systems might be very sparse. This fact would be discerned through the Beta Ten filter model, Fig. 6.1. This steep slope indicates a small population of larger particles. Test contaminant size, however, should not be stipulated at a single size range, such as 0-10 μm , as in Ref. [5], although it simplifies the test time and effort tremendously. A drawback of the procedure of Ref. [5] is the lack of capability to demonstrate the sensitivity of servovalves to various particle size ranges. As discussed in Chapter III, the spool-type valves which most of the flow control servovalves are composed of, often show high contaminant lock sensitivity to particular particle size ranges. For example, one servovalve might not be sensitive to 0-10 μm lower cut size, or its hysteresis might not increase much as contaminant concentration increases. On the other hand, the same servovalve might show a very large hysteresis in very low concentrations of 0-20 μm contaminant.

As stated in Ref. [5] and discussed in Chapter III, large particles are much more destructive on components' surfaces than smaller particles.



The evaluation technique of servovalve contaminant wear sensitivity could not be representative without the effect of particle impingement erosion due to contaminants. Therefore, 0-5 μm , 0-10 μm , and 0-20 μm lower cut dust are chosen to be standard test contaminant for servovalves.

The detailed test method is presented in the next paragraphs. The format used conforms to that of ISO Standards.

METHOD OF MEASURING AND REPORTING THE CONTAMINANT SENSITIVITY OF ELECTROHYDRAULIC FLOW CONTROL SERVOVALVES

1. Purpose

The purpose of this procedure is to provide a uniform test procedure and interpretation technique for evaluating the contaminant sensitivity of servovalves.

2. Scope

This recommended practice applies to all flow control servovalves which regulate flow rate.

3. Terms and Definitions

3.1 For definition of terms used, see Reference [15.1].

3.2 Contaminant injection - refers to the act of introducing classified test contaminants to the system fluid.

3.3 Contaminant concentration - denotes the contaminant weight per unit volume of fluid.

3.4 Contaminant lock sensitivity - the susceptibility of a spool type valve to the presence of contaminant. This is the measure of

silting force and is measured in terms of the degradation in hysteresis.

3.5 Contaminant wear sensitivity - the deterioration in a spool control orifice to the presence of contaminant. This wear is measured in terms of the degradation in pressure gain.

3.6 Test duration - the amount of time after each contaminant injection in which the test valve is exposed to contaminated fluid.

4. Units

The International Systems of Units (SI) is used here in accordance with Reference [15.2].

5. Graphic Symbols

Graphic symbols used herein are in accordance with Refs. [15.3] and [15.4]. Where [15.3] and [15.4] are not in agreement, Reference [15.2] governs.

6. Summary of Designated Information

Specify the following information on all requests for this test:

6.1 A full description of the valve

6.2 The type of fluid

6.3 The fluid temperature if different from Clause 7.1

6.4 The test pressure

6.5 The test flow rate

6.6 The test contaminant if different from Clause 7.3

6.7 The input requirement

7. Test Condition

- 7.1 Fluid temperature - shall be 43° C (110°F).
- 7.2 System volume - shall be numerically equal to one half the flow rate of the pump used for the test.
- 7.3 Test contaminant - Classified AC Fine Test Dust, 0-5 μm , 0-10 μm , 0-20 μm , 0-30 μm which are produced from AC Fine Test Dust per Reference [15.5].
- 7.4 Test contaminant concentration - 50 mg/L for wear test, 25 mg/L, 50 mg/L, and 100 mg/L for contaminant lock test.
- 7.5 Test Pressure - the maximum rated valve pressure drop for the test valve.
- 7.6 Test input current - 100 percent of input requirement for contaminant lock test. Cyclic input of 1 Hz with 50 percent of rated input amplitude for contaminant wear test.
- 7.7 Initial cleanliness level - the contaminant concentration level of the circulating fluid shall be less than 10 mg/L.

8. Test Condition Accuracy

Maintain the test condition accuracy within the limits shown in Table 6.1.

Test Condition	Accuracy \pm
Flow	2%
Pressure	2%
Input Current	2%
Temperature	2°C (3.6°F)
Contamination Concentration	10%

Table 6.1 - Accuracy Limits

9. Letter Symbols

The following symbols are used in this document:

P_s : Supply Pressure

P_v : Valve Pressure Drop

I_r : Rated Current

K_p : Pressure Gain

T : Fluid Temperature

Q_1 : Control Flow

10. Test Equipment

10.1 Hydraulic flow source insensitive to contaminant

10.2 Clean-up filter capable of achieving the initial cleanliness level

10.3 Heat exchanger which does not act as a contaminant trap

10.4 Reservoir with a conical shaped bottom

10.5 Flow diffuser at the point where the main return line empties into the reservoir

10.6 Three-way valve to by-pass system filter during contaminant injection period

- 10.7 Relief valve to maintain constant pressure supply to the test valve.
- 10.8 Flow meters which are insensitive to contaminant
- 10.9 Pressure transducers
- 10.10 Lines connecting hydraulic components sized so that turbulent mixing exists throughout
- 10.11 Injection chamber to introduce a required amount of contaminant into the test system
- 10.12 Test circuit as shown in Fig. 6.2
- 11. Test System Qualifying Procedure
 - 11.1 Install a direct connection in the test circuit in place of the test valve.
 - 11.2 Adjust system volume so that it equals 45 percent to 55 percent of the lowest volumetric flow rate per minute at which the test system is intended to be used.
 - 11.3 Circulate the fluid through the system filter until the contaminant background is less than 10 mg/L.
 - 11.4 By-pass the filter
 - 11.5 Add unclassified AC Fine Test Dust per Reference [15.6] to the fluid to bring the contaminant concentration to 100 mg/L.
 - 11.6 Inject the contaminant of Clause 11.5 in the form of a well-mixed slurry uniformly over a period of one minute.
 - 11.7 Operate the system at the minimum flow rate as described in Clause 11.2.

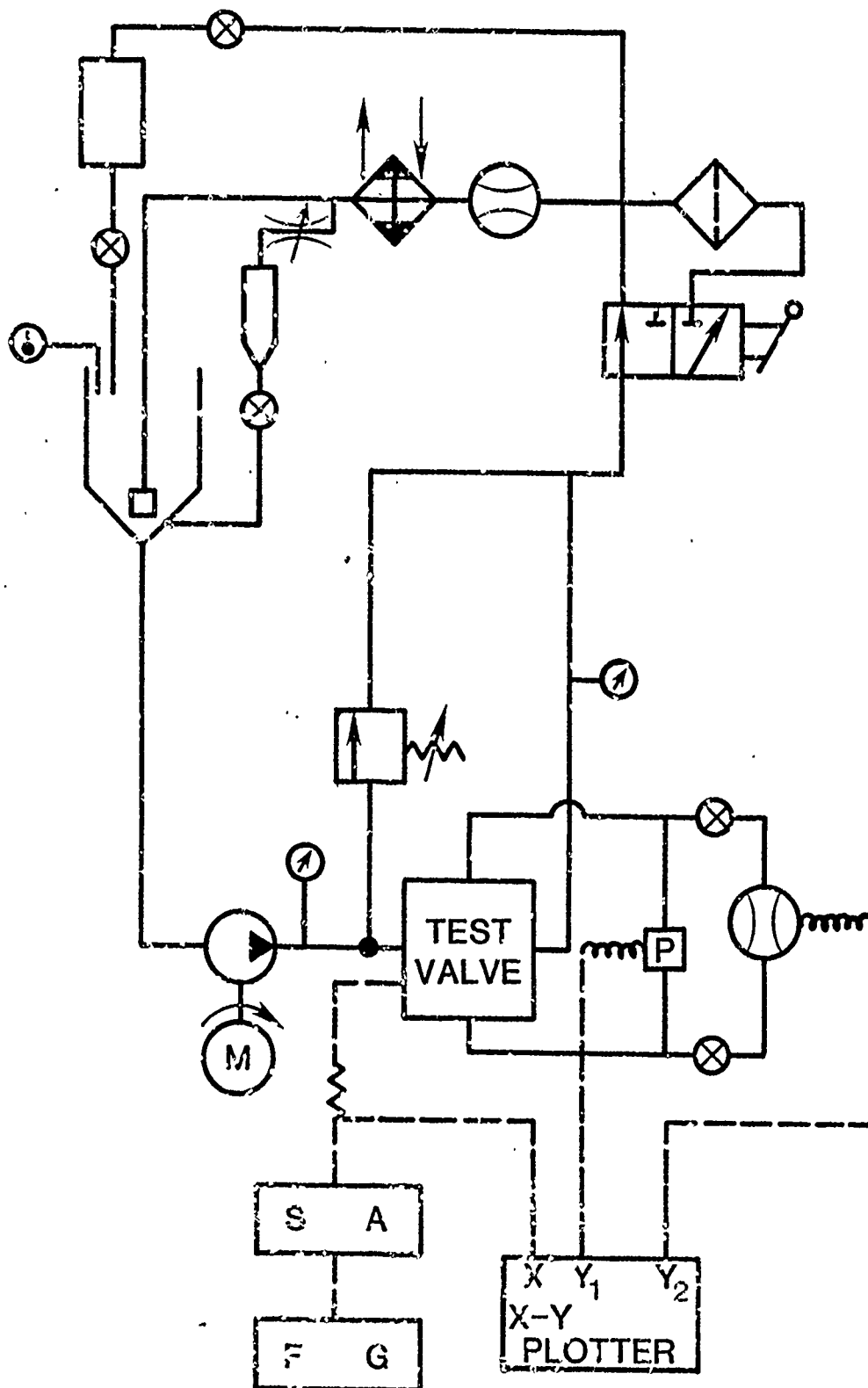


Fig. 6.2 Test Circuit

- 11.8 Extract four fluid samples from the system per Reference [15.6] at 15 minute intervals from the completion of contaminant injection.
- 11.9 Circulate fluid through the filter until the contaminant background is less than 10 mg/L.
- 11.10 Measure the contaminant concentration level of each sample per Reference [15.4].
- 11.11 Consider the system qualified for testing if the contaminant concentration levels of Clause 11.10 are within ± 10 percent of the initial requirement of Clause 11.5.
- 11.12 Repeat this qualification procedure when any modification to the flow path or to the reservoir is made.
- 12. Test Procedure
 - 12.1 Contaminant lock sensitivity
 - 12.1.1 Filter the fluid until the contaminant concentration level is less than 10 mg/L without the test valve.
 - 12.1.2 Install the test valve into the test circuit, Fig. 6.2.
 - 12.1.3 Set the valve pressure drop to the specified level.
 - 12.1.4 Record flow curve at the rated valve pressure drop per Reference [15.1].
 - 12.1.5 By-pass system filter
 - 12.1.6 Set the valve pressure drop at specified value.
 - 12.1.7 Set the test circuit for recording flow curve.
 - 12.1.8 Adjust the input current so that the test valve is set at null.

- 12.1.9 Prepare a slurry of classified AC Fine Test Dust of 0-5 μm , which will bring the contaminant concentration level of the fluid up to 25 mg/L.
- 12.1.10 Introduce the slurry into the test circuit through the injection chamber over a period of one minute.
- 12.1.11 Record the flow curves after one minute of stationary time.
- 12.1.12 Set the test valve at null.
- 12.1.13 Repeat Clauses 12.1.12 and 12.1.13 three times.
- 11.1.14 Reduce the supply pressure to the lowest level to prevent unnecessary wear.
- 12.1.15 Filter the fluid until the contaminant concentration level is less than 10 mg/L.
- 12.1.16 Repeat Clauses 12.1.3 and 12.1.16 for contaminant concentration levels, 50 mg/L and 100 mg/L.
- 12.1.17 Repeat Clauses 12.1.3 through 12.1.17 for contaminant sizes, 0-10 μm and 0-20 μm .
- 12.2 Contaminant wear sensitivity
 - 12.2.1 Perform Clauses 12.1.1 through 12.1.3.
 - 12.2.2 Record pressure gain per Reference [15.1].
 - 12.2.3 By-pass system filter.
 - 12.2.4 Set the valve pressure drop at specified level.
 - 12.2.5 Apply sinusoidal input current whose frequency and amplitude are 1 Hz and 50 percent of rated current, respectively.

- 12.2.6 Prepare a slurry of classified AC Fine Test Dust of $Q-5 \mu\text{m}$, which will bring the contaminant concentration level of the fluid up to 50 mg/L.
- 12.2.7 Introduce the slurry into the test circuit through injection chamber over a period of one minute.
- 12.2.8 Allow the contaminant to circulate through the test valve for a period of 30 minutes.
- 12.2.9 Reduce the supply pressure down to the minimum level as well as the sinusoidal current input to zero to prevent further wear.
- 12.2.10 Filter the fluid until the contaminant concentration level is less than 10 mg/L.
- 12.2.11 Record pressure gain per Reference [15.1].
- 12.2.12 Repeat Clauses 12.2.3 through 12.2.11 for contaminant sizes, 0-10 μm and 0-20 μm .
- 13. Data Preparation
 - 13.1 Record test valve identification and operating conditions for contaminant lock and contaminant wear sensitivities in Tables 6.2 and 6.3.
 - 13.2 Tabulate test data in Table 6.2. Hysteresis increase is averaged and obtained by subtracting the hysteresis in clean fluid from that in controlled contaminant condition.

Table 6.2 Contaminant Lock Sensitivity Data Sheet

CONTAMINANT LOCK SENSITIVITY

DATE TESTED:_____ TEST LOCATION:_____

SERVOVALVE:_____ NO.:_____

_____ SYSTEM VOLUME:_____

VALVE PRESSURE DROP:_____ TEST FLUID:_____

RATED FLOW:_____ FLUID VISCOSITY:_____

TEMPERATURE:_____ TYPE OF CONTAMINANT:_____

CONTAMINANT SIZE (μm)	CONCENTRATION (mg/L)	AVG. HYSTERESIS INCREASE (%)
0-5		
0-10		
0-20		
0-30		

Table 6.3 Contaminant Wear Sensitivity Data Sheet

CONTAMINANT WEAR SENSITIVITY

DATE TESTED: _____

TEST LOCATION: _____

SERVOVALVE: _____

NO.: _____

SYSTEM VOLUME: _____

VALVE PRESSURE DROP: _____

CONCENTRATION: _____

RATED FLOW: _____

FLUID VISCOSITY: _____

INPUT CYCLE: _____

TYPE OF CONTAMINANT: _____

INPUT CURRENT, AMP.: _____

TEMPERATURE: _____

CONTAMINANT SIZE (μm)	ACTUAL PRESSURE GAIN UNIT:	PRESSURE GAIN DEGRADATION RATIO
INITIAL		
0-5		
0-10		
0-20		

- 13.3 Tabulate wear test data in Table 6.2. The pressure gain is measured per Reference [15.1].
- 13.4 Plot on linear coordinates the hysteresis increase versus the respective maximum particle size from the data tabulated in Clause 13.2 (Example Fig. 6.3).
- 13.5 Plot on linear coordinates the pressure gain versus the respective maximum particle size from the data tabulated in Clause 13.3 (Example Fig. 6.4).
14. Identification Statement
- Use the following statement in catalogs and sales literature when electing to comply with this voluntary standard: "Contaminant sensitivity obtained in accordance with ISO Standard."
15. References
- 15.1 Aerospace Recommended Practice 490.D
- 15.2 International Standard Rules for the Use of the International System of Units and a Selection of the Decimal Multiples and Sub-Multiples of S.I. Units, ISO/R, 1000, 1976.
- 15.3 International Standard Graphic Symbols for Hydraulic and Pneumatic Equipment and Accessories for Fluid Power Transmission, ISO/R, 1219-1970. Agrees with ANSI/Y32, 10-1967.
- 15.4 American National Standard Fluid Power Diagrams, ANSI/Y14, 14-17-1966.
- 15.5 Air Cleaner Test Code - SAE J726C

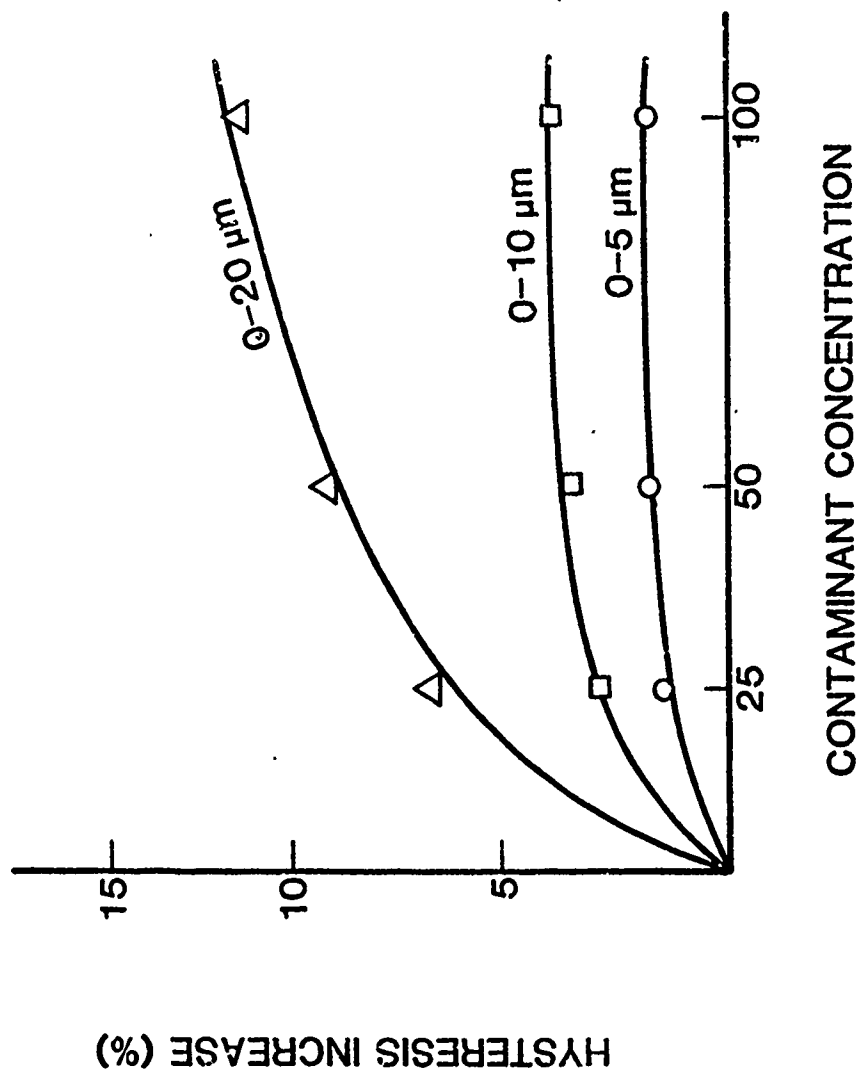


Fig. 6.3 Hysteresis Increase Characteristic Curves

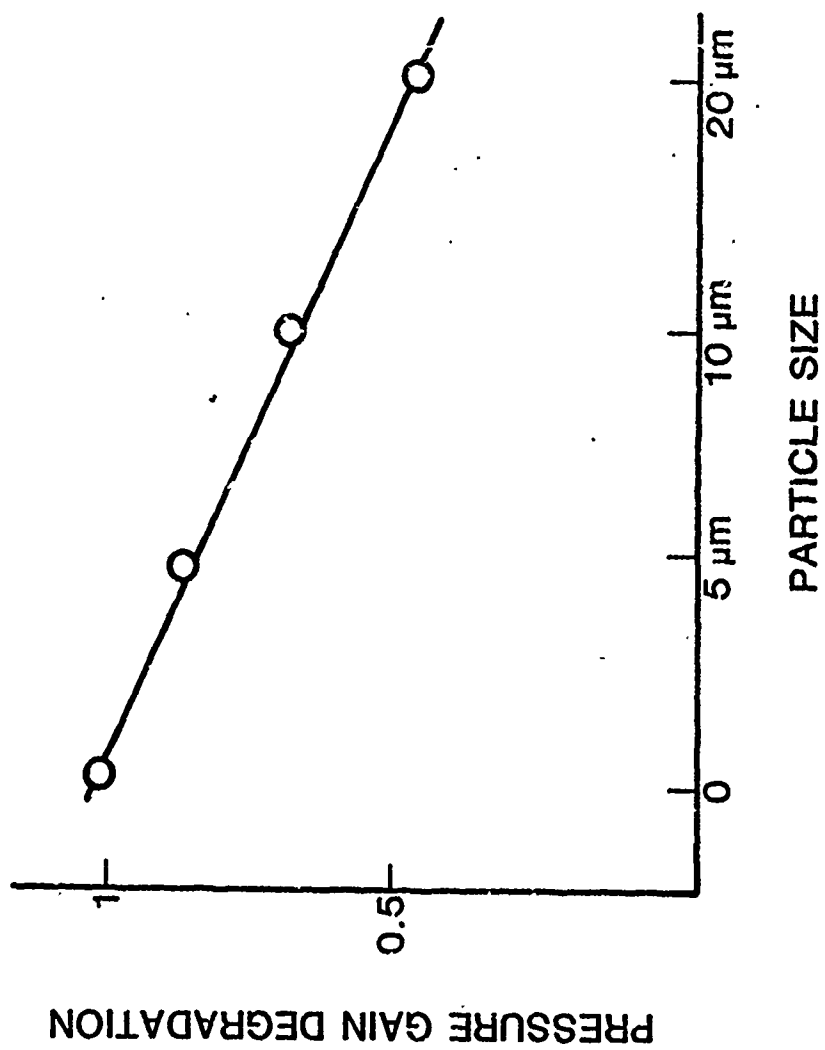


Fig. 6.4 Pressure Gain Degradation Curve

15.6 Hydraulic Fluid Power - Particulate Contamination Analysis -
Extraction of Fluid Samples from Lines of an Operating System -
ISO 4021.

CHAPTER VII - TEST RESULTS

Servo valve contaminant sensitivity tests were conducted on three servo valves from different manufacturers. The contaminant lock and contaminant wear tests were performed using the same specimens. The contaminant lock test was conducted first in each case because of the destructive nature of the wear test. The specimens were designated A, B, and C.

Some changes were made in the test procedures during the project in an effort to optimize the tests in terms of time, effort, and accuracy. The procedure shown in the previous chapter is the recommended test.

Specimen A was exposed for 30 minutes to 25 mg/L of 0-5 μm lower cut test dust. A set of flow curves was recorded in the no load condition as well as the loaded condition. After 30 minutes of test, the test system was filtered to reduce the background contaminant level to less than 10 mg/L. The concentration level was then increased to 50 mg/L and 100 mg/L with the same cut dust, and flow curves were recorded in the same manner. The test pattern was repeated for 0-10 μm , 0-20 μm , and 0-30 μm . At 100 mg/L of 0-30 μm dust, hysteresis was excessive, and the test was terminated.

At the end of the contaminant lock test, this specimen showed excessive null shift; and, as a result, the flow curve became asymmetric because of the long operation time in contaminant condition. A contributing factor to the failure of this valve might be the fact that

the control current was zero but the spool was not at null while the specimen was idled for one minute before hysteresis measurement. This situation was avoided or compensated in subsequent tests.

The wear test for Specimen A was performed after the contaminant lock test, although the specimen was obviously worn out because a new specimen from the manufacturer was not available. The concentration of the wear test was kept constant at 50 mg/L throughout for Specimen A. The test procedure introduced in Chapter VI was followed.

As a result of the damage done to Valve A, the procedure was improved to minimize exposure time of specimens in dirty fluid as well as to set the spools at null for the stationary time period.

For Specimen B, the no load flow curve was recorded in only 10 minutes in dirty fluid. The test system was then filtered until the background concentration level was reduced to less than 10 mg/L. At the beginning of the test, Specimen B was exposed to 100 mg/L of 0-5 μ m lower cut dust for 30 minutes. At this time, the valve pressure drop was varied from 100 psi to 2000 psi and then to 3000 psi to see the effect of supply pressure to flow curve. The hysteresis was recorded at each pressure. After cleaning the test system, the contaminant injection schedule was 25, 50, and 100 mg/L of each of three particle size ranges: 0-5, 0-10, and 0-20 μ m.

The wear test for Specimen B was conducted in exactly the same way as for Specimen A, except that the contaminant concentration level increased to 100 mg/L throughout.

Specimen C was tested for contaminant lock sensitivity using hysteresis measured from the pressure gain curve. Maximum hysteresis was measured from the curve within ± 40 percent of the valve pressure drop. For example, the straight line of pressure gain for the curve for positive-to-negative pressure drop was first drawn per SAE ARP 490D. Similarly, a straight line for negative-to-positive valve pressure drop was drawn. The hysteresis was defined at the maximum distance between the lines.

The contaminant injection schedule for Specimen C was determined so that the contaminant exposure time of the specimen was further decreased by adding the contaminant to the test system continuously. Initially, 25 mg/L of 0-5 μm dust was injected and hysteresis was recorded. After 10 minutes, another amount of contaminant was added to raise the system concentration level to 50 mg/L, and again hysteresis was recorded for 10 minutes of test time. Additional contaminant was again injected to raise the concentration level to 100 mg/L for the last 10 minutes of the test. Hysteresis was again recorded. This procedure was repeated for 0-10 μm and 0-20 μm test dust.

The wear test for Specimen C was conducted at the same condition as for Specimen A.

CONTAMINANT LOCK SENSITIVITY

The performance degradation due to contaminant lock was determined from the hysteresis increase derived from flow curves when the servo-valves were cycled between positive and negative rated current per SAE

ARP 490D. Maximum hysteresis values were measured in the region of ± 20 percent of rated current. The reason is because the performance around null is critical to servo systems due to the fact that servo-valves in position control systems respond in the null region most of the time. The measuring capability of the flowmeter is also an important factor. A flowmeter was used to record flow curves and hysteresis to prevent contaminant settlement which might occur if a cylinder were used for the measurement. The flowmeter, however, has limited accuracy within ± 10 percent of maximum measurable flow rate.

PERFORMANCE DEGRADATION DUE TO CONTAMINANT LOCK

The hysteresis increase for each injection is shown on the contaminant lock sensitivity report sheet in Tables 7.1 to 7.3. These values are plotted in Fig. 7.1 to 7.3. In the figures, theoretical fitted curves were overlaid on actual data points.

THE OMEGA RATING AND FILTER REQUIREMENT

From the theoretical curves, contaminant lock coefficients, X and Y , are known. X_β and Y_β in the Beta 10 filter model are then calculated from Eq. (4-4). A summary of calculations of coefficients X and Y is tabulated in Table 7.4. The lock coefficients of X_β and Y_β are substituted into Eq. (4-2) to produce the curves showing the relationship between the Beta 10 filter model and hysteresis increase, as depicted in Figs. 7.4 to 7.6. Finally, Omega rating values for the servovalves tested are shown.

TABLE 7-1

SERVOVALVE CONTAMINANT SENSITIVITY TEST RESULTS

CONTAMINANT LOCK SENSITIVITY

Date Tested:

Test Location:

Servo valve: A

No.: 1

Rated Flow: 5 gpm

System Volume:

Valve Pressure Drop: 3000 psi

Fluid Viscosity:

Temperature: 110°F

Type of Contaminant:

Test Fluid:

CONTAMINANT SIZE (μ M)	CONCENTRATION mg/L	AVERAGE HYSTERESIS Increase %
0-5	25	1.5
	50	1.9
	100	2.7
0-10	25	1.6
	50	2.0
	100	3.0
0-20	25	1.8
	50	1.9
	100	4.5
0-30	25	3.0
	50	10.2
	100	32.4

TABLE 7-2

SERVOVALVE CONTAMINANT SENSITIVITY TEST RESULTS

CONTAMINANT LOCK SENSITIVITY

Date Tested:

Test Location:

Servovalve: B

No.: 2

System Volume:

Valve Pressure Drop: 3000 psi

Test Fluid:

Rated Flow: 7.5 gpm

Fluid Viscosity:

Temperature: 110°F

Type of Contaminant:

CONTAMINANT SIZE (μ M)	CONCENTRATION mg/L	AVERAGE HYSTERESIS	
		Increase	%
0-5	25	2.6	
	50	2.6	
	100	2.2	
0-10	25	2.1	
	50	2.3	
	100	2.5	
0-20	25	4.2	
	50	4.6	
	100	8.8	
0-30			

TABLE 7-3

SERVOVALVE CONTAMINANT SENSITIVITY TEST RESULTS

CONTAMINANT LOCK SENSITIVITY

Date Tested:

Test Location:

Servo valve: C

No.: 3

System Volume:

Valve Pressure Drop: 3000 psi

Test Fluid:

Rated Flow: 5 gpm

Fluid Viscosity:

Temperature: 110°F

Type of Contaminant:

CONTAMINANT SIZE (μ M)	CONCENTRATION mg/L	AVERAGE HYSTERESIS Increase %
0-5	25	0
	50	0
	100	0
0-10	25	0.2
	50	0.9
	100	0.9
0-20	25	1.3
	50	13.4
	100	15.1
0-30		

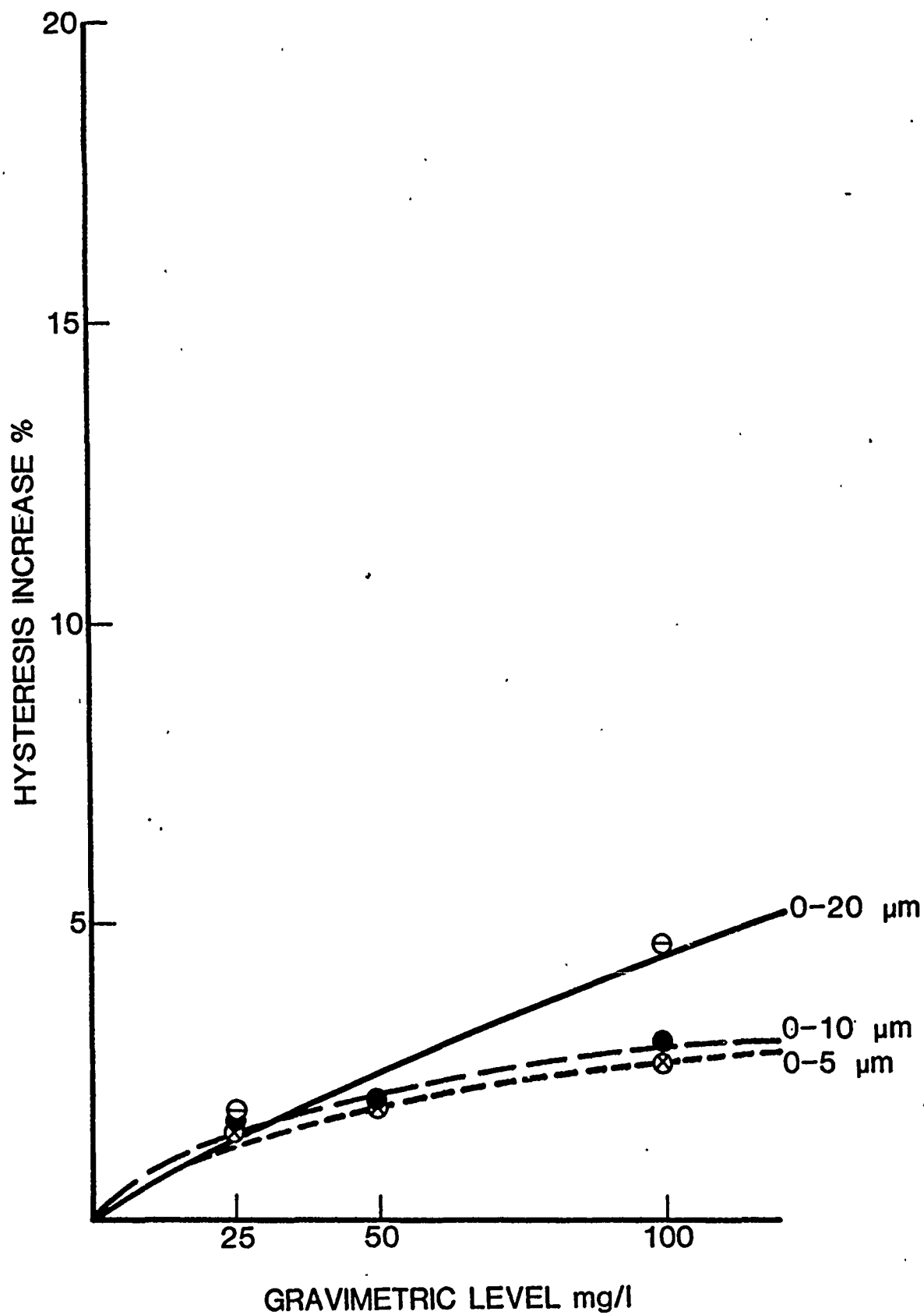


Fig. 7.1 Test Result of Servovalve A -- Hysteresis Increase

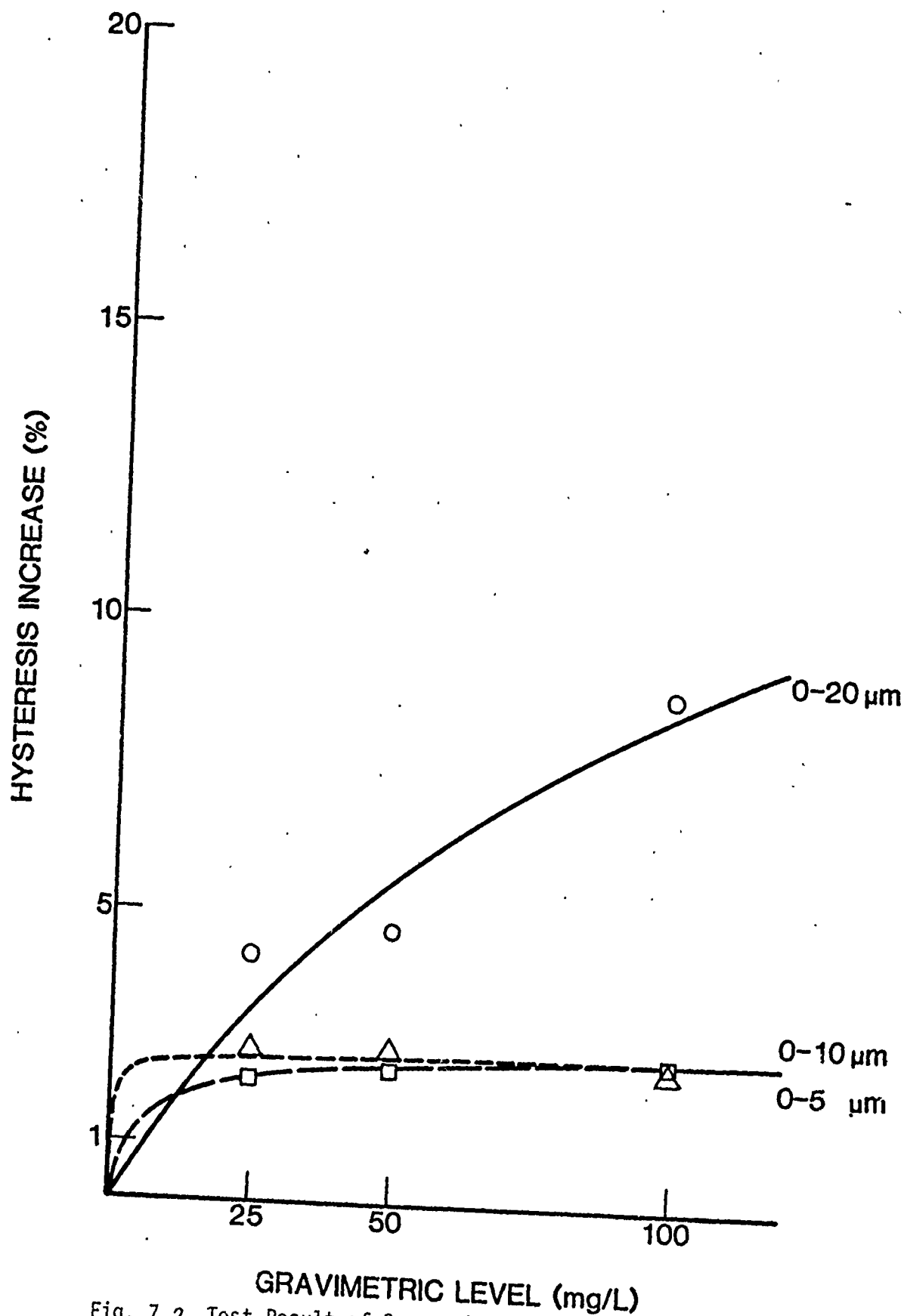


Fig. 7.2 Test Result of Servovalve B -- Hysteresis Increase

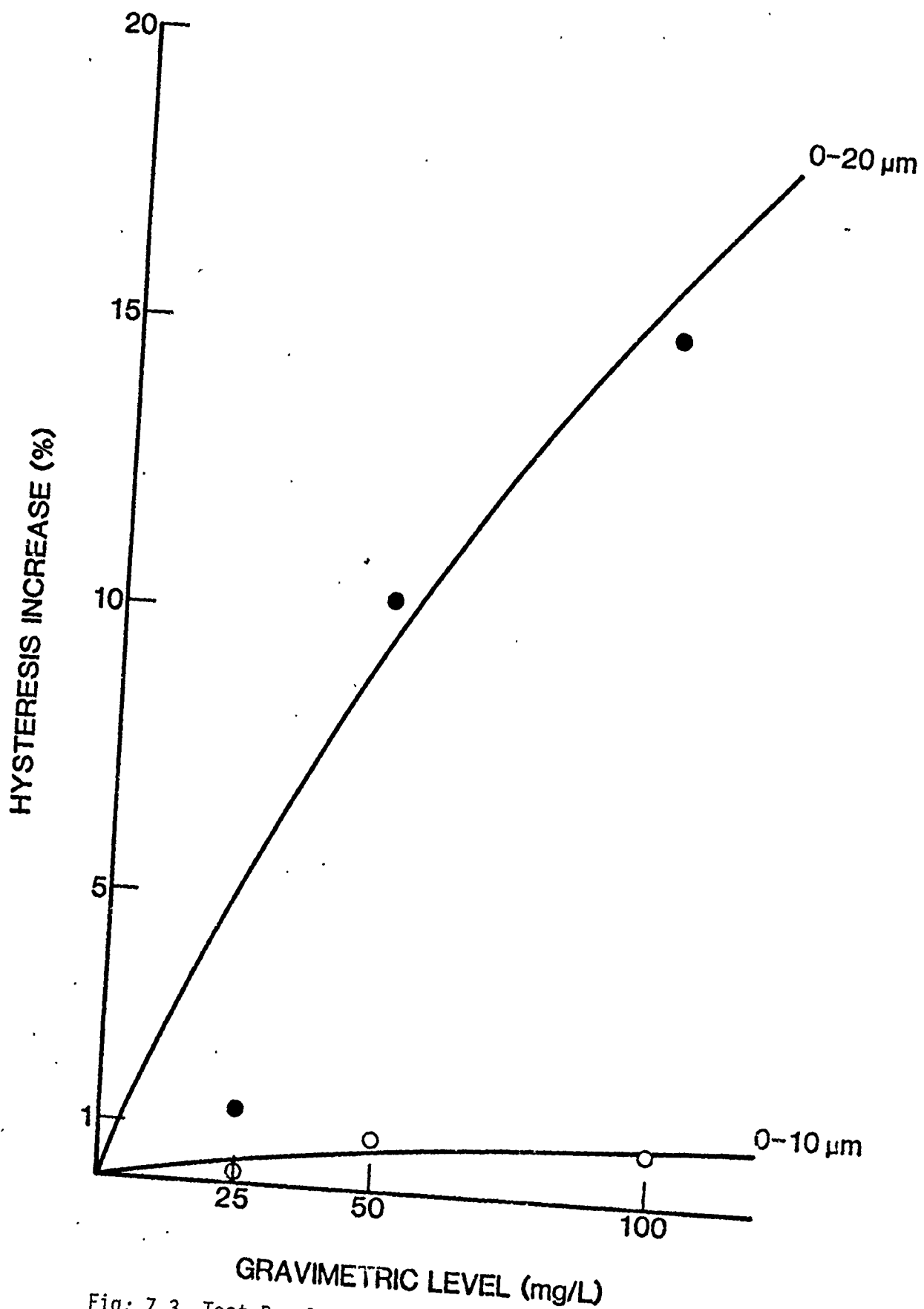


Fig: 7.3 Test Results of Servo Valve C -- Hysteresis Increase

Table 7.4 Summary of Calculation on Coefficients X & Y

SERVO- VALVE	CONTAM- INANT SIZE (μm)	X_i	Y_i	X_β	Y_β
A	0-5	4.75	0.0410	5.2572	0.0395
	0-10	5.663	0.0329		
	0-20	34.589	0.0031		
B	0-5	2.548	20.2418	2.8897	17.5328
	0-10	2.913	0.4623		
	0-20	24.491	0.0135		
C	0-5	0		1.368	0.0021
	0-10	2.531	0.0166		
	0-20	69.026	0.0070		

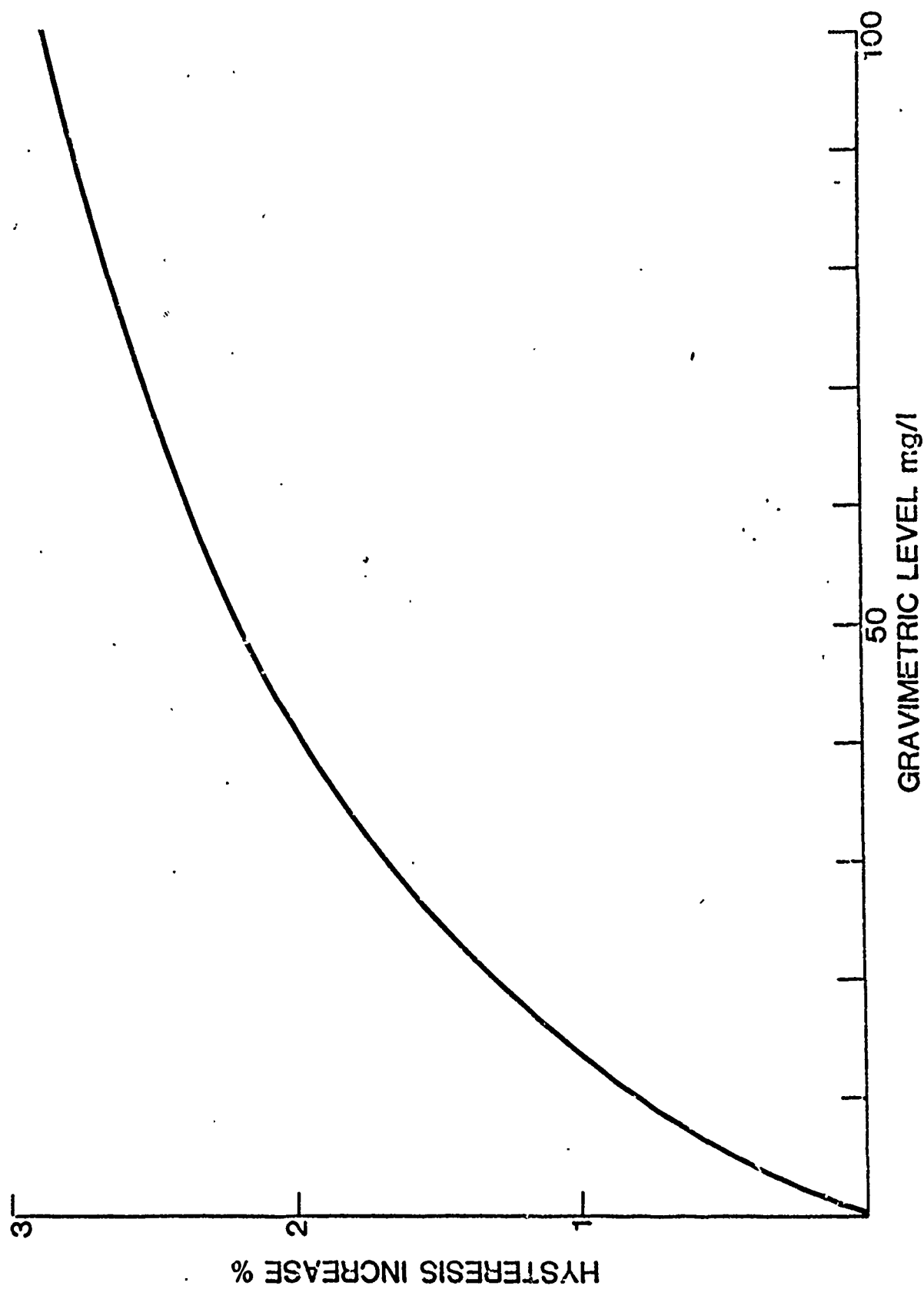


Fig. 7.4 Hysteresis Increase of Beta Model for Servovalve A

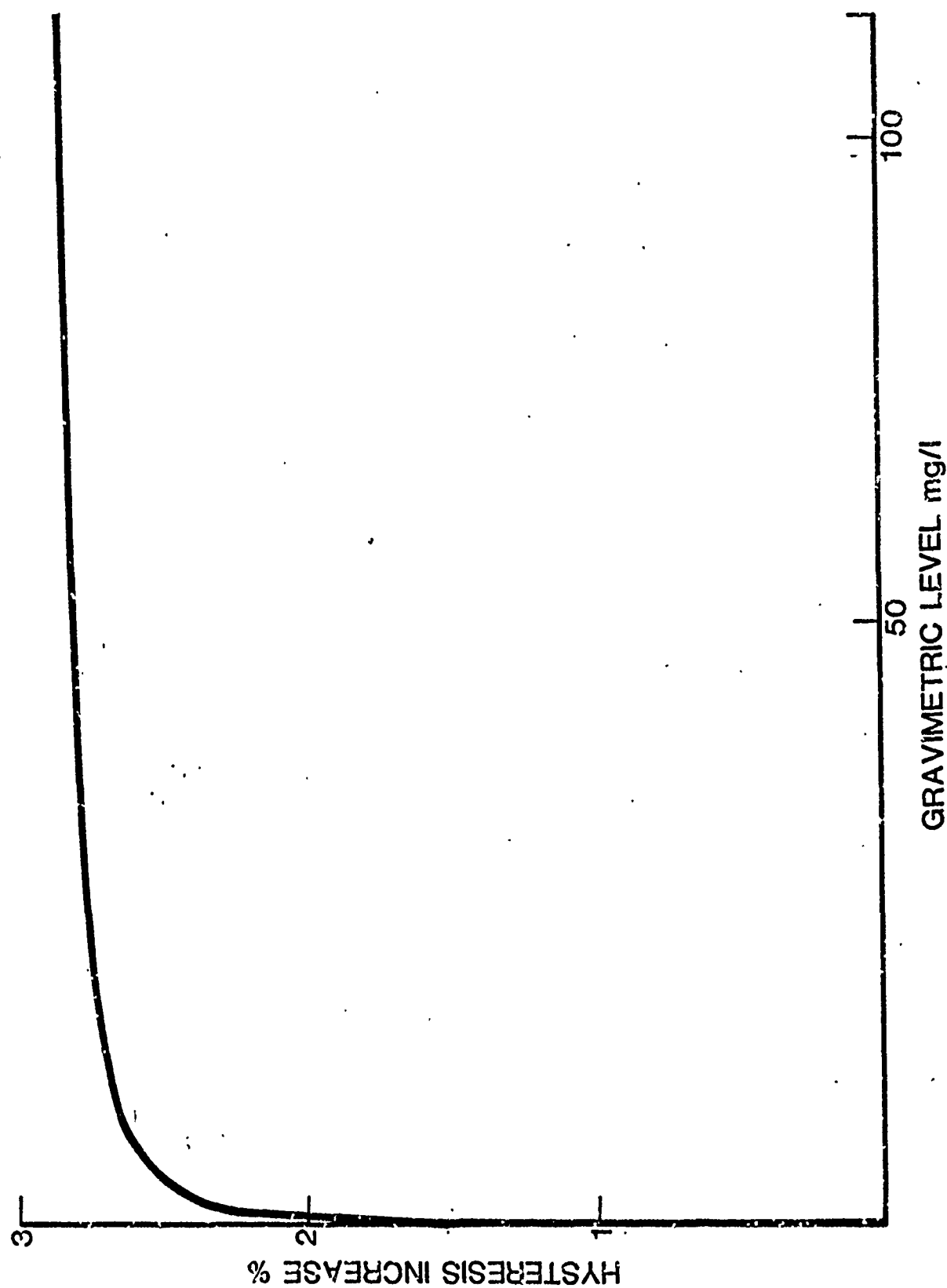


Fig. 7.5 Hysteresis Increase on Beta Model for Servovalve B

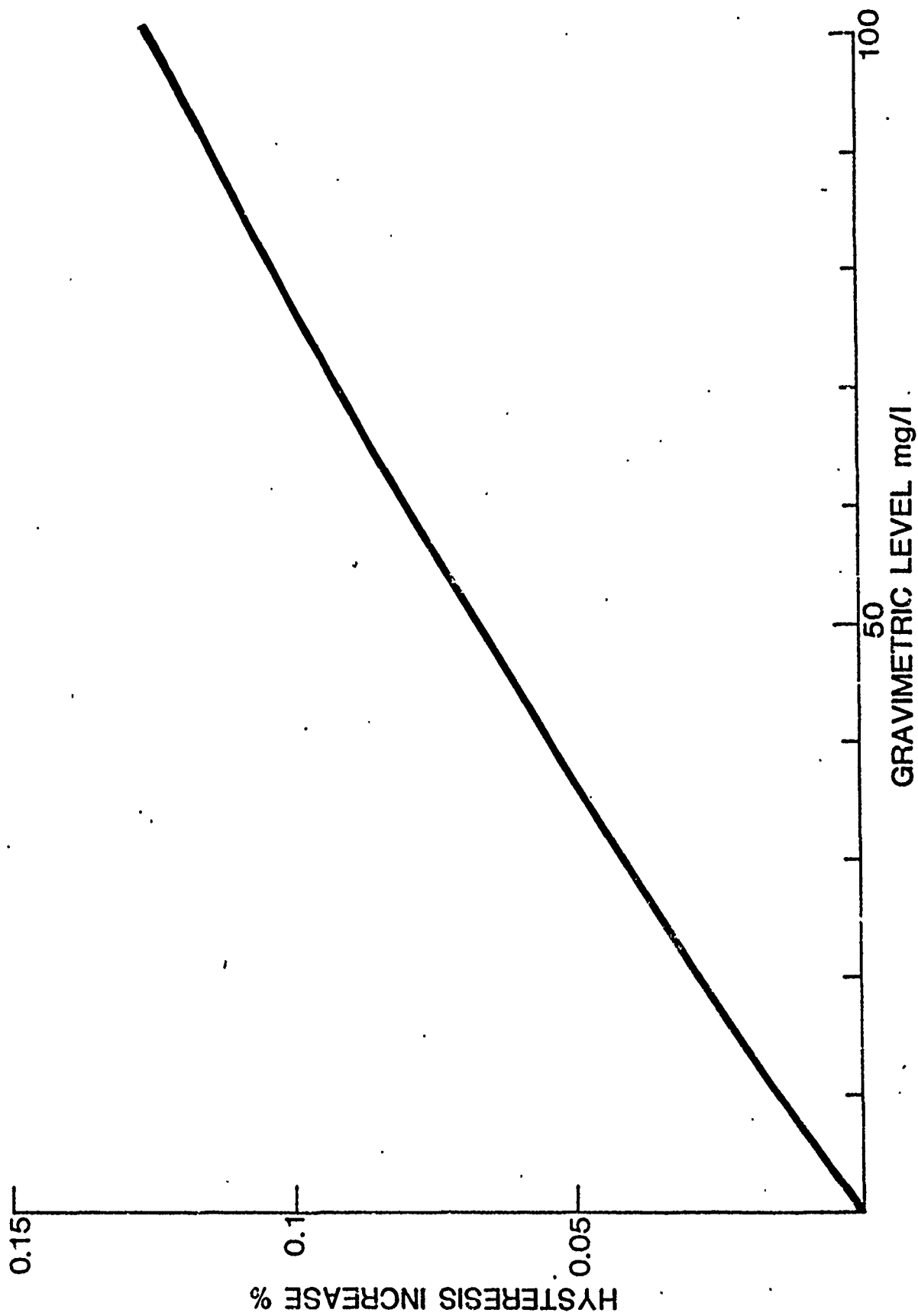


Fig. 7.6 Hysteresis Increase of Beta Model for Servovalve C

PERFORMANCE DEGRADATION DUE TO CONTAMINANT LOCK

The hysteresis increases for each particle size injection plotted in Figs. 7.1 through 7.3 for the tested valves. The fitted curves were obtained by calculating the least square errors of Eq. (4-2). From the figures, it can be seen that Servovalve "A" demonstrated insensitivity to contaminant size 0-20 μm ; whereas, the other servovalves exhibited large hysteresis width, indicating significant sensitivity to that size range.

Figure 7.2 shows that Servovalve B was sensitive to contaminants in even smaller particle size ranges and low gravimetric levels, although the gravimetric level did not significantly affect the valve performance of Valve B for smaller particle sizes. Hysteresis increases were almost constant from 25 mg/L to 100 mg/L as shown in Fig. 7.2.

Servovalve C showed no hysteresis increase for 0-5 μm size contaminants and only a small increase for 0-10 μm contaminants, as shown in Fig. 7.3. This servovalve, however, was very sensitive to the 0-20 μm size range. Hysteresis increased up to 15 percent at 100 mg/L concentration. Fortunately, for this servovalve, larger contaminants might not be a problem if a good filter is provided to remove the particles which are greater than 10 μm .

CONTAMINANT LOCK OMEGA RATING

As a process to find the fitted curves to data points, the coefficients, X_i and Y_i , in Eq. (4-2) were calculated and are tabulated

in Table 7.1. The values of these coefficients and the contribution of each particle size interval to hysteresis increase are calculated from Eq. (4-3). These values are then substituted into Eq. (4-4) to obtain X_B and Y_B in the Beta ten filter model.

This transformation to the Beta model gives the relationship between hysteresis increase and gravimetric level, as shown in Figs. 7.4 to 7.6. By setting the specification of allowable hysteresis increase to 2.5 percent, the acceptable gravimetric values for each of the servovalves can be found. The Omega rating values are then found from Fig. 4.1, which represents the gravimetric level vs Beta-ten values.

The Omega ratings for the valves tested are shown in Table 7.5.

Servovalves	Omega Rating Values
A	1.4
B	6.0
C	1.1

Table 7.5. Summary of Contaminant Lock
Omega Rating

To obtain specified performance, the hydraulic system must have filters with Beta 10 of 1.4 for Servovalve A, 6.0 for B, and 1.1 for C.

CONTAMINANT WEAR

Evaluations on contamination wear for servovalves were conducted after the lock sensitivity test. Sinusoidal current input was applied to the specimens at valve pressure drop of 3000 psi with no load. Throughout the test, the control flow rate and input current were monitored

by a digital oscilloscope to control excessive null shift, although no significant null shift was observed during the wear test.

PERFORMANCE DEGRADATION DUE TO CONTAMINANT WEAR

Figure 7.7 represents the pressure gain degradation for three test specimens. The gains are presented in the figures based on the reference values obtained at the beginning of the wear test or after the contaminant lock test. It was observed and reconfirmed from all the specimens that servovalves' control orifices are quickly worn off by contaminants. The susceptibility of the servovalves to contaminant wear can be easily recognized from the pressure gain degradation curves. The degradation curve for Specimen A was obtained after the contaminant lock test (Fig. 7.7). The sharp orifices of the specimens were probably already rounded at that time. It is likely, therefore, that a new valve of this type would have shown an even higher degradation slope than was seen with this used valve.

There are two degradation curves for Specimen B in Fig. 7.7. The solid line represents experimental data for a 100 mg/L contaminant concentration. For comparison with other data, the degradation curve was calculated using the normalized formula explained earlier in this report. Thus, the dotted line predicts the degradation curve for Specimen B under contaminant concentration of 50 mg/L. It is seen that the specimen demonstrated excellent performance on the particle size interval of 0-5 μm . The degradation ratio to the reference value is 0.996. The variation of pressure gain of this specimen is shown in Fig. 7.8.

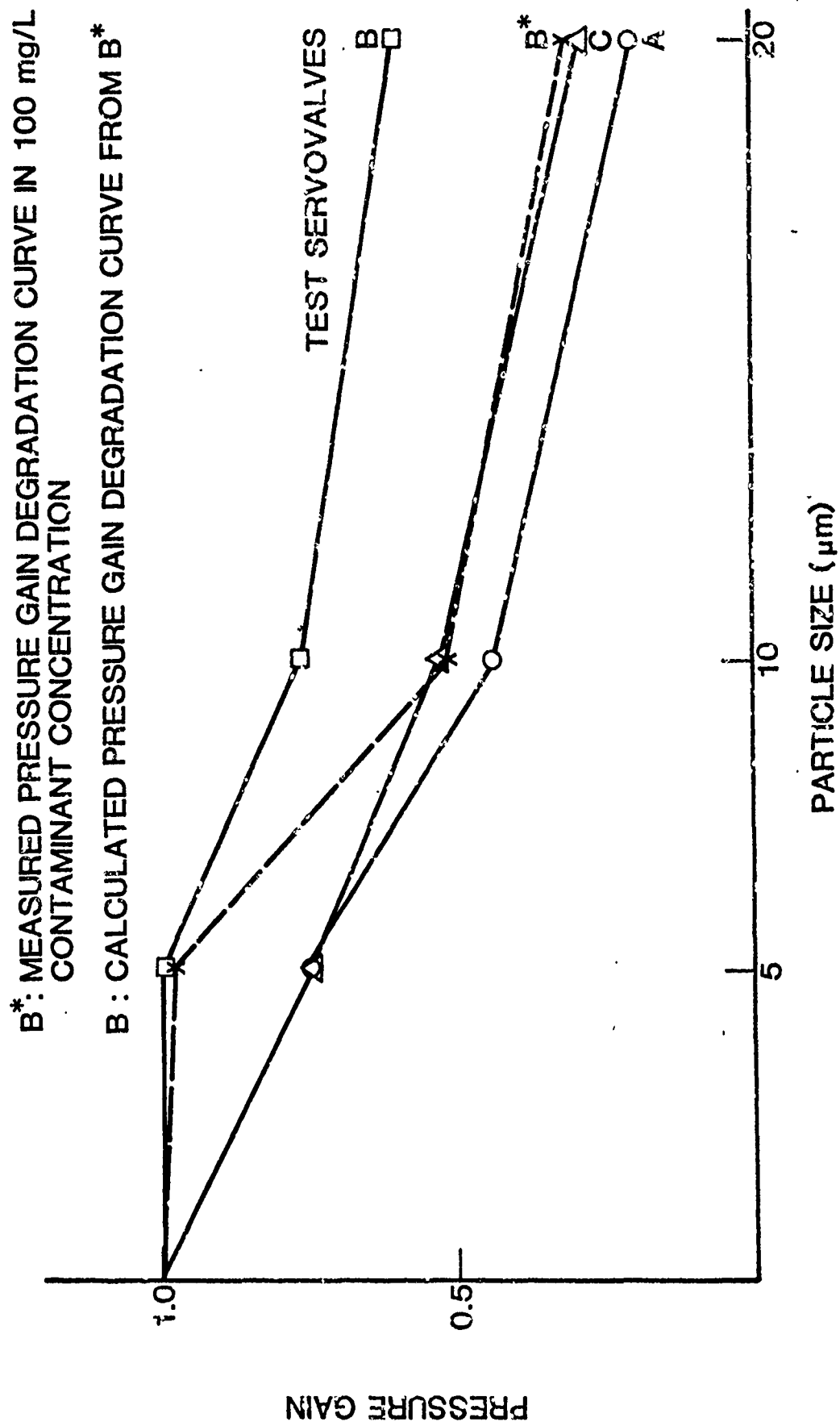


Fig. 7.7 Measured Pressure Degradation for Servovalves A, B, and C.

PRESSURE GAIN AFTER THE END
OF CONTAMINANT LOCK TEST
WAS SET AT 1.

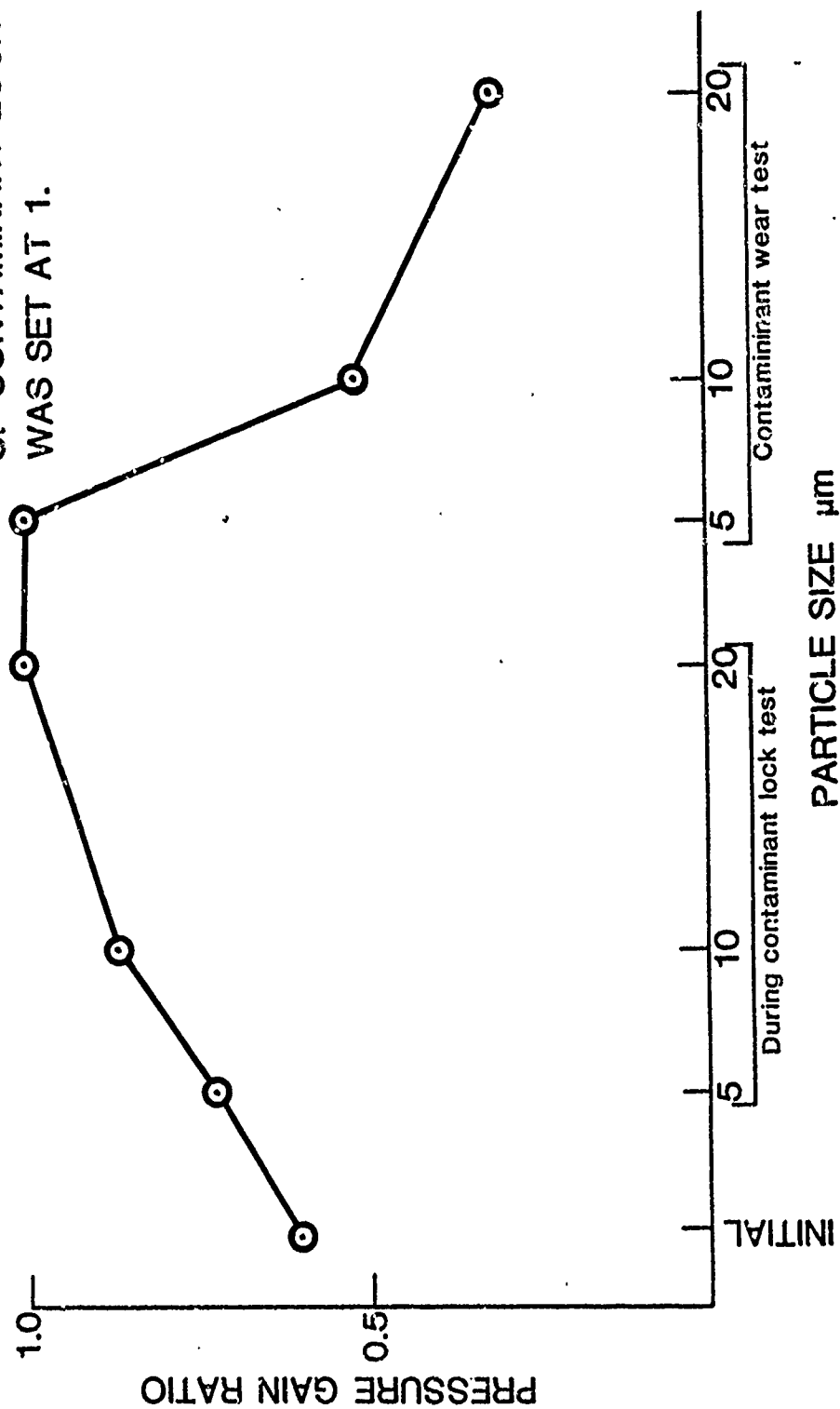


Fig. 7.8 Total Pressure Gain Profile for Valve B

The figure shows that the pressure gain initially increased to a value twice as large as the value when the specimen was new. Then, it dropped to approximately 60 percent of the original pressure gain. No explanation can be offered for this apparent ambiguity.

Figure 7.7 also shows the pressure gain degradation of Specimen C. As with the other specimens, it degraded very quickly. By the end of the test, its value dropped to 30 percent of the reference pressure gain.

OMEGA RATING

Based on the pressure gain degradation, servovalve tolerance profiles for 1000 hour life were calculated according to the wear theory discussed in previous chapters. The calculation was accomplished using a computer. The pump data reduction program for contamination sensitivity has been modified to obtain profiles for servovalves, since main structure is very similar. Allowable pressure gain degradation was set at 20 percent of initial pressure gain. If a specification did allow for servovalves to degrade by (say) 50 percent, then the degradation allowance could be set at 50 percent. Then, less efficiency could be selected to obtain 1000 hour life.

Effect of the particles greater than 20 μm was extrapolated from the experimental data of 0-5 μm , 0-10 μm and 0-20 μm . Then, these experimental data and extrapolated data (up to 50 μm) were provided into the modified data reduction program to obtain the profiles.

Servo valve tolerance profile curves are drawn on the contamination chart with a Beta ten filter model which is approximated by straight lines. Figure 7.9 shows the contaminant wear tolerance profiles for Specimens A, B, and C, respectively.

Omega rating values for the specimens can be found from the chart. The Omega rating value is obtained from the point that the profile curves indicate minimum along the Beta ten curves. For example, the Omega rating of Specimen A in Fig. 7.11 is found to be 1700 because no point on the profile goes beyond the line for a Beta ten of 1700. Similarly, Omega values for the rest of the specimens can be easily obtained; Omega values are summarized in Table 7.6.

Servo valves	Omega Rating
A	1700
B	140
C	1700

Table 7.6. Summary of Contaminant Wear
Omega Rating

From the results of the contaminant wear tests, servo valves definitely need excellent filters to keep desired performance for a specified period of time. There is one order of magnitude difference between Servo valves A and B in Omega rating; however, there is really no difference in selecting filters for them. Above a Beta ten of 75, a minute difference in particle counts makes a significant change in the

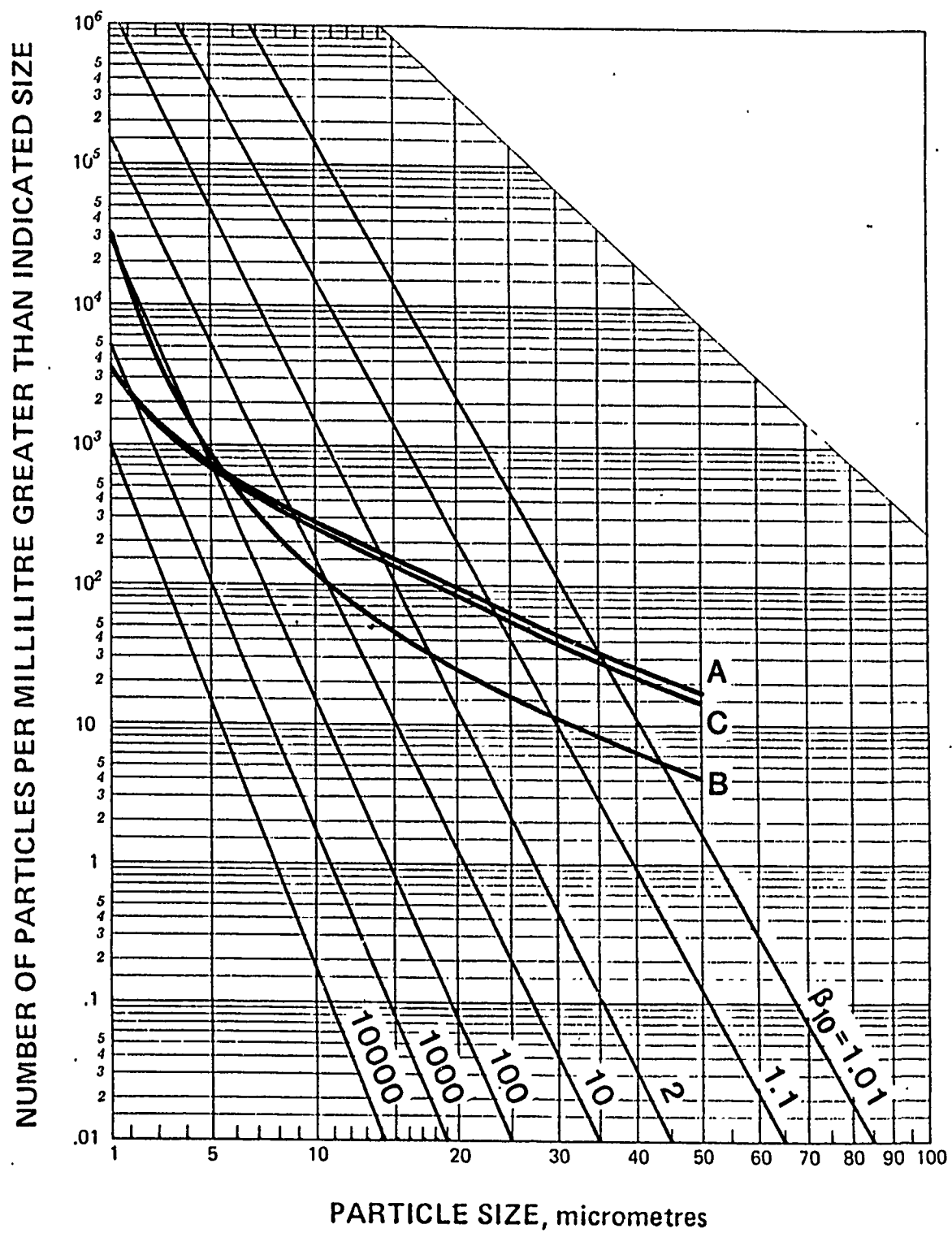


Fig. 7.9 Contaminant Tolerance Profiles

Beta rating. This is also seen from the efficiency of filters. A Beta ten of 100 means that the filter has 99 percent efficiency to capture particles greater than 10 μm . A filter rated at Beta ten of 1000 has 99.9 percent efficiency.

CHAPTER VIII - CONCLUSIONS AND RECOMMENDATIONS

This test procedure for the contaminant sensitivity for servovalves was established after review of previous attempts by other organizations to evaluate their contaminant sensitivity. Two different test procedures and data reduction techniques were found to be necessary to evaluate contaminant lock and contaminant wear sensitivities. The sensitivities for servovalves are represented on two different Omega rating values. Each rating value not only provides comparative figures among servovalves but also represents the filter requirements to achieve the desired performance. There could also be indications of possible degree of catastrophic and degradation failures.

According to the test procedure and data reduction technique developed, three commercially available servovalves were evaluated for susceptibility to particulate contaminants. These servovalves were found to be rather tolerant of the contaminant induced friction force on the spools which gives rise to contaminant lock. Consequently, the contaminant lock Omega values for the test servovalves were relatively low. A number of filters available in the market could supply sufficiently clean fluid for these servovalves. According to filter tests conducted at the FPRC in recent years, approximately half the filters tested are better than Beta ten of 6, the level required by one of the test servovalves. Therefore, these servovalves are as insensitive to contaminant as other hydraulic components as far as contaminant lock is concerned.

On the other hand, the contaminant wear tests showed that the test servovalves are very susceptible to contaminant and require very good filtration to fulfill specifications. Contaminant particles impinging on control orifices at high speed wore off the sharpness of the orifice corners in a short period of time. This not only changed the servovalve pressure gain but also increased the leakage flow; thus, it might be very critical to the servosystems, which have to overcome very strong loads with little compliance or which have limitation on hydraulic power consumption.

Pressure gain change for these servovalves tested showed excessive variation in 90 minutes of operation with 50 mg/L contaminant concentration. After the end of the wear test for each servovalve, a loss of almost 70 percent of the original pressure gain was seen. Since contaminant concentration is also a measure of time factor, it can be projected that the same degradation would occur in 900 minutes (15 hours) with a 5 mg/L contamination concentration or 75 hours at 1 mg/L. Although this calculation is too simple to predict total life, it is obvious that present day servovalves are very susceptible to contaminant wear.

It would be worthwhile to mention that other servovalve parameters, such as flow gain, vary at the same time that pressure gain changes. Since flow gain contributes to the loop gain of the total servo system, severe stability problems can be expected when flow gain varies.

The following conclusions can be drawn from the work done during this project:

1. No previous work provided a satisfactory technique for evaluating the contaminant sensitivity of servovalves.
2. The testing done using the developed procedure indicates that the differences in the contaminant tolerance of different servovalves can be readily detected.
3. As a result of the testing done using the procedures developed during this project, it was concluded that contaminant wear is a more severe problem than contaminant lock in servovalves.

It is recommended that this procedure be adopted by MERADCOM for evaluating the contaminant sensitivity of servovalves and that only the most tolerant valves be utilized in military systems.

REFERENCES

1. Williams, L. J., "Fluid Contamination Effects on Servovalve Performance," Mccg Technical Bulletin 115.
2. Nair, K. S., "Survey on Applications of Servovalves for Industrial and Mobile Hydraulics," The BFPR Journal, 1981, 14:425-429.
3. Kinney, W. L., et.al., "Hydraulic Servo-Control Valves, Part VI, Research on Electrohydraulic Servovalves Dealing with Oil Contamination, Life and Reliability, Nuclear Radiation and Valve Testing," Wright Air Development Center, Air Research and Development Command, United States Air Force, Wright-Patterson Air Force Base, Ohio, WADC Technical Report 55-29 Part VI, 1958.
4. Arnold, J. T., et.al., "Electrohydraulic Servo-Control Valves, Reliability Test of a Number of Representative Electrohydraulic Servovalves," Lockheed Aircraft Corporation. Missile Systems Division, Sunnyvale, California, Report No. R14-213, Dec. 1960.
5. Black, R. L., "Contaminant Sensitivity Testing of Hydraulic Servovalves," Twenty-ninth Annual Meeting of the National Conference on Fluid Power, Sept. 1973.
6. Kusama, H., et.al., "Hydraulic Lock on Spool Valve (Third Report - Role of Dirts on Lock and Effect of Dither)," Bulletin of the Tokyo Institute of Technology, No. 100, 1970, P. 81.
7. Inoue, R., "Contaminant Lock in Spool Type Directional Control Valves," The BFPR Journal, 13.2, 1980.

8. Nikitin, G. A., and S. V. Chirkov, "The Effect of Fluid Contamination on the Operating Reliability of Aircraft Hydraulic Systems," Translation Division, Foreign Technology Division, Wright-Patterson Air Force Base, Ohio, FTD-MT-24-463-69.
9. Gillum, J. R., "MERADCOM/OSU Assessment and Rating of the Contaminant Sensitivity of Relief Valves," U.S. Army Mobility Equipment Research and Development Command, Fort Belvoir, Virginia, Report No. FPRC M111980, 1980.
10. Pai, R. M., "Particle Impingement Erosion," M.S. Thesis, Oklahoma State University, 1981.
11. Neilson, H. H., and A. Gilcrist, "Erosion by a Stream of Solid Particles," Wear, Volume 11, 1968, pp. 111-122.
12. Bensch, L. E., and E. C. Fitch, "A New Theory for the Contaminant Sensitivity of Fluid Power Pumps," The BFPR Journal, Section 72-cc, Annual Report No. 6, September 1972, p. 99.

PART II

SOLENOID VALVES

CHAPTER 1 - INTRODUCTION

As the use of electrohydraulic solenoid valves has increased, the need for a reliable, repeatable, and reproducible test procedure for determining the sensitivity of such valves to particulate contaminants has become urgent. Many companies, especially those involved with government procurement contracts, have developed their own proprietary tests to demonstrate that their components can operate under certain contaminant levels. The objective of these tests has been specifically to demonstrate the survivability of the valves under a specified level, not to determine the actual sizes and concentrations of contaminant to which they are sensitive. For this reason, the proprietary tests do not provide a basis for comparing the contaminant sensitivity of similar valves.

The absence of a standardized contaminant sensitivity test hampers the consumer and operator in several ways. Principal among these are:

- * There is no basis for comparing valves.
- * There is no basis for determining the filtration requirements for a specific valve.

The work discussed in this report has resulted in the development of a comprehensive procedure for determining the contaminant sensitivity of solenoid operated hydraulic valves. The procedure results in the

data required to provide a figure of merit for rating the susceptibility of solenoid valves to both wear and jamming resulting from injections of known sizes and amounts of AC Fine Test Dust.

The remainder of this section discusses the theory of solenoid valve contaminant sensitivity, describes the test stand developed for the tests, presents the test procedure, and analyzes the test results. Section II of this report discusses servovalve contaminant sensitivity in the same way.

The objectives of the project which is the subject of this report include:

1. Develop test procedures to evaluate the contaminant sensitivity of solenoid valves.
2. Conduct contaminant sensitivity tests on representative solenoid valves.
3. Develop interpretation techniques for the test results to determine the valve contamination protection requirements.

CHAPTER II - REVIEW OF PREVIOUS STUDIES

Through the extensive research work at the FPRC, it has been determined that there are two major failure modes in hydraulic valves due to the existence of particulate contaminants in the fluid of the hydraulic system. One of the failure modes is wear. Although the performance degradation by wear is conspicuous with valves that have a poppet system inside, normally, spool-housing type valves do not have critical failure or degradation due to wear. With spool-housing type valves, wear takes place in the clearance between spool and housing and at the entrance edge of the clearance.

The progress of wear is rather gradual; therefore, normally, another failure mode, contaminant lock, is a much more obvious and dangerous failure mode among spool-housing type valves.

It has long been known that directional control valves with the spool-housing configuration are susceptible to contaminant lock when particulate contaminants exist in the hydraulic system fluid. In addition, this failure mode is unpredictable; and, when it takes place, it often leads to catastrophic failure because of sudden loss of control. Moreover, the roughened surface in the clearance due to wear can cause an increase in friction force, which results in the increased probability of contaminant lock occurrence.

There are three criteria previously developed at the FPRC to

evaluate the contaminant sensitivity of the solenoid valve from experimental data. They are:

- * PRESSURE RESPONSE RATIO
- * RESPONSE TIME
- * SILTING FORCE

To determine the pressure response ratio, the output pressure response of the solenoid valve is measured while the valve is operated under rated conditions. Output pressure response is the pressure differential between the upstream pressure level before and after the solenoid valve actuation.

The pressure response ratio can then be calculated by dividing the output pressure response when operating with contaminant fluid by the output pressure response with clean fluid. A decrease in the pressure response ratio indicates there is less pressure drop across a valve due to a bypass leakage inside the valve. Since the leakage is caused by wear inside the valve, this criterion is a measure of the wear inside the solenoid valve.

Response time is the lag time between an input of the electrical signal and a corresponding change in output pressure. There is a time delay for output pressure to reach a new output level after the input signal (voltage or current across solenoid) reaches its new level and actuates the spool of the valve. Under contaminant lock, response is slowed and may even become infinite. In other words, the spool shifts slowly or fails to shift at all. Therefore, response time is a measurable criterion of contaminant lock.

Silting force corresponds to the additional force required to shift the spool due to the existence of particulate contaminants in the valve clearances. The higher the silting force, the more severe the degrees of contaminant lock. Therefore, this criterion can also be used to measure the contaminant sensitivity of solenoid valves in relation to contaminant lock.

With regard to the magnetic field effect on the contaminant sensitivity of solenoid valves, in preliminary experimental work done at the FPRC, the contaminant lock mode was tested under silting force measurement criterion. For the measurement of silting force, a strain gauge type force transducer was used, as shown in Fig. 2.1. Also, Fig. 2.1 shows the hydraulic circuit used for this test. The solenoid valve used for this test was modified to accommodate both manual and solenoid operation. ACFTD was injected as the standard contaminant. As Fig. 2.2 shows, under the valve's magnetic field, there is an obvious increase in silting force with the contaminant size of 5 micrometres or above.

Subsequently, this experiment was conducted with 100 percent ferrous contaminants--carbonyl iron grade E, C, and L. The results of the test are shown in Fig. 2.3. Again, the effect of magnetic field on this solenoid valve contaminant sensitivity is obvious.

Through this early experimental activity at the FPRC, it is assured that the effect of a magnetic field created by solenoids is an important parameter to be considered for the establishment of a solenoid valve contaminant sensitivity rating system. In addition,

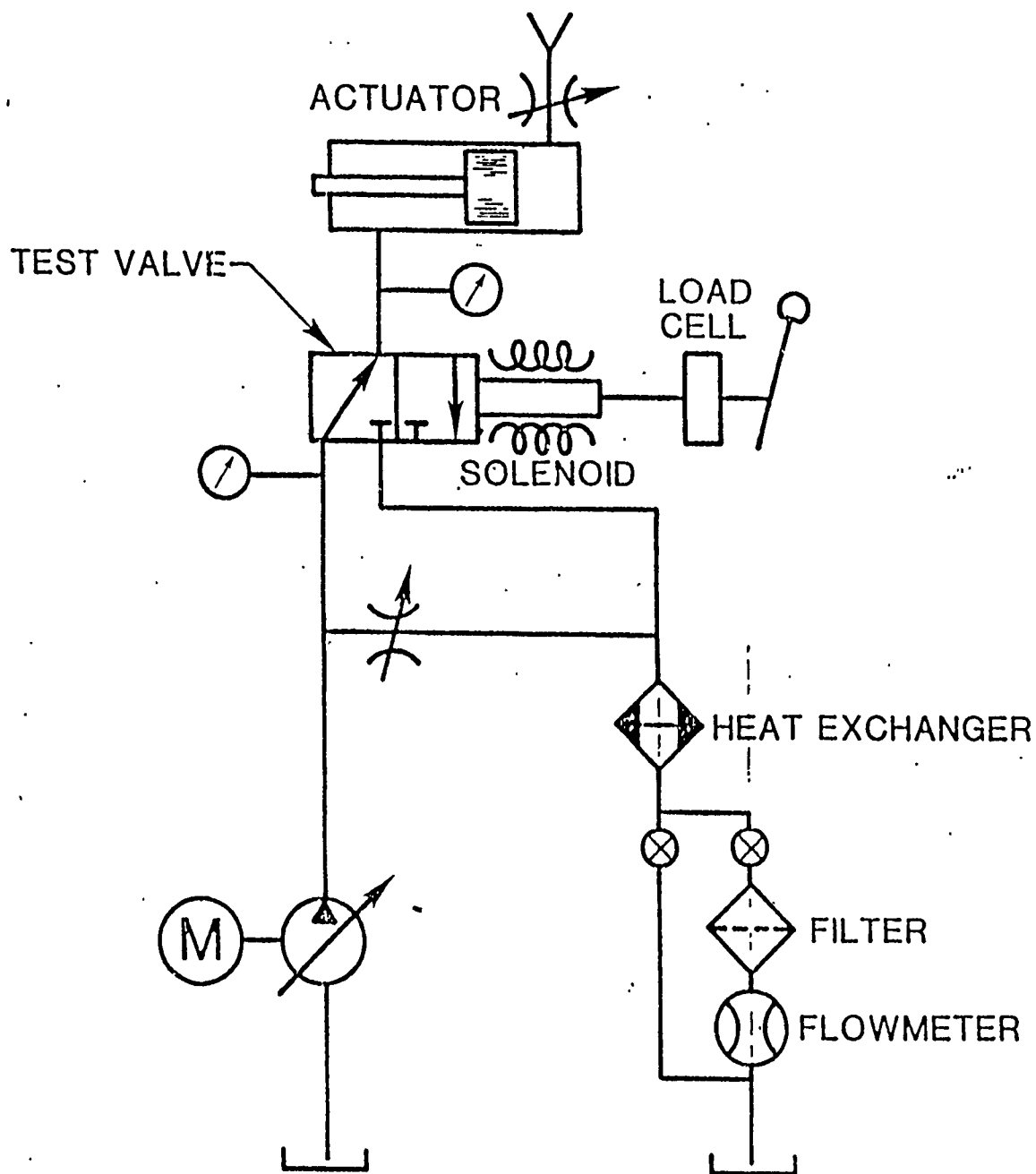


Figure 2-1. Test Circuit

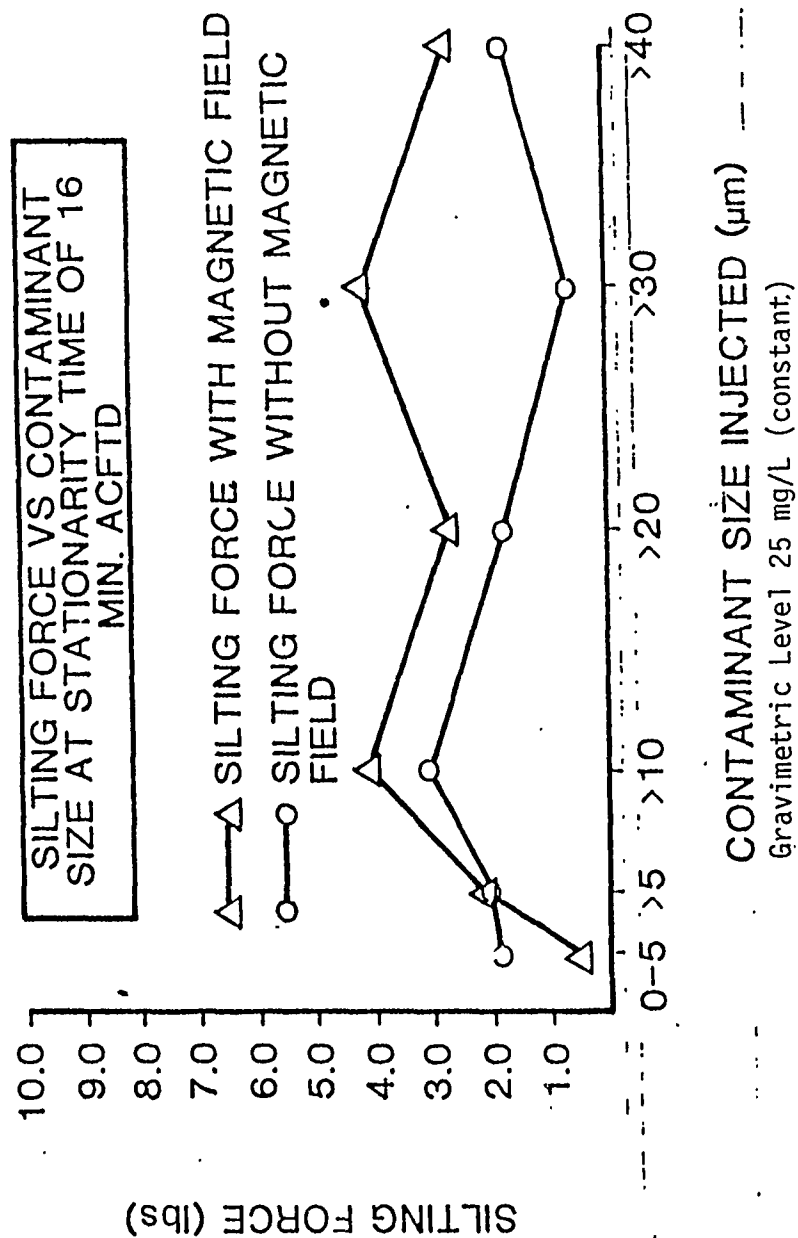


Figure 2-2.

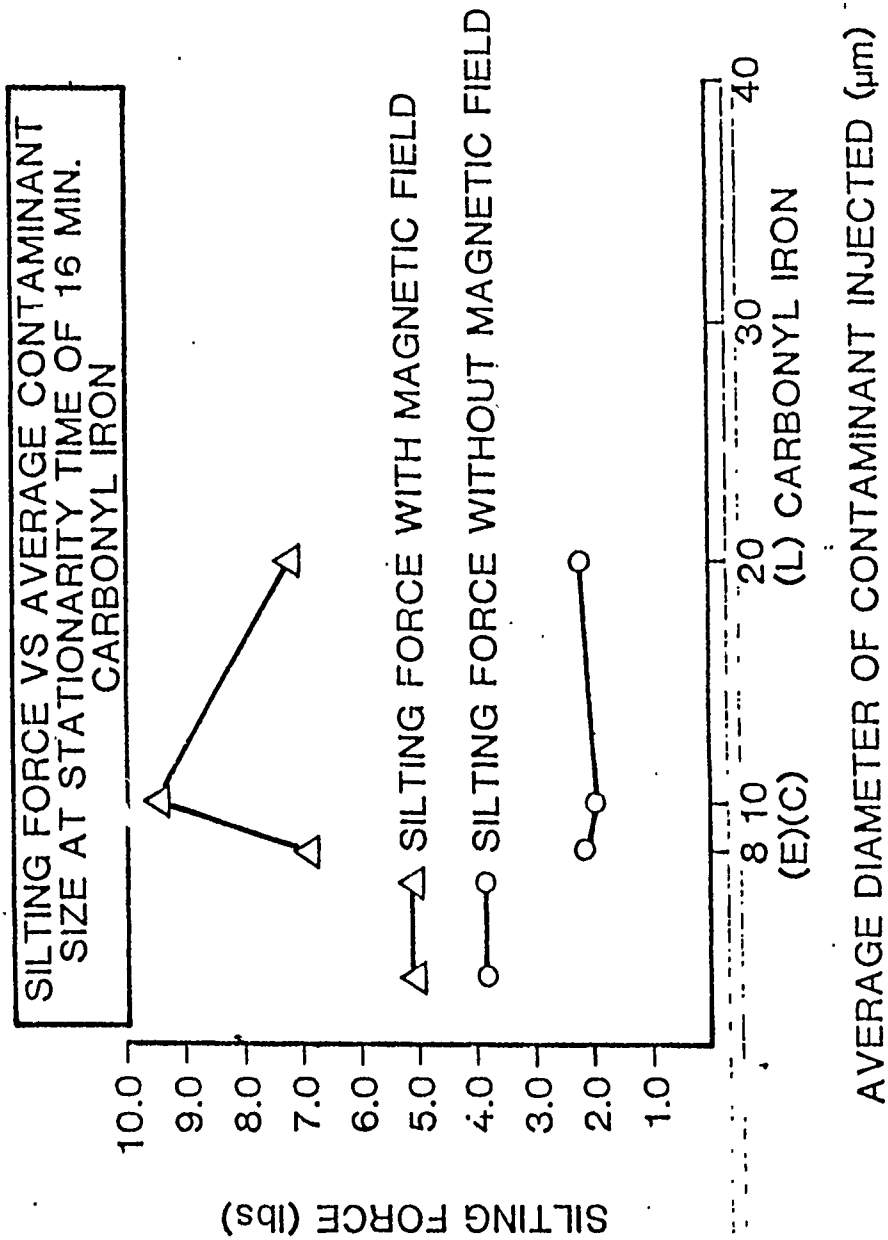


Figure 2-3.

it was demonstrated that the silting force measurement is a prospective criterion for a solenoid valve contaminant sensitivity rating system.

THEORETICAL DEVELOPMENT

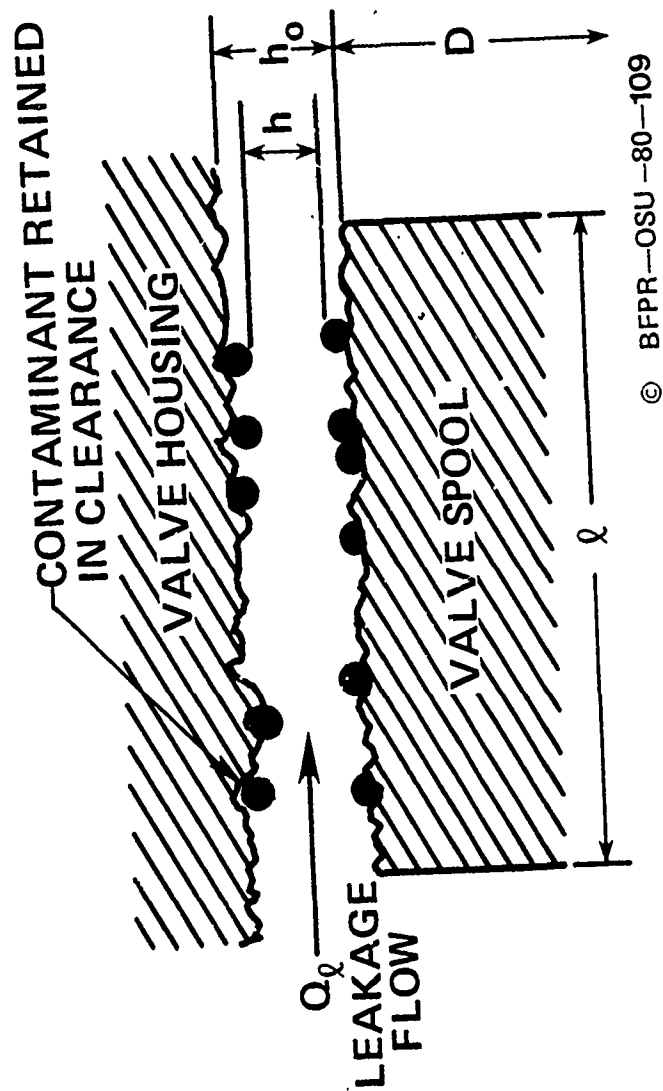
The theory of contaminant lock in solenoid valves was developed using the constant pressure filtration theory. The final equation which describes the nature of silting force contaminant lock is shown below (see Fig. 2.4):

$$F = X(1 - \frac{Y}{X}) \quad (2-1a)$$

where F = silting (contaminant lock) force
and X, Y = valve parameters

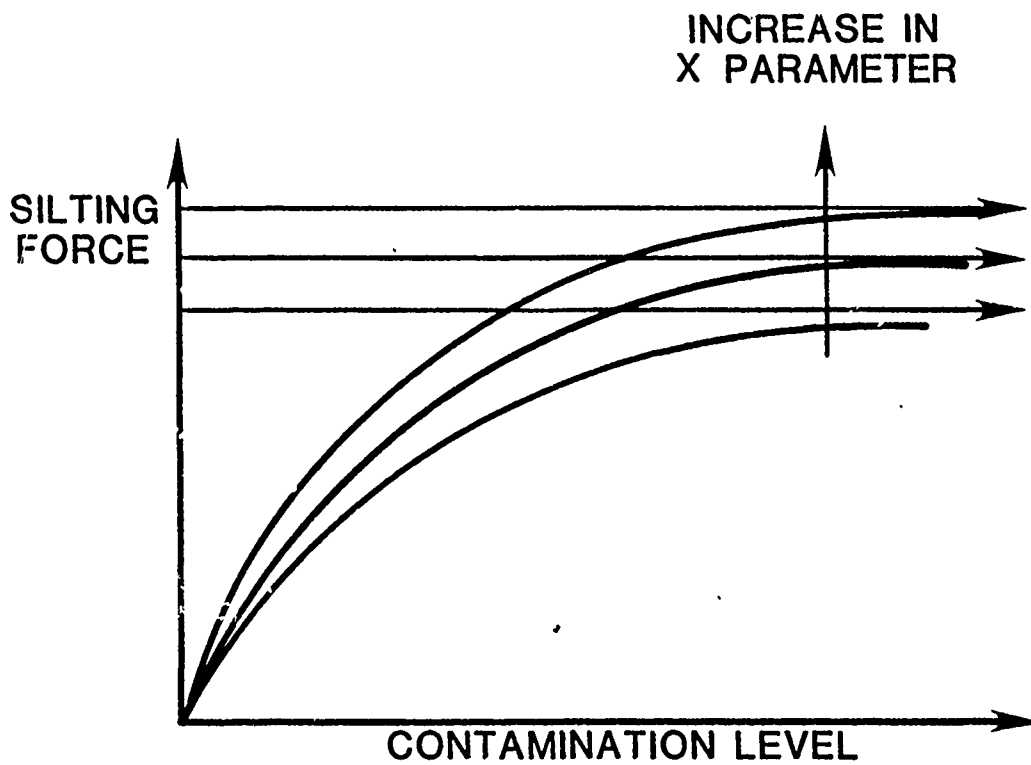
This equation indicates that silting force is a function of valve geometry (X parameter) and the hydraulic system condition plus the nature of contaminants (Y parameter).

The effect of the X parameter on silting force is described in Fig. 2.5 (a). As the X parameter increases, the maximum limit silting force increases. Thus, an increase in the diameter of the spool or spool length causes the X parameter to increase and results in higher maximum silting force. On the other hand, an increase in pressure, contamination level, and time allowed for contaminants to deposit in the clearances, or a decrease in viscosity will result in an increase in the Y parameter. Conversely, an increase in the Y parameter causes

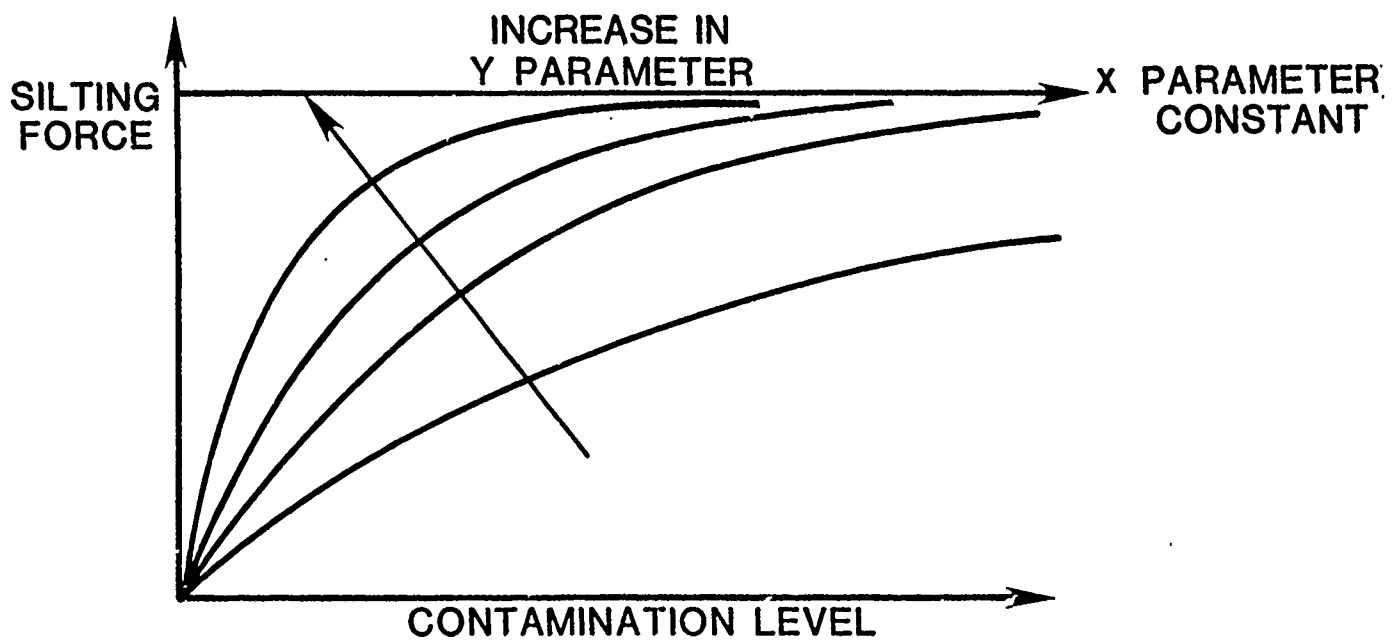


© BFPR—OSU —80—109

Fig. 2.4 The Nature of Silting Force Contaminant Lock



(a) X-Parameter Effect



(b) Y-Parameter Effect

Fig. 2.5 Effect of Increase in X and Y Parameters

a steep increase in the silting force with a slight increase in contamination level, especially at low contamination levels.

Experimentally, validity of this equation was verified through a contamination monitor project sponsored by the U.S. Department of Energy. In this project, a computer program was developed to determine the X and Y parameters from the test data.

CHAPTER III - DEVELOPMENT OF THE SOLENOID VALVE OMEGA RATING

It is desirable to define the contaminant sensitivity of solenoid valves by a single figure of merit - termed the Omega Rating - in much the same manner as has been done previously for pumps, hydraulic motors, and other types of valves.

The Omega Rating value is defined as the Beta 10 filter required to ensure that the contaminant silting force of the valve will be less than 0.5 lbf after a one-minute stationary time interval when the contaminant ingress rate into the system is 10^8 particles 10 μm or larger per minute.

Based on this 10^8 ingress, Fig. 3.1(a) indicates the particle size distribution that would occur downstream of filters with the indicated Beta 10 ratings. To determine the Omega rating of a solenoid valve, the relationship between the silting force equation, Eq. 2.1(a), and these particle distribution profiles must be established. To simplify this relationship, all Beta 10 profiles were assumed to be parallel to the Beta 10 of 2 and 10 profiles. This is, in fact, a reasonable step, due to the fact that most filters tested at the FPRC over the past ten years have Beta 10 ratings between those two values. Additionally, the shifting of the profiles, as shown in Fig. 3.1(b), bases the distribution toward a higher number of particles in the range spool type valves are sensitive, Fig. 3-2, and therefore makes any analysis based on those distributions somewhat conservative.

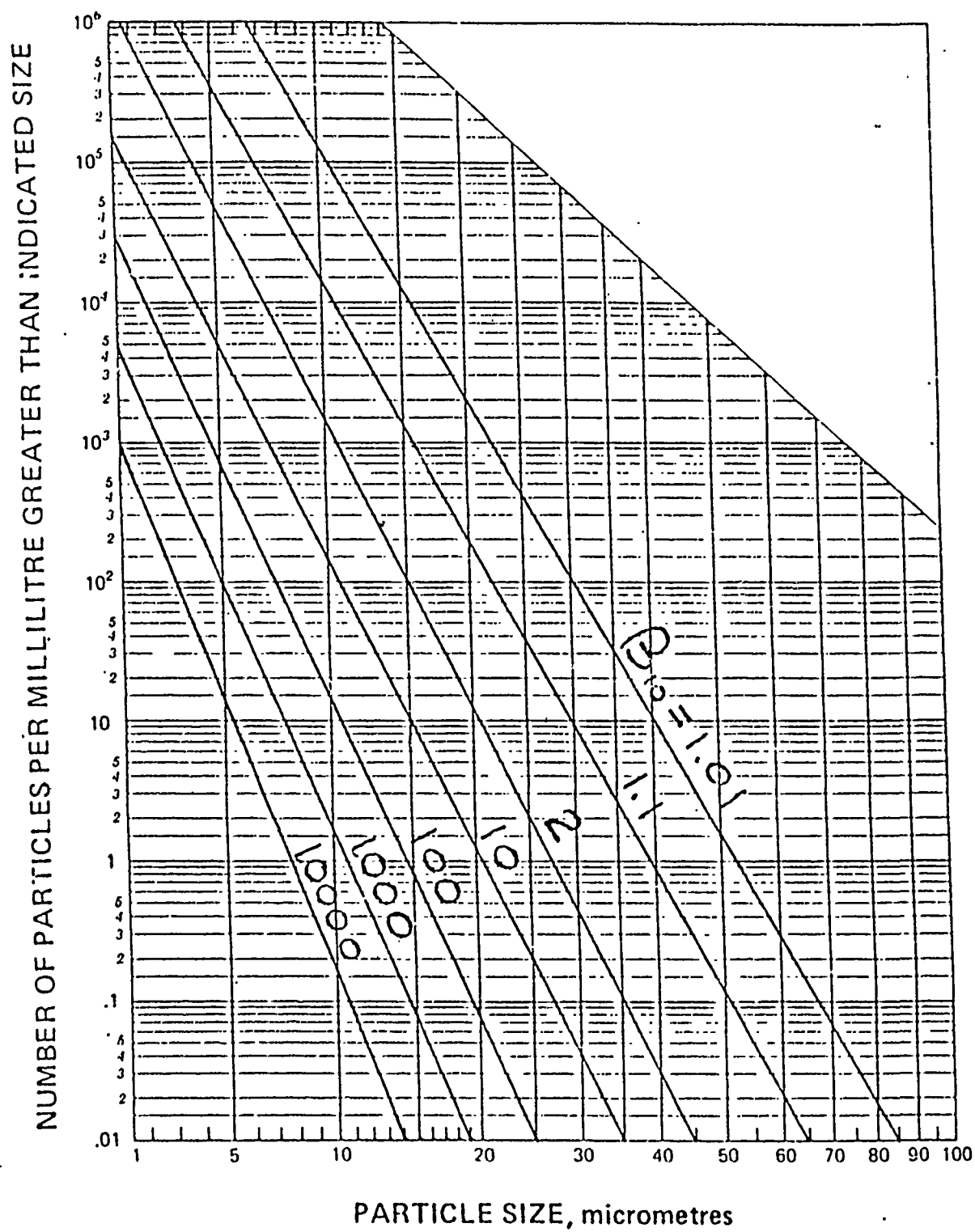


Fig. 3.1(a) Beta 10 Profile

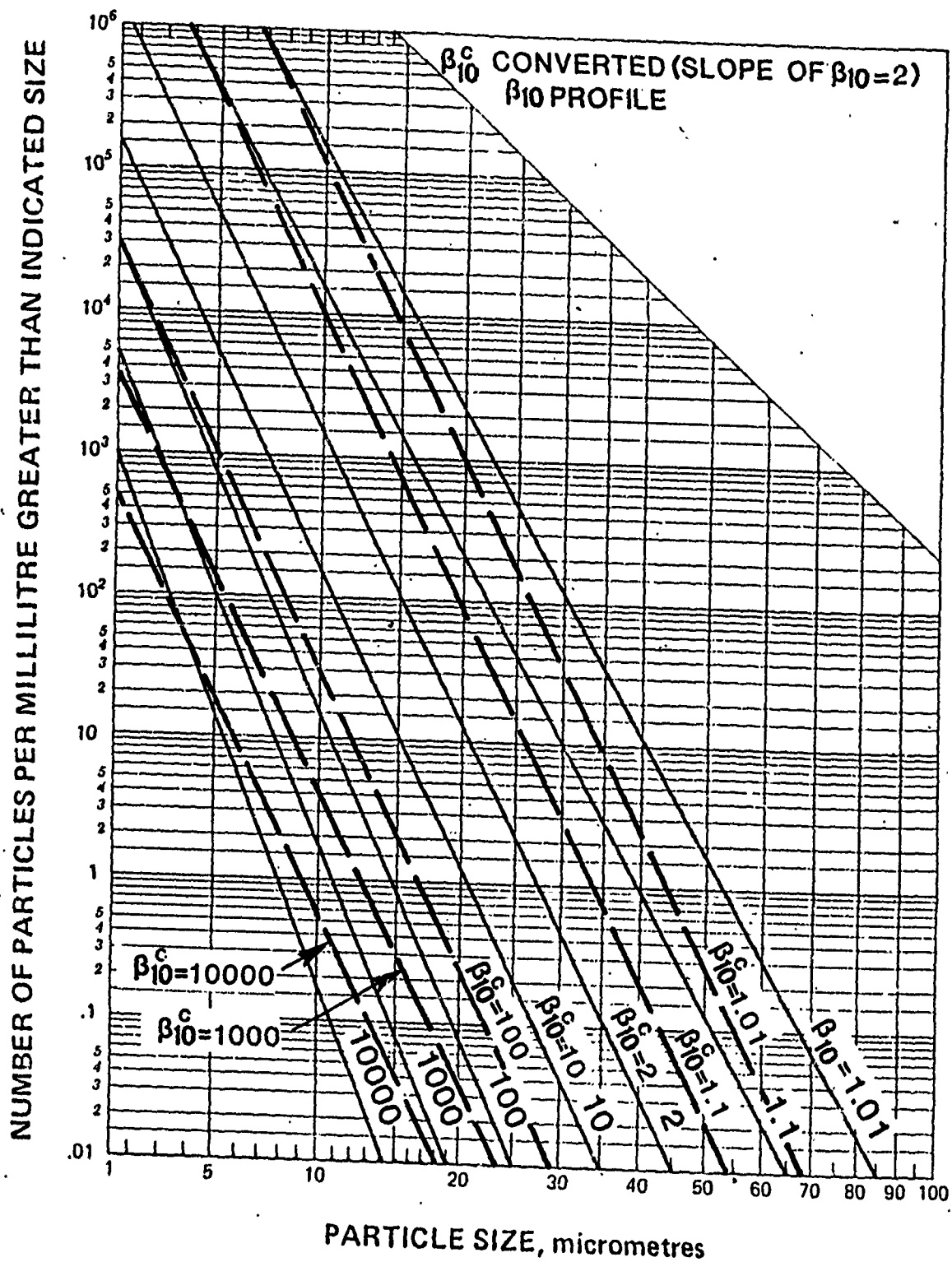


Fig. 3.1(b) Modified Beta 10 Profile

VALVE CONTAMINANT LOCK SENSITIVITY VS CONTAMINANT SIZE

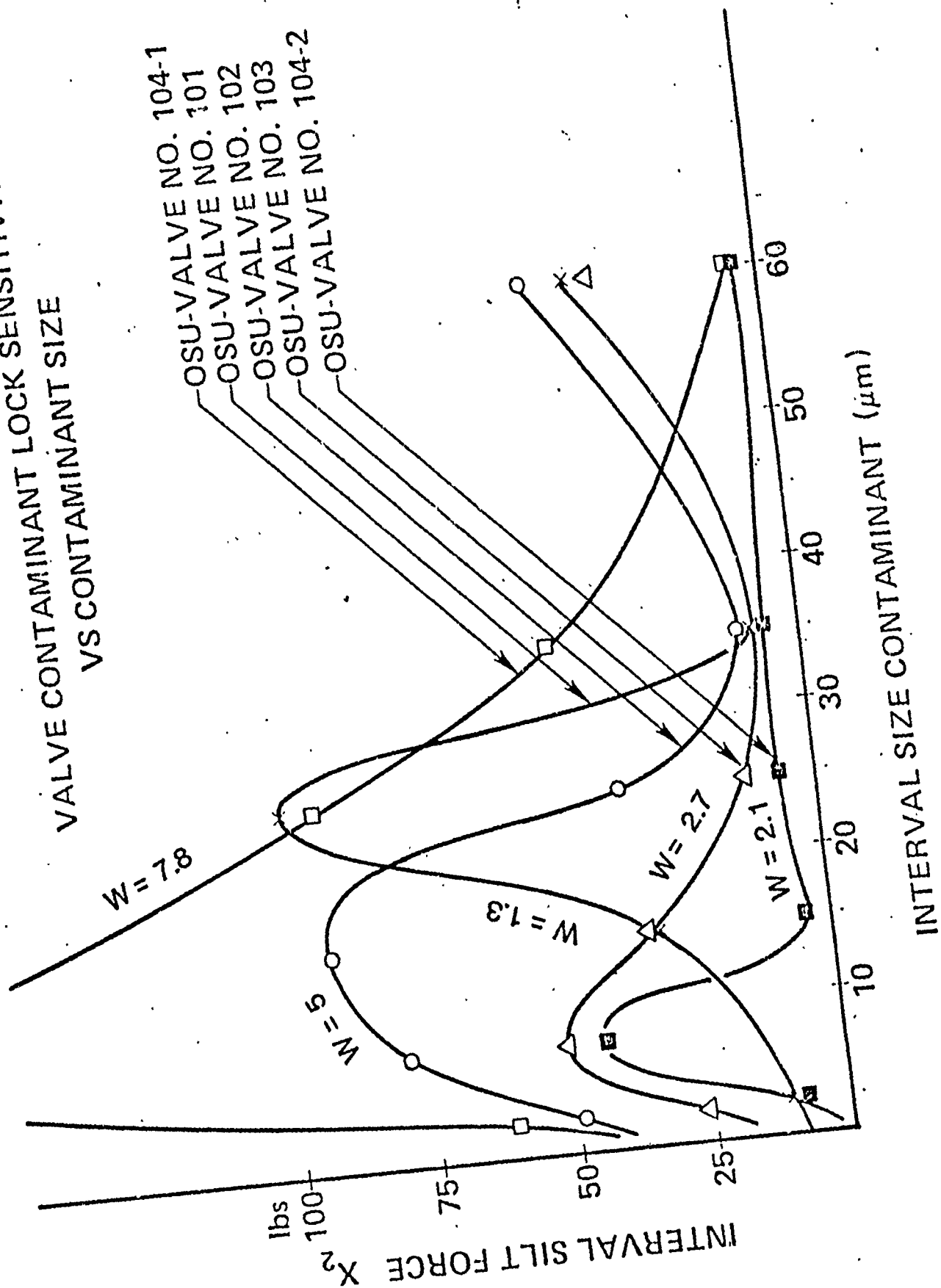


Fig. 3.2

Based on this converted or shifted profile, each solenoid valve will have its own characteristic curve based on the silting force equation, as shown in Fig. 3.3. When the other parameters of G_B are set constant, there is a one-to-one relationship between the silting force, F , and the reference gravimetric level, G_B . This gravimetric level can be converted directly to its corresponding Beta 10 value, as shown in Fig. 3.3. This, then, is the relationship between the filter rating and contaminant sensitivity of the solenoid valve.

Unfortunately, there is no standard contaminant with the particle size distribution corresponding to the Beta 10 = 2 profile. Therefore, it is necessary to test the valves with standard ACFTD, to convert the results to correspond to the desired profile. To accomplish the conversion to the Beta 10 profile, the distribution for Beta 10 = 2 was analyzed, Table 3.1. Based on this analysis, the percentages of particles in the various size ranges can be combined to give the following relationships:

$$X_B = 0.964 X_{0-5} + 0.035 X_{5-10} + 0.001 X_{10-20} \quad (3-1)$$

$$Y_B = 0.964 Y_{0-5} + 0.035 Y_{5-10} + 0.001 Y_{10-20} \quad (3-2)$$

It is possible to separate ACFTD into the 0-5, 5-10, 10-20, etc., fractions; however, the distributions achieved vary significantly from laboratory to laboratory. Therefore, while using these double-cut fractions for testing appears attractive on the surface, it is likely that the test results would not be satisfactorily repeatable. On the

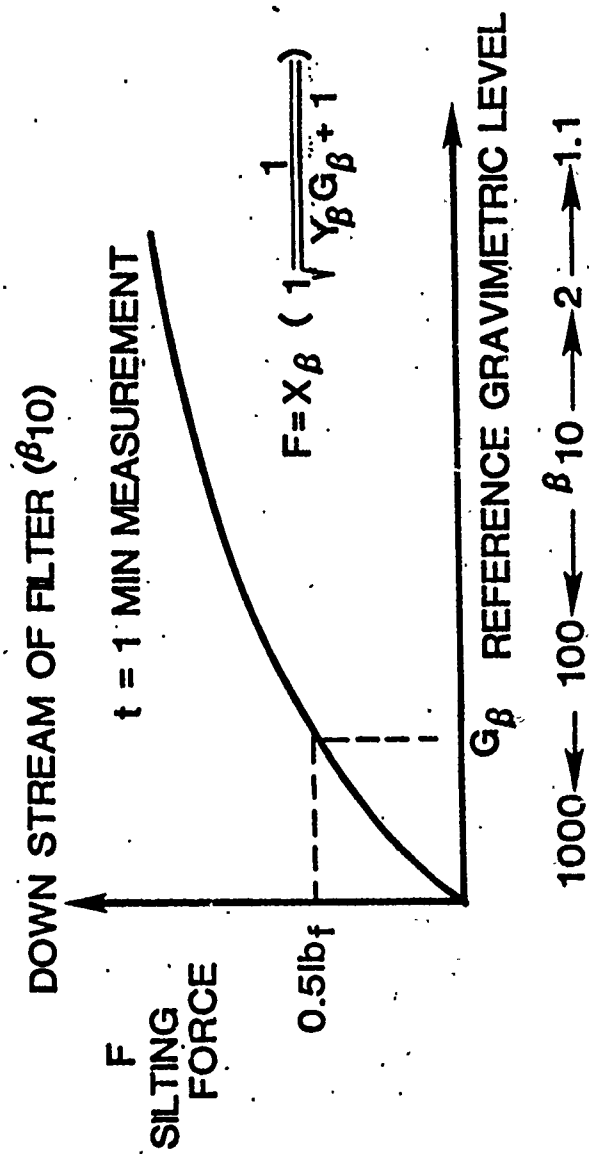


Fig. 3.3 Silting Force vs. Reference Gravimetric Level

Table 3.1 Particle Size Distribution of Converted Beta Ten Profile

INDICATED SIZE (μm)	NUMBER OF PARTICLES GREATER THAN INDICATED SIZE
1	1.4×10^6
5	5×10^4
10	1.5×10^3
20	1.2×10

N_T ; ASSUMED TOTAL NUMBER OF PARTICLES FOR
 $\beta_{10} = 2$ IS 1.4×10^6

INTERVAL	NUMBER OF PARTICLES IN THE INTERVAL (N_i)	PERCENTAGE $N_i/N_T \times 100$
0-5	1.35×10^6	96.4
5-10	4.85×10^4	3.5
10-20	1.49×10^3	0.1

other hand, single-cut fractions of ACFTD have been thoroughly analyzed, and they are known to display the distributions shown in Table 3.2. Using this table, the following equations can be postulated:

$$X_{0-5} = X_{0-5} \quad (3-3a)$$

$$X_{0-10} = 0.742 X_{0-5} + 0.258 X_{5-10} \quad (3-3b)$$

$$X_{0-20} = 0.687 X_{0-5} + 0.239 X_{5-10} + 0.074 X_{10-20} \quad (3-3c)$$

$$Y_{0-5} = Y_{0-5} \quad (3-4a)$$

$$Y_{0-10} = 0.742 Y_{0-5} + 0.258 Y_{5-10} \quad (3-4b)$$

$$Y_{0-20} = 0.687 Y_{0-5} + 0.239 Y_{5-10} + 0.074 Y_{10-20} \quad (3-4c)$$

By using Eqs. 3-1 through 3-4, the silting force test results from ACFTD can be converted into the modified Beta 10 profile test result. Consequently, the Omega rating of a solenoid valve can be found. The algorithm for this conversion is shown in Fig. 3.4.

TEST RESULT PRESENTATION: OMEGA RATING

The whole test result must be finalized into silting force vs. pressure difference. The use of tables such as Table 3.3 is helpful. Note that the silting force is found by subtracting initial friction force (measured force under clean fluid) from the measured force under contaminated fluid.

Having those experimental data, X and Y parameters can be found through the computer program presented below. First, its theory of numerical analysis is shown; then, the developed computer program based upon the theory is shown next.

Table 3.2 Particle Distribution of Lower Cut Dust

INTER- VAL µm	THE LOWER CUT DUST						
	0-10	0-20	0-30	0-40	0-50	0-60	0-70
0/5	74.2%	68.7%	67.9%	67.8%	67.7%	67.7%	67.7%
5/10	25.8	23.9	23.6	23.6	23.5	23.5	23.5
10/20		7.4	7.4	7.4	7.4	7.4	7.4
20/30			1.1	1.0	1.0	1.0	1.0
30/40				0.2	0.3	0.26	0.26
40/50					0.1	0.11	0.10
50/60						0.03	0.03
60/70							0.01

Fig. 3.4

ALGORITHM TO FIND SOLENOID VALVE Ω

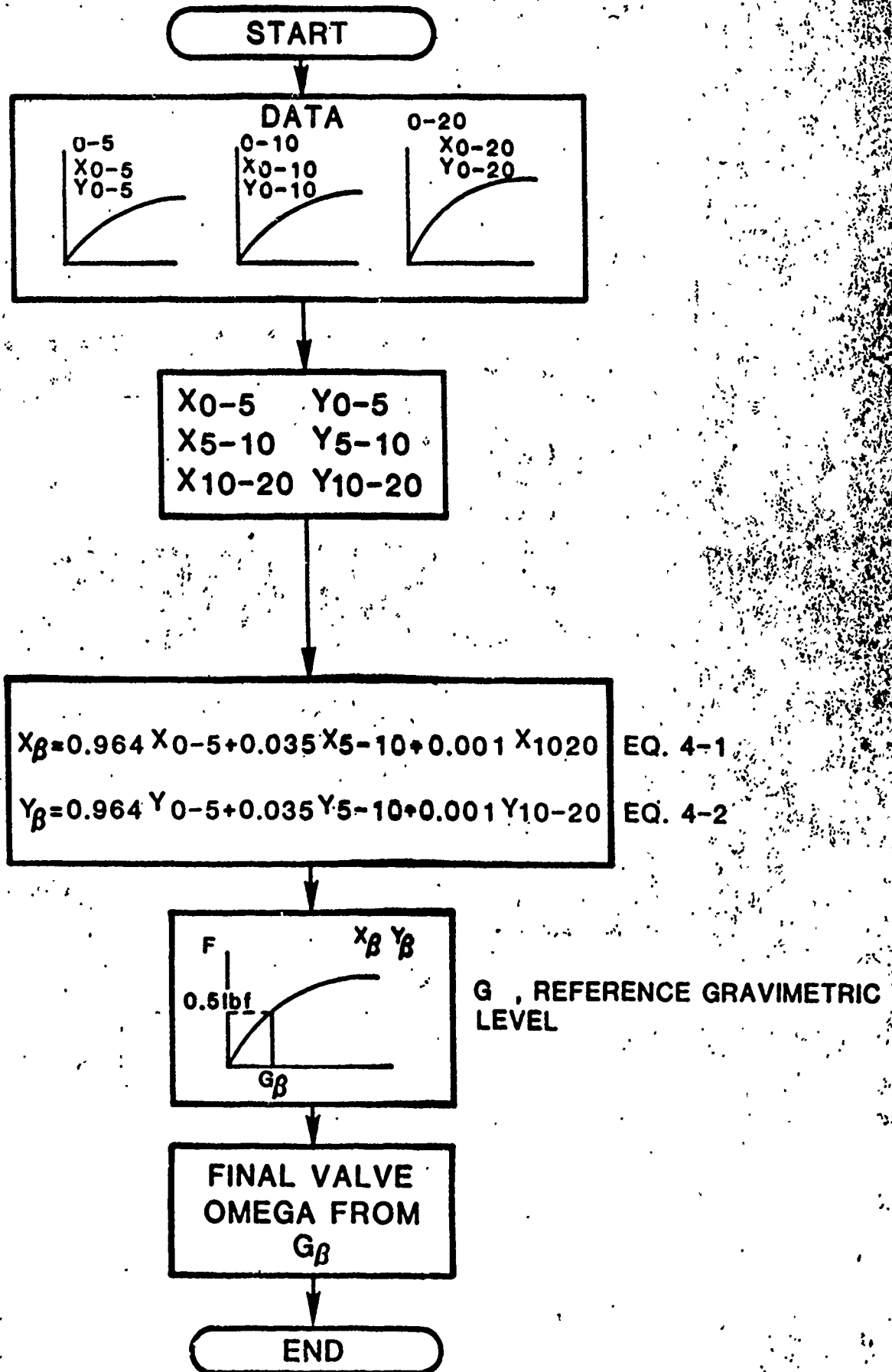


Table 3.3

TABLE FOR SILTING FORCE vs. PRESSURE DIFFERENCE (ΔP)

VALVE NAME _____

TESTED POSITION _____

FORCE (lbf)	MEASURED FORCE / SILTING FORCE (lbf)							
	MEAS. FORCE-CLEAN FLUID F.							
ΔP								
ACFTD LOWER CUT								
CLEAN C \rightarrow S FLUID S \rightarrow C								
0-5 μm								
0-10 μm								
0-20 μm								

The equation mentioned in Eq. (2-1) can be written as

$$F = X \left(1 - \frac{1}{\sqrt{X(YG) \Delta P^{1.1}}} \right) \quad (3-5)$$

$$\frac{(1 + d \sigma(YG)) \sqrt{X(YG) \Delta P^{1.1}}}{X} = \frac{Y}{d} \quad (3-6)$$

$$F_i = X (1 - P_i) \quad (3-7)$$

This is a linear graph with a constant slope of $-X$. Set P_i arbitrary to get F_i (i is used for later summation equation):

$$\hat{F}_i = X - X P_i \quad (3-8)$$

The deviation (or error) ϵ from the actual data is :

$$\epsilon = F_i - \hat{F}_i \quad (3-9)$$

Let the summation of total deviation of square be:

$$E = \sum_{i=1}^n \epsilon_i^2 \quad (3-10)$$

Finding the minimum error point in terms of X , $\frac{\partial E}{\partial X} = 0$.

This results in
$$X = \frac{\sum F_i - \sum F_i P_i}{\sum P_i^2 - 2 \sum P_i + n} \quad (3-11)$$

This X can be found through the ration process of the value of P_i to minimize E , error.

Once X has been found, corresponding P_i is found. However, P_i is a function of (YG) (Eq. 3-6); thus, YG is found. Since back parameters of X and YG of Eq. (3-5) are set, only two unknowns, ΔP and F , remain. If ΔP is set to a certain pressure, then corresponding silting force F can be calculated.

The hard copy of the computer program and its algorithm are shown in Figs. 3-5 and 3-6. For the purpose of Omegatizing solenoid valves, the relationship of silting force versus gravimetric level has to be determined. With the use of the computer program in Fig. 3.6 on the experimental data of silting force (F) versus pressure difference (ΔP), the constant of X and YG can be found. Note that YG is constant because the gravimetric level of the system was set constant through the whole experiment except tests with clean fluid.

Using the known value of YG, it is possible to find Y only by dividing YG with a constant G. In addition, if the pressure difference ΔP is set constant at rated pressure, the choice of rated pressure was decided to have a fair evaluation of each valve's contaminant sensitivity; e.g., it's not reasonable to evaluate contaminant sensitivity of the valve designed for 10,000 psi with 5000 psi; and, multiplied by Y, this will give another constant $Y\Delta P$. Hence, using the two constants X and $Y\Delta P$ and letting G be variable, the next equation can be derived:

$$F = X \left(1 - \frac{1}{\sqrt{(Y\Delta P)G + 1}} \right) \quad (3-12)$$

DATA

#	ΔP_i	F_i
1	.	.
.	.	.
.	.	.
.	.	.
n	.	.

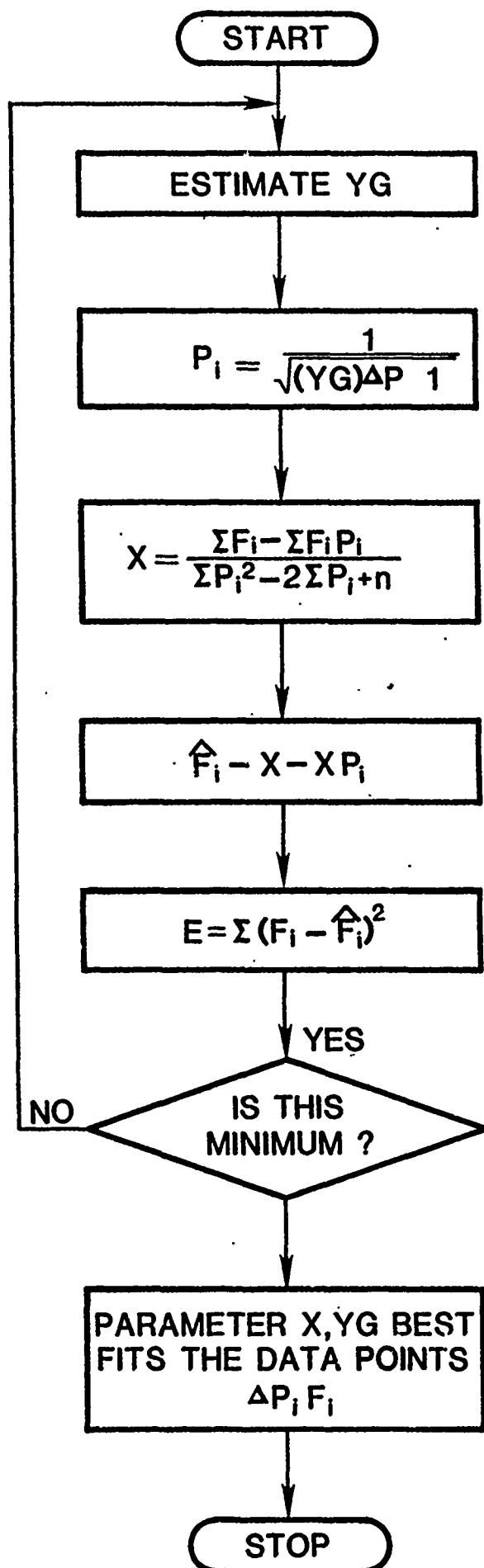


Fig. 3.5 Solenoid Omega Computer Algorithm


```

L
00010 C THIS PROGRAM IS TO FIT THE THEORETICAL CURVE TO GIVEN
00020 C DATA POINTS
00030 C LIST OF VARIABLES
00040 C     K - NUMBER OF DATA GIVEN
00050 C     F - ARRAY OF SILTINGFORCE DATA
00060 C     G - ARRAY OF PRESSURE DIFFERENCE DATA
00070 C     P - ARRAY CALUCULATED FROM THE VALUE OF Y
00080 C     X - CONSTANT OF THEORETICAL EQUATION
00090 C     Y - CONSTANT OF THEORETICAL EQUATION
00100 C     E - ERROR,FUNCTION OF Y
00110 C     STORED VARIABLES FOR COMPARISON TO FIND THE MINIMUM
00120 C     ERROR CORRESPONDING Y
00130 C         Y1
00140 C         Y2
00150 C         Y3
00160 C         E1
00170 C         E2
00180 C         E3
00190 C IN - READ INPUT
00200 C LP - LINE PRINTER
00210 C FF - SILTING FORCE FOUND BY THEORETICAL EQUATION
00220 C GG - PRESSURE DIFFERENCE SET TO FIND SILTING FORCE
00230 C     USING THEORETICAL EQUATION
00240 C
00250 C SUBPROGRAM USED -- PROG
00260 C     DIMENSION P(10),F(10),FP(10),PS(10),G(10),BF(10)
00270 C     COMMON X,E,E2,E3,Y1,Y2,Y3
00280 C     DATA IN,LP/5,6/
00290 C READ DATA POINTS OF SILTING FORCE AND PRESSURE DIFFERENCE
00300 C
00310 C     WRITE(LP,5)
00320 C     5 FORMAT(/5X,'FIRST INPUT NUMBER OF DATA YOU HAVE,THEN PUNCH IN'
00330 C     $       /4X,'PRESSURE DIFFERENCE & SILTING FORCE RESPECTIVELY')
00340 C     READ(IN,*)K,(G(I),F(I),I = 1,K)
00360 C SET THE INITIAL INCREMENT OF Y AND INITIAL NUMBER OF Y
00370 C     D = .00001
00380 C     Y = .00001
00390 C INITIALIZE STORAGE SPACE OF Y AND E
00400 C     Y2 = 0.0
00410 C     Y3 = 0.0
00420 C     E2 = 0.0
00430 C     E3 = 0.0
00440 C FILL THE STORAGE SPACE OF Y AND E
00450 C     DO 20 I = 1,3
00460 C         CALL PROG(P,F,FP,PS,G,BF,D,Y,K)
00470 C         Y = Y + D
00480 C     20 CONTINUE
00490 C CHECK TO SEE IF ERROR E IS MINIMUM
00500 C     30 CALL PROG(P,F,FP,PS,G,BF,D,Y,K)
00510 C         IF(E3,EQ,E2) GO TO 55
00520 C         IF(E3,GT,E2) GO TO 50
00530 C     ERROR IS NOT MINIMUM
00540 C         Y = Y + D
00550 C         GO TO 30
00560 C     ERROR E PASSED MINIMUM POINT ,SET BACK Y CORRESPONDING
00570 C     BEFORE MINIMUM E ; AND START Y BY ONE TENTH OF PREVIOUS
00580 C     INCREMENT D
00590 C     50 D = (Y3 -Y1)/10.
00600 C         Y = Y1 + D
00610 C         GO TO 30
00620 C PRINT THE HEADINGS OF DATA TABLE
00630 C     * NUMBER OF DATA GIVEN
00640 C     * DATA POINTS OF PRESSURE DIFFERENCE AND SILTING

```

```

00670 60 FORMAT(/11X,'NUMBER OF DATA GIVEN ',I2)
00680 WRITE(LP,70)
00690 70 FORMAT(/2X,'DATA',6X,'PRESSURE DIFFERENCE (PSI)',5X,
00700 $ 'SILTING FORCE (LB)')
00710 C PRINT THE GIVEN DATA POINTS
00720 DO 85 I = 1,K
00730 WRITE(LP,80)I,G(I),F(I)
00740 80 FORMAT(' ',3X,I1,13X,F6.1,19X,F9.4)
00750 85 CONTINUE
00760 C PRINT THE CONSTANTS OF THEORETICAL EQUATION AND ERROR
00770 90 WRITE(LP,100)X,Y,E
00780 100 FORMAT(/3X,'X IS ',F11.7,5X,' YG IS ',F11.7,5X,
00790 $ 'ERROR IS ',F11.7,/)
00800 C PRINT THE HEADINGS FOR THE RESULTS CALUCULATED FROM
00810 C THEORETICAL EQUATION
00820 WRITE(LP,110)
00830 110 FORMAT(/5X,'RESULT OF THEORETICAL EQUATION',
00840 $ //4X,' ',7X,'PRESSURE DIFFERENCE (PSI) ',
00850 $ 5X,'SILTING FORCE (LB)')
00860 C INITIALIZE GRAVIMETRIC LEVEL GG AND SILTING FORCE FF
00870 GG = 0.0
00880 FF = 0.0
00890 DO 130 I = 1,30
00900 GG = GG + 100.
00910 FF = X * (1. - 1./SQRT(Y * GG + 1.))
00920 C PRINT THE RESULT OF THEORETICAL EQUATION FOUND
00930 WRITE(LP,140)I,GG,FF
00940 140 FORMAT(' ',2X,I2,13X,F6.1,19X,F9.4)
00950 130 CONTINUE
00960 STOP
00970 END
00980 C SUBROUTINE TO FIND ERROR E CORRESPONDING
00990 C
01000 C LIST OF VARIABLES
01010 C VALUE USED IN SUBROUTINE HAS THE SAME FORM AS IN
01020 C MAIN ROUTINE
01030 C FP - F TIMES P
01040 C PS - P SQUARED
01050 C SF - SUM OF F
01060 C SP - SUM OF P
01070 C SFP - SUM OF FP
01080 C SPS - SUM OF PS
01090 C X - CONSTANT SOUGHT FOR THEORETICAL EQUATION
01100 C BF - SILTING FORCE CALUCULATED THROUGH Y
01110 C E - ERROR
01120 C
01130 SUBROUTINE PROG(P,F,FF,PS,G,BF,D,Y,K)
01140 DIMENSION P(K),F(K),FP(K),PS(K),G(K),BF(K)
01150 COMMON X,E,E2,E3,Y1,Y2,Y3
01160 C INITIALIZE VARIABLES
01170 SF = 0.0
01180 SFP = 0.0
01190 SPS = 0.0
01200 SP = 0.0
01210 E = 0.0
01220 DO 1 I = 1,K
01230 P(I) = 1./SQRT(Y * G(I) + 1.)
01240 FP(I) = F(I) * P(I)
01250 PS(I) = P(I)**2
01260 SF = SF + F(I)
01270 SP = SP + P(I)
01280 SFP = SFP + FP(I)
01290 SPS = SPS + PS(I)
01300 1 CONTINUE

```

```

01320      X = (SF -SFF)/(SPS - 2.*SP + FLOAT(K))
01330      DO 2 I = 1,K
01340      BF(I) = X - X * P(I)
01350      E = E + (F(I) - BF(I))**2
01360      2 CONTINUE
01370 C    STORE CALUCULATED E AND Y TO FIND MINIMUM E
01380      Y1 = Y2
01390      Y2 = Y3
01400      Y3 = Y
01410      E1 = E2
01420      E2 = E3
01430      E3 = E
01440      RETURN
01450      END
END OF DATA

```

This equation shows the relationship of silting force and gravimetric levels. If we denote $Y\Delta P$ as just aY , since it is a constant, the equation becomes:

$$F = X \left(1 - \frac{1}{\sqrt{Y G + 1}} \right) \quad (3-13)$$

This is the same equation as in Eq. (2-1(a)). Summarizing the process to Omegatize a solenoid valve, first from the experimental data, parameters X and YG in Eq. (3-5) are found. Secondly, those parameters can be converted into Eq. (2-1(a)) form, and parameters X_{o-5} , X_{o-10} , X_{o-20} , Y_{o-5} , Y_{o-10} , and Y_{o-20} can be found. Finally, through the process in Fig. 3.4, the solenoid valve tested can be "Omegatized".

To ease the process of assigning an Omega value to the valve, Tables 3.4, 3.5, and Figs. 3.6 and 3.7 were developed. The multifactor of Table 3.6 was found by solving Eqs. (3-1) through (3-6) for X_B and Y_B . The equation in Fig. 3.6 was derived from Eq. (2-1(a)) by solving for G . After G_B is found, which corresponds to 0.5 lbf using Fig. 3.7, it is possible to find the Omega rating of the tested solenoid valve.

Table 3.4 Solenoid Valve Omega Rating Test Data Recording Form

PARTICLE SIZE INTERVAL	^G GRAVIMETRIC LEVEL (CONSTANT)	ΔP PRESSURE DIFFERENCE	YG PARAMETER	$Y = \frac{YG}{Y_G}$	$Y = Y \Delta P$	χ	COMMENT
0-5							
0-10							
0-20							

OSU VALUE # _____

Table 3.5 Solenoid Valve Omega Rating Test Work Sheet

ⁱ PARTICLE SIZE INTERVAL	X_i PARAMETER	MULTI- FACTOR	CONTRIBUTION OF X_i TO X_β
0-5		x 0.8633 =	①
0-10		x 0.1231 =	②
0-20		x $\frac{1.351}{10^{-2}}$ =	③

$$X_\beta = \textcircled{1} + \textcircled{2} + \textcircled{3} = \underline{\hspace{2cm}}$$

ⁱ PARTICLE SIZE INTERVAL	Y_i PARAMETER	MULTI- FACTOR	CONTRIBUTION OF X_i TO X_β
0-5		x 0.8633 =	①
0-10		x 0.1231 =	②
0-20		x $\frac{1.351}{10^{-2}}$ =	③

$$Y_\beta = \textcircled{1} + \textcircled{2} + \textcircled{3} = \underline{\hspace{2cm}}$$

OMEGA RATING OF _____

SILTING FORCE, F \longrightarrow GRAVIMETRIC LEVEL, G_{β}

$$G_{\beta} = \frac{1}{Y_{\beta}} \left\{ \left(\frac{X_{\beta}}{X_{\beta} - F} \right) - 1 \right\}$$

$X_{\beta} =$

$Y_{\beta} =$

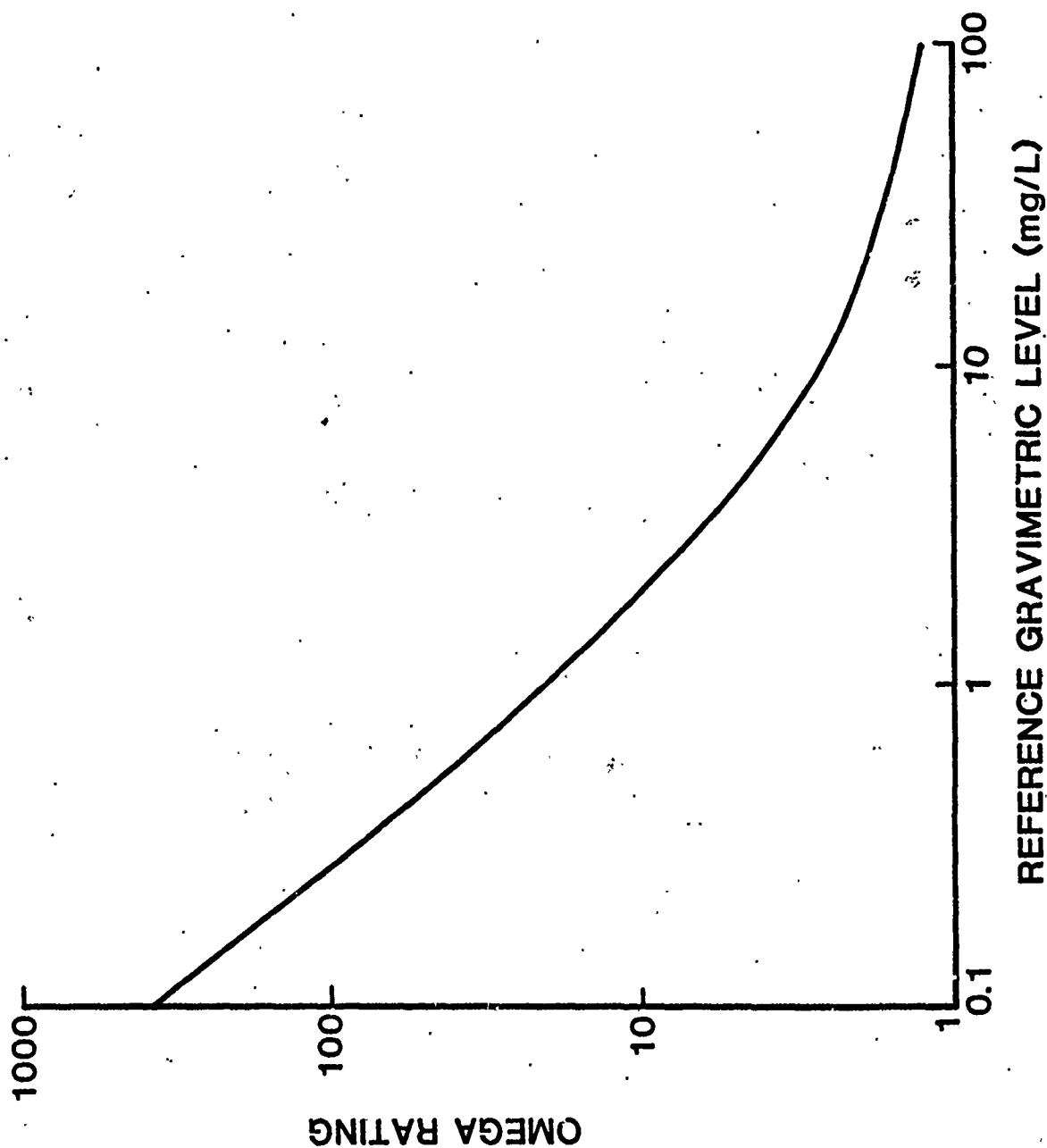
$F_{\beta} = 0.5$ lbf of silting force

$G_{\beta} =$ _____ mg/L

OMEGA RATING OF THE VALVE IS _____

OMEGA CONVERSION CHART

Fig. 3.7



CHAPTER IV - TEST PROCEDURE

The test procedure presented in this chapter is designed to provide a complete set of data with which to describe the contaminant sensitivity of solenoid valves. The procedure is presented in a format that would be suitable for presentation to a standards committee of the Society of Automotive Engineers.

1. Purpose

To provide a uniform procedure for evaluating the contaminant sensitivity of fluid power solenoid valves.

2. Scope

This recommended practice applies to all hydraulic solenoid valves which control directions of fluid flow.

3. Terms & Definitions

3.1 Test flow - any steady flow rate required to achieve the designated pressure drop across ports of interest.

3.2 Test pressure - the pressure drop across ports of interest.

3.3 Maximum rated flow - the maximum amount of fluid can be directed by the solenoid valve as specified by the manufacturer.

3.4 Maximum rated pressure - the maximum pressure at the supply port as specified by the manufacturer.

3.5 Center to side shift - energizing solenoid to shift the spool of a valve from the center position to the side.

3.6 Side to center shift - de-energizing solenoid to shift the spool of a valve from the side to the center.

3.7 Rated voltage - maximum voltage and its phase of application as specified by the manufacturer.

4. Units

4.1 The International System of Units (SI) is used herein in accordance with Reference paragraph [14.5].

5. Graphic Symbols

Graphic symbols used herein are in accordance with Reference paragraphs [15.2] and [15.3]. Where References [15.2] and [15.3] are not in agreement, Reference [15.2] governs.

6. Summary of Designated Information

6.1 Specify the following information on all requests for this test.

6.1.1 A full description of the valve.

6.1.2 The type of fluid

6.1.3 The fluid temperature if different from (7.1)

6.1.4 The test pressure

6.1.5 The test flow rate

6.1.6 The test contaminant

7. Test Condition

7.1 Fluid temperature - shall be 40°C (104°F)

7.2 System Volume - shall be numerically equal to one-half the maximum rate flow per minute of the test valve as recommended by manufacturers.

- 7.3 Test Contaminant - classified AC Fine Test Dust, 0-5 μm and 0-20 μm , which are produced from AC Fine Test Dust per Reference [14.6].
- 7.4 Test Contaminant - concentration - 100 mg/L.
- 7.5 Test Pressure - 4 different pressure differences across the valve for each shift to the spool.
- 7.5.1 For the center-to-side shift case, the pressure difference of supply pressure port and return line port is measured.
- 7.5.2 The differential pressures are chosen at equal intervals without exceeding the maximum rated pressure at the supply port; e.g., using 4500 psi maximum rated pressure valve:
- First differential pressure is 4000 psi.
- Second differential pressure is 3000 psi.
- Third differential pressure is 2000 psi.
- Fourth differential pressure is 1000 psi.
- 7.5.3 For side-to-center shift case, the pressure difference of a control and the other.
- 7.5.4 Choice of each differential pressure is the same as in 7.5.2.
- 7.6 Initial cleanliness level - the contaminant concentration level of the circulating fluid shall be less than 10 mg/L.

8. Test Condition Accuracy

Maintain the test condition accuracy within the limits shown in Table 4.1.

9. Letter Symbol

The following symbols are used in the document:

- C→S - energizing solenoid from de-energized state to shift the spool of the solenoid valve from the center position to a side.
- S→C - de-energizing solenoid from energized state to shift the spool of the solenoid valve from the side position to the center.

10. Test Equipment

- 10.1 Hydraulic flow source insensitive to contaminant.
- 10.2 Clean-up filter capable of achieving the initial cleanliness level.
- 10.3 Heat exchanger which does not act as a contaminant trap.
- 10.4 Reservoir with a conical shaped bottom.
- 10.5 Flow diffuser at the point where the main return line empties into the reservoir.
- 10.6 Four-way valve to by-pass system filter during contaminant injection periods.
- 10.7 Needle valve to direct all flow through the test valve.
- 10.8 Flow measuring device which is insensitive to contaminant.
- 10.9 Pressure sensing device.

TABLE 4.1

TEST CONDITION	MAINTAIN WITHIN \pm
PRESSURE	2%
TEMPERATURE	2°C (3.6°F)
CONTAMINANT CONCENTRATION	10%

- 10.10 Lines connecting hydraulic components sized so that turbulent mixing exists throughout.
- 10.11 Test circuit as shown in Fig. 4.1.
- 10.12 Injection chamber which is free of contaminant traps.
- 10.13 Injection chamber for the uniform introduction of contaminant to the test circuit.

11. Test System Qualifying Procedure

- 11.1 Install a direct connection in the test circuit in place of the test valve.
- 11.2 Adjust system volume so that it equals 45 percent to 55 percent of the lowest volumetric flow rate per minute at which the test system is intended to be used.
- 11.3 Circulate the fluid through the system filter until the contaminant background is less than 10 mg/L.
- 11.4 By-pass the filter.
- 11.5 Add unclassified AC Fine Test Dust per Reference [15.6] to the fluid to bring the contaminant concentration to 100 mg/L.
- 11.6 Inject the contaminant of Clause 11.5 in the form of a well-mixed slurry uniformly over a period of one minute.
- 11.7 Operate the system at the minimum flow rate as described in Clause 11.2.
- 11.8 Extract four fluid samples from the system per Reference [14.7] at 15 minute intervals from the completion of contaminant injection.

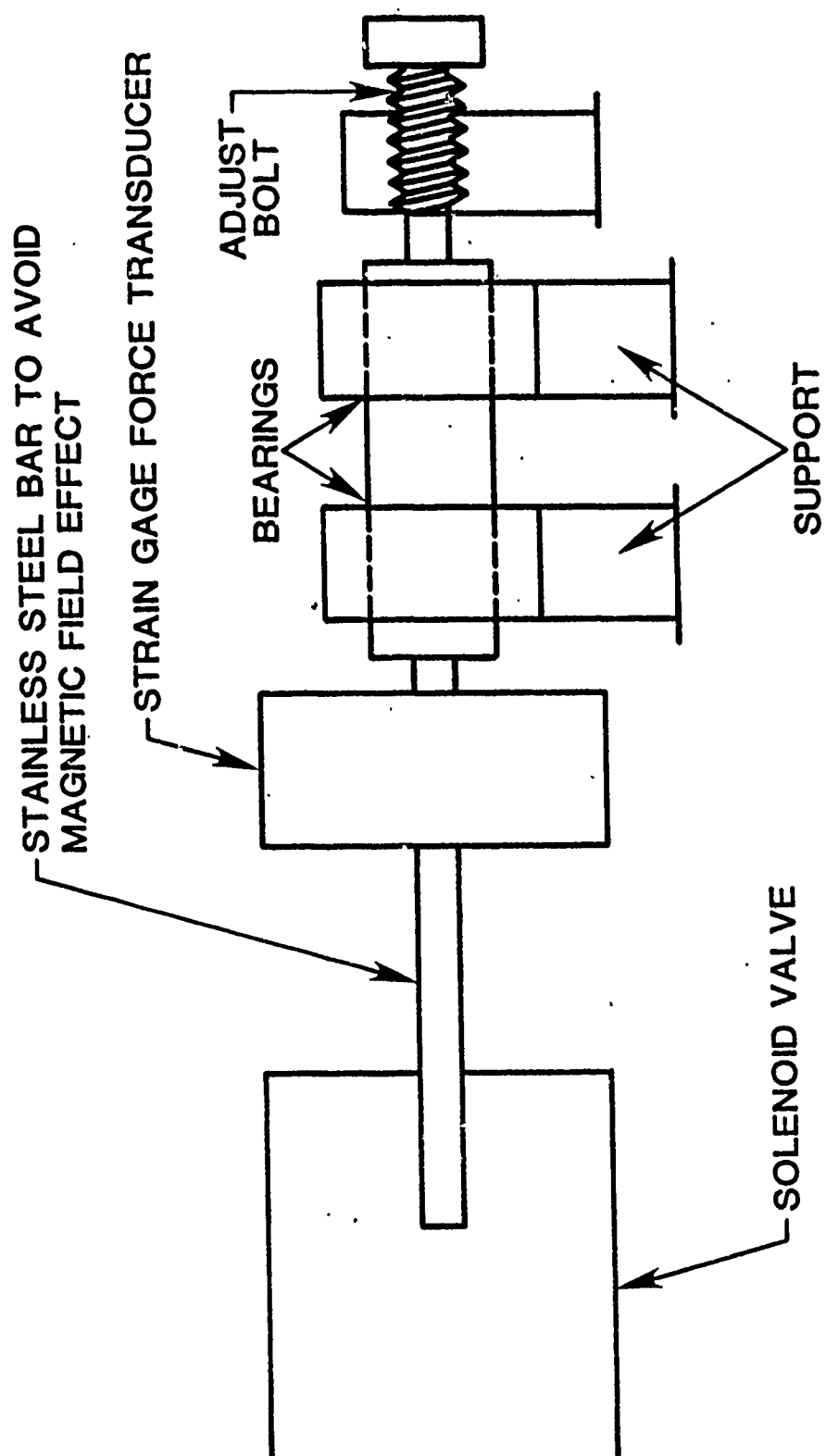


Fig. 4.1 Test Circuit

- 11.9 Circulate fluid through the filter until the contaminant background is less than 10 mg/L.
- 11.10 Measure the contaminant concentration level of each sample per Reference [14.4].
- 11.11 Consider the system qualified for testing if the contaminant concentration levels of Clause 11.10 are within ± 10 percent of the initial requirement of Clause 11.5.
- 11.12 Repeat this qualification of procedure when any modification to the flow path or to the reservoir is made.
- 12. Force Test of a Solenoid Valve
 - 12.1. Install the solenoid valve as shown in Fig. 1.
 - 12.2. Align the stainless bar to the side of manual override of the solenoid valve.
 - 12.3 Measurement for the case of shifting the valve spool from center to side (C→S).
 - 12.3.1 Use adjust bolt to push the manual override with the stainless steel bar until the manual override touches the spool of the valve.
 - 12.3.2 De-energize solenoids.
 - 12.3.3 Apply the voltage across the solenoids that are located on the opposite side of the stainless steel bar to create a force pushing against the stainless steel, Fig. 4.2(a).
 - 12.3.4 Record the change in voltage across the solenoid and force applied, as shown in Fig. 4.3.

12.4 Measurement for the case of shifting the valve spool from side to center (S→C).

12.4.1 Energize Solenoid A on the side of the stainless steel bar.

12.4.2 Insert the stainless steel bar until the spool, plungers and stainless steel bar make direct contact, Fig. 4.2(b).

12.4.3 Slowly de-energize Solenoid A.

12.4.4 Record the voltage across Solenoid A and force measured, Fig. 4.3.

12.4.5 After completely de-energizing Solenoid A, energize Solenoid B gradually.

12.4.6 Record the voltage across Solenoid B and force measure as in Fig. 4.3.

13. Test Procedure

13.1 Install the test valve into the test circuit.

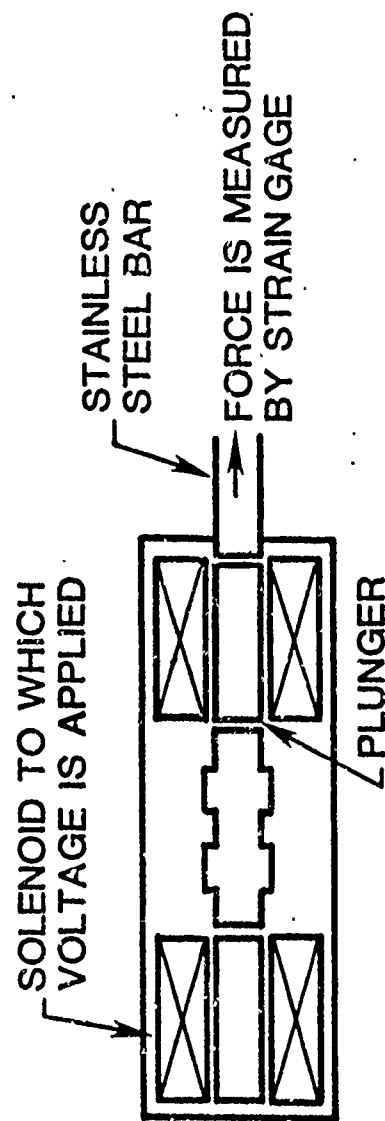
13.2 Filter the fluid until the contaminant concentration level is less than 10 mg/L.

13.3 Record static response test for the valve spool shift from the center to side (C→S) as follows:

13.3.1 Set the supply pressure equal to the rated pressure of the valve.

13.3.2 Energize solenoid to the rated voltage, then de-energize. Repeat three times.

(a) "C-S" SHIFT



(b) "S-C" SHIFT

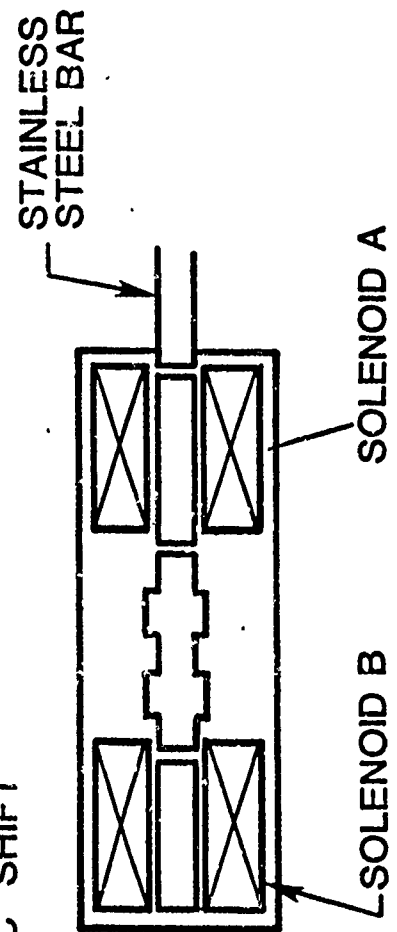


Fig. 4.2 Solenoid Valve Actuation Mechanism

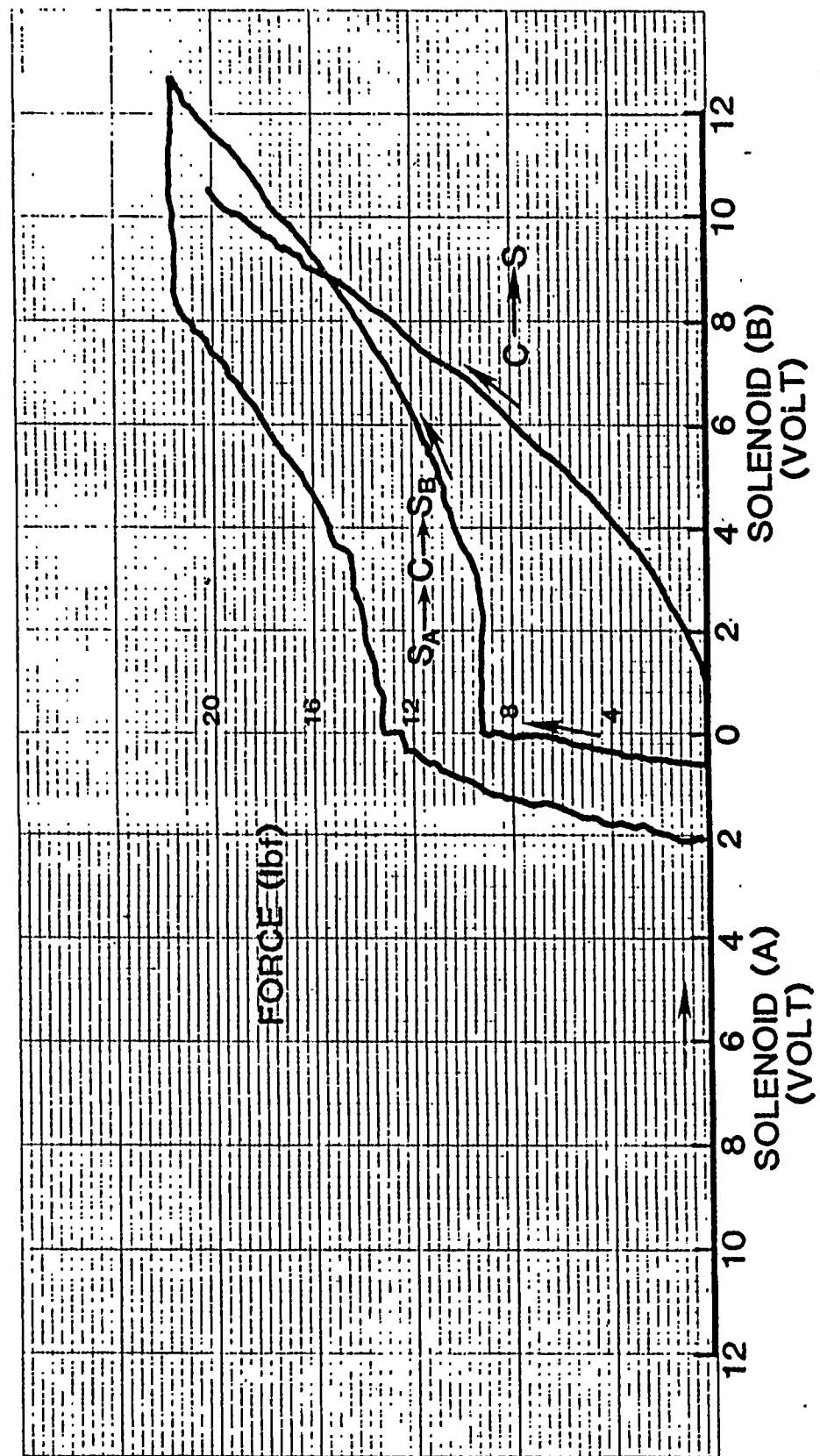


Fig. 4.3 Force & Voltage Characteristic Curve

- 13.3.3 De-energize solenoid and allow 1 minute of stationary time.
- 13.3.4 Record the variation in voltage across the solenoid and pressure across the valve ΔP_{PR} as the solenoid is slowly energized immediately after 1 minute of stationary time.
- 13.3.5 Increase gradually the voltage across solenoid up to its rated voltage.
- 13.3.6 Repeat 13.3.2 to 13.3.5 three times for repeatability of data.
- 13.4 Record static response test for the valve spool shift from the side to center (S→C).
 - 13.4.1 Set the supply pressure equal to the rated pressure of the valve.
 - 13.4.2 Energize solenoid to the rated voltage, then de-energize. Repeat three times.
 - 13.4.3 Energize solenoid to a side and allow 1 minute of stationary time.
 - 13.4.4 As the solenoid is gradually de-energized, immediately after 1 minute of stationary time, record the variation in voltage across the solenoid and pressure across the valve ΔP_{AB} .
 - 13.4.5 Decrease the voltage across the solenoid down to zero voltage.

- 13.4.6 Repeat 13.4.2 to 13.4.5 three times for repeatability of data.
- 13.5 Prepare a slurry of classified AC Fine Test Dust (0-20 μm) which will bring the contaminant concentration level of the fluid up to 100 mg/L.
- 13.6 Inject the slurry in the injection chamber of the test system.
- 13.7 Introduce the contaminant to the test hydraulic system uniformly over a period of one minute using the injection chamber.
- 13.8 Allow the contaminant to circulate through the test valve for a period of two minutes.
- 13.9 Test the valve according to the steps in 13.3.
- 13.10 Repeat 13.9 for three more different pressures that are approximately equally spaced pressures between zero pressure and the valve's rated pressure.
- 13.11 Test the valve according to the steps in 13.4.
- 13.12 Repeat 13.11 for three more different pressures that are approximately equally spaced pressures between zero pressure and the valve's rated pressure.
- 13.13 Evaluate the silting force of C \rightarrow S and S \rightarrow C according to 12 from the voltage data of the solenoid.
- 13.14 Find the silting forces by subtracting the force under clean fluid from the force under contaminated fluid for both C \rightarrow S and S \rightarrow C.

13.15 Compare silting force of C→S and S→C. The one that has the higher silting force result is still being tested.

13.16 Repeat the chosen shift test (13.9-13.10 or 13.11-13.12) for the injection of 0-10 μm and 0-5 μm AC Fine Test Dust following the steps in 13.5 to 13.7.

14 References

14.1 American National Standard Glossary of Terms for Fluid Power, ANSI/893.2 - 1971.

14.2 International Standard Graphic Symbols for Hydraulic and Pneumatic Equipment and Accessories for Fluid Power Transmissions, ISO/R, 1219-1970. Agrees with ANSI.Y32, 10-1967.

14.3 American National Standard Fluid Power Diagrams, ANSI/Y14, 14-17-1966.

14.4 Assessing Cleanliness of Hydraulic Fluid Power Components and Systems - SAE J1227.

14.5 International Standard Rules for the Use of the International System of Units and a Selection of the Decimal Multiples and Sub-Multiples of S.I. Units, ISO/R, 1000-1969.

14.6 Air Cleaner Test Code - SAE J726C.

14.7 Hydraulic Fluid Power - Particulate Contamination Analysis - Extraction of Fluid Samples from Lines of an Operating System - ISO 4021.

CHAPTER V - TEST STAND

In order to conduct the tests described in the previous chapter, a contaminant sensitivity test facility was constructed. It was determined that the test stand must meet the following criteria:

1. It must accept a variety of valves up to four-way, three position.
2. It must have facilities for a controlled rate of injection of contaminants into the fluid stream.
3. The components in the test system must not be contaminant sensitive, and they must neither generate nor trap the test contaminant, so that the gravimetric level of the contaminants will remain constant.
4. It must be compatible with mineral base fluids as well as the entire range of fire resistant fluids.
5. It must have a cleanup system to remove the contaminants after each test.

To meet these criteria, a stand was fabricated using the schematic diagram shown in Fig. 5.1. The stand was provided with a manifold suitable for mounting a variety of valves on their individual adapters.

The injection chamber provides the means for injecting the ACFTD contaminants at a controlled rate. The chamber is constructed of glass so that the injection process can be observed and to ensure

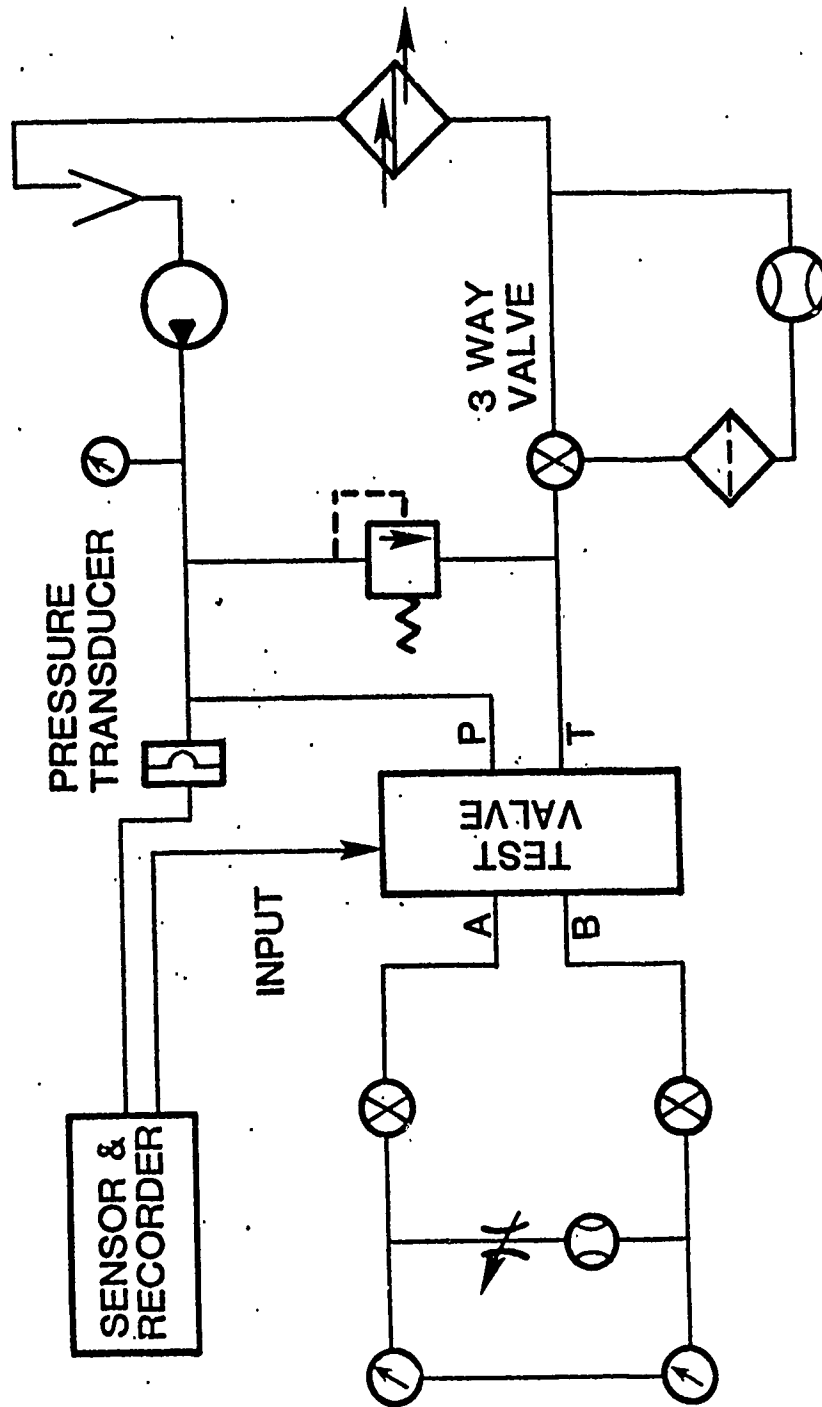


Fig. 5.1 Schematic of Test Circuit

that the contaminant does not adhere to the side walls. The base of the chamber is conical.

Contaminant is put into the chamber as a slurry. The injection valve is then opened to allow the slurry to flow into the test reservoir, where it is thoroughly mixed with the test fluid by the agitating action of the diffuser through which all return fluid flows. Residual contaminants are removed from the injection chamber by allowing a portion of the return fluid to flow through the chamber.

The components used in the stand were chosen based either on previously conducted contaminant sensitivity tests or on known contaminant insensitive designs. For instance, the main system pump has a demonstrated high contaminant tolerance, while the charge pump uses a centrifugal design which is not only insensitive to contaminants but which also does little damage to the ACFTD particles.

The flow meter on the high pressure portion of the system was target-type. A rotameter was used on the low pressure side of the system. The shut-off valves and three-way valves were of stainless steel construction to resist abrasion, while the pressure relief valve had been tested at the FPRC and was known to be very contaminant tolerant.

To ensure that a constant contaminant gravimetric level could be maintained by the test system, qualification tests were conducted in accordance with Clause 11 of the Test Procedure of Chapter IV with the exception that a gravimetric level of 250 mg/L was used rather

than the 100 mg/L specified in the procedure. This was done because it was originally proposed to test the valves at this higher contaminant concentration. Unfortunately, the higher level caused some long-term damage to the test stand components, so it was decided to reduce the concentration.

The qualification test results are shown in Fig. 5.2. The ability of the stand to maintain the injected level for at least one hour is clearly shown.

To ensure compatibility with fire resistant hydraulic fluids, most system components were fabricated of stainless steel. Where elastomeric seals were required, Viton seals were specified.

The filter elements used in the cleanup circuit have a Beta 10 rating of greater than 75.

MAJOR TEST STAND COMPONENTS

The following is a listing of the major components used in the fabrication of the valve test stand:

Hydraulic System

- Hydraulic pump

Dynex/Rivett fixed displacement piston pump model PF4015-1584

- Hydraulic Pressure Relief Valve

Vickers Balanced Piston type relief valve model CG-03-H-20

- Heat Exchangers

Basco two pass all 304 stainless steel model 04024

- Injection Chamber

Made of glass tube

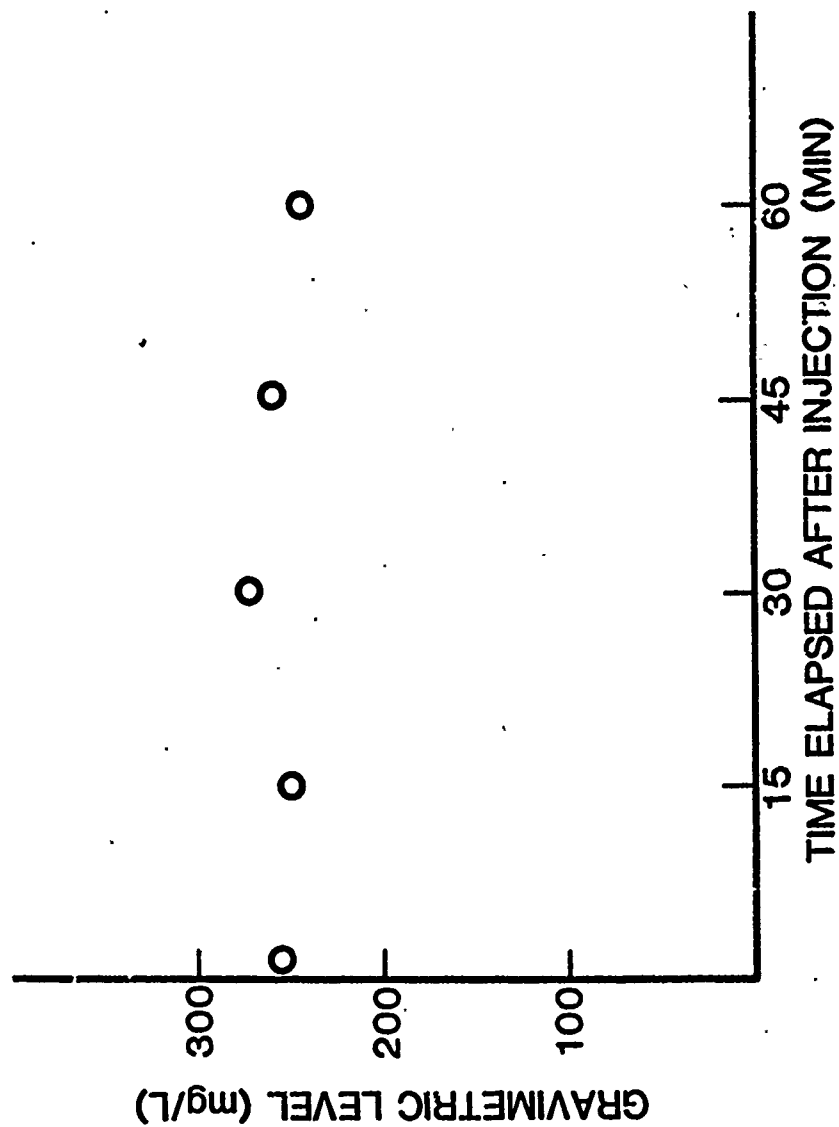


Fig. 6.1 Test Stand Qualification Test Result

- . Reservoir

Conical shape with diffuser at the end of hydraulic tubing

- . Charge Pump

Dayton centrifugal pump and electrical motor model GK580

- . Filter Elements

Hilco Model PL-718-26

Instrumentation

- . Flowmeter

Ramapo target type model Mark V- $\frac{1}{2}$ -SSB

- . Rotameter

Fischer and Porter model 10A 1755S

- . Differential Pressure Gauge

Sensotec Model A-5

- . Strain Gauge Amplifier

Daytronic Strain Gage Conditioner/Indicator Model 3278

- . Strain Gauge Amplifier

Ramapo digital flow indicator Model SGA-350 RMD

- . Servovalve Amplifier

Thompson Controls Model T6-R

- . Low Frequency Oscillator

Hewlett Packard Model 202 CR

- . X-Y Recorder

Hewlett Packard Model 7046A

TEST CONTAMINANTS

Air Cleaner Fine Test Dust (ACFTD) was selected as the test contaminant. This contaminant has been approved both nationally and internationally as a standard for contamination control tests. The result of chemical analysis of AC Fine Test Dust is tabulated in Table 6.1 for different size ranges with the raw dust reported by the manufacturer. Mechanical properties of the test contaminants are listed below:

Density = $2.66 \times 10^{-3} \text{ kg/cm}^3$

Poisson's Ratio = 0.2

Young's Modulus of Elasticity = $2.74 \times 10^3 \text{ MPa}$

Contaminant sensitivity tests on servovalves are conducted using lower cut classified AC Fine Test Dust (zero to some size "D") because of the resemblance of the size distribution of these cuts to the result of downstream particle size distribution of the system filter associated with the standard multipass test.

CHAPTER VI - RESULTS OF VALVE TESTS

To verify the solenoid valve contaminant sensitivity theory and Omega concept, four solenoid valves were tested according to the procedure of Chapter III. Each valve was four-way, three-position, closed-center and manufactured by a different company. The closed-center configuration was chosen because it was assumed to be the most sensitive to contaminants due to the high pressure drop across the closed position. The solenoids of two of the valves were 12 VDC. The others were 120 VAC.

SUMMARY OF RESULTS

The results of the four tests are summarized in Table 6.1. Because the Omega rating is directly related to the filter Beta 10 profile, a lower Omega rating is indicative of a lower contaminant sensitivity; that is, a higher contaminant tolerance.

It is interesting to note that the two valves using AC-powered solenoids had lower Omega ratings than the DC-powered units. While it is not the intention of the FPRC, or in fact of this test procedure, to determine the reasons for the ratings, it is interesting to speculate on the rating difference.

One possible explanation for the better performance of the AC-powered valves is that the alternating current was actually providing a dithering motion to the valve spool when the spool is to shift. This movement could cause a re-arranging, re-aligning, or possibly even a

destruction of trapped contaminant, which would subsequently allow the spool to shift. This is possibly seen in the results of Valve 130, where some slight delay was seen between the energizing of the solenoid and the movement of the spool under contaminated fluid.

COMPARISON

The Omega values of tested solenoid valves are tabulated in Table 6.1. It was demonstrated that solenoid valves that have AC (alternating current) solenoid show lower Omega values. This is probably not due to the fact that those valves have less contaminant sensitive structures but because the AC solenoid applies oscillatory force on the spool of the solenoid valves. Since the alternating current changes direction as well as magnitude, the magnetic field created by the solenoid is also changing. It was noted that, when a contaminant lock situation existed, the solenoid emitted a hum, indicating that the unit was vibrating. In several instances, the contaminant lock was broken and the spool moved after a few seconds. The variation of solenoid force resulting from the AC induced vibration on Valve #129 is shown in Fig. 6.1. It is seen that the spool is pulsed 120 times per second.

Hence, it is reasonable to say that, even if the same maximum force were applied by an AC and a DC solenoid, the AC device would have some advantage over the DC unit. It can be hypothesized that, because of the AC solenoid's oscillatory force application, contaminants lodged in the clearance of a valve may be dislodged, reoriented, or crushed

Table 6.1 Summary of Omega Ratings of Tested Valves

OSU VALVE NUMBER	Ω OMEGA RATING	RATED PRESSURE	RATED FLOW	POWER SUPPLY	X_β	γ_β	RANK
127	69	4500	11	12 VDC	27.47	9.56×10^{-2}	4
128	13.2	5000	5	12 VDC	53.75	1.221×10^{-2}	3
129	6.9	4600	12	110/115 VAC 50/60 Hz	192.4	1.776×10^{-3}	2
130	≈ 1	6000	3	115 VAC 60 Hz	0.3850	8.633	1

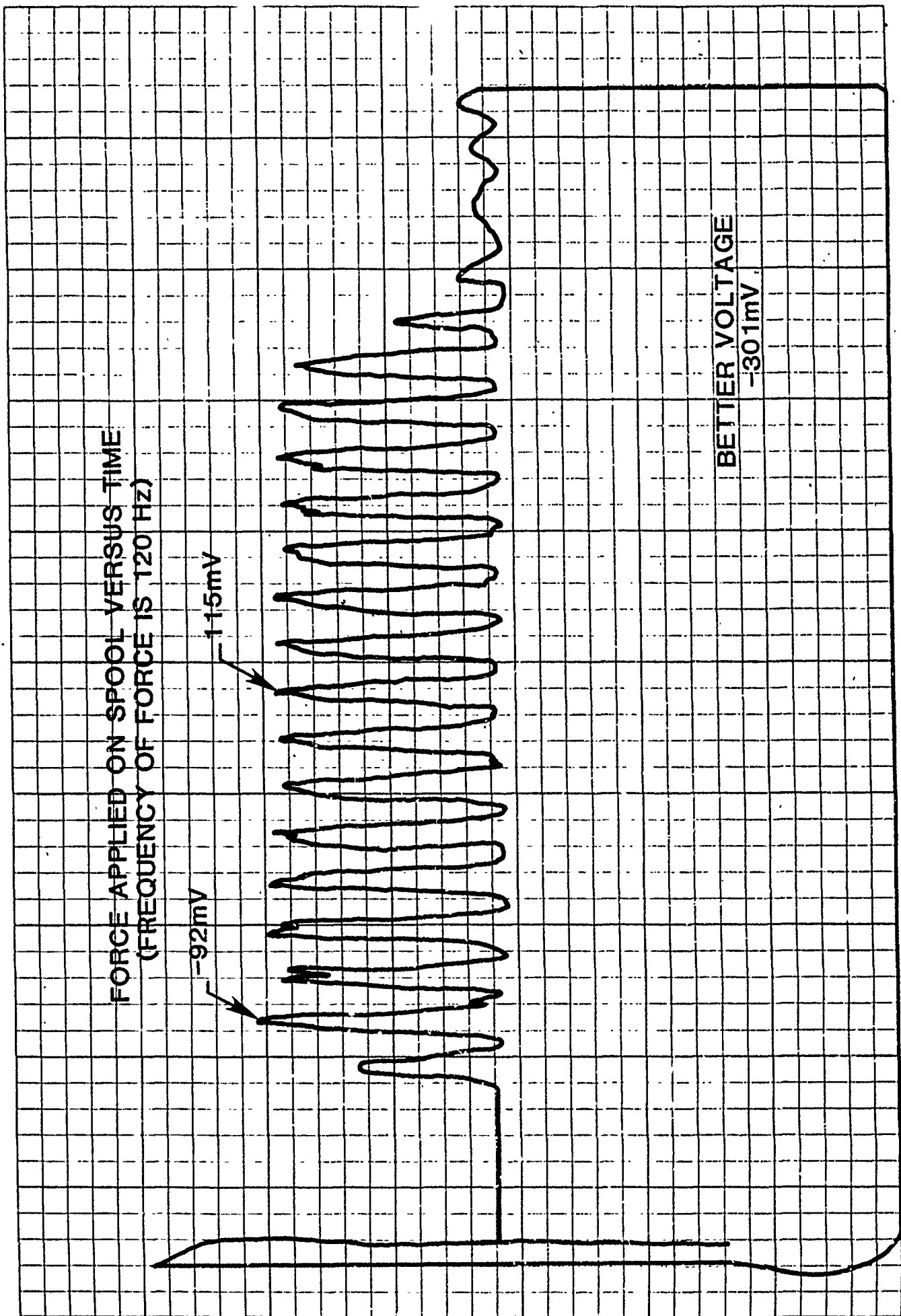


Fig. 6.2 Variation of Solenoid Force Due to the AC Induced Vibration

by the dither and allow the spool to move. On the other hand, a DC solenoid can apply a force of constant magnitude and direction only; therefore, once the spool is locked by contaminants, there is no possibility of breaking the spool loose to relieve the situation, except possibly by manual movement of the spool if such a facility exists on the valve.

OSU Valve #130 showed excellent contaminant tolerance. Although it displayed a slight hesitation at a 2 mg/L concentration of 0-5 micrometre test dust, the spool never failed to respond to the input signal.

The Omega values of all the test valves are shown in Table 6.1. As for pumps, motors, and other types of valves, the lower the Omega rating, the more tolerant the valve is to contaminant and the lower the Beta rating of the filter required to provide protection for it.

Valves #127 and 128 both used DC solenoids and showed the highest Omega ratings. This was probably directly attributable to the use of the DC solenoids.

CHAPTER VII

CONCLUSIONS AND RECOMMENDATIONS

As a result of the work described in this report, the following conclusions were reached:

1. Contaminant lock is a far more serious mode of failure in solenoid valves than is wear. Consequently, the activities of this project were directed toward a procedure for evaluating contaminant lock only. It may be advantageous in the future to investigate contaminant wear more closely in order to further differentiate between those valves with good contaminant lock characteristics.
2. The test procedure, test stand, and Omega rating system described in this report are suitable for evaluating the contaminant lock characteristics of solenoid valves.
3. On the basis of the valves tested, solenoid valves operated by AC power appear to have better Omega ratings than those operated on DC power.

The following recommendations are made:

1. MERADCOM should provide the necessary support and funding to promote this procedure as a national and/or international standard.
2. MERADCOM should require that all prospective solenoid valve suppliers provide Omega ratings obtained in accordance with this procedure along with other pertinent data.

PART III

HYDRAULIC CYLINDERS

CHAPTER I - INTRODUCTION

Hydraulic cylinders are the workhorses of the hydraulic industry. They supply the forces necessary to accomplish many important jobs. They lift and lower huge cranes, steer monstrous earth movers, crush automobiles, and manipulate heavy loads. Practical hydraulic systems would be impossible without cylinders. Although hydraulic cylinders are extremely powerful, they are still very sensitive and are damaged quite easily by contaminant entrained in the system fluid.

A problem may develop in a hydraulic cylinder directly due to the current state of the seal-rubbing surface interface. This problem is called drift, which is the loss of output force caused by internal leakage in the cylinder. Drift can be serious when it is desired for a hydraulic cylinder to maintain a force for a long period of time. It is highly desired that the fluid in the cylinder will stay pressurized at its load condition without being constantly re-supplied; otherwise, the force it is trying to exert will not be maintained. In practice, the loss of position holding capability of a cylinder may be devastating to property and human lives.

The main cause of cylinder rod drift is pressurized fluid escaping past piston seals through the microsurface of the barrel, thus causing a reduction in the force a cylinder can exert. The rate with which the fluid escapes in this way is a function of the current roughness state of the surfaces of the barrel and the seal which rubs against it. This

type of leakage is self-accelerating. The fluid tends to erode, especially in the seal, a deeper and deeper channel. Thus, a seal-barrel interface worn by contamination to the extent that fluid is getting through micro-grooves in the interface is very undesirable. The reason is that no further wear due to relative motion need take place for the seal to become totally useless.

From a practical standpoint, the condition of the barrel surface is affected by two distinct factors -- the initial surface finish given to the barrel during manufacture and any wear which has resulted during the operation of the cylinder. This latter factor is affected by both the surface-to-surface tribological (asperity) wear and the wear caused by particulate contamination in the fluid. These particles may be trapped by the seal and abrade the barrel surface in a sandpaper-like fashion, or they may be carried in the leaking fluid jet and aggravate the erosion caused by that jet. In either case, the effect is undesirable and could be alleviated by reduction in the amount of contaminant in the fluid.

It is believed that the effect of particulate contamination on the barrel surface is directly related to the original surface finish of the barrel and the seal characteristic. Due to the highly complicated tribological interface or topography of the barrel surface and seal, until now, no contaminant sensitivity assessment technique has been successfully developed for fluid power cylinders. This study advances a contaminant sensitivity test procedure for fluid power cylinders which

allows the user to identify the contaminant tolerance of fluid power cylinders effectively. In the next three chapters, the cylinder contaminant sensitivity rating method is presented, the test facility is outlined, and the contaminant sensitivity test procedure is outlined.

CHAPTER II - THE CYLINDER CONTAMINANT SENSITIVITY RATING METHOD

All fluid power components degrade when exposed to fluid-borne contamination and exhibit specific contaminant service lives for various states of contamination. The contaminant service life of a fluid power component is the time during which component performance degrades to a pre-determined level of acceptable performance. The Omega rating system developed at the FPRC/OSU has been proven effective in evaluating the contaminant sensitivity of most commonly used hydraulic components; for instance, pumps, motor, relief valves, etc. However, the Omega rating system has not been extended to fluid power cylinders. Due to the success of the Omega rating method when applied to other hydraulic components, Ahlberg (former Senior Project Engineer (FPRC)) conceived a method by which the Omega rating concept could be applied to fluid power cylinders. This section describes Ahlberg's approach and the difficulty presented in practical applications.

According to Bensch and Fitch, the performance degradation of a fluid power component is expressed as:

$$\frac{dP}{dt} = - \sum_i (n_i) \frac{dN_i(t)}{dt} \quad (2.1)$$

where P is the selected performance parameter; $S_i(n_i)$ is the sensitivity of the component to a concentration of n_i particles in the size interval i per unit volume; and $N_i(t)$ is the number of particles in the size interval i to which the component is exposed at some instant in time, t .

The performance parameter chosen to express cylinder performance degradation is the theoretical displacement flow minus the cyclic leakage flow past the piston. The theoretical displacement flow is:

$$Q_T = V \cdot A \quad (2.2)$$

where Q_t is the rate of flow, V is the stroking velocity, and A is the annulus area formed between the piston and the rod.

The chosen cylinder performance parameter is defined as:

$$Q(t) = Q_T - (L/t) \cdot \frac{1}{S} \quad (2.3)$$

where $Q(t)$ is the performance parameter, L is the volume of leakage passing the piston, t is the time over which the leakage is collected, and S is the number of stroke cycles over which the leakage is collected.

Unless discovered otherwise, the contaminant sensitivity of a cylinder will be assumed to be linearly proportional to the concentration of fluid-borne contaminant.

$$S_i(n_i) = \alpha_i n_i \quad (2.4)$$

where d_i is the contaminant sensitivity coefficient for the size interval i . The rate of particle exposure to a fluid power cylinder is expressed as:

$$\frac{dN_i(t)}{dt} = Q(t) n_i \quad (2.5)$$

By substituting Eq. (2.4) and Eq. (2.5) into Eq. (2.1) and rearranging, Eq. (2.6) results:

$$\int_{Q_0}^{Q(t)} \frac{dQ}{Q} = -\alpha_i n_i^2 \int_0^t dt \quad (2.6)$$

where Q_0 is the original value of the performance parameter $Q(t)$, which is measured after break-in but before the first injection of contaminant when performing a contaminant sensitivity test. Integrating Eq. (2.6) yields:

$$Q(t) = Q_0 \exp(-\alpha_i n_i^2 t) \quad (2.7)$$

Eq. (2.7) can be solved for δ_i as:

$$\alpha_i = \frac{-\ln(Q(t)/Q_0)}{n_i^2 t} \quad (2.8)$$

Therefore, the reference contaminant life equation for fluid power cylinders is:

$$T = -\ln(Q(t)/Q_0) / \sum_{i=1}^{i_{max}} \alpha_i n_i^2 \quad (2.9)$$

Theoretically, the contaminant sensitivity coefficient, δ_i , for size interval i can be obtained from Eq. (2.8) if the flow degradation ratio ($Q(t)/Q_0$) is known. Accordingly, the reference contaminant life of a specific cylinder can be derived from Eq. (2.9). In order to find out the flow degradation ratio, several approaches have been developed at the FPRC; for example, the dynamic leakage method, static leakage method, pressure differential method, etc. Although the test methods used are different from each other, the final purpose is the same -- to monitor the variation of internal leakage between seal and barrel surfaces such that the parameter $Q(t)$ can be obtained.

Eq. (2.3) shows that the cylinder performance flow rate, $Q(t)$, is the difference between the theoretical displacement flow, Q_T , and the internal leakage. In practical application, the internal leakage flow is several orders less than the displacement flow. This property induces the insensitivity of $Q(t)$ with respect to the variation of the internal

leakage. Table 2.1 illustrates test results obtained by conducting cylinder contaminant sensitivity tests. The cylinder used has a theoretical displacement flow of 8 litres/min. The measured static internal leakage flow is about 0.5 millilitres/min. As compared to the theoretical displacement flow, the internal leakage is trivial.

The seal mechanism is another factor which increases the complexity of utilizing the conventional Omega rating system, Eq. (2.9), to evaluate fluid power cylinder contaminant sensitivity. Unlike the tribological wear process that occurs in most hydraulic components (a process in which, once contaminant-induced wear takes place, a relevant clearance increase occurs between the critical surfaces), the seal will compensate for the increased clearance due to its inherent elasticity. The clearance compensation mechanism results in the catastrophic failure of the sealing function. Mathematically, a discontinuity may occur in manipulating the catastrophic failure data. This discrepancy again causes difficulty in finding the contaminant sensitivity coefficients. Table 2.1 shows that there is no significant flow degradation that results from injecting different particle size contaminants. The postulated clearance compensation mechanism is therefore supported.

From the above discussion, it is realized that, in order to investigate fluid power cylinder contaminant sensitivity, it is necessary that an effective parameter be identified to evaluate the performance degradation rather than simply measuring flow degradation directly.

Table 2.1 Cylinder Test Results -- Average Leakage

PARTICLE SIZE (μm)	AVERAGE LEAKAGE (mL/min.)
0-5	.58
0-10	.39
0-20	.482
0-40	.592
0-80	.477

A straightforward way to accomplish this is to correlate performance degradation in terms of wear rate. Ferrography has been proven as an effective wear analysis technique if there is a significant amount of ferrous wear debris generated in a tribological system. Because of the non-intrusive wear analysis property exhibited, Ferrography became the first candidate selected to investigate the cylinder wear characteristic in this study. However, most of the seals were made of nonmetallic material; for example, Teflon. It therefore became apparent that the wear characteristic could not be adequately analyzed by employing ferrography.

It is well known that the particle concentration level in a carefully controlled chamber is very sensitive to the external ingress of particles. These external particles may enter the controlled chamber through the clearance between the seal and cylinder barrel by means of the pressure differential across the seal or the motion of the piston. In other words, the leakage flow carries particles from the high pressure side to the low pressure side of the container. The higher the leakage flow, the more particles that are transferred. Accordingly, by monitoring the variation in the particle concentration level at the low pressure side of the chamber, an indication can be found for the variation of leakage flow which passed the seal and barrel surfaces. Furthermore, the internal leakage of the fluid power cylinder is a function of wear behavior which occurs between the seal and barrel. Consequently, the variation of particle concentration level in the controlled chamber

provides effective information by which to rate the contaminant sensitivity of fluid power cylinders.

Fig. 2.1 illustrates the particle ingress process which occurs in a fluid power cylinder. Whenever the high particle concentration chamber is pressurized, some of the particles become entrained in the low pressure side as a result of internal leakage. The variation rate of the particle concentration level at the low pressure side is expressed as:

$$\frac{dN_L(t)}{dt} = \frac{N_H(t) \cdot Q(t)}{V_L} \quad (2.10)$$

where $N_L(t)$ is the particle concentration level at the low pressure side at time t ; $N_H(t)$ is the particle concentration level at high pressure side at time t ; $Q(t)$ is the leakage flow rate through the seal and barrel at time t ; and V_L is the fluid volume at the low pressure side.

Suppose that the particle concentration of the high pressure side level, N_H , is constant. Integrating Eq. (2.10) yields:

$$N_L(t) = \frac{N_H}{N_L} \int_0^t Q(t) dt \quad (2.11)$$

Because the characteristic of $Q(t)$ is unknown, there is no analytical solution of Eq. (2.11). In order to simplify Eq. (2.11), it is assumed that the leakage flow is averaged during a reasonable sampling interval. As a result, the particle concentration level at the low pressure side during the i th sampling interval is:

$$N_{L,i} = N_{L0,i} + \frac{N_H}{N_L} \cdot \bar{Q}_i \cdot S \quad (2.12)$$

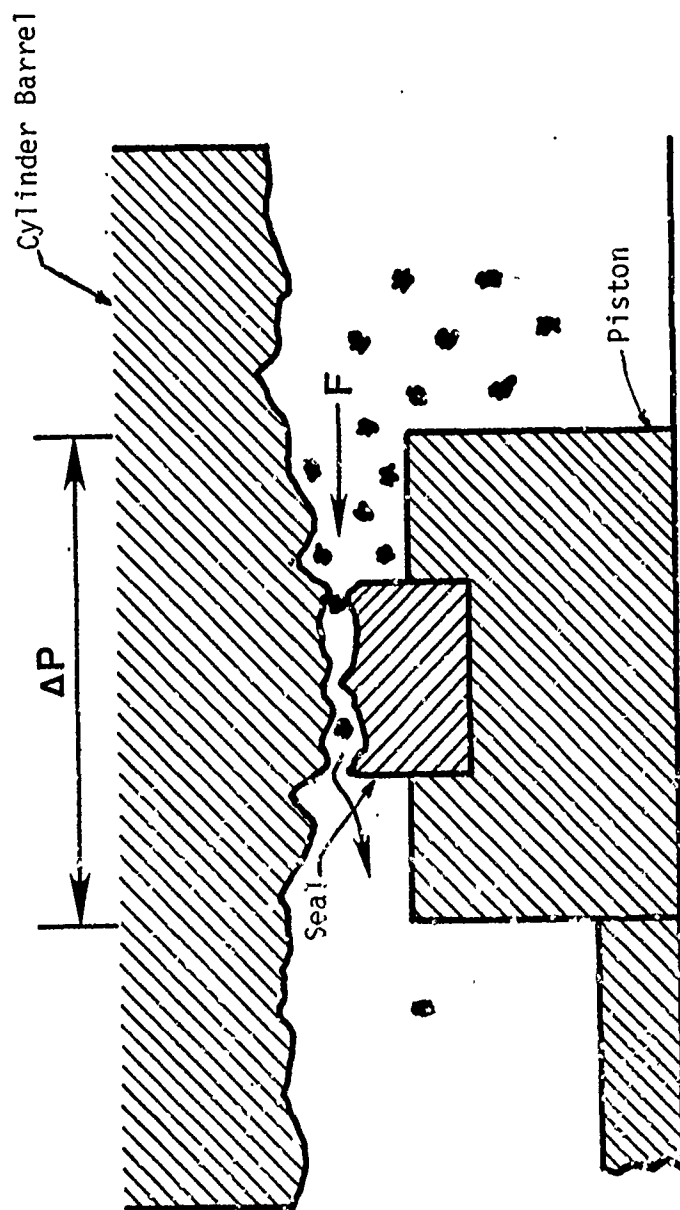


Fig. 2.1 Particle Ingression Process

where $N_{0,i}$ is the initial particle concentration at the low pressure side during the i th sampling interval, \bar{Q}_i is the averaged leakage flow rate at the i th sampling interval, and S is the sampling time.

The advantage of using Eq. (2.12) to rate cylinder contaminant sensitivity can be appreciated by examining the following example. Assume that the high pressure side particle concentration level is 300 mg/L, the low pressure side fluid volume is 50 milliliters, the initial particle concentration, $N_{0,i}$, is zero, sampling time is one hour, and the leakage flow rate is 0.01 mL/min. Substituting these data into Eq. (2.12), it is found that $N_{e,i}$ is 3.6 mg/L concentration change. However, the cumulative leakage flow is only 0.6 milliliters. Thus, the resolution using the particle concentration level approach is significantly higher than measuring the volume of leakage flow.

Contaminant sensitivity of fluid power cylinders can be evaluated by setting an acceptable reference particle concentration level at the low pressure chamber. Failure of the piston seal is characterized by the number of cycles distance at which the particle concentration level at the low pressure side exceeds the reference level. Fig. 2.2 illustrates the cylinder contaminant sensitivity rating concept. The higher the cycle distance obtained, the higher the contaminant tolerance possessed by the fluid power cylinder. The following chapter describes the test facility developed to verify the established cylinder contaminant sensitivity rating technique.

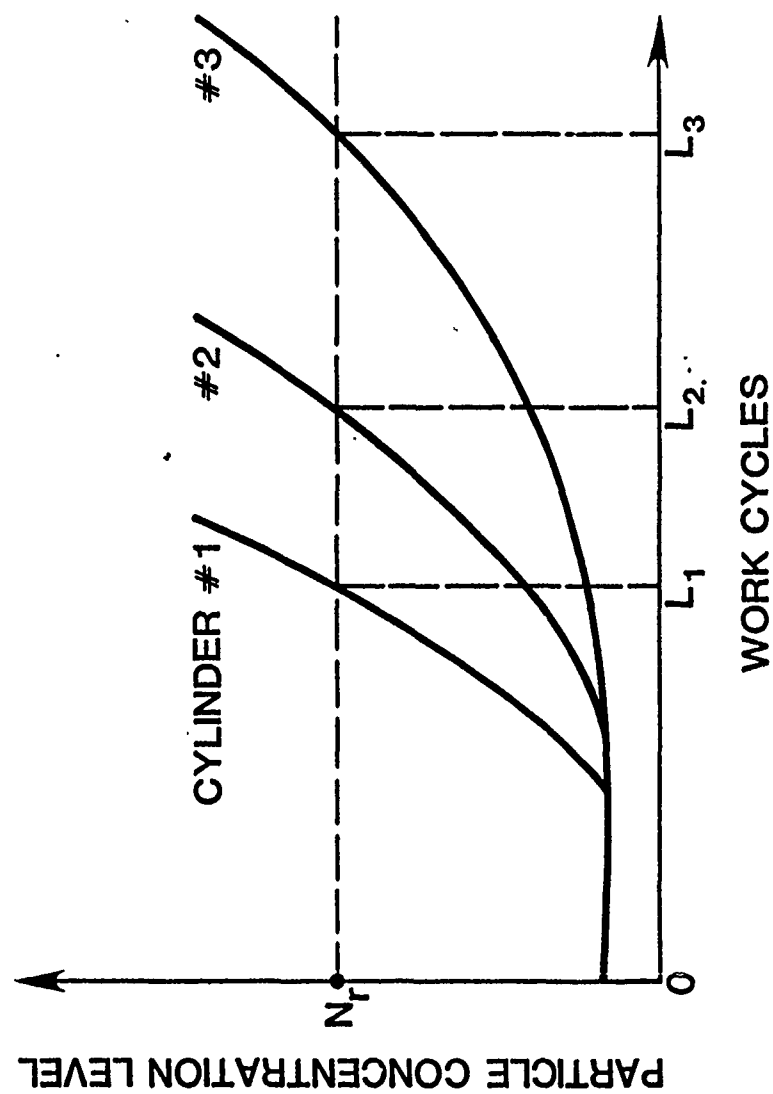


Fig. 2.2 Cylinder Contaminant Sensitivity Rating Concept

CHAPTER III - CYLINDER TEST FACILITY

Fig. 3.1 is a schematic circuit diagram of the cylinder contaminant sensitivity test system. Several parts of this system are labeled and identified in the figure. The basic premise limiting the design of this test stand is:

- * The cylinder must be stroked against a load by fluid pressure.
- * The fluid stroking the cylinder must be at a controlled pressure and contaminant level.
- * The mechanism pressurizing the fluid must not damage the contaminant.
- * The mechanism pressurizing the fluid must not be degraded by the contaminant.

By virtue of these conditions, a normal pump pressurization system was ruled out. Basically, the test stand consists of a driving cylinder, 2 (Component No. 2 in Fig. 3.1), two pumping cylinders, 3 and 4, one load cylinder, 19, and one test cylinder, 20. The drive cylinder, 2, which is operated by a separate clean fluid hydraulic power source, has its stroke limited by two limit switches controlling a hydraulic control valve, 1.

The drive cylinder is coupled by a through shaft to both pumping cylinders, 3 and 4, which are connected to the two ports of the test cylinder, 20, individually. As the drive cylinder, 2, strokes upward (see Fig. 3.2), the pumping cylinder, 3, displaces the clean fluid and delivers it to the rod end side chamber of the test cylinder to the stroke test cylinder rod. Because the test cylinder rod is coupled directly to the load cylinder, 19, the piston of the load cylinder rises. By virtue

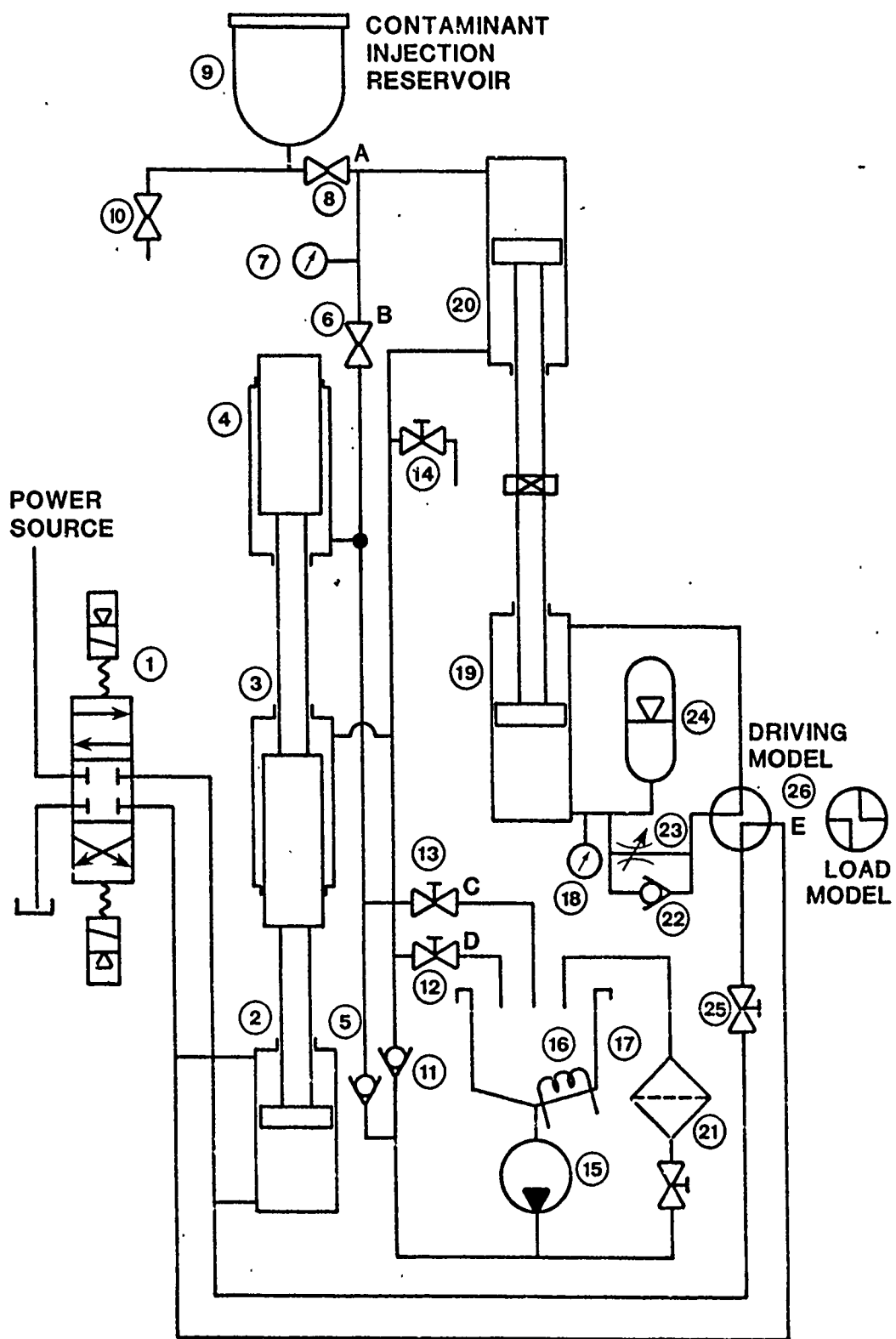


Fig. 3.1 Test Circuit

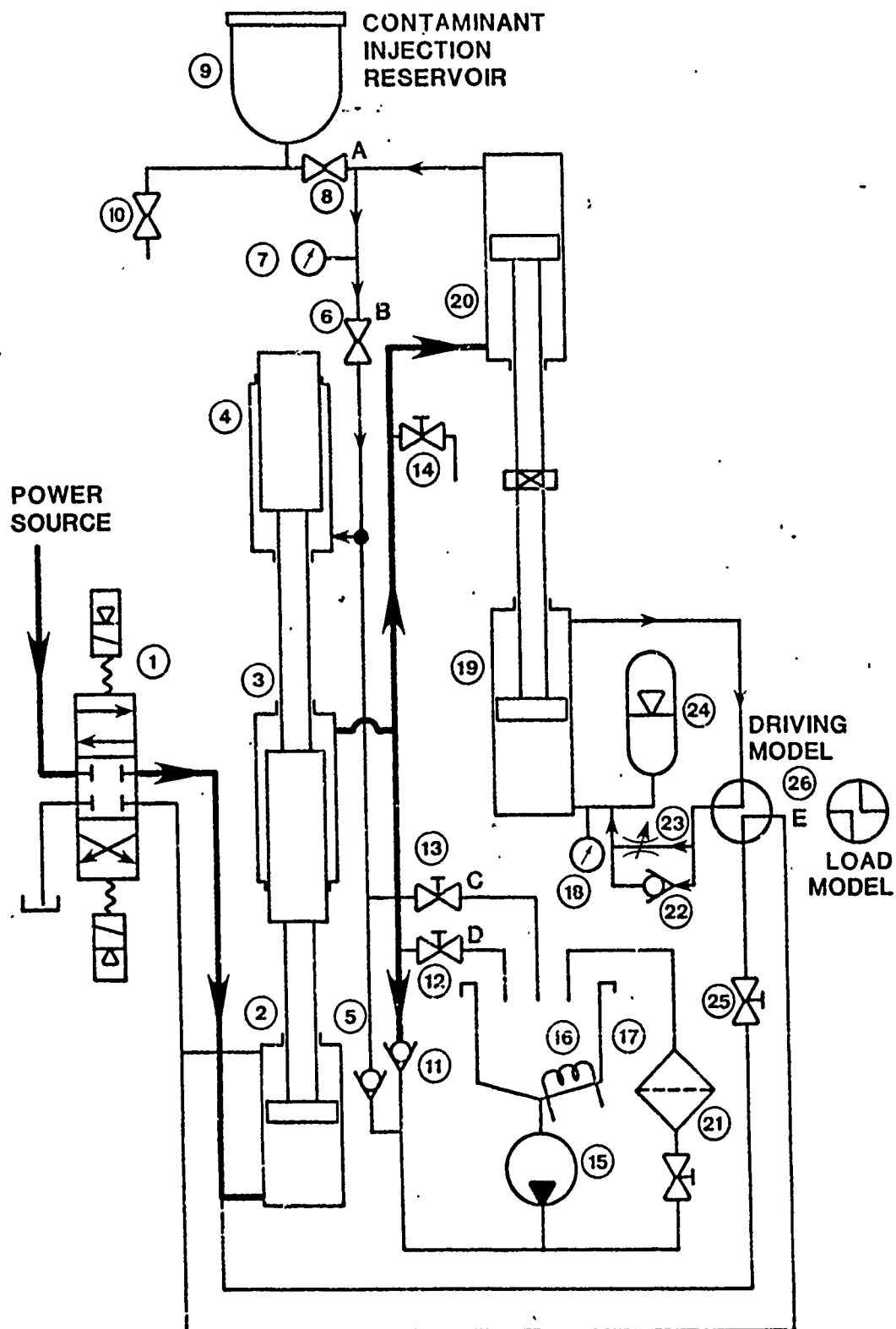


Fig. 3.2 Schematic of Pressure Path -- Upward Process

of this, the fluid in the rod end side of the load cylinder is compressed and forced to pass elements 26, 23, and 22 into the lower chamber. Due to the flow passing through the check valve, 23, in the free direction, there is no resistance to the fluid. In other words, the pressure established in the test cylinder chambers is relatively low. This high pressure contaminant section with low pressure clean fluid mechanism section prevents the clean fluid in the lower chamber of the test cylinder from entraining into the upper chamber where the fluid has been contaminated to the desired reference level. Consequently, the particle concentration level in the upper chambers can be maintained.

On the other hand, as the drive cylinder strokes downward (see Fig. 3.3), the fluid in the lower chamber of the pumping cylinder, 4, is compressed. As a result, the piston rod at the test site retracts. The fluid in the lower chamber of the load cylinder is therefore compressed. By virtue of this, the oil pressure rises until the load control valve, 23, is tripped and relieves the excess fluid to the high chamber of the load cylinder. Therefore, a high pressure is established in the upper chamber of the test cylinder in order to push the rod to overcome the high pressure force generated in the lower chamber of the load cylinder, thus simulating a load in the fluid power cylinder application. Furthermore, the high pressure in the upper chamber of the test cylinder forces contaminants to pass through the clearance between the seal and cylinder barrel surfaces, which accelerates the contaminant wear of the cylinder. More significantly, the ingression of particles

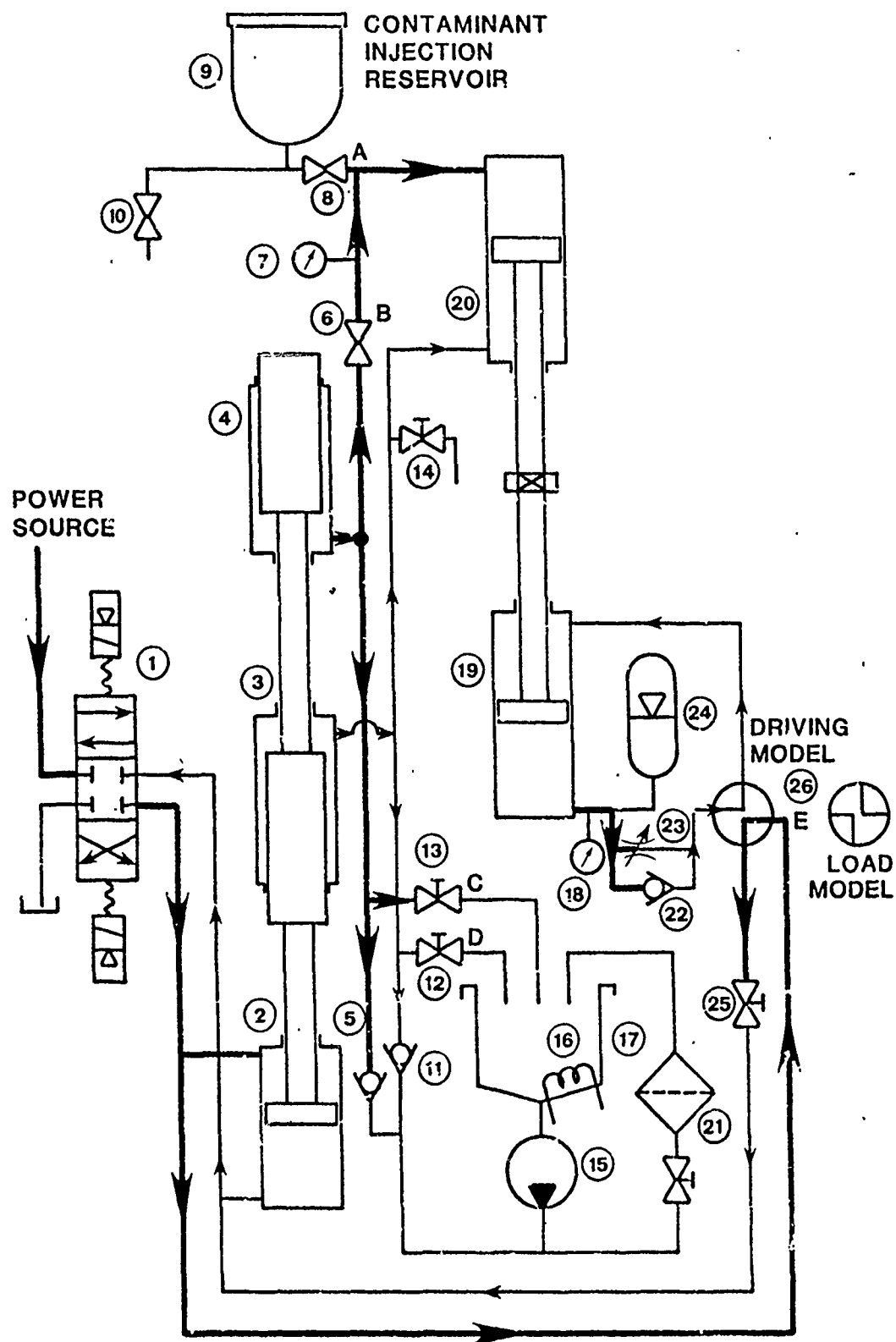


Fig. 3.3 Schematic of Pressure Path -- Downward Process

from the upper chamber (fluid inside is contaminated) to the lower chamber (clean fluid) of the test cylinder provides a feasible way to investigate the contaminant sensitivity of fluid power cylinders by means of the variation of particle concentration in the lower chamber of the test cylinder.

The cylinder test system requires a hydraulic power supply to furnish the fluid power to the drive cylinder. The system operating pressure is maintained at some specified value set independently by a relief valve.

In addition to the power supply, there is a temperature control system for the test cylinder. The reservoir has a heating element immersed in its fluid. Fluid temperature is controlled by the temperature control system. The temperature in the reservoir is sensed and controlled by regulating the electric power to the heater and maintaining the desired fluid temperature.

CHAPTER IV - FLUID POWER CYLINDER CONTAMINANT TEST PROCEDURE

1.0 Purpose

- 1.1 The purpose of this test procedure is to determine the contaminant sensitivity of fluid power cylinders.

2.0 Test system verification (Qualification).

- 2.1 Install the test cylinder with its proper position, (Fig. 4.1).
- 2.2 Circulate system fluid through the filtering system with the test circuit completely unloaded until the contaminant background is less than 2 mg/L.
- 2.3 Disconnect the filtering system.
- 2.4 Achieve a contamination level of AC Fine Test Dust of $300 \text{ mg/L} \pm 30 \text{ mg/L}$ in the test site fluid. The system is qualified when the particle concentration level is maintained within $300 \text{ mg/L} \pm 30 \text{ mg/L}$ for a period of 30 minutes.

3.0 Preliminary preparation.

- 3.1 Operate the cylinder under clean fluid conditions at the test speed and 40 C (100 F). Use the following schedule for cylinder break-in:

1000 stroke cycles at 25 percent of test pressure
1000 stroke cycles at 75 percent of test pressure
1000 stroke cycles at 100 percent of test pressure

- 3.2 Take fluid sample from the rod end side chamber of the test cylinder. This is the initial clean background particle concentration level.

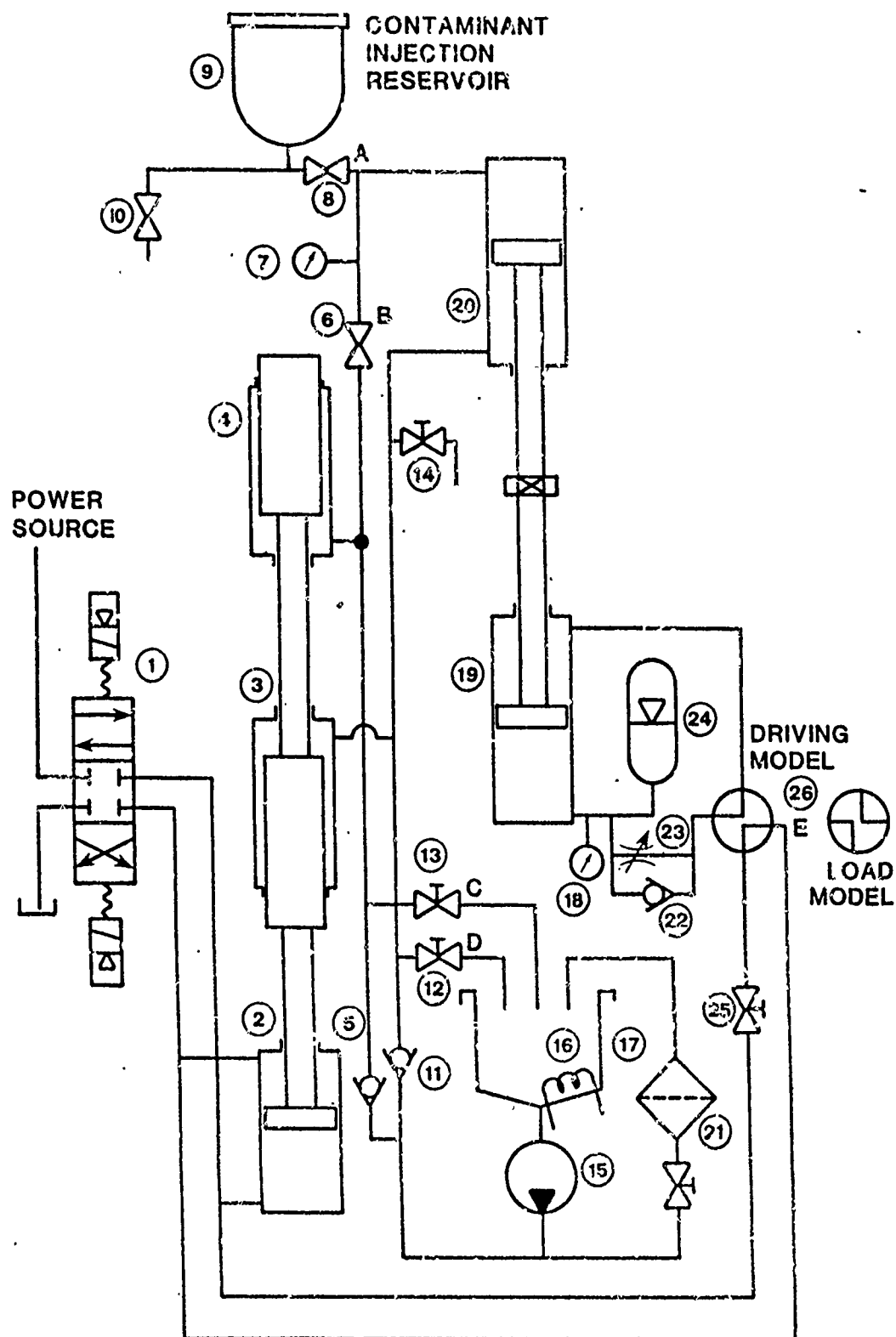
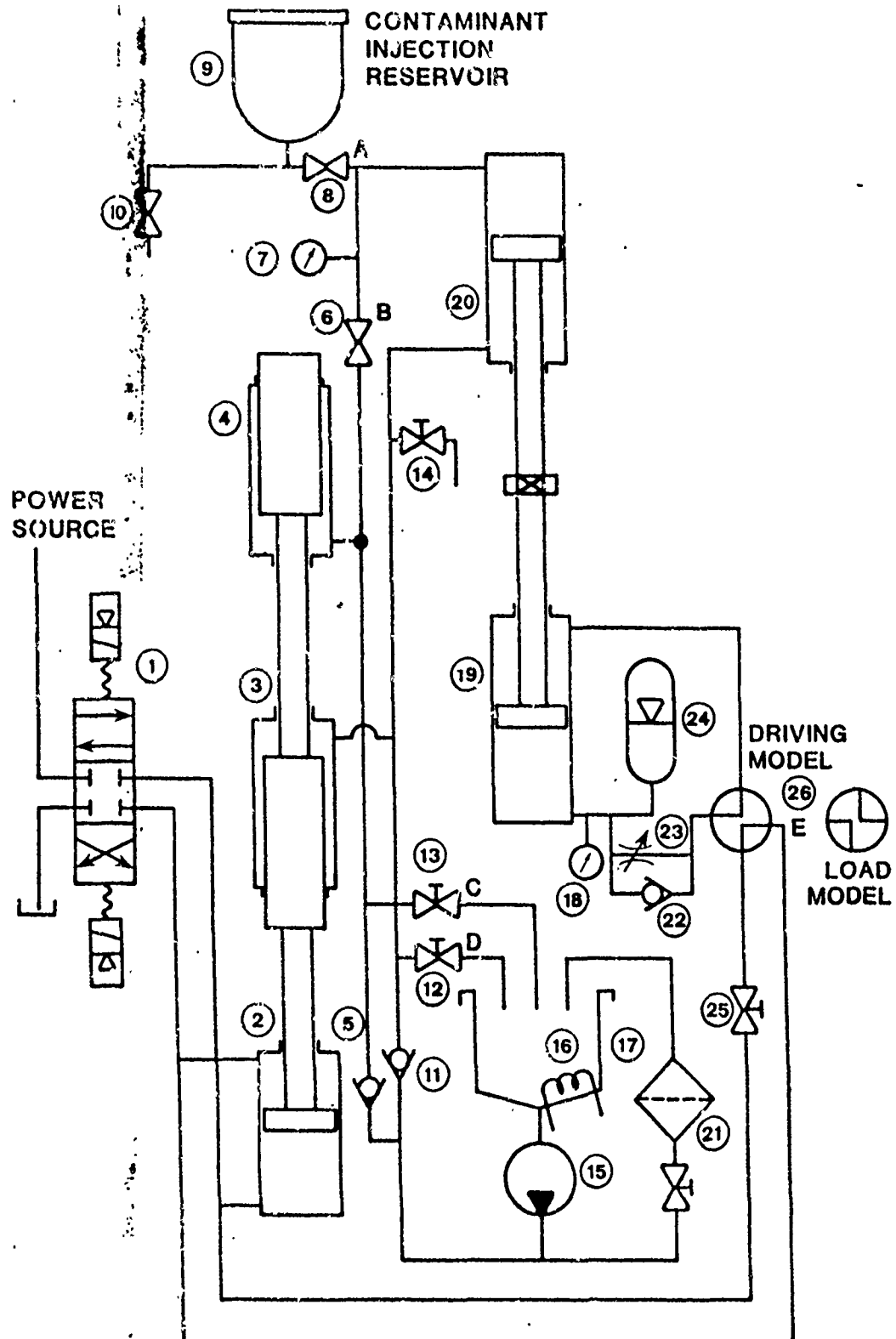


Fig. 4.1 Test Circuit



- 3.3 Inject ACFTD to obtain a $300 \text{ mg/L} \pm 30 \text{ mg/L}$ concentration level.
- 4.0 Contaminant sensitivity test.
- 4.1 Operate the cylinder at test speed, test pressure, and test temperature for 2000 stroke cycles.
- 4.2 Take a fluid sample from the rod end side chamber.
- 4.3 Repeat Steps 4.1 and 4.2 until 10,000 cycles.
- 5.0 Presentation of test results.
- 5.1 Analyze fluid sample particle concentration level.
- 5.2 Record all information required in Table 4.1.
- 5.3 Draw the characteristics of particle concentration level versus working cycles at 10 micrometer size.
- 5.4 Calculate the work cycles reaching the reference concentration level.
- 5.5 Take the product of the work cycles obtained in Clause 5.4 and the cylinder stroke distance. The result is the work cycle distance, which is the parameter used to represent cylinder contaminant sensitivity.

Table 4.1

CYLINDER CONTAMINANT SENSITIVITY TEST REPORT

CYLINDER I. D. NO. _____ TEST DATE / /

TEST SPEED _____ TEST FLUID _____

STROKE DISTANCE _____ TEST DUST _____

TEST PRESSURE _____ GRAVIMETRIC LEVEL _____

TEST TEMPERATURE _____

PARTICLE SIZE	WORK CYCLES						REMARK
	0	2000	4000	6000	8000	10000	

CHAPTER V - EXPERIMENTAL VERIFICATION

In order to demonstrate the creditability of the fluid power-cylinder contaminant sensitivity methodology, a series of cylinder tests were conducted. The plan for the test program is presented in Table 5.1. As can be seen, the first three tests used cylinders which have the same design specification but different surface roughness profiles. The purpose of this arrangement is to investigate the effect of cylinder barrel surface roughness on the contaminant sensitivity of fluid power cylinders. Cylinders with good, fair and poor surface roughness are designated as Cylinders A, B, and C, respectively. Cylinders D and E are off-the-shelf products from different manufacturers. All the cylinders used in this research have the same design specification but different barrel surface roughness, (Table 5.1).

Cylinder barrel surface roughness was examined by using the stylus-type surface texture characterization instrument. Stylus-type instruments are the only measuring tools approved by ANSI B46.1-1978 for the measurement of surface texture characterization parameters. The parameter used in this study to describe surface texture characterization is the Arithmetic Average Roughness, which is normally designated as R_a , AA, or CLA. The arithmetic average deviation from the mean center line is expressed as:

$$R_a = \frac{1}{L} \int_{x=0}^{x=L} |y| dx \quad (5.1)$$

Table 5.1 Test Program

TEST I. D.	CYLINDER I. D.	SURFACE ROUGHNESS (Ra, μm)
1	A	0.6
2	B	6
3	C	10
4	D	1.0
5	E	3

CYLINDER SPECIFICATIONS:

ID: 63.0 \pm 0.1 mm

OD: 76.5 \pm 0.5 mm

STROKE DISTANCE: 3 INCHES

where L is the sampling length, and Y is the ordinate of the curve of the profile.

Cylinders were tested according to the procedure specified in Chapter IV. AC Fine Test Dust was used as the abrasive contaminant. After a 300 mg/L particle concentration level was achieved, the test cylinder was subjected to the break-in test for a total of 3000 cycles at three different levels of operating pressure. The contaminant sensitivity test was then performed at the rated pressure of 10,000 stroke cycles, and fluid samples were taken at each 2000 cycles point.

Table 5.2 illustrates the test results obtained from each cylinder test. The particle concentration shown is the number of particles of size greater than 10 micrometers. The test results are plotted in Fig. 5.1. In the figure, the smoothly fitted curves were overlaid on actual data points. A reference particle concentration level of 3000 particles/ml greater than 10 micrometers is set as the failure criterion. This selection was made based on experience gained from testing cylinders that could no longer maintain the required working pressure when the lower pressure chamber particle concentration was over 3000 particles/ml greater than 10 micrometers. The cross point of the contaminant sensitivity characteristic curve with the reference concentration level represents the service life of the cylinder under tests. In other words, the higher the stroke cycles obtained to reach the reference concentration level, the greater the tolerance of the cylinder to the contaminant. Consequently, the effectiveness of the

Table 5.2 Test Results -- Ingression Approach

TEST I. D.	WORK CYCLES					
	0	2000	4000	6000	8000	10000
1	226.7*	1197.7	1223.7	2112.0	2818.0	1745.0
2	316.0	2511.7	1756.7	3627.0	39262.7	24558.4
3	584.6	48488.7	23614.0	+	+	+
4						
5						

* NUMBER OF PARTICLES PER mL GREATER
THAN 10 μm

+ TEST FAILED

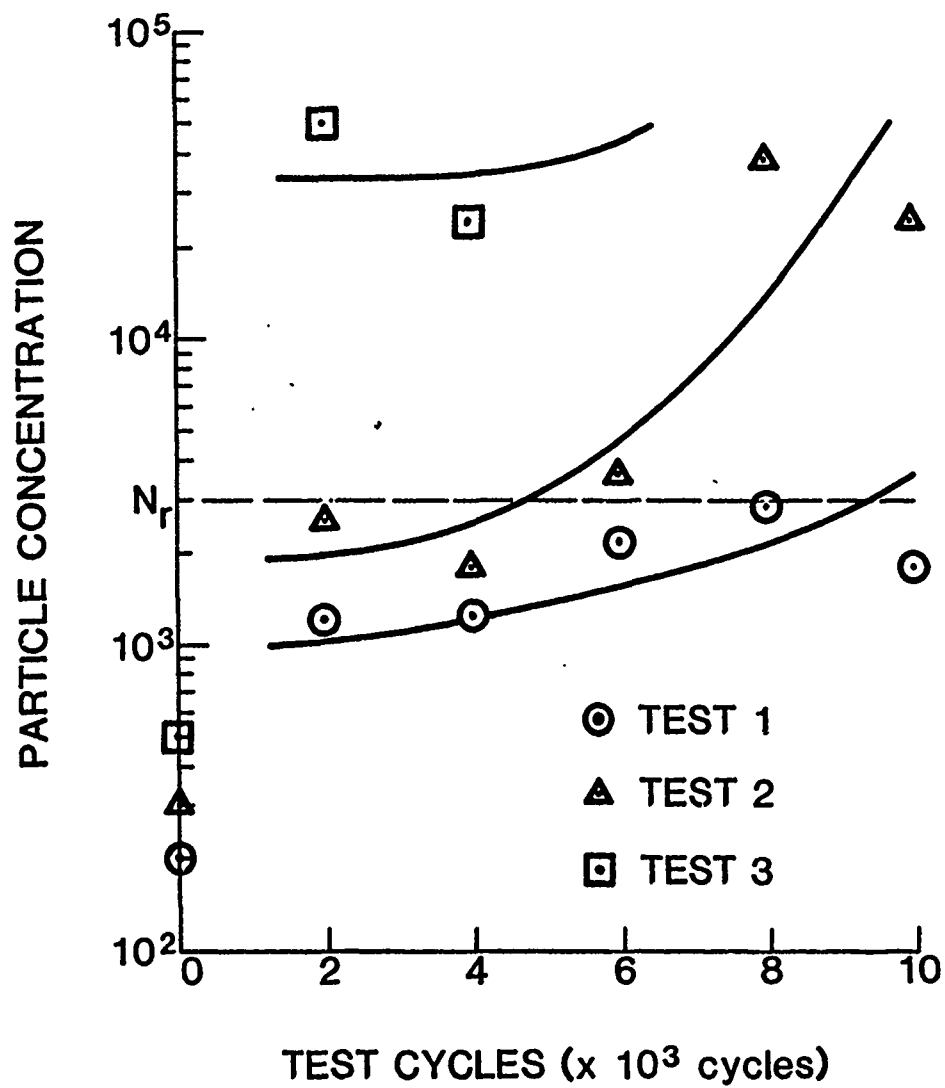


Fig. 5.1 Cylinder Contaminant Sensitivity Test Results

developed technique, using the variation of particle ingression through the piston seal and cylinder barrel, to monitor the degree of cylinder contaminant sensitivity is verified and proven.

CHAPTER VI - DISCUSSION AND CONCLUSION

Many efforts have been made to establish an effective and dependable cylinder contaminant sensitivity assessment method. Some of the efforts made relative to the current program include the use of dynamic leakage techniques, static leakage techniques, and the ferrography wear analysis method. No dependable results were obtained through these approaches. The main problem stems from the fact that most piston seals are made of elastomeric materials. The elastomer bears an inherent elastic property so that the seal may compensate for the increased clearance induced by the abrasive wear. This wear compensation mechanism is desirable in component design. However, from the standpoint of detecting leakage flow through the piston seal and cylinder barrel to indicate the wear degree, the compensation mechanism is most undesirable. The wear compensation mechanism limits the contaminant sensitivity study by directly using either a dynamic or static flow leakage measurement technique.

The nonmetallic property of elastomers also prevents the use of ferrography to accurately monitor the wear process between a seal and cylinder. Although ferrography may be applicable to correlate the wear rate in terms of the amount of wear debris generated from a cylinder barrel, it may not be informative in wear process analysis, since the wear of the seal also contributes to cylinder performance degradation.

The use of the particle ingression concept in monitoring the degree of cylinder contaminant sensitivity has been proven to be an effective and sensitive approach through the efforts of this study. It was established that particle concentration at the low pressure chamber of the test cylinder remains fairly stable before the cylinder fails to work; however, particle concentration increases dramatically (about two times) when the cylinder fails. The stroke cycle point where the test particle concentration level reaches the reference concentration level indicates the failure of the cylinder under the specified test condition. The higher the value of the failure point, the less sensitive the cylinder is to the contaminant. This criterion therefore provides an efficient and simple means of comparing cylinder contaminant sensitivity characteristics and rating their tolerance.

REFERENCES

1. White, C. M., and D. F. Denny, "The Sealing Mechanism of Flexible Packings," Ministry of Supply, Scientific and Technical Memorandum No. 3/47, Printed by BHRA Fluid Engineering, 1972, First Published (1948).
2. Bensch, L. E., and R. K. Tessmann, "An Evaluation of the Relative Contaminant Sensitivity of Hydraulic Cylinders," Report No. FPRC 77-F-1, 1977.
3. Phillips, J. F., "A Theory on the Contaminant Sensitivity of Elastomeric, Reciprocating, Hydraulic Pressure Seals," M. S. Thesis, Oklahoma State University, Stillwater, Oklahoma, 1973.
4. Fitch, E. C., "A Fundamental Performance Appraisal Concept for Reciprocating Pressure Seals," Paper H2, Seals in Fluid Power Symposium, Published by BHRA Fluid Engineering, 1 March 1973.
5. Gustafsson, J., and B. Svensson, "An Investigation of the Effect of Surface Finish Upon Seals Function in Hydraulic Cylinders," (Written in Swedish and translated at the Fluid Power Research Center), Siefra Industri AB and Sandvile AB research report, April 1972.
6. Shneider, Yu, G. et al., "Effect of Surface Finish on Leakage Between Seal Mating Surfaces," Russ Engineering, (cover to cover translation of Vestnik Mashinostroenifa by Production Engineering Research Association), 49, 6, 1969.

7. Pybus, B., "The Omega Rating of Hydraulic Cylinders, Part 1: The Test Stand," The BFPR Journal, 17, 1, 41-44, 1934.
8. He, Z. C. and A. Y. Zhao, "Experimental Research of Cylinder Contaminant Wear Sensitivity," The BFPR Journal, 18, 1985 (To be published).